AUBURN UNIVERSITY

Samuel Ginn College of Engineering

Final Report for ALDOT Project 931-072

Designing and Evaluating Infiltration Swales for Retaining and Infiltrating Roadway Stormwater Runoff

Submitted to

The Alabama Department of Transportation

Prepared by

Parker J. Austin,

Diego A. Ramirez Florez,

Yuting Ji

Michael A. Perez, PhD, PE, CPESC

Xing Fang, PhD, PE, BC.WRE, F.EWRI, F.ASCE

Wesley N. Donald, PhD

December 8, 2025

Highway Research Center

Harbert Engineering Center

Auburn, Alabama 36849

1. Report No. 931-072	2. **Government Accession No.**	**3. Recipient Catalog No.**
4. **Title and Subtitle** Designing and Evaluating Infiltration Swales for Retaining and Infiltrating Roadway Stormwater Runoff		5. **Report Date** December 8, 2025 6. **Performing Organization Code** Report No. 931-072
7. Author(s) Parker J. Austin, Diego A. Ramirez Florez, Yuting Ji, Michael A. Perez, Xing Fang, Wesley N. Donald		8. **Performing Organization Report No.** 931-072
9. **Performing Organization Name and Address** Highway Research Center Department of Civil Engineering 238 Harbert Engineering Center Auburn, AL 36849		10. **Work Unit No. (TRAIS)** 11. **Contract or Grant No.**
12. **Sponsoring Agency Name and Address** Alabama Department of Transportation 1409 Coliseum Boulevard Montgomery, AL 36130-3050		13. **Type of Report and Period Covered** Technical Report 14. **Sponsoring Agency Code**
15. **Supplementary Notes**		

16. **Abstract**

The Alabama Department of Transportation (ALDOT) employs infiltration swales, linear vegetated channels with engineered soil media, as a green infrastructure stormwater control measure along roadsides to reduce runoff discharge. This study evaluated the performance of infiltration swales and their media through laboratory experiments, field testing, and hydrologic modeling. Laboratory testing using 6-in. columns and falling-/constant-head tests guided material performance characterization. Two 40-ft long swales (ALDOT and modified infiltration swale) were constructed at the Auburn University - Stormwater Research Facility to compare infiltration behavior under varying rainfall frequencies, soil moisture conditions, underdrain settings, and seasonal differences. Moisture sensors tracked water movement within the swales, and surface storage and settlement were monitored. Results showed the ALDOT infiltration swale performed adequately and met infiltration goals. The modified infiltration swale, which included an amended topsoil and optimized media matrix, provided higher infiltration rates. The ALDOT swale averaged an infiltration rate of 1.6 ft/d and a drawdown time of 12.25 hrs, while the modified swale achieved 5.2 ft/d and 5.06 hrs, respectively. Drier soils, longer inter-event dry periods, and warmer months resulted in higher infiltration rates in both designs. Moisture data indicated that infiltrated water reached the bottom of the modified swale in 0.13 hours compared to 1.8 hours for the ALDOT swale. Hydrologic modeling demonstrated that both swales reduce discharge, with the modified design providing the largest reductions under design storms and long-term rainfall. Assessment of surface profile elevations found no indication of settling in either swale.

17. Key Words Infiltration swales, stormwater, green infrastructure		**18. Distribution Statement** No restrictions	
19. Security Classification (of this report) Unclassified	**20. Security Classification (of this page)** Unclassified	**21. No. of Pages** 259	**22. Price** None.

Research Report

Designing and Evaluating Infiltration Swales for Retaining and Infiltrating Roadway Stormwater Runoff

Submitted to

The Alabama Department of Transportation

Prepared by

Parker J. Austin,
Diego A. Ramirez Florez,
Yuting Ji
Michael A. Perez, PhD, PE, CPESC
Xing Fang, PhD, PE, BC.WRE, F.EWRI, F.ASCE
Wesley N. Donald, PhD

December 8, 2025

DISCLAIMERS

The contents of this report reflect the views of the authors who are responsible for the facts and accuracy of the data presented herein. The contents do not necessarily reflect the official views or policies of Alabama DOT, Auburn University, or the Highway Research Center. This report does not constitute a standard, specification, or regulation. Comments contained in this report related to specific testing equipment and materials should not be considered an endorsement of any commercial product or service; no such endorsement is intended or implied.

NOT INTENDED FOR CONSTRUCTION, BIDDING, OR PERMIT PURPOSES

Michael A. Perez, PhD, PE, CPESC
Wesley Donald, PhD
Xing Fang, PhD, PE, BC.WRE, F.EWRI, F.ASCE
Research Supervisors

ACKNOWLEDGEMENTS

Material contained herein was obtained in connection with a research project, "Designing and Evaluating Infiltration Swales for Retaining and Infiltrating Roadway Stormwater Runoff," ALDOT Project 931-072, conducted through the Auburn University Highway Research Center. Funding for the project was provided by the Alabama Department of Transportation (ALDOT). The funding, cooperation, and assistance of many individuals from each of these organizations are gratefully acknowledged. The authors particularly acknowledge the contributions of the following individuals for serving on the project advisory committee (PAC):

Stan Biddick (PAC Chair)	Bureau Chief	Design Bureau	ALDOT
Scott Rogers	Environmental Coordination Engineer	Design Bureau	ALDOT
Nick Franklin	Stormwater Engineer	Design Bureau	ALDOT
Stacey Glass	Bureau Chief	Construction Bureau	ALDOT
Richard Klinger	Environmental Construction Engineer	Construction Bureau	ALDOT
Mark Waits	Asst. Bureau Chief, Roadways	Maintenance Bureau	ALDOT
Benjamin Yates	Asst. State Maintenance Engineer	Maintenance Bureau	ALDOT
Howard Peavy	State Agronomist (ret.)	Maintenance Bureau	ALDOT
Scott George	Bureau Chief	Materials & Tests Bureau	ALDOT
Virgil Clifton	Asst. Bureau Chief (ret.)	Research Bureau	ALDOT
Kristy Harris	Program Analyst / Pavements & Materials	Federal Highway Administration	

ABSTRACT

Urbanization, characterized by the increase of impervious surfaces including roads, parking lots, and buildings, presents challenges for stormwater management. The expansion of impervious surfaces disrupts natural infiltration processes, leading to increased volumes and peak flow rates of stormwater runoff. Post-construction stormwater control measures (SCMs) that integrate Low Impact Development (LID) and Green Infrastructure (GI) principles rely on evapotranspiration, infiltration, filtration, and water reuse, to mimic pre-development hydrology and manage the quantity and quality of stormwater runoff. The Alabama Department of Transportation (ALDOT) employs infiltration swales, linear vegetated channels with engineered soil media, as a green infrastructure stormwater control measure along roadsides to reduce runoff discharge.

This study evaluated the performance of infiltration swales and their media through laboratory experiments, field testing, and hydrologic modeling. Laboratory-scale experiments were conducted to evaluate material properties and assess infiltration capacity of various matrices. Testing was conducted primarily in 6 in. (15.2 cm) diameter cylinders using falling head and constant head infiltration tests. Two 40-ft long swales (ALDOT and modified infiltration swale) were constructed at the Auburn University - Stormwater Research Facility to compare infiltration behavior under varying rainfall frequencies, soil moisture conditions, underdrain settings, and seasonal differences. The construction process included geotechnical and soil investigation, site selection, excavation, media material placement, moisture content installation, and site stabilization for both infiltration swale designs. The evaluation focused on infiltration rates and drawdown times under various rainfall-event scenarios designed to assess the influence of external factors on infiltration performance. These factors included variations in rainfall-event frequency, underdrain valve settings (open vs. closed), initial soil moisture conditions (wet vs. drier), and seasonal variations. Moisture content sensors were also installed within the swale media and surrounding soil at different depths and locations to track the movement of infiltrated water. Additionally, settlement of the swales was monitored from construction completion, and surface storage volumes were measured.

Results showed the ALDOT infiltration swale performed adequately and met infiltration goals. The modified infiltration swale, which included an amended topsoil and optimized media matrix, provided higher infiltration rates. The ALDOT swale averaged an infiltration rate of 1.6 ft/d and a drawdown time of 12.25 hrs, while the modified swale achieved 5.2 ft/d and 5.06 hrs, respectively. Drier soils, longer inter-event dry periods, and warmer months resulted in higher infiltration rates in both designs. Moisture data indicated that infiltrated water reached the bottom of the modified swale in 0.13 hours compared to 1.8 hours for the ALDOT swale. Hydrologic modeling demonstrated that both swales reduce discharge, with the modified design providing the largest reductions under design storms and long-term rainfall. Assessment of surface profile elevations found no indication of settling in either swale.

TABLE OF CONTENTS

LIST OF TABLES

LIST OF FIGURES

CHAPTER 1. INTRODUCTION

The drainage design for a roadway construction project in the Alabama Department of Transportation (ALDOT) is required to follow the ALDOT Guideline for Operation GFO 3-73 (ALDOT 2014). Based on the Guideline, ALDOT developed calculation guidance for drainage design using small frequently occurring storms, i.e., the 95th percentile daily rainfall events, to calculate runoff volume and peak discharge. Runoff volume is calculated using the 95th percentile rainfall event and a volumetric runoff coefficient R_V. Peak discharge is calculated from the Natural Resources Conservation Service (NRCS) unit peak discharge diagram using the rainfall, basin area, modified curve number, and time of concentration. GF 3-73 requires the use of decentralized practices and features near the source of the runoff, which cause post-development hydrology to mimic pre-development hydrology of the site to the maximum extent practicable for all small, frequent rain events, working within the constraints of the project, at all locations of discharge. ALDOT has promoted using the infiltration swales in the drainage channels of roadways as decentralized practices and features.

1.1 BACKGROUND

The increase in urbanization and population growth has led to a heightened demand for the expansion of highway and roadway networks. According to a report by Transportation for America, the largest 100 urbanized areas in the United States added 30,511 new freeway lane-miles of road between 1993 and 2017, representing a 42% increase. Interestingly, this rate of freeway expansion significantly outstripped the 32% growth in population in those regions over the same period (Transportation For America 2013). This development of infrastructure has resulted in a notable increase in impermeable surface cover compared to the natural pre-development area.

Impermeable surfaces are hardened surfaces, usually in the form of pavement, asphalt, or concrete, that do not allow water to pass through. The presence of impervious surfaces significantly impacts a watershed's runoff characteristics. The rise in impermeability is acknowledged as a key factor contributing to the increase in peak flow and the overall volume of surface stormwater runoff. This is primarily due to reduced infiltration capabilities compared to the predevelopment conditions (Abida and Sabourin 2006). According to the US Environmental Protection Agency (EPA), when impermeable surfaces reach 10% to 20% of the total area, surface runoff doubles. This trend continues, with a 100% impervious cover resulting in five times more runoff than a forested watershed (USEPA 2020). As for peak flow increase, some studies have shown that a 10% increase in impervious cover can result in a 30% to 50% increase in peak flow rates (National Research Council 2009).

The rise in runoff peak flow and volume is demonstrably linked to several negative environmental consequences. Notably, stormwater runoff acts as a conveyance mechanism for pollutants deposited on highways and roadways. These pollutants are then transported to sensitive habitats and potentially contaminate drinking water sources. Despite

comprising only 3% of the landmass in the United States, urban areas generate a significant amount of stormwater pollution. This runoff is estimated to be the leading cause of impairment for a substantial portion of the nation's waterways, affecting 13% of rivers, 18% of lakes, and a troubling 32% of estuaries (National Research Council 2009). Other negative impacts include increased frequency and intensity of flooding, deterioration of urban stream health, excess nutrient and contaminant loading, impacts on biological aquatic organisms, lower local groundwater recharge, and erosion of slopes and streambanks (Bell et al. 2020; Bhaduri et al. 2000).

In response to growing concerns about water quality degradation in the United States, Congress enacted the Clean Water Act (CWA) of 1972. The CWA aimed to restore and maintain the health of the nation's waters by regulating point source discharges and implementing other pollution control measures. Recognizing the significant contribution of stormwater runoff to water quality issues, the CWA was amended in 1987 to establish the National Pollutant Discharge Elimination System (NPDES) program. The NPDES, enforced by the EPA, focused on reducing pollutants from industrial processes and wastewater and municipal sewage discharge (National Research Council 2009). This also laid the groundwork for the Municipal Separate Storm Sewer System (MS4) program which targets stormwater runoff from urbanized areas. It regulates the collection and discharge of stormwater through a network of municipal storm drains, sewers, and other conveyances. The MS4 program applies to municipalities and other designated urban entities, such as universities, hospitals, and airports. The program is further divided into phases, with Phase I targeting larger municipalities and Phase II focusing on smaller ones and specific areas within urbanized areas. Runoff from roadways designed/constructed/managed by ALDOT is covered through a Phase I MS4 permit issued by the Alabama Department of Environmental Management (ADEM). The MS4 program doesn't directly issue permits; however instead, it requires municipalities and other entities to develop and implement Stormwater Management Programs (SWMPs) to control pollution in their stormwater discharges (USEPA 2024). An SWMP outlines the strategies, policies, and practices that will be implemented to achieve specific water quality objectives.

To achieve effective SWMPs, municipalities and other entities implement stormwater control measures (SCMs), also referred to as best management practices (BMPs). These practices aim to manage stormwater runoff, protect water quality, and mitigate the impacts of urbanization on natural hydrological processes. SCMs are structural or non-structural practices specifically designed to manage stormwater runoff. Structural practices are landscape features designed to counter the increase in peak flow and runoff by detaining, retaining, infiltrating, and/or treating runoff (Bell et al. 2020). Some of these SCMs are labeled as "post-construction" which signifies the features are to operate as long-term, permanent solutions well after the construction phase has been concluded. Some SCM types include wetlands, wet ponds, dry detention ponds, infiltration beds, permeable pavement, etc. (UNC 2024).

In adherence to the requirements of the MS4 program and its associated SWMPs, ALDOT utilizes stormwater control measures to manage stormwater runoff and protect

public health and the environment. ALDOT uses many different types of SCMs, but a relatively new one they started implementing around the state is called infiltration swales.

1.2 Definition And Purpose Of Infiltration Swales

Infiltration swales (Figure 1.1) are a commonly employed SCM implemented by ALDOT along roadways. These linear vegetated channels function by promoting the infiltration of stormwater runoff through an engineered soil media. This infiltration process allows the stormwater to subsequently percolate into the underlying native soils and potentially reach the local groundwater table. This functionality allows infiltration swales to mimic the pre-development hydrology of a site by mitigating the increase in peak flow rates and runoff volumes generated by impervious surfaces. Infiltration swales offer a compelling solution for stormwater management due to their combined capabilities. Their potential for high infiltration rates reduces runoff volumes, while the vegetated channels and check dams promote velocity flow reductions, potentially managing both peak flow rates and total runoff volumes.

Beyond managing peak flow and runoff volume, ALDOT utilizes infiltration swales to comply with MS4 requirements and promote the principles of Low Impact Development (LID) and Green Infrastructure (GI). Both LID and GI share a common goal: managing stormwater runoff locally and in a more sustainable manner that mimics natural hydrology. However, they differ in scope and emphasis. GI encompasses a broader range of practices and elements that utilize natural processes to manage stormwater runoff. These elements, such as parks, rain gardens, and bioswales, often deliver additional environmental and social benefits beyond stormwater management, including improved air quality, habitat creation, and recreational opportunities. GI principles are integrated into the planning and design of communities and infrastructure projects, promoting a holistic approach to urban development. LID, on the other hand, focuses on a specific set of engineered practices designed to manage stormwater runoff close to its source. Examples of LID practices include infiltration trenches, permeable pavements, and bio-retention facilities. These practices aim to reduce the overall volume and flow rate of runoff entering traditional conveyance systems. While LID primarily targets stormwater management, some practices can contribute to broader environmental goals when strategically implemented (Dylewski et al. 2007; USEPA 2024).

The infiltration swale design process is essential to understanding how the engineered media matrix affects the swale's functionality and infiltration performance. The ALDOT infiltration swale (ALDOTIS) design is an existing design currently used across the state of Alabama and was provided to Auburn University for testing and enhancement. Figure 1.1 represents the current ALDOTIS design.

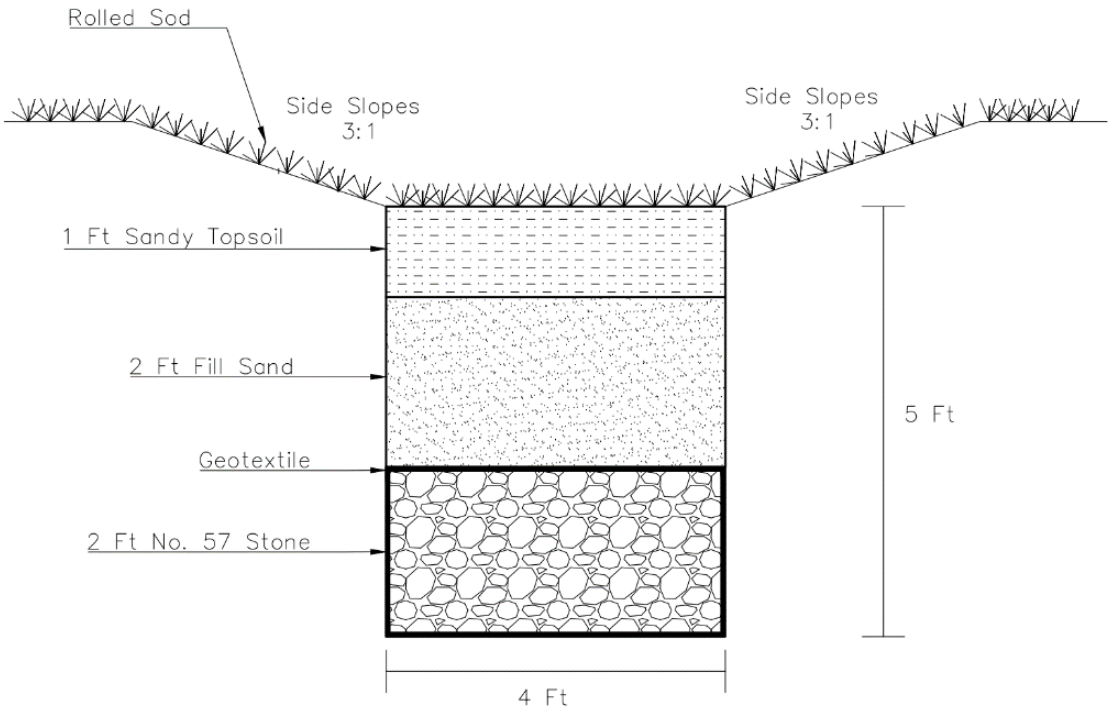

(a) cross section

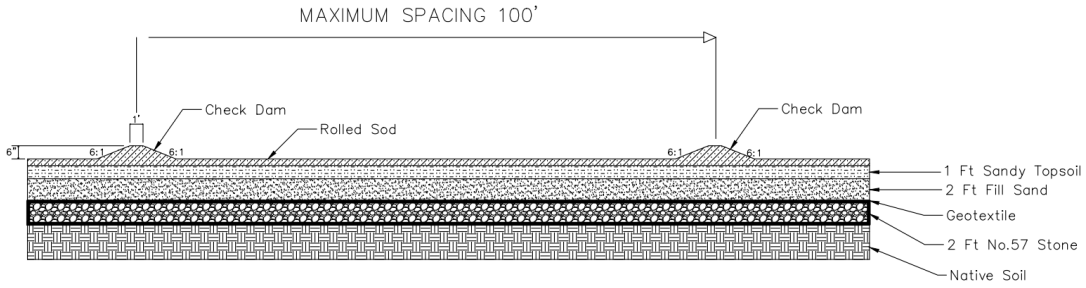

(b) profile view

Figure 1.1. ALDOTIS Field-Scale Drawing

This infiltration swale design is a vegetated lined grass channel composed of an engineered soil media matrix that lies underneath the bottom of the swale. This component is 4 ft (1.2 m) in width and 4–5 ft (1.2–1.5 m) in depth underneath the surface of the swale's channel. Figure 1.1(a) shows ALODT's engineered soil media matrix from the top is composed of 1 ft (0.3 m) of sandy topsoil, 2 ft (0.6 m) of fill sand, and 2 ft (0.6 m) of #57 stone. The #57 stone layer is wrapped on all four sides by a separation geotextile fabric to block any smaller soil particles from filling the voids in between the #57 stone. If the engineered media matrix does not have the topsoil and fill sand layers, it becomes an infiltration trench with a gravel storage layer only. If the engineered media matrix does not have the gravel storage layer, it becomes a rain garden with topsoil and sand layers. The ALDOTISs have three heterogeneous layers and are called bio-retention cells (BRCs), one type of LIDs, for SCMs.

1.3 LITERATURE REVIEW SUMMARY

This section provides a brief and condensed summary of literature reviewed as part of this project. A comprehensive literature review is available in two Master's degree theses (Austin 2024; Ramirez Florez 2024). Infiltration swales are a type of post-construction infiltration-based SCM that are used around the United States. While existing literature on the specific infiltration swale design employed in this study may be limited, extensive research exists on grass swales, a closely related SCM. Infiltration swales investigated in this study incorporate engineered media matrix (soil and gravel storage layers) beneath the grass layer to enhance infiltration compared to traditional grass swales without it. Given their shared core functionality as grass swales with an added infiltration media, findings from grass swale studies can be readily applied to understand the performance of infiltration swales. Infiltration swales, including grass swales, can be effective in reducing the amount of stormwater runoff volumes and peak flows if coordinated, planned, constructed, and maintained correctly. Field studies on grass swales, which lack an engineered media, have documented substantial reductions in runoff volumes through infiltration. These studies report reductions of up to 50% in semi-arid regions with low initial soil moisture content, suggesting the potential effectiveness of infiltration swales in similar conditions (Ramirez Florez 2024). Grass swales and infiltration swales both provide stormwater quantity and quality treatment; however, grass swales can only manage smaller storm events (Abida and Sabourin 2006). Infiltration swales, with an added engineered media matrix, can potentially decrease runoff from a wider range of storm events.

In terms of a general design, infiltration swales are a vegetated open channel conveyance system that uses check dams and an engineered media matrix to capture and infiltrate stormwater runoff. The core component of an infiltration swale is the engineered media matrix. The media can be either heterogeneous (composed of various materials) or homogeneous (uniform material). The ALDOT swale investigated in this study employs a heterogeneous media mixture. Infiltration swales function by promoting permeation of runoff into the engineered soil media matrix. This matrix, comprised of high permeable soil materials, facilitates water movement through its layers and into the underlying native soils, ultimately reaching the local groundwater table. The engineered media matrix has pollutant removal properties; however, water quality research is not within the scope of this study. The engineered media matrix is the component of the infiltration swale that is under the base of the swale's channel and is broken into different soil layers to help stimulate infiltration. This ability allows the swale to mimic the pre-hydrology of a site and manage the increase in peak flow and volume of runoff from impervious surfaces through its potential for high infiltration rates over a linear surface area. Figure 1.2(a) shows a general depiction of an infiltration swale and the engineered media matrix component while Figure 1.2(b) shows its functionality.

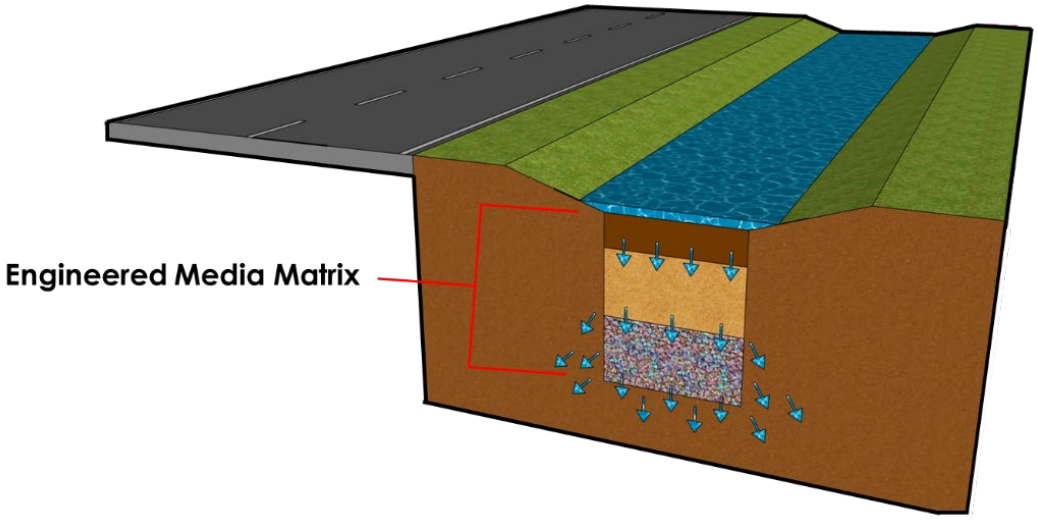

(a) infiltration swale rendering

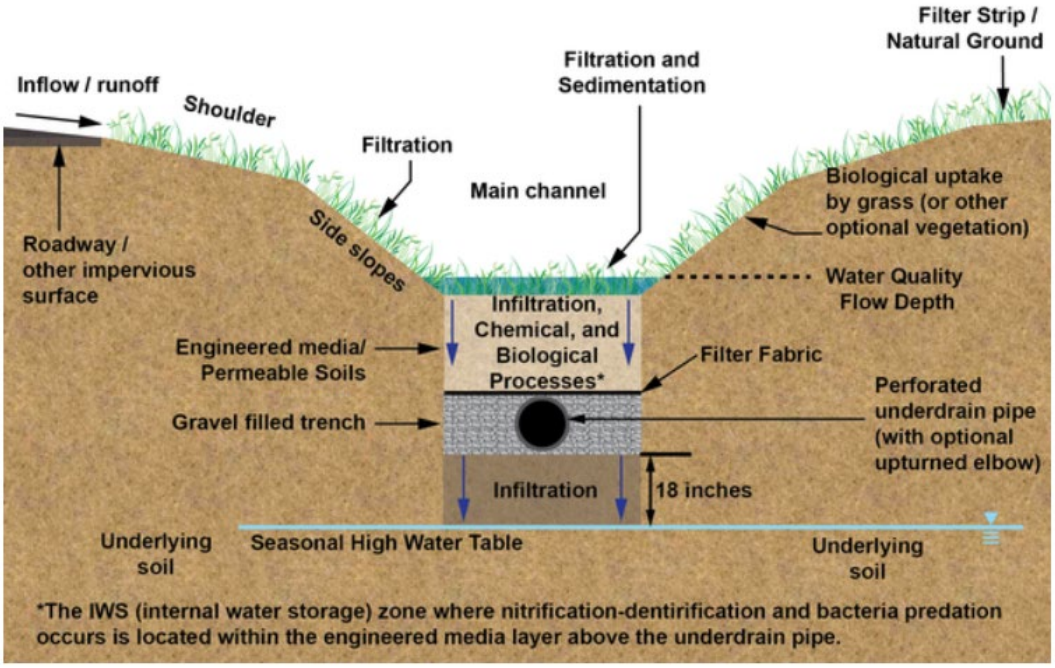

(b) general infiltration swale design (Figure 6 rom Ekka and Hunt (2020))

Figure 1.2. Infiltration Swale Schematic

Despite the widespread use of post-construction infiltration-based SCMs including infiltration swales across the United States by various departments of transportation (DOTs) and organizations, a lack of standardization exists. This results in diverse interpretations, including variations in nomenclature, design criteria, geometric configurations, media compositions, construction techniques, and maintenance procedures. For instance, other common infiltration-based SCMs include dry detention ponds, grass swales, bioswales, biofiltration swales, media filters, etc.(UNC 2024). Some organizations use these SCMs for

specific purposes, including focusing on managing the quantity, volume, and peak flow of stormwater runoff or focusing on the quality of runoff by treating and filtering pollutants out.

The focus of this literature review is broken into three parts: (1) using grass swale studies to compare infiltration rates, (2) investigating main factors that affect infiltration-based SCM performance, and (3) investigating other DOT's infiltration-based SCMs to compare to ALDOT's infiltration swale design. To establish a common ground for the subsequent literature, the next section provides definitions for several key terms frequently used within the post-construction stormwater management community.

1.1 DOT SCM SUMMARY

A review of infiltration-based SCM practices across the United States revealed several key design criteria that influence their performance. These criteria are essential for optimizing infiltration efficiency and ensuring the long-term functionality of these facilities.

- **Longitudinal Slope:** Most reviewed facilities possess relatively flat longitudinal slopes, ranging from 0.5% to a maximum of 5%. State agencies consistently emphasize the importance of a flat slope for promoting infiltration. Lower slopes encourage slower flow velocities, allowing stormwater runoff to linger on the surface and infiltrate into the media. Conversely, steeper slopes create higher velocities that bypass infiltration and can lead to erosion and scour within the SCM. With ditch checks/dams, lower slopes can pond more water to facilitate/promote infiltration.
- **Drainage Area:** The optimal drainage area for infiltration-based SCMs is generally considered to be 5 acres (2 ha) or less. Excessively large drainage areas overwhelm the SCM and compromise its infiltration capacity. Larger areas contribute to higher peak flow velocities, further exacerbating erosion and scour.
- **Native Surrounding Soil:** The infiltration performance of these facilities is significantly influenced by the surrounding native soil. Ideally, the soil should be classified as (Hydrological Soli Group) HSG A or B, with an infiltration rate exceeding 0.5 in/hr. (1.27 cm/hr.). Some states entirely avoid infiltration-based SCMs in areas with HSG C or D soils, while others incorporate underdrains for such sites. Low infiltration rates in native soils prevent timely exfiltration of stormwater runoff from the media before the next storm event, leading to ponding and potential flooding that can take days to resolve.
- **Drawdown Time:** Most state agencies require their infiltration-based SCMs to achieve a complete drawdown within 48 hours. The reviewed literature documented drawdown times ranging from 12 hours (reported for North Carolina's bio-retention basins) to a maximum of 48 hours. Drawdown times exceeding 48 hours can lead to increased pollutant concentrations within the stagnant water and create mosquito breeding habitats. The stagnant polluted water can potentially contaminate the groundwater table or other nearby waterways.
- **Depth of Seasonal High Groundwater Table:** The depth of the seasonal high groundwater table significantly impacts the recommended drawdown time. Across

the country, reported minimum depths varied from 1 ft (0.3 m) in Alabama to 5 ft (1.5 m) in California. A deeper groundwater table allows infiltrated runoff to exfiltrate and drain from beneath the SCM, facilitating a faster drawdown. Conversely, a shallow groundwater table creates water mounding underground that restricts exfiltration into the native soils, thereby reducing infiltration capacity and potentially causing drawdown times to exceed 48 hours.

- **Check Dams:** Including the benefits of low longitudinal slopes, check dams serve to interrupt flow and reduce flow velocity within the SCM. By creating impoundments, check dams allow the runoff to slow down and make contact with the surface, promoting infiltration. Facilities lacking check dams may experience reduced infiltration due to runoff bypassing the media and continuing downstream.

A summary table consolidating the key findings from this literature review, including the six design criteria and minimum media depth, is presented in Table 1.1

Table 1.1. Summary of Presented Infiltration-Based SCMs

State DOT	Infiltration SCM	Design Criteria	Min. Media Depth
AL	Infiltration Swale	Long. Slope ≤ 5% Drainage Area ≤ 5 ac. (2.02 ha) Native soils HSG A or B Check Dams Groundwater Table ≥ 1 ft (0.305 m) Max. 48 hr. drawdown	30 in. (76.2 cm)
GA	Infiltration Trench	Long. Slope ≤ 1% Drainage Area ≤ 5 ac. (2.02 ha) Native soil ≥ 0.5 in/hr. (1.27 cm/hr.) No Check Dams Groundwater Table ≥ 4 ft (1.2 m) Max. 48 hr. drawdown	48 in. (121.9 cm)
	Enhanced Dry Swale	Long. Slope ≤ 4% Drainage Area ≤ 5 ac. (2.02 ha) No Native Soil Restrictions Optional Check Dams Groundwater Table ≥ 2 ft (0.61 m) Max. 48 hr. drawdown	36 in. (91.4 cm)
MN	Infiltration Trench	Long. Slope ≤ 1% Drainage Area ≤ 5 ac. (2.02 ha) Native soil HSG A, B, or C No Check Dams Groundwater Table ≥ 3 ft (0.91 m) Max. 48 hr. drawdown	46 in. (116.8 cm)
	Bioinfiltration Basin		33 in. (83.8 cm)
NC	Filtration Basin	Long. Slope ≤ 0.5% Drainage Area ≤ 5 ac. (2.02 ha) Native soil ≥ 0.52 in/hr. (1.32 cm/hr.) No Check Dams Groundwater Table ≥ 2 ft (0.61 m) Max. 24 hr. drawdown	18 in. (45.7 cm)
	Bioretention Basin	Long. Slope ≤0.5% Drainage Area ≤ 5 ac. (2.02 ha) Native soil ≥ 0.52 in/hr. (1.32 cm/hr.) No Check Dams Groundwater Table ≥ 2 ft (0.61 m) Max. 12 hr. drawdown	24 in. (60.9 cm)
WS	Media Filter Drain	Long. Slope ≤ 5% Drainage Area ≤ 0.12 ac. (0.05 ha) Native soil HSG A or B Flow Spreader, no check dams Groundwater Table ≥ 3 ft (0.91 m) Max. 48 hr. drawdown	33 in. (83.8 cm)
NY	Surface Sand Filter	Long. Slope ≤ 2% Drainage Area ≤ 10 ac. (4.05 ha) Native soil ≥ 0.5 in/hr. (1.27 cm/hr.) No Check Dams Groundwater Table ≥ 3 ft (0.91 m) Max. 48 hr. drawdown	33 in. (83.8 cm)
	Organic Filter		39 in. (99.1 cm)
CA	Bioswale	Long. Slope ≤ 2% Drainage Area – small or large Native soil ≥ 0.5 in/hr. (1.27 cm/hr.) Check Dams Groundwater Table ≥ 2 ft (0.61 m) Max. 12 hr. drawdown	23 in. (58.4 cm)

Bio-retention cells (BRCs) are versatile and widely utilized LID facilities (or modules) for reducing runoff volumes and mitigating peak flow in urban stormwater management. This LID module, which primarily relies on infiltration, evapotranspiration, drainage through the underdrain, and storage to control stormwater, can be adapted to various conditions. The hydrologic performance of the BRCs is influenced by design parameters such as soil composition, dimensions (depth, length, and width) and structure (layer layout), and drainage configuration. There are several studies (Khan et al. 2013; Yang and Chui 2018) that underscore the importance of optimizing structure and design for different conditions to enhance the effectiveness of BRCs for urban runoff control.

BRCs consist of three layers: surface pond areas containing mulch or growing grasses, engineered soil media, and storage volume. An underground drainage system is optional and may be required by certain conditions/jurisdictions. All these components help manage runoff by filtering pollutants, infiltration, and temporary water storage (Yang and Chui 2018). The standard design of BRCs depends on jurisdictions and is affected by drainage area, bio-retention surface area, pond depth, medium depth and composition, subsurface drainage configuration, surrounding soil properties, rainfall characteristics (depth, duration, and intensity), vegetation, and temperature. (He and Davis 2011). The medium of the BRCs is a mixture of sand (typically the main medium component), fine sand (silt and clay), and organic matter that supports the growth of plants (i.e., vegetation in the module's surface layer). This vegetation, whose primary function is to withstand drought and temporarily inundate to store water, usually trees, shrubs, forbs, or grasses, plays a crucial role in the efficiency of BRCs (Winston et al. 2016).

Bio-retention can not only reduce runoff peaks, runoff volumes, and pollutant loads and increase the time of concentration, groundwater infiltration, and evapotranspiration but also alter the water balance to decrease direct discharge by evapotranspiration and exfiltration(Davis et al. 2009). Properly designed bio-retention systems can handle various storm events, including small and moderate storms where runoff can be captured entirely and infiltrated(Winston et al. 2016). Saturated hydraulic conductivity (k_s) of the soil layer has the greatest influence on the efficiency of BRCs, determined by physical parameters such as the composition and density of the soil media, vegetation on the surface, and the soil clog condition after infiltration(Paus et al. 2015). When k_s is increased, it improves the hydrological performance of BRCs (Paus et al. 2015). The efficiency of infiltration of BRCs is influenced by the soil composition, the most prominent being the proportion of the soil mixture connected to field capacity, k_s, and soil moisture content. Internal water storage (IWS), which reduces runoff by seepage into native soil and evapotranspiration, is usually made of stone and contains drainage pipes. Moreover, the thickness of the IWS region is one of the main factors affecting the efficiency of BRCs (Winston et al. 2016). Drainage of BRCs is a vital configuration, especially in areas with poorly drained native soils, which prevents excessive accumulation of water. Although BRCs are widely used and there is much research on these vital LIDs, further studies are still needed to optimize the size standard of BRCs, especially in terms of balancing peak flow mitigation and volume reduction (Yang and Chui 2018).

There are various published methods for the design and sizing of rain gardens or bio-retention systems such as applications of Darcy's equation to determine the runoff infiltrated (SEMCOG 2008) or the CN method (Lucas 2004) to determine the runoff to a LID facility. Some more complex programs have also been developed over the years by various researchers, e.g., RECHARGE developed by Dussaillant et al. (2004) solves Richards Equation to simulate recharge, runoff, and evapotranspiration through different layers of rain gardens. The EPA SWMM model developed/updated the capability to model various LIDs since 2009 (version 5)(Rossman 2010; Rossman and Huber 2016).

1.4 PROJECT OBJECTIVES

The objective of this research project was to better understand infiltration swale design and enhance infiltration capacity through effective planning, site data collection, and testing. The project sought to better understand the factors influencing the performance of infiltration swales and to provide the knowledge base needed to effectively and efficiently design and implement infiltration swales along Alabama roadways. To meet this objective, a two-phased approach was developed. The first phase focused on small-scale infiltration swale testing in the laboratory to understand infiltration mechanics and develop a simple method to quantify media porosity. The second phase involved full-scale testing to develop an understanding of rainfall and runoff characteristics and long-term performance of infiltration swales and hydrological modeling of swales. The following tasks were completed through the two phases of the project:

- **Task 1: Literature Review & Survey:** The literature review included a search of scholarly research, best practices guidelines, and state and federal suggested LID/GI practices. The findings of the literature review served as the basis for the subsequent tasks in the research. In addition to a literature review, this task included a state-of-the-practice survey of DOTs across the U.S. and the collection of design, construction, and maintenance information on current LID/GI practices being used by state DOTs
- **Task 2: Small-Scale Infiltration Swale to Quantify Porosity and Infiltration Mechanics:** The second task was to construct a small-scale infiltration swale in the Auburn University Civil and Environmental Engineering's (CEE) Stormwater Laboratory to understand and visualize infiltration mechanics when water moves through the soil matrix media. Results from these experiments were used to finalize the infiltration swale design and understand its performance in capturing stormwater runoff.
- **Task 3: Design, Construct, and Calibrate Experimental Field-Scale Infiltration Swales:** The third task of the project was the construction of a test apparatus at the AU-SRF to facilitate field-scale testing of infiltration swales. Two 40-ft long swales were constructed, one per current ALDOT specifications and the second per modifications recommended through Task 2 efforts.

- **Task 4: Perform Controlled Experiments and Observe Performance under Rainfall Events:** The performance of the infiltration swales was monitored during controlled tests as well as during naturally occurring rainfall events.
- **Task 5: Determine Factors Affecting Long-Term Performance of Infiltration Swales:** long-term monitoring throughout the project period was used to identify maintenance concerns that may affect the performance of the infiltration swales.
- **Task 6: Understand Performance of Infiltration Swales under Long-term Rainfall Conditions:** Through Task 6, we conducted a hydrological analysis of infiltration swales and developed case studies using EPA SWC, EPA SWMM, and Bentley's CivilStorm to model and analyze rainfall and runoff characteristics for watersheds with infiltration swales.
- **Task 7: Final Report and Development of Best Practices:** A comprehensive final report documenting research efforts and results was developed. The report includes all findings from the research effort, including recommended best practices for the design, construction, and maintenance of ALDOTISs.

1.5 REPORT ORGANIZATION

This report is divided into six chapters that address the objective of improving guidance for the design and use of infiltration swales. The first chapter serves as an introduction, summary of literature review, and provides an overview of the project objective and outlining the report's organization. Chapter 2 presents the findings of the small-scale and intermediate-scale testing efforts. Chapter 3 focuses on field-scale testing of the two investigated swale designs. Chapter 4 provides a summary of the hydrologic modeling task. Finally, based on the research findings, Chapter 5 provides the summary and conclusions of the study and final recommendations.

1.6 EXECUTIVE SUMMARY

Chapter 5 provides 21 conclusion points based on the in-depth laboratory, field-scale, and modeling studies. A more concise executive summary is provided below.

1. A sandy topsoil with ~88% sand content and less than 2% silty content was used in this study to construct infiltration swales for small-scale column tests and field-scales tests. For small-scale tests, the measured infiltration rates for topsoil and the current ALDOT swale design are greater than 1.0 ft/day (as ft/d afterwards) in some tests, which is higher than the minimum required infiltration rate specified in the LID Manual of Alabama; and are less than 1.0 ft/d in many other tests (the lowest is 0.16 ft/d). For field-scale tests, the average infiltration rates were greater than 1.0 ft/d (1.3–2.6 ft/d). Variations in infiltration rates of topsoil are due to soil consolidation (2 ft water head in tests, also linking to the impact of maintenance of machine mowing) and soil's heterogeneity. Therefore, the current ALDOTIS design could perform satisfactorily (>1.0 ft/d infiltration rate) sometimes but may not perform well in other situations. ALDOT's topsoil (Section 650) for highway construction follows ASTM D 5268 and has 2–20% by weight of organic material, 10–90% by weight of sand

content, and 10–90% by weight of silt and clay content, in portion of sample passing 10 Sieve (2 mm). Based on ASTM D 5268, ALDOT's topsoil could have quite different particle size distributions, e.g., 30% silt and clay and 60% sand. In comparison to the topsoil used for this study (~88% sand), another topsoil could have quite a different permeability, smaller than 1.0 ft/day, when it has more fine silt and clay. This may not be important for various highway construction projects, but smaller permeability is crucial to infiltration-based LIDs. Using topsoil with different permeabilities can result in quite variable performance of the infiltration swale to control the surface runoff and retain/store inflow.

2. A modified infiltration swale design is proposed and tested. To enhance the ALDOT topsoil's infiltration rate, amended topsoil with 20% pine bark fines and 80% of the original topsoil by weight was used. The modified swale design has 6 in. (15 cm) amended topsoil, 10 in. (25 cm) sand, 6" (15 cm) pea gravel (replacing the geotextile), and #57 stone layer (height depending on the swale depth, e.g., 26" stone of 4-ft swale). The amended topsoil had an average infiltration rate of 5.6 ft/d, i.e., 8.9 times higher than the infiltration rate obtained with topsoil alone, which was 0.63 ft/day (0.19 m/day). For both small-scale column tests and field-scale experiments, the modified swale outperformed the current ALDOT swale to infiltrate surface runoff.

3. Modeling simulations show that both the current ALDOT and modified infiltration swales reduce the runoff under design storm conditions (2.2–2.8 in. over Alabama). Under long-term historical simulations for a southern Alabama project site, these infiltration swales could capture additional 30.5–33.5% relatively smaller rainfall events to produce no runoff. Therefore, implementing infiltration swales along roadways is encouraged for stormwater control and management.

4. Modeling simulations show that lower soil hydraulic conductivity leads to lower utilization rate of the storage layer (stone), which wastes the investment on making the swale deeper with more stone or storage space. For example, when the soil-layer's hydraulic conductivity is 1.0 ft/d, under 2.6 in. design storm in the Southern Alabama project site, the maximum storage depth is less than 2.5 in. when the storage layer (stone) is 12 in. or 24 in. for the ALDOTIS design at 4 or 5 ft total depth. Therefore, increasing the hydraulic conductivity of the infiltration swales topsoil layer is encouraged.

5. Large-scale testing also assessed maintenance needs associated with the infiltration swales. Surveys of the swale surfaces showed no indication of settling over time. With the modified swale providing higher hydraulic conductivity, the surface layer dries faster, reducing the chances of sod damage and compaction from mowing activities. Continued monitoring will be performed at the AU-SRF experimental swales to assess settling due to heavy equipment and mowing operations.

CHAPTER 2. SMALL AND INTERMEDIATE SCALE TESTING

The assessment of infiltration swale media performance in this research study was conducted through the systematic collection and analysis of data and observations. Multiple parameters were measured to evaluate the effectiveness of infiltration swale media, including permeability, infiltration rates under constant and falling water heads, settlement of materials, and moisture content. In this research, the following tests were designed and conducted to evaluate the water infiltration capacities of materials and infiltration swale media. In the small-scale phase, modified constant head permeability tests were conducted on the permeameter structure. Falling and constant head infiltration rate tests were performed using the clear infiltrometers. In the intermediate-scale phase, falling and constant head infiltration rate tests were conducted on the infiltration swale box. Construction and calibration of all these small- and intermediate-scale testing devices were detailed by Ramirez Florez (2024)

The small-scale phase of the project began with modified constant head permeability tests conducted in the permeameter apparatus. Samples of materials and infiltration swale media, representing the ALDOT and GDOT designs, underwent the modified constant head permeability test to determine their hydraulic conductivity. Additionally, fill sand samples at various degrees of compaction underwent this test for extended periods, specifically 9 hours, to investigate how density and the consolidation process impact their permeability.

In the next stage, the team initiated the implementation of falling head infiltration rate tests on a small-scale using clear infiltrometers. Initially, due to the low permeability observed in topsoil, this test was conducted on both topsoil and amended topsoil samples to identify a top layer mixture with improved infiltration rate capacities. Following this, alternative engineered media matrices, some derived from the ALDOT design with specific modifications, underwent evaluation through this test to identify designs with superior performance, which was called F3 design (with more information later).

Finally, infiltration media designs selected in the previous stages underwent testing under constant and falling head infiltration rates on a small-scale in the infiltrometers until the optimal F3 design was identified, which demonstrated an appropriate performance in the short and long term. Design F3 was then tested on an intermediate-scale alongside the ALDOT design in the infiltration swale chamber. Constant and falling head tests were conducted in the infiltration chamber. These two designs were simultaneously monitored by a moisture content monitoring system.

2.1 Porosity, Bulk Density, and Particle Size Distribution of Materials

Bulk density and porosity provide insights into the structure of a material, affecting its permeability. High bulk density and low porosity may suggest lower permeability. However, it is important to note that soil permeability is not solely determined by bulk density and the percentage of pores within the material; it is also influenced by the shape and inter-granular distribution of these pores (Elhakim 2016), as well as the intermolecular interactions

between particles that tend to adhere to each other (Kozlowski and Ludynia 2019). The materials used in this research were subjected to bulk density and porosity test and the results are shown in Table 2.1.

Table 2.1. Bulk Density and Porosity Tests Results.

Material	Bulk density	Porosity
Topsoil	1.35 g/cm^3	43%
#57 stone	1.44 g/cm^3	46%
Pea gravel	1.44 g/cm^3	41%
Fill sand	1.68 g/cm^3	33%
Pine Bark Fines	0.17 g/cm^3	73.5%

The materials used in this research were subjected to particle size distribution tests. Regarding the topsoil, and the #57 stone, these tests were useful to verify that they meet with the current ALDOT requirements. Figure 2.1 shows the particle size distribution curves of the topsoil, fill sand, pea gravel, and #57 stone.

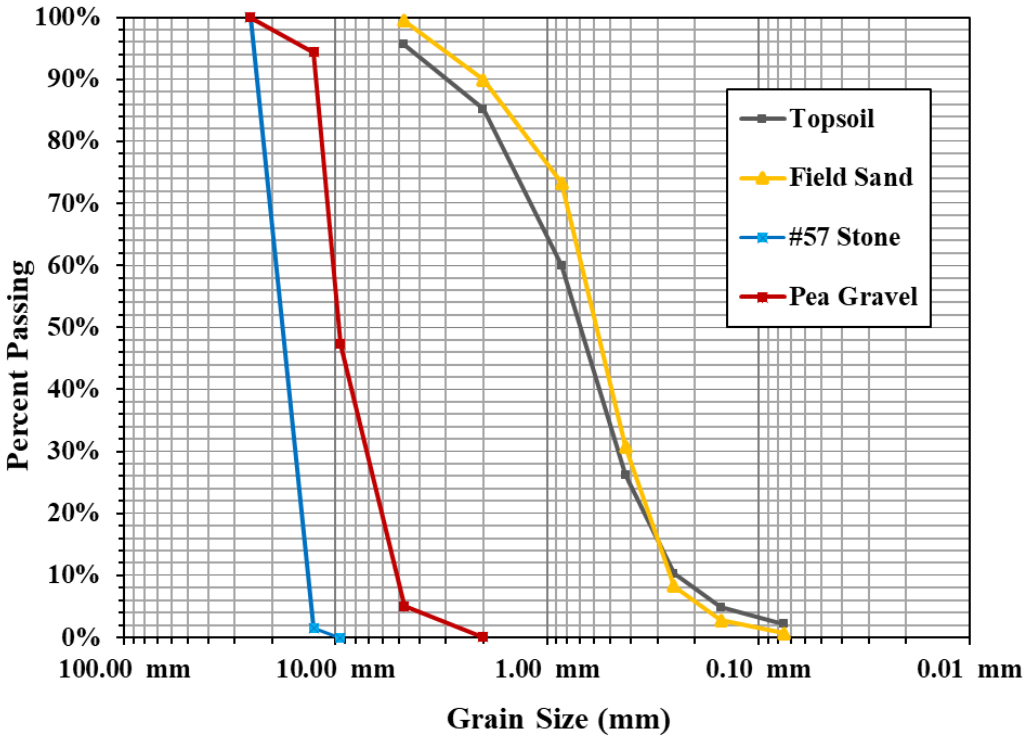

Figure 2.1 Particle Size Distribution Curves.

Topsoil, #57 stone, and pea gravel have similar bulk density and porosity (Table 2.1), but quite different particle size distributions (Figure 2.1) that resulted in quite different permeabilities (Table 2.2). The particle size distribution curves indicate that topsoil has finer particles and a

more well-graded size distribution than fill sand. This difference is one of the reasons why the topsoil exhibits lower permeability than fill sand (Table 2.2), despite having higher porosity.

ALDOT's topsoil (Section 650 (ALDOT 2022)) for highway construction follows ASTM D 5268 and has 2–20% by weight of organic material, 10–90% by weight of sand content (0.05–2 mm, from the Soil Science Society of America), and 10–90% by weight of silt (0.002–0.05 mm) and clay (< 0.002 mm) content, in portion of sample passing 10 (2 mm) Sieve. The sandy topsoil (Figure 1.1) used in this study has about 88% sand content and less than 2% silty content (Figure 2.1). It should also be noted that ALDOT does not have any specifications on sandy topsoil.

2.2 Modified Constant Head Permeability Tests

The modified constant head permeability test was first conducted on samples of topsoil, fill sand, and #57 stone—the current materials used in ALDOT's infiltration swale media design (Figure 1.1). In addition to the ALDOT's materials, the permeability of pea gravel was assessed with the aim of incorporating this material into alternative designs. Fill sand samples at different densities were tested over extended periods to evaluate the effects of density and consolidation on them. Finally, samples representing both ALDOT and Georgia DOT infiltration swale designs underwent this test to assess their hydraulic conductivity.

2.2.1 Permeability Tests On Infiltration Swale Materials.

Loose samples of topsoil, fill sand, #57 stone, and pea gravel were tested on the permeameters apparatus to know their permeability at 20 °C. The testing results obtained are shown in Table 2.2.

Table 2.2. Modified Permeability Constant Head Results.

Materials	Height of sample in. (cm)	Permeability, k, at 20 °C in./min (cm/min)
Topsoil	33 (83.82)	0.016 (0.04)
Fill sand	33 (83.82)	1.56 (3.96)
#57 stone	33 (83.82)	2,403 (6,104)
Pea gravel	33 (83.82)	215 (547)

According to results from the constant permeability tests, the critical and limiting layer on the current ALDOT design was determined to be topsoil because it has very low permeability that is about 100 times smaller than fill sand's permeability. Even the topsoil's permeability is higher than the minimum required infiltration rate specified in the LID Manual of Alabama (Dylewski et al. 2007), which is 1.0 ft/d (0.0083 in./min), the infiltration swale is seldom subject to a 2-ft (0.6 m) constant head of water. Based on ASTM D 5268, ALDOT's topsoil could have quite different particle size distributions in different project sites, e.g., 30% silt and clay and 60% sand. In comparison to the topsoil used for this study (Figure 2.1, ~88% sand), another topsoil can have quite different permeability, much smaller than 0.016

in./min (1.92 ft/d, Table 2.2), with more fine silt and clay. This may not be important for various highway construction projects, but smaller permeability is crucial to infiltration-based LIDs. Using topsoil with different permeabilities can result in quite variable performance of the infiltration swale to control the surface runoff and retain/store inflow.

2.2.2 PERMEABILITY TEST ON FILL SAND AT DIFFERENT DENSITIES.

The modified constant head permeability test was conducted on 11 fill sand samples, each 3.0 ft (0.91 m) in height (See Figure 2.2), at various degrees of compaction over a 9-hour period. The constant water head above the sand is 24 in. (78.7 cm). The degree of compaction represents the percentage of the sample's density compared to the optimum dry density obtained from the Proctor test for fill sand, which was 109.5 lb/ft^3 (1.75 g/cm^3).

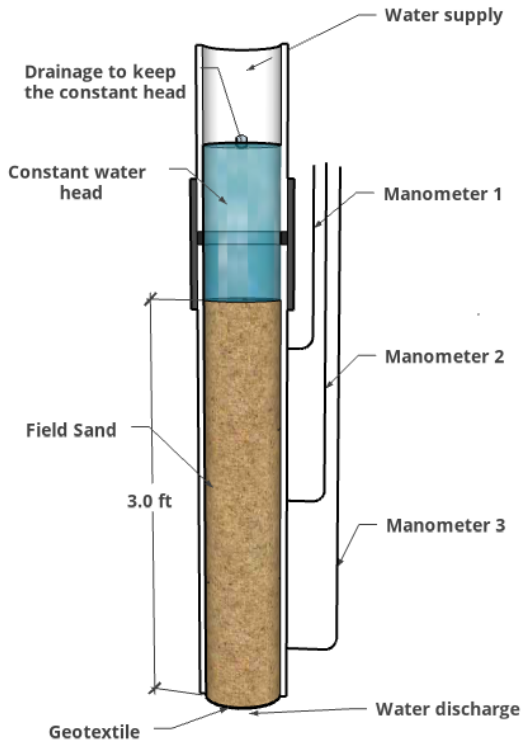

Figure 2.2. Layout Constant Head Permeability Test on Sand.

Hourly measurements were taken for water discharge, temperature, and water head in manometers 1 and 3 to calculate the permeability, *k*. A permeability vs. time curve was generated for each fill sand sample using the permeabilities calculated at each hour during the test. Table 2.3 shows the results obtained in the modified constant head permeability tests of fill sand samples.

Table 2.3. Fill sand Configuration and Permeability Results

Fill sand Sample	Final Density lb/ft³ (g/cm³)	Degree of compaction (%)	Initial k 20°C in./min (cm/min)	Final k 20°C in./min (cm/min)	Permeability Reduction (%)	Compaction method
S1	104.9 (1.68)	95.8	0.31 (0.79)	0.30 (0.77)	2.5	mechanical
S2	106.1 (1.70)	97.0	0.19 (0.48)	0.17 (0.44)	8.3	mechanical
S3	91.1 (1.46)	83.1	2.11 (5.35)	1.17 (2.98)	44.3	loose
S4	94.9 (1.52)	86.6	1.49 (3.68)	1.26 (3.19)	13.3	mechanical
S5	93.6 (1.50)	85.4	1.26 (3.20)	1.06 (2.69)	15.9	mechanical
S6	98.0 (1.57)	89.5	1.44 (3.65)	1.08 (2.74)	24.9	loose
S7	101.1 (1.62)	92.3	0.87 (2.22)	0.72 (1.84)	17.1	mechanical
S8	93.6 (1.50)	85.6	0.96 (2.43)	0.89 (2.25)	7.4	consolidated with water
S9	93.0 (1.49)	85.2	1.09 (2.77)	1.00 (2.54)	8.3	consolidated with water
S10	93.6 (1.50)	85.4	0.91 (2.30)	0.83 (2.11)	8.3	consolidated with water
S11	93.6 (1.50)	85.5	0.87 (2.22)	0.84 (2.14)	3.6	consolidated with water

Note: Initial permeability: permeability of the sample at the start of the test.
Final permeability = permeability at 9 hours after the start of the test.
Permeability reduction = reduction in permeability during the 9-hour test.

The graph of the permeability vs. time curves of the 11 fill sand samples obtained from the modified permeability tests are shown in Figure 2.3.

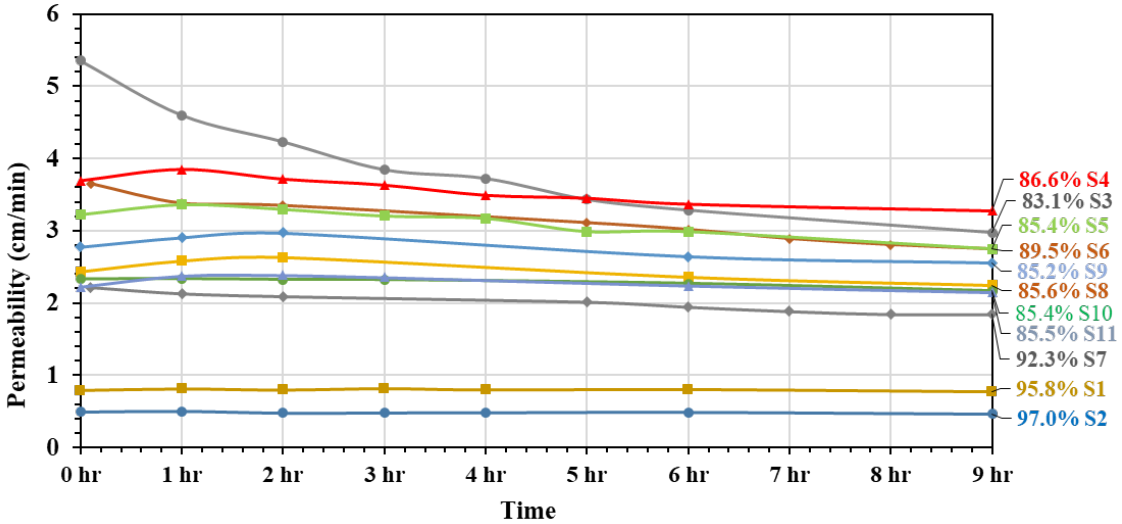

Note: Each curve is labeled with the degree of compaction of the sample followed by the sample's name. The degree of compaction represents the percentage of the sample's density compared to the optimum dry density.

Figure 2.3. Permeability vs. Time Curves – Fill sand Samples.

The prolonged modified constant head permeability test on fill sand samples at different degrees of compaction revealed that the final density of this material, when placed without any compaction and subjected to a flowing water column (Samples S8 to S11), is 85.5% of its optimum density. In the field, this material undergoes the same consolidation phenomenon due to ponding water or compaction phenomenon due to machine mowing. Consequently, if the sand is loosely installed without compaction, consolidation over time will lead this material to achieve a density of 85.5%. Therefore, in subsequent tests, this material was consolidated with water after being placed in the infiltrometers to attain the 85.5% degree of compaction, corresponding to 93.62 lb/ft^3 (1.50 g/cm^3).

At 9 hours of tests, the highest permeability of fill sand is 7.3 times larger than the lowest permeability in Figure 2.3. This variation is small compared to the variations in the field (Bjerg et al. 1992). However, the variations of fill sand's hydraulic conductivity or permeability have a very little effect on the soil-layer's hydraulic conductivity of ALDOTIS with topsoil and sand layers (Figure 1.1) since topsoil's permeability is much smaller than sand's permeability and controls the soil-layer's permeability.

The fill sand under 97% compaction has a permeability of 0.17 in./min or 20.4 ft/d after 9 hours of the constant head test is still 10 times larger than the permeability of the topsoil. Therefore, it is topsoil, not fill sand to limit the overall infiltration rate of the engineered media of the ALDOT infiltration design, which will be further approved in the next sets of tests (section 1.1.3). Typical bio-retention cells contain one homogenous layer of sand or other engineered media with high porosity and infiltration rate, for example, Jiang et al. (2019) tested ten different bio-retention media with the basic mixture of sand, soil, and wood chip plus other modifiers (flyash, green zeolite, and water treatment residual). These media should support plant growth, cost-effectiveness, local available to promote runoff and pollution control. A homogeneous topsoil or native soil layer (e.g., 1 or 2 ft [0.3 or 0.6 m] thickness) with low permeability is seldom used as a part of bioretention media.

2.2.3 72 HOURS - PERMEABILITY TEST ON FILL SAND.

Two fill sand samples, initially at densities of 88.1% and 91.8% of the optimum density, underwent a 72-hour modified constant head permeability test to evaluate the effects of consolidation on this material. The properties and permeability results are presented in Table 2.4.

Table 2.4. Fill sand Samples Properties Subjected to 72-hour Modified Permeability Test.

Material	Initial Bulk density lb/ft³ (g/cm³)	Optimum density lb/ft³ (g/cm³)	Initial degree of compaction	Final Bulk density lb/ft³ (g/cm³)	Final degree of compaction	Initial Perm. in./min (cm/min)	Final Perm. in./min (cm/min)
Fill sand	96.8 (1.55)	109.2 (1.75)	88.1%	98.0 (1.57)	89.5%	1.39 (3.53)	0.85 (2.15)
Fill sand	100.5 (1.61)	109.2 (1.75)	91.8%	101.1 (1.62)	92.3%	0.85 (2.17)	0.50 (1.28)

Figure 2.4 illustrates the permeability vs. time curves for the two fill sand samples during the 72-hour modified constant head test.

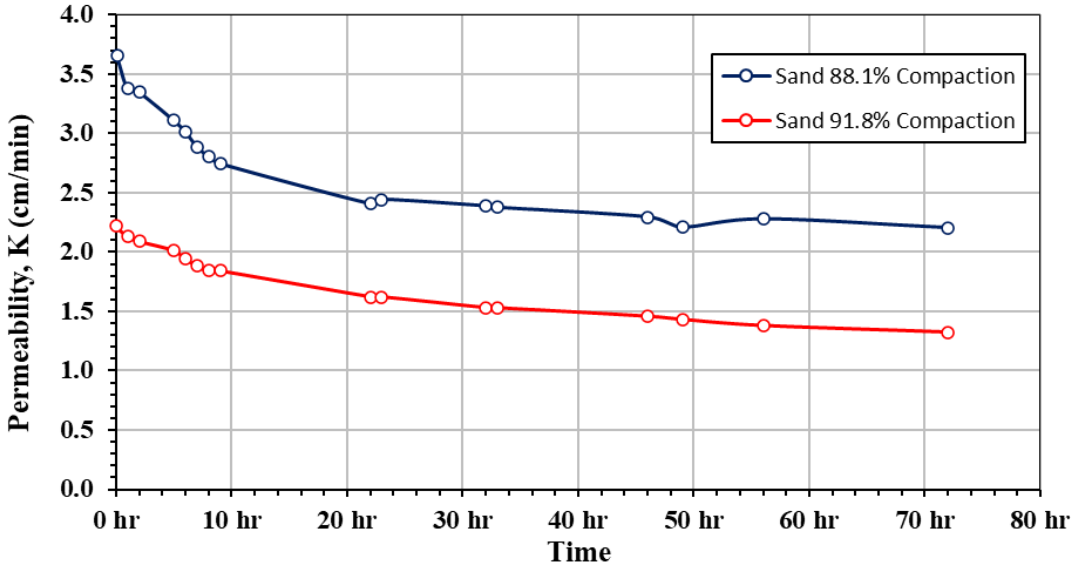

Figure 2.4. Permeability vs. Time Curves – 72-hour Test - Fill sand Samples.

The sample with 88.1% of the optimum density exhibited an initial permeability of 3.53 cm/min, and after 72 hours, its permeability decreased to 2.15 cm/min, representing a reduction of 39%. In terms of density, it changed from 88.1% to 89.5% of its optimum density. For the sample with 91.8% of the optimum density, the initial permeability was 2.17 cm/min, and after 72 hours, the permeability reduced to 1.28 cm/min, indicating a reduction of 41%. The density of this sample changed from 91.8% to 92.3%.

These tests show that after subjecting the materials to a water column for an extended period, the consolidation effects generated when a water column flows through the materials significantly reduce their infiltration capacities. In these two samples, it can be seen that, on average, the reduction was 40%, which is important when constructing infiltration swale media, as these field practices will

invariably be subjected to this phenomenon. However, these fill sand samples, after 72 hours of compaction, still have 30–50 times higher permeability than topsoil samples do.

2.2.4 PERMEABILITY TESTS ON ALDOT AND GDOT DESIGNS.

Five samples, representative of the ALDOTIS design alternatives, and two samples, representative of the GDOT infiltration swale design, underwent the modified constant head permeability test. The configuration of all seven samples with different thicknesses of three layers, along with the corresponding test results, is detailed in Table 2.5 (averaged with three replicate tests).

Table 2.5. Modified Permeability Tests Results – ALDOT and GDOT Designs.

Design	Topsoil layer height in. (cm)	Fill sand layer height in. (cm)	#57 stone layer height in. (cm)	Permeability, k (20 °C) in./min (cm/min)
ALDOT 1	9.4 (24)	14.2 (36)	9.4 (24)	0.019 (0.050)
ALDOT 2	11.8 (30)	12.6 (32)	8.7 (22)	0.015 (0.039)
ALDOT 3	8.3 (21)	16.5 (42)	7.9 (20)	0.013 (0.033)
ALDOT 4	8.3 (21)	16.5 (42)	8.3 (21)	0.004 (0.011)
ALDOT 5	10.6 (27)	15.0 (38)	7.5 (19)	0.002 (0.004)
GDOT 1	22.4 (57)	1.6 (4)	9.1 (23)	0.001 (0.002)
GDOT 2	22.0 (56)	2.4 (6)	8.7 (22)	0.002 (0.004)

The total depth of the engineered soil media is about 33 in. (84 cm) for the small-scale permeability tests. Water was added to the media to saturate soil layers and the permeability was measured under a steady outflow flow condition (Ramirez Florez 2024). These measured permeabilities give/represent the overall infiltration rate of the swale design. The #57 stone layer ranges from 9.4 in. (24 cm) to 7.5 in. (19 cm), allows water to pass through quickly, and does not limit the infiltration rate. The measured permeability of the first three ALDOT design alternatives is about the same as the measured permeability of 33 in. of topsoil (Table 2.2), which is greater than 0.00833 in./min (1.0 ft/d). One would expect the permeability of ALDOT 4 sample is about the same as ALDOT 3 sample and the permeability of ALDOT 5 sample is about the same as ALDOT 2 sample. However, the permeabilities of ALDOT 4 and 5 samples are much smaller (3 or 7 more times smaller) and much less than 1.0 ft/d. This could be contributed from topsoil's heterogeneity. In the field, one would expect topsoil's properties could vary more. Two GDOT designs that had much larger thickness of topsoil and less fill sand resulted in much smaller permeability (0.12–0.24 ft/d < 1.0 ft/d). The results of the modified permeability tests on the ALDOT and Georgia DOT designs confirmed again that the low permeability of topsoil is the limiting factor of the infiltration capability of the engineered media so that the top layer's permeability must be improved to enhance the infiltration performance of the media.

2.3 FALLING HEAD INFILTRATION RATE TEST IN PERMEAMETERS

The falling head infiltration rate tests were initially conducted in the permeameters apparatus. In the subsequent stage, they were performed in the clear infiltrometers to gain better insights into the interaction between materials and water, as well as the consolidation process. Topsoil samples, amended topsoil samples compound by a mixture of topsoil and pine bark fines, and six different infiltration swale media designs, including the current ALDOT design, were subjected to the falling head infiltration rate test.

2.3.1 TOPSOIL – FALLING HEAD INFILTRATION RATE TESTS.

Three similar loose topsoil samples, each 6 in. (15.24 cm) high, underwent three falling head infiltration rate tests using a water column of 2.0 ft (0.61 m). The results are presented in Table 2.6.

Table 2.6. Topsoil - Falling Head Infiltration Rate Tests Results.

Topsoil sample	Falling head test			Average	Overall Average ± STD
	Test 1	Test 2	Test 3		
Sample 1	0.76 ft/d (0.23 m/d)	0.35 ft/d (0.11 m/d)	0.27 ft/d (0.08 m/d)	0.46 ft/d (0.14 m/d)	0.63 ± 0.33ft/d (0.19 ± 0.10 m/d)
Sample 2	0.86 ft/d (0.26 m/d)	0.41 ft/d (0.12 m/d)	0.28 ft/d (0.09 m/d)	0.52 ft/d (0.16 m/d)	
Sample 3	1.39 ft/d (0.42 m/d)	0.94 ft/d (0.29 m/d)	0.39 ft/d (0.11 m/d)	0.91 ft/d (0.28 m/d)	

Note: STD stands for standard deviation from all the data used to determine overall average.

According to the results (except test 1 of sample 3), the topsoil exhibited an infiltration rate lower than the minimum requirement specified in the Alabama LID Manual (Dylewski et al. 2007), which is 1.0 ft/d (0.30 m/d). Additionally, it was observed that infiltration rate decreased during subsequent testing (28–36% decreases from Test 1 to Test 3), indicating consolidation may be occurring in the column.

2.3.2 TOPSOIL MIXED WITH PINE BARK FINES – FALLING HEAD INFILTRATION RATE TESTS.

To minimize consolidation of the topsoil layer, pine bark fines were added. Literature showed that incorporating porous material into the topsoil layer may enhance infiltration capacity, as demonstrated by Jiang et al. (2019). Pine bark fines selected for the column experiments were sourced from a commercially available product, Evergreen All-Purpose Top Soil (Lowes Item No. 648834). The material is also available in bulk, which was ultimately sourced for the full-scale testing experiments (Figure 2.5). Pine bark fines have much lower bulk density and much larger porosity in comparison to topsoil (Table 2.1). Twelve samples, each 6 in. (15.2 cm) in height, were prepared for falling head infiltration rate tests. Ten of these samples were composed of a mixture of topsoil and pine fine barks at different weight proportions, one

consisted of only topsoil, and another comprised solely of pine bark fines. Table 2.7 provides details on these samples and the infiltration rates obtained in the falling head tests.

(a) bulk order

(b) store bought

Figure 2.5. Pine Bark Fines

Table 2.7. Falling-Head Infiltration Rate Results.

Top layer sample composition		Infiltration rate ft/d (m/d)			
Topsoil % by weight	Pine bark fines % by weight	Test 1	Test 2	Test 3	Avg.
100	0	1.00 (0.30)	0.57 (0.17)	0.31(0.09)	0.63 (019)
95	5	0.87 (0.27)	0.55 (0.17)	0.87 (0.27)	0.76 (0.23)
93	7	0.96 (0.29)	1.67 (0.51)	0.03 (0.01)	0.89 (0.27)
90	10	0.92 (0.28)	0.87 (0.27)	1.63 (0.50)	1.14 (0.35)
85	15	1.50 (0.45)	2.32 (0.71)	3.29 (1.00)	2.37 (0.72)
80	20	5.70 (1.73)	3.40 (1.04)	7.70 (2.35)	5.60 (1.71)
75	25	14.3 (4.35)	17.0 (5.19)	21.3 (6.5)	17.5 (5.35)
70	30	12.9 (3.9)	30.6 (9.3)	35.1 (10.7)	26.2 (7.99)
60	40	45.0 (13.7)	15.7 (4.8)	16.3 (5.0)	25.6 (7.81)
50	50	222 (67.2)	411 (125)	320 (97.5)	318 (96.8)
25	75	262 (79.8)	320 (97.5)	411 (125)	331 (101)
0	100	2,160 (658)	1,440 (439)	1,920 (585)	1,840 (561)

In Figure 2.6, the infiltration rate curve is plotted against the percentage content of pine bark fines in the mixture.

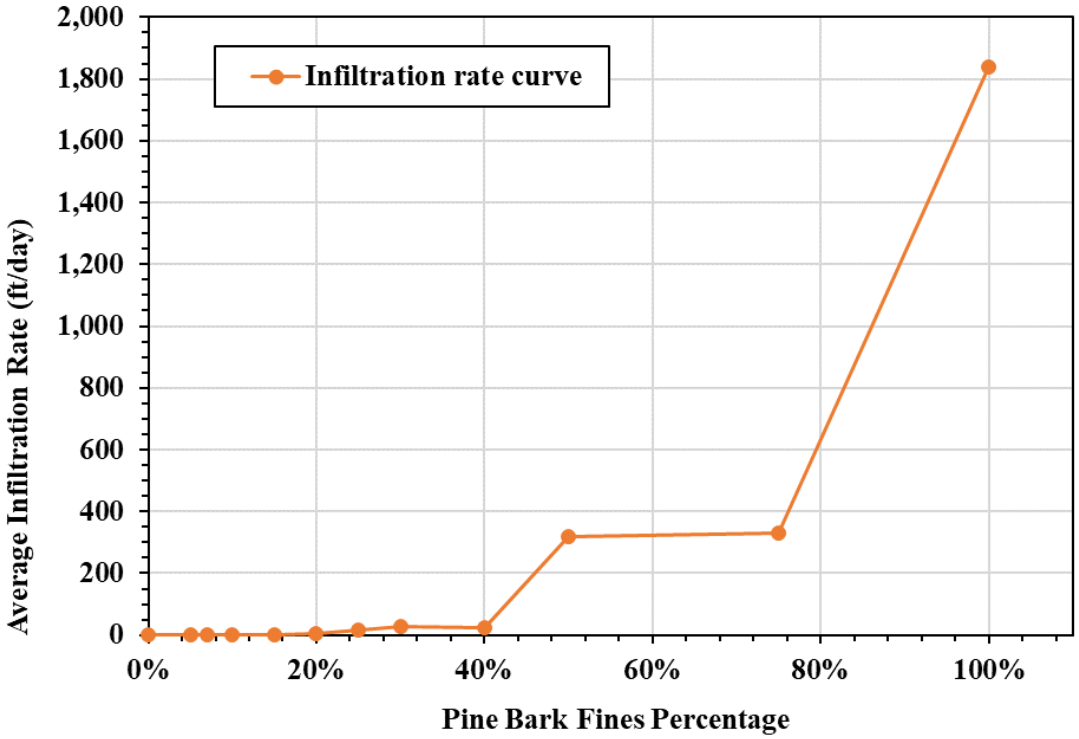

Figure 2.6. Average Infiltration Rate Vs. Pine Bark Fines Percentages by Weight

The results indicated that the higher the percentage of pine bark fines in the amended topsoil, the greater the infiltration rate of the mixture. Specifically, the amended topsoil design, composed of 80% topsoil and 20% pine bark fines by weight, demonstrated an average infiltration rate of 5.60 ft/d (1.71 m/d)—8.89 times higher than the infiltration rate obtained with topsoil alone, which was 0.63 ft/d (0.19 m/d). Consequently, this amended topsoil design was selected and integrated into some of the future alternative designs evaluated in this research due to its significant improvement in infiltration capacities compared to using a top layer composed entirely of 100% topsoil. From here out, every time amended topsoil is mentioned, it refers to the mixture composed of 20% pine bark fines and 80% topsoil by weight.

2.3.3 A, B, C, D, and E Designs – Falling Head Infiltration Rate Tests.

Three samples of each engineered media design were subjected to three falling head infiltration rate tests. Design A, the first representative prototype of the current ALDOT engineered media, consisted of a 10.0 in. (25.4 cm) topsoil layer, a 12.0 in. (30.5 cm) fill sand layer, and an 8.0 in. (20.3 cm) geotextile-wrapped #57 stone layer. Design B was similar to Sample A, with the only difference being the use of amended topsoil instead of 100% topsoil. Design C was comprised of a 6.0 in. (15.2 cm) amended topsoil layer, a 16.0 in. (40.6 cm) fill sand layer, and an 8.0 in. (20.2 cm) geotextile-wrapped #57 stone layer. Design D included a 6.0 in. (15.2 cm) amended topsoil layer, a 15 in. (38.1 cm) fill sand layer, a 1.0 in. (2.5 cm) pea

gravel layer, and an 8.0 in. (20.3 cm) #57 stone layer not wrapped in geotextile. Design E consisted of a 6.0 in. (15.2 cm) layer of amended topsoil, a 4.0 in. (10.2 cm) layer of pea gravel, and an 18.0 in. (45.7 cm) layer of #57 stone not wrapped in geotextile (See Figure 2.7). Table 2.8 summarizes the configuration of these samples.

Table 2.8. Designs A, B, C, D, and E Configuration.

Design	**Topsoil**	**Amended topsoil**	**Fill sand**	**Pea gravel**	**#57 stone**	**Geotextile wrapped #57 stone layer**
A	10 in. (25.4 cm)	-	12 in. (30.5 cm)	-	8 in. (20.3 cm)	Yes
B	-	10 in. (25.4 cm)	12 in. (30.5 cm)	-	8 in. (20.3 cm)	Yes
C	-	6 in. (15.2 cm)	16 in. (40.6 cm)	-	8 in. (20.3 cm)	Yes
D	-	6 in. (15.2 cm)	15 in. (38.1 cm)	1 in. (2.5 cm)	8 in. (20.3 cm)	No
E	-	6 in. (15.2 cm)	-	4 in. (10.2 cm)	18 in. (45.7 cm)	No
Layer compacted density lb/ft^3 (g/cm^3)	88.8 (1.42)	61.2 (0.98)	93.6 (1.50)	101.1 (1.62)	98.6 (1.58)	

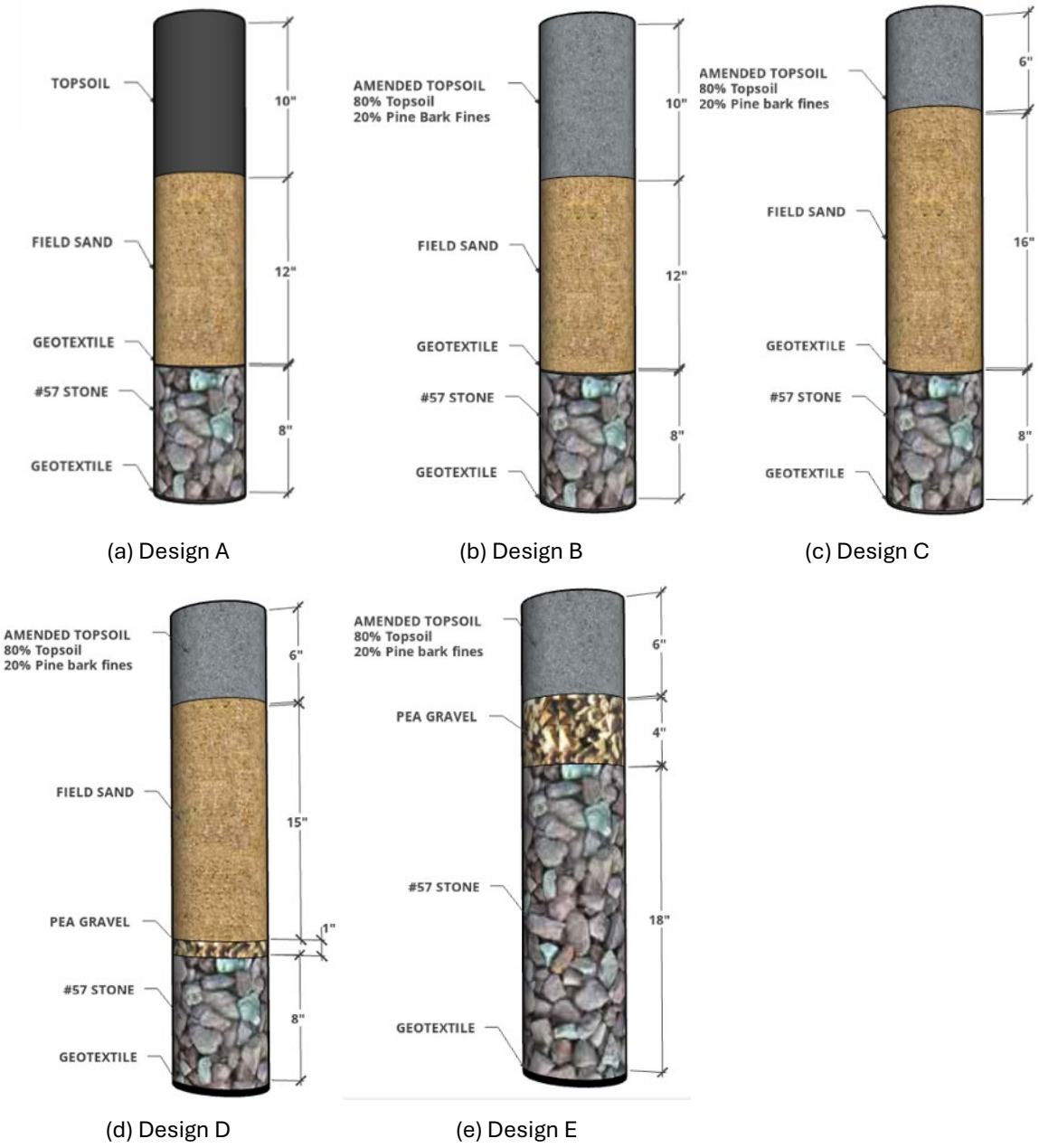

Figure 2.7. Designs A, B, C, D, and E Layout.

Table 2.9 summarizes the results of the three falling head infiltration rate tests conducted on each of the three samples representing Designs A, B, C, D, and E.

Table 2.9. Falling Head Infiltration Rate Results for Designs A, B, C, D, and E.

Design	Test 1	Test 2	Test 3	Avg.
A	0.33 ft/d (0.10 m/d)	0.30 ft/d (0.09 m/d)	0.29 ft/d (0.09 m/d)	0.31 ft/d (0.09 m/d)
B	0.99 ft/d (0.30 m/d)	2.24 ft/d (0.68 m/d)	3.51 ft/d (1.07 m/d)	2.25 ft/d (0.69 m/d)
C	1.13 ft/d (0.34 m/d)	1.33 ft/d (0.41 m/d)	1.50 ft/d (0.46 m/d)	1.32 ft/d (0.40 m/d)
D	0.98 ft/d (0.30 m/d)	0.93 ft/d (0.28 m/d)	0.86 ft/d (0.26 m/d)	0.92 ft/d (0.28 m/d)
E	1.27 ft/d (0.39 m/d)	1.85 ft/d (0.56 m/d)	1.68 ft/d (0.51 m/d)	1.60 ft/d (0.49 m/d)

The results of these tests were valuable in detecting that the average infiltration rate of Design B was 7.26 times higher than the infiltration rate of Design A, representing the current ALDOT design. This indicates that changing the topsoil to amended topsoil increased the infiltration capacity of the ALDOT design by 7.26 times, from 0.31 ft/d (0.09 m/d) to 2.25 ft/d (0.69 m/d), when subjected to three falling head infiltration rate tests.

Since fill sand has much larger permeability (Table 2.20, in theory, one would expect Design C to have a higher infiltration rate than Design B. However, the average measured infiltration rate of Design C is 58.7% lower than Design B, even though both averages are greater than 1.0 ft/d. This could be explained by topsoil and pine bark fines heterogeneity or variations of particle size distributions in those 10 in. or 6 in. of the mixture. In the field, due to soil heterogeneity and variable particle size distribution, one would expect the hydraulic conductivity or infiltration rate of topsoil in different project sites to have very large variability. Spatial variations of soil's saturated hydraulic conductivity have been studied for decades by many researchers (Gohardoust et al. 2017; Goyal et al. 2019; Zhang et al. 2020).

2.3.4 Constant and Falling Head Infiltration Rate Test in Clear Columns

From this point forward, all tested designs underwent three falling head infiltration rate tests and three constant head infiltration rate tests. Initially, for designs A-1G and F, falling head infiltration rate tests were conducted first, followed by constant head infiltration rate tests. However, the order of the tests was later reversed. All samples were initially subjected to constant head tests to simulate extended use, followed by three falling head infiltration rate tests to assess their long-term performance under falling head conditions.

2.3.5 A-1G and F Designs: Three Falling and Three Constant Infiltration Rate Tests.

Three samples of each of designs A-1G and F were subjected to three falling head infiltration rate tests followed by three constant head infiltration rate tests. Design A-1G, representing the ALDOT design with a subtle modification (See Figure 2.8[a]), had a geotextile layer installed over the #57 stone to separate it from the fill sand. At the bottom, stainless wire-mesh with apertures of 0.25 by 0.25 in. (0.64 by 0.64 cm) was used instead of a geotextile

layer. Omitting the geotextile layer at the bottom aimed to determine if it was causing a reduction in the infiltration rate.

In relation to Design F, tested in this phase (Figure 2.8[b]), it shared similarities with Design B but featured a 6.0 in. (15.2 cm) pea gravel layer between the fill sand and #57 stone, replacing the geotextile layer used in Design B. Additionally, stainless wire-mesh was employed at the bottom. The configuration of Design F comprised 10 in. (25.4 cm) of amended topsoil, 12 in. (30.5 cm) of fill sand, 6.0 in. (15.2 cm) of pea gravel, and 8.0 in. (20.3 cm) of #57 stone. Table 2.10 displays the materials comprising each design with their respective heights and densities, while Figure 2.8 illustrates their layout.

Table 2.10. Designs A-1G and F Configuration.

Design	Topsoil	Amended topsoil	Fill sand	Pea gravel	#57 stone	Geotextile
A-1G	10 in. (25.4 cm)		12 in. (30.5 cm)		8 in. (20.3 cm)	single layer separating fill sand from #57 stone
F		10 in. (25.4 cm)	12 in. (30.5 cm)	6 in. (15.2 cm)	8 in. (20.3 cm)	None
Layer compacted density lb/ft^3 (g/cm^3)	88.8 (1.42)	61.2 (0.98)	93.6 (1.50)	101.1 (1.62)	98.6 (1.58)	-

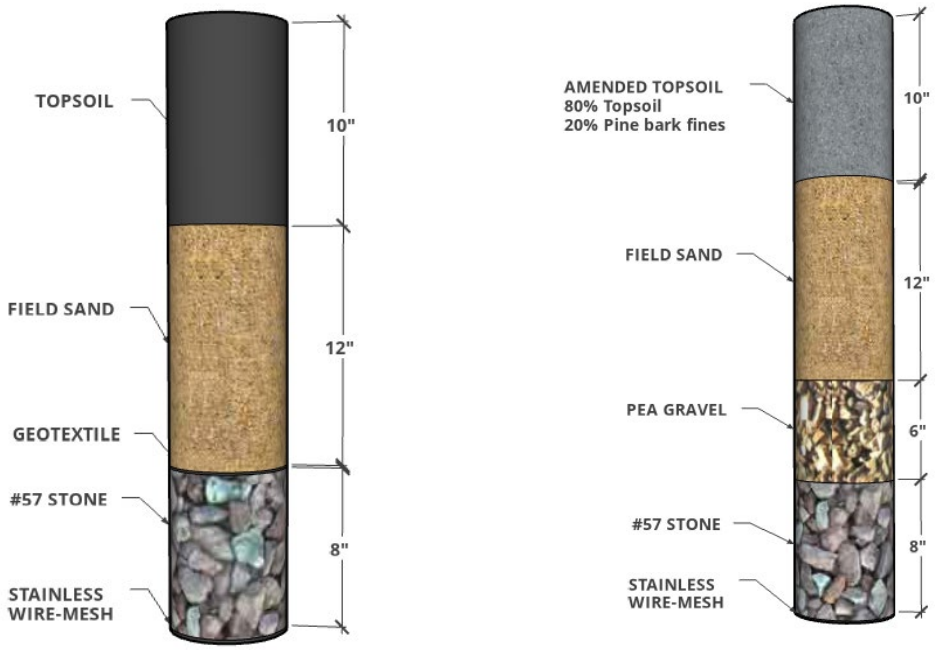

(a) A-1G design w/o bottom geotextile (b) F design

Figure 2.8. Designs A-1G and F Layout.

The results of the falling and constant head infiltration rate tests for Designs A-1G and F are presented in Table 2.11. They include average measured infiltration rates, their standard deviations, and minimum and maximum values from three repeated tests on each design under the falling and constant head testing. These results show variations in measured infiltration rates under repeated tests.

Table 2.11. Infiltration Rate Test Results for A-1G and F.

Design	Falling head infiltration rate (avg.)	Constant head infiltration rate (avg.)
A-1G	0.62 ± 0.27 ft/d (0.19 ± 0.08 m/d) (0.34, 1.18 ft/d) (0.10, 0.36 m/d)	0.46 ± 0.06 ft/d (0.14 ± 0.02 m/d) (0.40, 0.56 ft/d) (0.12, 0.17 m/d)
F	5.99 ± 2.72 ft/d (1.83 ± 0.83 m/d) (2.26, 11.08 ft/d) (0.69, 3.38 m/d)	7.66 ± 1.97 ft/d (2.33 ± 0.06m/d) (4.80, 9.45 ft/d) 1.46, 2.88 m/d

The results indicate that the removal of the geotextile layer at the bottom of the ALDOT design, as done in the A-1G design, doubles the infiltration rate under falling water head conditions, increasing from 0.31 ft/d to 0.62 ft/d. In the case of Design F, which closely resembled Design B except for replacing the geotextile above and below the #57 stone layer with a 6 in. (15.2 cm) pea gravel layer, the results demonstrate that this replacement leads to 2.66 times increase in the infiltration rate under falling water head conditions of the engineered media, increasing from 2.25 ft/d (0.69 m/d) to 5.99 ft/d (1.83 m/d). The constant head test showed that Design F yielded an infiltration rate of 7.66 ft/d (2.33 m/d), 16.6 times higher than Design A-1G.

2.3.6 F1 and F2 Designs: Constant and Falling Head Infiltration Rate Tests.

Three samples of each of Designs F1 and F2 (Figure 2.9) underwent three constant head infiltration rate tests followed by three falling head infiltration rate tests. Both Designs F1 and F2 consisted of the same material layers as Design F. However, these two designs were intended to investigate how a reduction in the height of the amended topsoil layer, coupled with an equivalent increment in the fill sand layer, would impact the infiltration rate of the engineered media.

The configuration of Design F1 included 6.0 in. (15.2 cm) of amended topsoil, 16.0 in. (40.6cm) of fill sand, 6.0 in. (15.2 cm) of pea gravel, and 7.0 in. (17.8 cm) of #57 stone (See Figure 2.9[a]). Similarly, Design F2 comprised 8.0 in. (20.3 cm) of amended topsoil, 14.0 in. (35.6 cm) of fill sand, 6.0 in. (15.2 cm) of pea gravel, and 7.0 in. (17.8 cm) of #57 stone (See Figure 2.9[b]). Table 2.12 provides a detailed breakdown of the materials comprising each design along with their respective heights and densities.

Table 2.12 Designs A-1G and F Configuration.

Design	Amended topsoil	Fill sand	Pea gravel	#57 stone
F1	6 in. (15.2 cm)	16 in. (40.6 cm)	6 in. (15.2 cm)	7 in. (17.8 cm)
F2	8 in. (20.3 cm)	14 in. (35.6 cm)	6 in. (15.2 cm)	7 in. (17.8 cm)
Layer compacted density lb/ft^3 (g/cm^3)	61.2 (0.98)	93.6 (1.50)	101.1 (1.62)	98.6 (1.58)

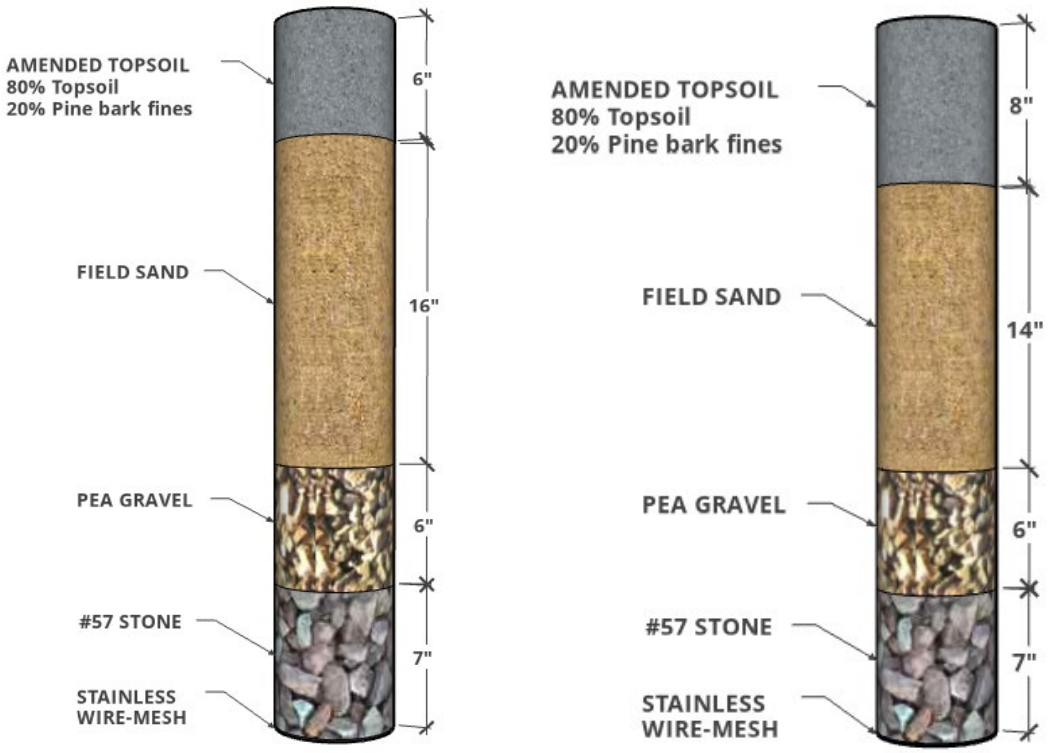

(a) Design F1 (b) Design F2

Figure 2.9. Design F1 and F2 Layout.

The results of the constant and falling head infiltration rates tests of Designs F1 and F2 are shown in Table 2.13.

Table 2.13. Constant and Falling Head Infiltration Rate Test Results for Designs F1 and F2.

Design	Constant head Avg.	Falling head Avg.
F1	4.75 ± 1.36 ft/d (1.45 ± 0.41 m/d) (3.32, 7.41ft/d) (1.01, 2.26 m/d)	1.11 ± 0.16 ft/d (0.34 ± 0.05m/d) (0.89, 1.35ft/d) (0.27, 0.41m/d)
F2	6.73 ± 1.39 ft/d (2.05 ± 0.43 m/d) (5.22, 8.82ft/d) (1.59, 2.69 m/d)	1.58 ± 0.38 ft/d (0.48 ± 0.12m/d) (1.17, 2.17ft/d) (0.36, 0.66m/d

The results indicated that Design F2 achieved an infiltration rate of 6.73 ft/d under constant head conditions and 1.58 ft/d under falling head conditions, which was 42% higher than the infiltration rate of Design F1 in both constant and falling head infiltration rate tests. However, when comparing the performance of Design F2 to that of Design F, it was observed that Design F yielded higher infiltration rates in both constant, 7.66 ft/d (2.33 m/d), and falling, 5.99 ft/d (1.83 m/d), head infiltration rate tests.

2.3.7 Settlement Tracking and Adjustment of Densities

The transparency of the infiltrometers allowed for a more precise monitoring of the settlement in each of the material layers composing the specimens (See Figure 2.10). This tracking was carried out during the constant head and falling head infiltration tests conducted on Designs A-1G, F, F1, and F2, mentioned in the preceding two subsections. Given that these specimens were not only subjected to three falling head infiltration tests, as previously done, but also to three constant head infiltration tests lasting 9 hours each, the consolidation effects resulted in increased settlement in the upper layer of the specimens, composed of topsoil or amended topsoil.

(a) topsoil after all tests (b) amended topsoil after all tests

Figure 2.10. Settlement Tracking of Samples After Being Subjected to Three Constant and Three Falling Head Infiltration Rate Tests.

After monitoring the settlement of the layers, the densities of the topsoil and amended topsoil were updated, as shown in Table 2.14.

Table 2.14. Densities of Topsoil and Amended Topsoil.

Material	Density before settlement tracking - lb/ft^3 (g/cm^3)	Updated Density: after settlement tracking - lb/ft^3 (g/cm^3)
Topsoil	88.6 (1.42)	96.8 (1.55)
Amended topsoil	61.2 (0.98)	68.7 (1.10)

2.3.8 A* AND B* DESIGNS: CONSTANT AND FALLING HEAD INFILTRATION RATE TESTS.

It was decided to retest Designs A and B, considering that the final density of the upper layer would be the compacted density mentioned in the previous subsection. The designs with the compacted density of the upper layer were named A* and B*. Table 2.15 provides a detailed breakdown of the materials comprising these designs along with their respective heights and densities. Figure 2.11 illustrates the layout of Designs A* and B*.

Table 2.15 Designs A* and B* Configuration.

Design	Topsoil	Amended topsoil	Fill sand	#57 stone	Geotextile wrapping #57 stone layer
A*	10 in. (25.4 cm)	-	12 in. (30.5 cm)	9.5 in. (24.1 cm)	Yes
B*	-	10 in. 25.4 cm)	12 in. (30.5 cm)	9.5 in. (24.1 cm)	Yes
Layer compacted density lb/ft^3 (g/cm^3)	96.8 (1.55)	68.7 (1.10)	93.6 (1.50)	98.6 (1.58)	-

(a) A* design, ALDOT Design considering final consolidation of topsoil

(b) Design B*, design B considering final consolidation of amended topsoil

Figure 2.11. Designs A* and B* Layout.

The results of the constant and falling head infiltration rates tests of Designs A* and B* are shown in Table 2.16.

Table 2.16. Constant and Falling Head Infiltration Rate Test Results for Designs A* and B*.

Design	Constant head – Avg.	Falling head– Avg.
A*	1.73 ± 0.45 ft/d (0.53 ± 0.14 m/d) (1.16, 2.31ft/d) (0.35, 0.71 m/d)	0.49 ± 0.31 ft/d (0.15 ± 0.09 m/d) (0.23, 1.28 ft/d) (0.07, 0.39 m/d)
B*	5.38 ± 1.23 ft/d (1.64 ± 0.38 m/d) (3.46, 7.69 ft/d) (1.05, 2.34 m/d)	1.10 ± 0.64 ft/d (0.24 ± 0.19m/d) (0.46, 2.25 ft/d) (0.14, 0.69m/d

The results of the constant head infiltration rate test showed that Design B* yielded 5.38 ft/d (1.64 m/d), which is 3.10 times higher than the infiltration rate of Design A*. In the falling head infiltration rate test, Design B* yielded 1.10 ft/d (0.30 m/d), representing a 2.24 times higher infiltration rate than Design A*.

2.3.9 F* AND F3 DESIGNS: CONSTANT AND FALLING HEAD INFILTRATION RATE TESTS.

Three samples of Design F* and three samples of Design F3 (Figure 2.12) were subjected to three constant head infiltration rate tests, followed by three falling head infiltration rate tests. Design F* is equivalent to the previously tested Design F, but with the updated density of the amended topsoil. Table 2.17 provides a detailed breakdown of the materials comprising these designs along with their respective heights and densities. Figure 2.12 illustrates the layout of Designs F* and F3.

Table 2.17 Designs F* and F3 Configuration.

Design	Amended topsoil	Fill sand	Pea gravel	#57 stone
F*	10 in. (25.4 cm)	12 in. (30.5)	6 in. (15.2 cm)	4 in. (10.2 cm)
F3	6 in. (15.2 cm)	10 in. (25.4 cm)	6 in. (15.2 cm)	9 in. (22.9 cm)
Layer compacted density lb/ft^3 (g/cm^3)	68.7 (1.10)	93.6 (1.50)	101.1 (1.62)	98.6 (1.58)

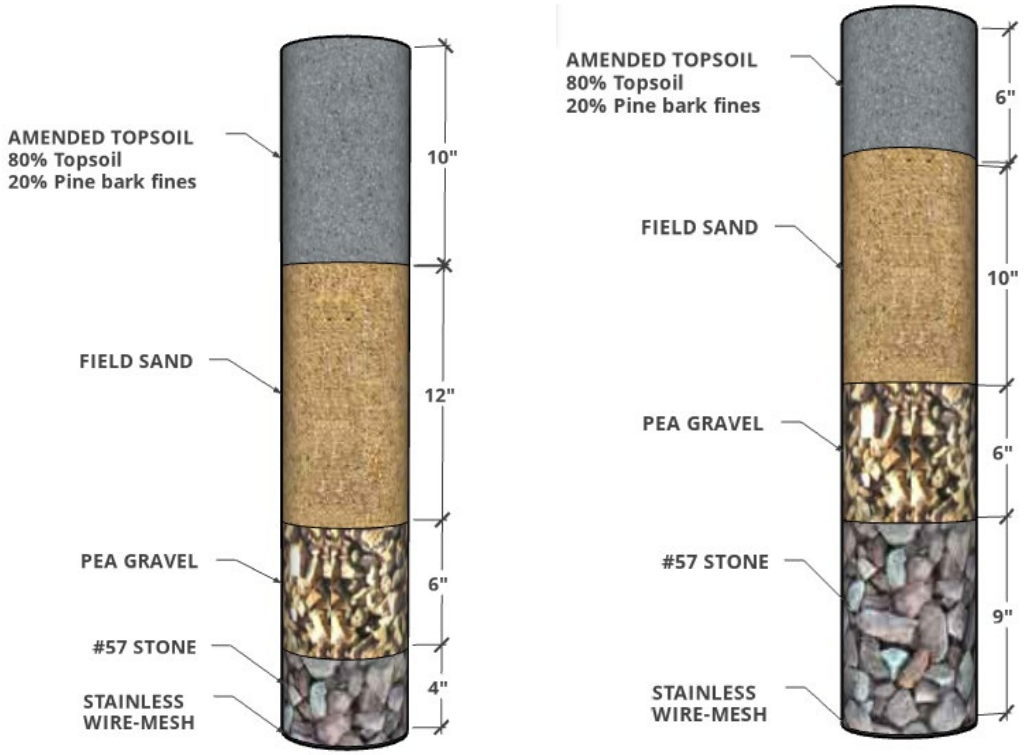

(a) F* design, sample F considering consolidation of amended topsoil

(b) Design F3

Figure 2.12. Designs F* and F3 Layout.

The results of the constant and falling head infiltration rates tests for Designs F* and F3 are shown in Table 2.18.

Table 2.18. Constant and Falling Head Infiltration Rate Test Results Designs F* and F3.

Design	Constant head test – Avg.	Falling head test –Avg.
F*	5.31 ± 0.76 ft/d (1.62 ± 0.23 m/d) (4.18, 6.43 ft/d) (1.27, 1.96 m/d)	1.26 ± 0.46 ft/d (0.38 ± 0.14 m/d) (0.73, 2.03 ft/d) (0.22, 0.62 m/d)
F3	5.75 ± 0.89 ft/d (1.75 ± 0.27 m/d) (4.52, 7.48 ft/d) (1.38, 2.28 m/d)	2.24 ± 0.31 ft/d (0.68 ± 0.09m/d) (1.94, 2.98 ft/d) (0.59, 0.91m/d

The results of the constant head infiltration rate tests showed that Design F3 yielded 5.75 ft/d (1.75 m/d), 1.08 times more infiltration rate than Design F*. In the falling head infiltration rate tests, Design F3 yielded 2.24 ft/d (0.68 m/d), 1.78 times more infiltration rate than design F*. The F3 design exhibited the best performance in the infiltration tests under constant and falling head conditions. For this reason, in the upcoming tests using the clear infiltrometers, Design F3 and A*, representing the ALDOT Design considering final consolidation, were tested with Bermuda grass sod placed over them for comparison.

2.3.10 ALDOT + Grass and F3 + Grass Designs: Constant and Falling Head Infiltration Rate Tests.

Three samples of ALDOT + Grass Design, and three samples of F3 + Grass Design were subjected to three constant head infiltration rate tests, and then to three falling head infiltration rate tests. Table 2.19 provides a detailed breakdown of the materials comprising these designs along with their respective heights and densities. Figure 2.13 illustrates the layout of Designs F* and F3.

Table 2.19. Designs ALDOT + Grass and F3 + Grass Configuration.

Design	Bermuda grass	Topsoil	Amended topsoil	Fill sand	Pea gravel	#57 stone	Geotextile wrapped #57 stone layer
ALDOT + Grass	Yes	10 in. (25.4 cm)		12 in. (30.48 cm)		9.5 in. (24.1 cm)	Yes
F3 + Grass	Yes		6 in. (15.2 cm)	10 in. (25.4 cm)	6 in. (15.2 cm)	9 in. (22.9 cm)	No
Layer compacted density - lb/ft^3 (g/cm^3)		96.7 (1.55)	68.7 (1.10)	93.6 (1.50)	101.1 (1.62)	98.6 (1.58)	

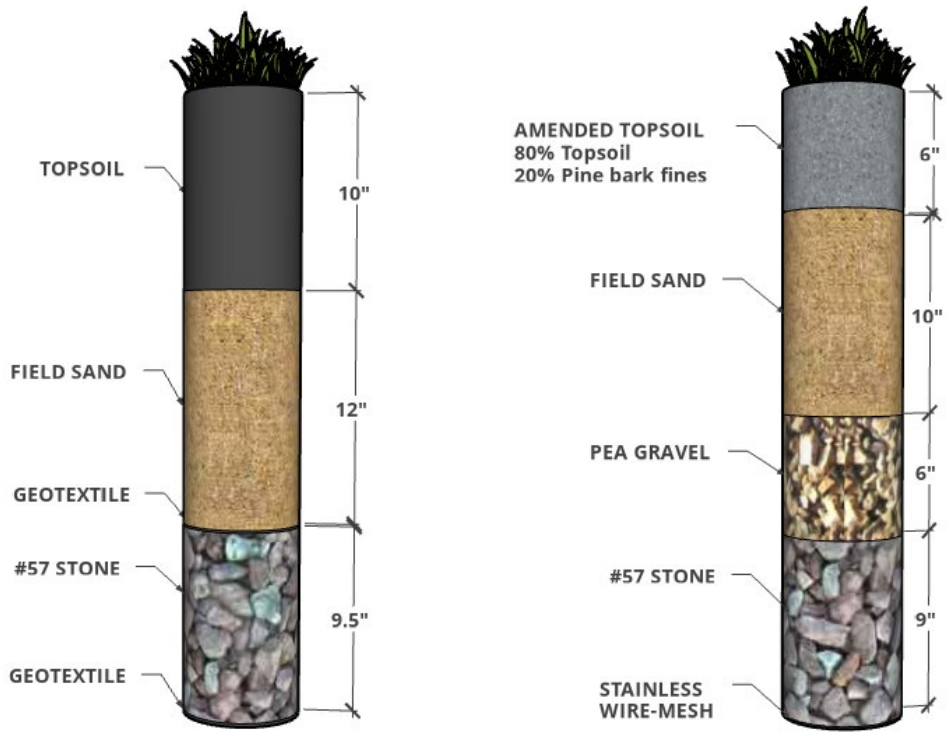

(a) ALDOT + Grass Design (b) F3 + Grass Design

Figure 2.13. ALDOT + Grass and F3 + Grass Layout.

The results of the constant and falling head infiltration rates tests of the ALDOT + Grass and F3 + Grass Designs are shown in Table 2.20.

Table 2.20. Infiltration Rate Test Results for ALDOT + Grass and F3 + Grass Designs.

Design	Constant head – Avg.	Falling head– Avg.
ALDOT + Grass	00.91 ± 0.08 ft/d (0.28 ± 0.02 m/d) (0.79, 1.04 ft/d) (0.24, 0.32 m/d)	0.31 ± 0.07 ft/d (0.01 ± 0.02 m/d) (0.24, 0.43 ft/d) (0.07, 0.13 m/d)
F3 + Grass	13.73 ± 4.78 ft/d (4.18 ± 1.46 m/d) (7.48, 21.31 ft/d) (2.28, 6.49 m/d)	11.66 ± 5.69 ft/d (3.55 ± 1.73 m/d) (3.52, 24.25 ft/d) (1.07, 7.39 m/d
Ratio of Average:	15.1	37.6

The results of the constant head infiltration rate test showed that Design F3 + Grass yielded 13.73 ft/d (4.18 m/d), 15.09 times more infiltration rate than ALDOT + Grass Design, which was reduced to 0.91 ft/d from 1.73 ft/d without grass (Table 2.16). In the falling head infiltration rate test the Design F3 + Grass yielded 11.66 ft/d (3.55 m/d), 37.61 times more infiltration rate than ALDOT + Grass Design, which was reduced to 0.31 ft/d from 0.49 ft/d without grass (Table 2.16).

Comparing the performance of the F3 + Grass design with its counterpart, F3, which does not include grass, it was observed that the performance of the F3 + Grass design was 2.39 times higher in constant head infiltration tests and 5.21 times higher in falling head tests (See Table 2.21). Therefore, with grass, ALDOT design reduced the infiltration rates by 53%-

63% for the constant and falling head tests; however, F3 design with grass performed much better with 2–5 times of increase in infiltration rates (Table 2.21).

Table 2.21. Comparison of Results Between F3 + Grass and F3

Design	Constant head – Avg.	Falling head– Avg.
F3 + Grass	13.73 ± 4.78 ft/d (4.18 ± 1.46 m/d) (7.48, 21.31 ft/d) (2.28, 6.49 m/d)	11.66 ± 5.69 ft/d (3.55 ± 1.73 m/d) (3.52, 24.25 ft/d) (1.07, 7.39 m/d
F3	5.75 ± 0.89 ft/d (1.75 ± 0.27 m/d) (4.52, 7.48 ft/d) (1.38, 2.28 m/d)	2.24 ± 0.31 ft/d (0.68 ± 0.09m/d) (1.94, 2.98 ft/d) (0.59, 0.91m/d
Ratio:	2.4	5.2

The reason for the higher infiltration rate of Design F3 + Grass is that in F3 Design without Grass, the pine bark fines particles located in the superficial layer of the amended topsoil separate from it and start to float (See Figure 2.14) in the water during the tests. This happens because they are less dense than water and lack a confining layer like Bermuda Grass. The separation of these pine bark fines creates zones with higher topsoil density within the amended topsoil layer, causing a reduction in the infiltration rate of the specimen. In the case of the F3 + Grass design, the layer of Bermuda grass installed over the specimen prevents the separation of the pine bark fines from the amended topsoil, keeping the mixture unchanged, which does not affect its infiltration rate.

Figure 2.14. Pine Bark Fines Floating During Tests on F3 Designs.

2.4 INFILTRATION SWALE CHAMBER EXPERIMENTS

In the intermediate-scale phase of the project the Design F3, obtained in the previous phase, and ALDOT Design were subjected to constant and falling head infiltration rate tests in the infiltration swale chamber.

2.4.1 ALDOT Design: Constant and Falling Head Infiltration Rate Tests.

The ALDOT design was placed into the infiltration swale chamber as shown Figure 2.15. It was subjected to nine constant head infiltration rate tests, and one falling head infiltration rate test. The original experimental test design for the constant head infiltration rate test contemplated a test duration of 6 hours. However, after the first test, the AU stormwater team decided to extend the test duration to 8 hours to collect more data, allowing for a better comprehension of the sample's performance.

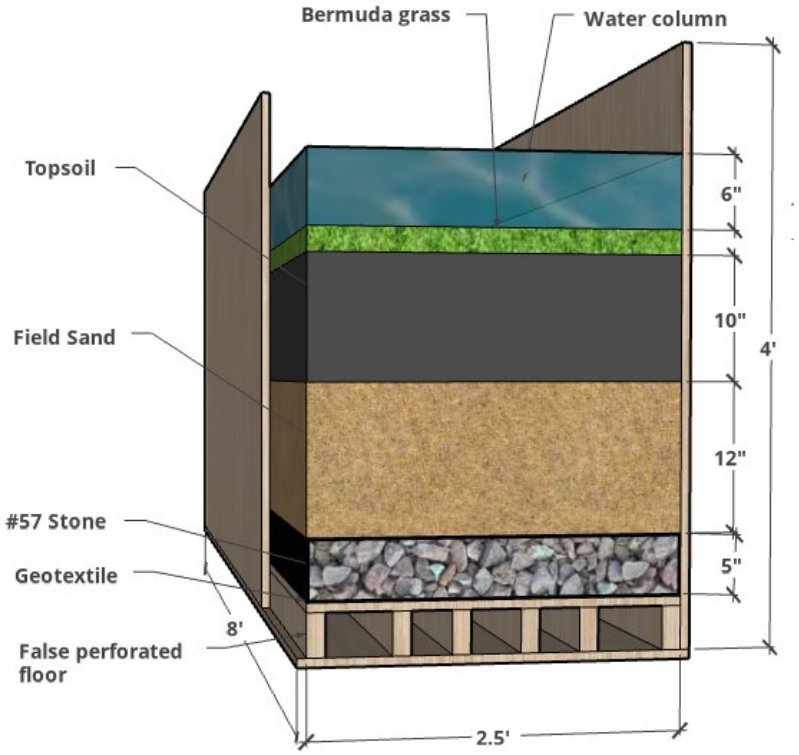

Figure 2.15. ALDOT Design Layout – Infiltration Swale Chamber

The results of the nine constant head infiltration rate tests conducted on the ALDOT Design are shown in Table 2.22.

Table 2.22. Results of Constant Head tests of ALDOT Design in Infiltration Swale Chamber.

	Infiltration rate - ft/d (m/d)								
Test	**1 hr**	**2 hr**	**3 hr**	**4 hr**	**5 hr**	**6 hr**	**7 hr**	**8 hr**	**Avg.**
1	9.15 (2.79)	9.76 (2.97)	9.76 (2.97)	10.07 (3.07)	10.07 (3.07)	10.30 (3.14)	N/A (N/A)	N/A (N/A)	9.85 (3.00)
2	4.58 (1.40)	6.41 (1.95)	6.29 (1.92)	8.54 (2.60)	8.09 (2.47)	8.34 (2.54)	8.37 (2.55)	8.39 (2.56)	7.38 (2.25)
3	4.22 (1.29)	5.90 (1.80)	6.23 (1.90)	6.23 (1.90)	6.59 (2.01)	6.64 (2.02)	6.76 (2.06)	7.63 (2.33)	6.27 (1.91)
4	4.58 (1.40)	5.19 (1.58)	5.85 (1.78)	6.41 (1.95)	6.36 (1.94)	5.49 (1.67)	5.77 (1.76)	5.82 (1.77)	5.68 (1.73)
5	3.97 (1.21)	5.72 (1.74)	6.05 (1.84)	6.08 (1.85)	6.25 (1.91)	6.76 (2.06)	6.76 (2.06)	6.92 (2.11)	5.81 (1.77)
6	4.58 (1.40)	5.85 (1.78)	6.01 (1.83)	6.15 (1.87)	6.66 (2.03)	6.56 (2.00)	6.66 (2.03)	6.64 (2.02)	6.14 (1.87)
7	4.63 (1.41)	5.64 (1.72)	5.92 (1.80)	6.08 (1.85)	6.23 (1.90)	6.28 (1.91)	6.43 (1.96)	6.28 (1.91)	5.94 (1.81)
8	6.20 (1.89)	5.64 (1.72)	5.92 (1.80)	6.08 (1.85)	6.08 (1.85)	6.13 (1.87)	6.25 (1.91)	6.28 (1.91)	6.07 (1.85)
9	3.64 (1.11)	5.19 (1.58)	5.57 (1.70)	5.72 (1.74)	5.57 (1.70)	5.72 (1.74)	6.33 (1.93)	6.20 (1.89)	5.49 (1.67)
Overall Average									6.51 (1.98)

The infiltration rate in the falling head infiltration rate test yielded by ALDOT Design in the infiltration swale chamber was 4.96 ft/d (1.51 m/d).

2.4.2 F3 Design: Constant and Falling Head Infiltration Rate Tests.

The F3 design (See Figure 2.16) underwent six constant head infiltration rate tests and one falling head infiltration rate test. The decision to conduct three fewer constant head infiltration rate tests compared to those performed on the ALDOT Design was due to the absence of a reduction in the infiltration rate after each test. This was in contrast to the ALDOT Design, where the infiltration rate decreased from the first to the fourth test.

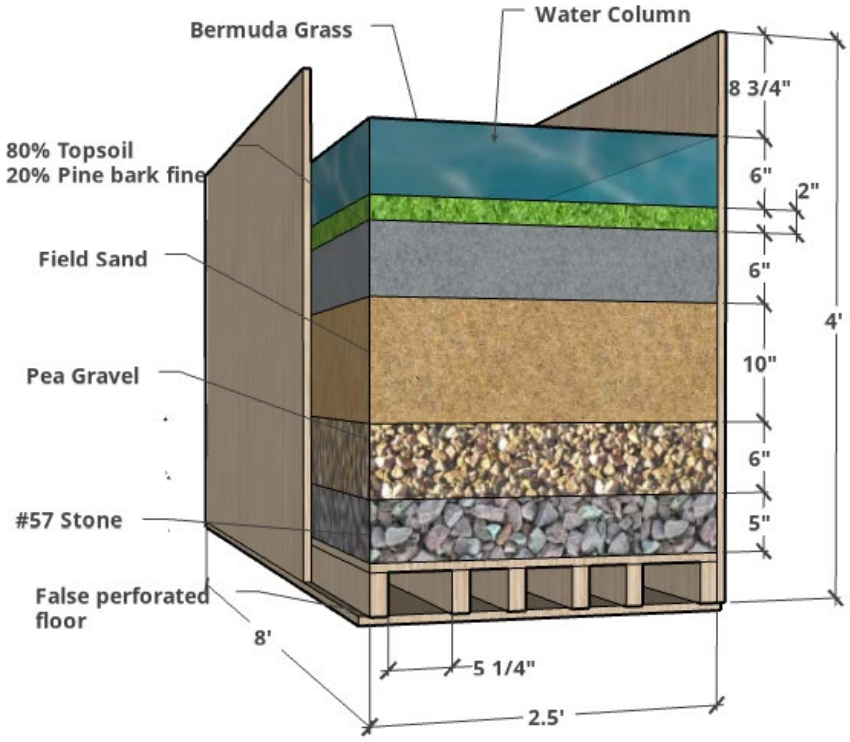

Figure 2.16. F3 Design Layout - Infiltration Swale Chamber.

The results of the six constant head infiltration rate tests conducted on the F3 Design are shown in Table 2.23.

Table 2.23. Results of Constant Head Tests of F3 Design in Infiltration Swale Chamber.

	Infiltration rate – ft/d (m/d)								
Test	**1 hr**	**2 hr**	**3 hr**	**4 hr**	**5 hr**	**6 hr**	**7 hr**	**8 hr**	**Avg.**
1	99.14 (30.22)	93.28 (28.43)	88.02 (26.83)	82.01 (25.00)	77.36 (23.58)	75.97 (23.16)	74.12 (22.59)	69.83 (21.28)	82.47 (25.14)
2	104.85 (31.96)	93.99 (28.65)	86.76 (26.44)	81.78 (24.93)	75.48 (23.01)	74.01 (22.56)	73.08 (22.27)	57.00 (17.37)	80.87 (24.65)
3	86.41 (26.34)	91.88 (28.01)	93.00 (28.35)	81.95 (24.98)	78.73 (24.00)	74.74 (22.78)	73.72 (22.47)	73.35 (22.36)	81.72 (24.91)
4	103.58 (31.57)	104.50 (31.85)	97.61 (29.75)	91.68 (27.94)	83.98 (25.60)	80.31 (24.48)	79.22 (24.15)	77.23 (23.54)	89.76 (27.36)
5	111.69 (34.04)	108.08 (32.94)	99.27 (30.26)	102.15 (31.14)	98.97 (30.17)	95.53 (29.12)	88.31 (26.92)	83.11 (25.33)	98.39 (29.99)
6	104.73 (31.92)	96.52 (29.42)	92.01 (28.04)	86.72 (26.43)	85.02 (25.91)	84.32 (25.70)	82.98 (25.29)	80.83 (24.64)	89.14 (27.17)
Overall Average									87.06 (25.54)

The infiltration rate in the falling head infiltration rate test yielded by F3 Design in the infiltration swale chamber was 75.79 ft/d (23.10 m/d).

2.4.3 COMPARISON OF RESULTS

Table 2.24 presents the outcomes of constant and falling head infiltration tests conducted on the ALDOT Design and the F3 Design in the infiltration swale chamber, along with the ratio between both.

Table 2.24. Comparison of Results of ALDOT and F3 Design in the Infiltration Swale Chamber

Design	Constant head – Avg.	Falling head – Avg.
ALDOT (Chamber)	6.51 ft/d (1.98 m/d)	4.96 ft/d (1.51 m/d)
F3 (Chamber)	87.06 ft/d (26.54 m/d)	75.79 ft/d (23.10 m/d)
Ratio: $\frac{F3\ Rate\ (Chamber)}{ALDOT\ Rate\ (Chamber)}$	13.37	15.28

Table 2.25 displays the ratio between the performance obtained by the F3 Design and the ALDOT Design in the infiltrometers and in the infiltration swale chamber during the constant and falling head infiltration tests.

Table 2.25. Comparison of Ratios Between the Results of F3 and ALDOT Designs Obtained in the Infiltrometers and in the Infiltration Swale Chamber.

	Ratio	Constant head – Avg.	Falling head – Avg.
Infiltrometers	$\frac{F3 + Grass\ Rate}{ALDOT + grass\ Rate}$	15.09	37.61
Infiltration swale chamber	$\frac{F3\ Rate}{ALDOT\ Rate}$	13.37	15.28

Table 2.26 displays the ratio between the performance obtained by F3 Design (tested in the infiltration chamber) and F3 + Grass Design (tested in the infiltrometers) and the ratio between the performance obtained by ALDOT Design (tested in the infiltration chamber) and ALDOT + Grass Design (tested in the infiltrometers).

Table 2.26. Comparison between Infiltration Chamber and Infiltrometers.

Ratio	Constant head – Avg.	Falling head – Avg.
$\frac{F3\ Rate\ (Infiltration\ chamber)}{F3 + Grass\ Rate\ (Infiltrometers)}$	$\frac{87.06\ ft/day}{13.73\ ft/day} = 6.3$	$\frac{75.79\ ft/day}{11.66\ ft/day} = 6.5$
$\frac{ALDOT\ Rate\ (Infiltration\ chamber)}{ALDOT + Grass\ Rate\ (Infiltrometers)}$	$\frac{6.51\ ft/day}{0.91\ ft/day} = 7.2$	$\frac{4.96\ ft/day}{0.31\ ft/day} = 16.0$

2.4.4 MOISTURE CONTENT ANALYSIS CONSIDERING EACH SENSOR SEPARATELY

A water volume content monitoring system was used to monitor the tests conducted in the infiltration swale chamber. Six sensors were installed in both the ALDOT Design and F3 Design. Three sensors were positioned in the top layer of the sample, halfway up the layer's

height, along the central longitudinal axis, spaced 2.0 ft (0.61 m). apart from center to center. The other three sensors were installed in the fill sand layer in the same manner. The distribution and position of the sensors on the ALDOT and F3 Designs are depicted in Figure 2.17 .

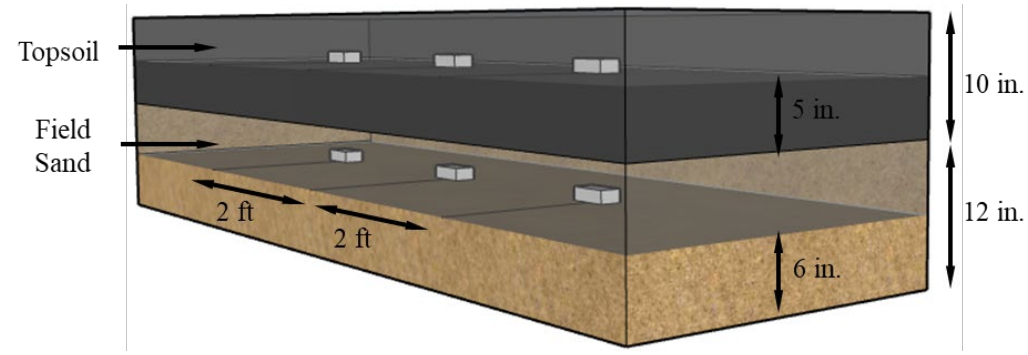

(a) Water content sensor distribution ALDOT Design.

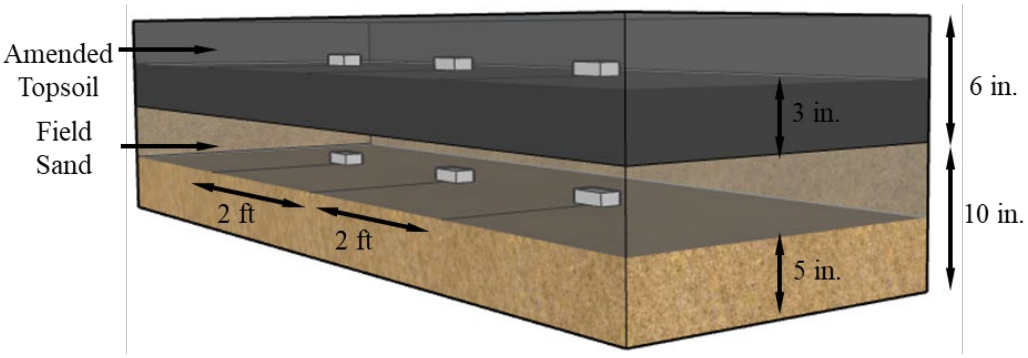

(b) Water content sensor distribution F3 Design.

Figure 2.17. Distribution of Sensors in ALDOT and F3 Designs.

Figure 2.18 illustrates the water volume content vs. time curves during the second constant head test conducted on the ALDOT design. The test began at hour 1 when water was introduced through the irrigation system. Subsequently, at hour 9, the water supply was stopped, concluding the test. Importantly, it should be noted that five days prior to this test, the ALDOT design underwent its first constant head test.

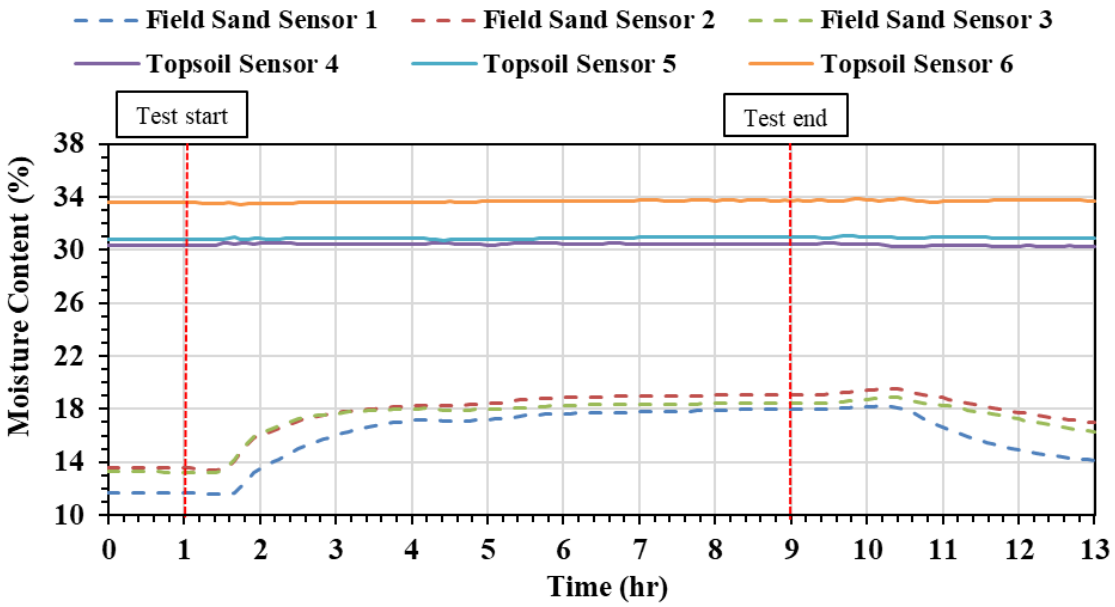

Figure 2.18. Moisture Content – ALDOT Design – Constant Head Test 2.

In this graph, it can be observed that the moisture content in the topsoil remains almost constant. This indicates that the topsoil has remained saturated since the last test, which occurred 5 days earlier. The information gathered from the sensors in the fill sand layer revealed a response 25 minutes after the test's commencement. Furthermore, the moisture content in the sand layer started to decrease 90 minutes after the test concluded.

Following the approach taken with the ALDOT design, the constant head infiltration rate test for the F3 design extended for 8 hours. Figure 2.19 depicts the curves of water volume content vs. time during constant head test 2 conducted on the F3 design. The test commenced in hour 1 with the initiation of water supply through the irrigation system. The test concluded at hour 9, 8 hours after the start, when the water supply was stopped. It is worth noting that, one day before this test, the F3 design underwent its initial constant head test.

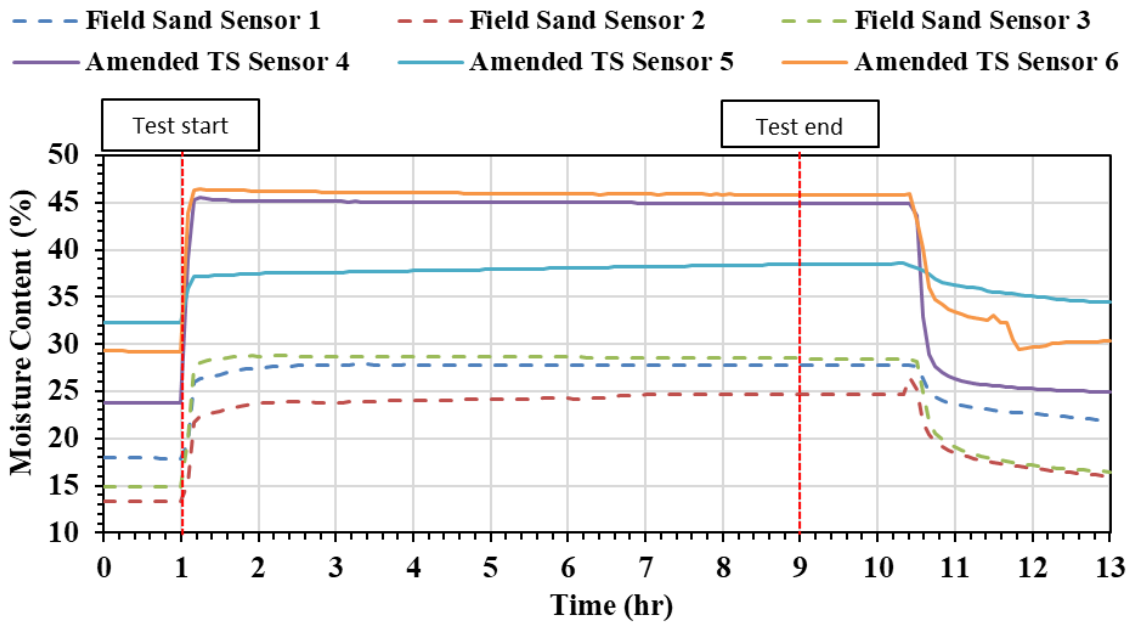

Figure 2.19. Moisture Content – F3 design – Constant Head Test 2.

The results indicated that the sensors in the amended topsoil and the fill sand of the F3 Design exhibited faster reactions than the sensors in the topsoil and the fill sand of the ALDOT Design. Furthermore, the moisture content achieved by the amended topsoil and the fill sand of the F3 design was higher than the moisture content attained by the topsoil and the fill sand of the ALDOT design. Regarding the drying process in the F3 Design, it was observed that this process commenced approximately 90 minutes after closing the irrigation system, and the moisture content in the amended and fill sand layer decreased more rapidly than the moisture content in the topsoil and the fill sand layer of the ALDOT Design.

2.4.5 Moisture Content Analysis Considering the Average of Each Layer.

In the ALDOT Design, the readings recorded by the three water volumetric content sensors installed in the topsoil were averaged, and the same was done with the readings from the three sensors installed in the fill sand. With these averages, a curve of water volume content vs. time was created for each layer during the nine constant head infiltration tests (See Figure 2.20).

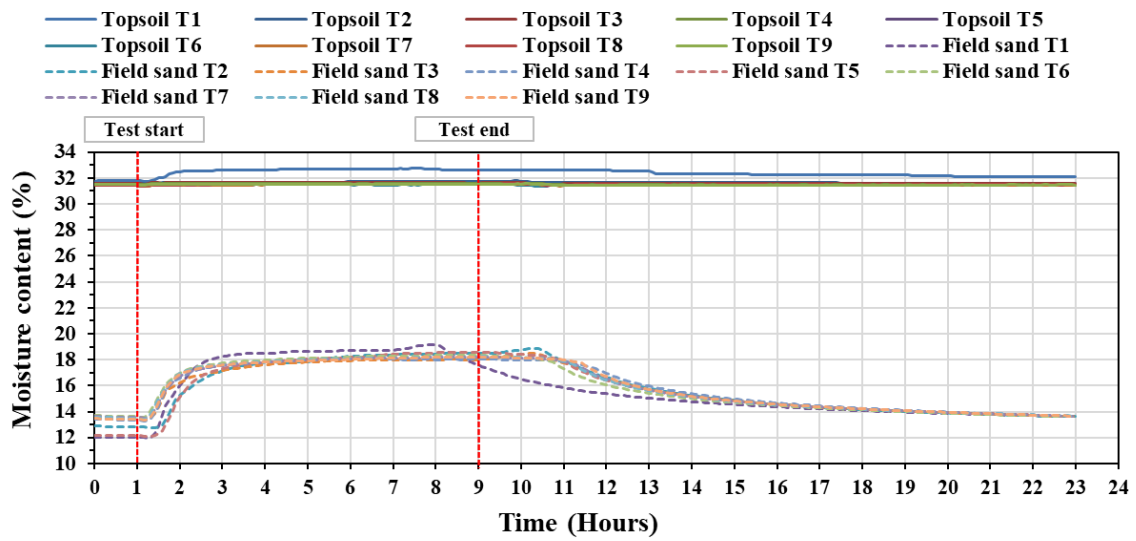

Figure 2.20. Layer Average Moisture Content vs Time - Per test – ALDOT Design.

For the F3 design, the same exercise was conducted as in the ALDOT design, with the readings recorded by the three water volumetric content sensors installed in the amended topsoil averaged, and the same done with the readings from the three sensors installed in the fill sand. With these averages, a curve of water volume content vs. time was created for each layer during the six constant head infiltration tests (See Figure 2.21).

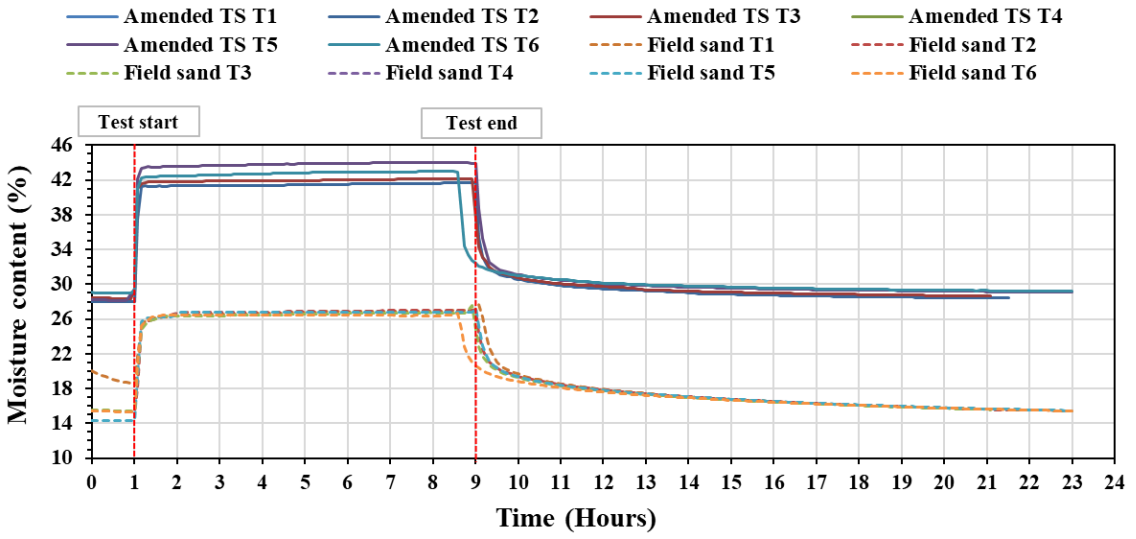

Figure 2.21. Layer Average Moisture Content vs Time - Per Test – F3 Design.

The curves from tests 2 to 8 representing the moisture content in the topsoil of the ALDOT Design were averaged to obtain the Average curve for all tests. The same was done with the curves from tests 2 to 8 representing the moisture content in the fill sand of the ALDOT Design. As can be observed, the curve of the first test conducted on the ALDOT

Design was not included in the average curve for all tests because it was not an 8-hour test but rather a 6-hour test. In the case of the F3 Design, the average curve for the amended topsoil and the fill sand was also calculated, including all six tests conducted on this specimen. (See Figure 2.22)

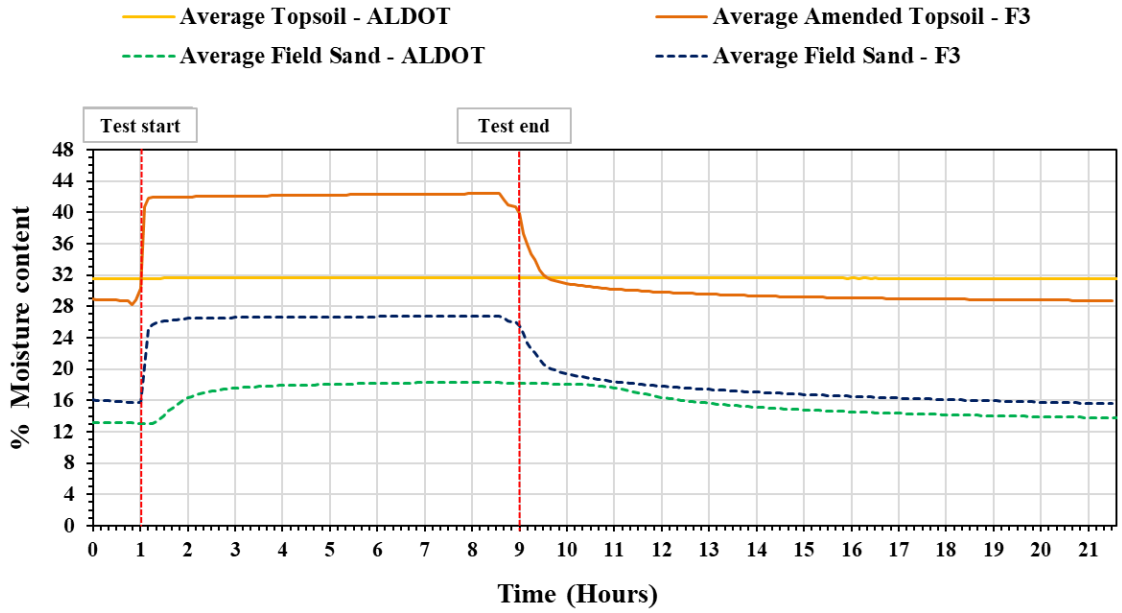

Figure 2.22. Moisture Content vs Time - Average Curve for All Tests.

The data from these curves were analyzed to determine the maximum and minimum moisture content reached by each layer, and also to calculate the time it takes for water to reach from the surface to the sensors installed in the fill sand layer of both specimens. Similarly, the drying rate of the layers after the constant head infiltration test was completed was calculated. **Table 2.27** summarizes all this information.

Table 2.27. Analysis of Moisture Content Sensors Data.

Design	Layer	Max. moisture content (%)	Moisture content at 9-hrs (%)	Moisture content at 21-hrs (%)	Drying ratio (%/hr)	Sensors' response time
ALDOT	Topsoil	31.7	31.7	31.6	0.0083	20 to 25 min
	Fill sand	18.3	18.2	13.7	0.37	20 to 25 min
F3	Amended topsoil	42.4	39.8	28.7	0.92	0 to 5 min
	Fill sand	26.8	25.6	15.6	0.83	0 to 5 min

From the curves shown in Figure 2.22 and the data in Table 2.27, the following conclusions can be drawn:

1. The amended topsoil of the F3 Design reaches a maximum moisture content of 42.4%, equivalent to 1.33 times the maximum moisture content reached by the topsoil of the ALDOT Design, which was 31.7%.

2. The Fill sand of the F3 Design reaches a maximum moisture content of 26.8%, equivalent to 1.46 times the maximum moisture content reached by the fill sand of the ALDOT Design, which was 18.3%.
3. The time it takes for water to travel from the surface of the F3 Design to the moisture sensors located in the fill sand is between 0 and 5 minutes, and the time it takes for water to travel from the surface of the ALDOT Design to the moisture sensors located in the fill sand is 20 to 25 minutes. This indicates that the water flow, and consequently the infiltration rate of the F3 Design, is higher than the infiltration rate of the ALDOT Design.
4. The drying rate of the amended topsoil and fill sand of the F3 Design is higher than the drying rate of the topsoil and fill sand layers of the ALDOT Design. The drying rate of the amended topsoil in the F3 Design is 0.92% per hour, which is 111 times greater than the drying rate of the topsoil in the ALDOT Design, which is 0.0083% per hour. The drying rate of the fill sand in the F3 Design is 0.83% per hour, 2.24 times greater than the drying rate of the fill sand in the ALDOT Design, which is 0.37% per hour.

2.5 Overall Analysis

The permeability tests allowed detecting that the critical layer of the ALDOT Engineered Media Design was the topsoil with a permeability of 0.002 in./min (0.004 cm/min). Additionally, they also revealed that loose sand, when subjected to a 9-hour constant head permeability test, consolidated to a density of 85.5% of its optimum density and a permeability of 0.83 in./day (2.11 cm/min). With these findings, the next step was to improve the permeability of the topsoil by mixing it with pine bark fines. After conducting falling head infiltration tests on 12 samples, the amended topsoil composed of 80% topsoil and 20% pine bark fines by weight was selected, which achieved an infiltration rate of 5.60 ft/d (1.70 m/d), 8.9 times higher than that of pure topsoil, which was 0.63 ft/d (0.19 m/d).

From here, the infiltration tests began. Initially, Designs A, B, C, D, and E were subjected to three falling head infiltration tests, with an initial water column of 2.0 ft. Design B showed the best performance with an average infiltration rate of 2.25 ft/d (0.14 m/d). Table 2.28 summarizes the characteristics of these designs and their results.

Table 2.28. Designs A, B, C, D and E: Characteristics and Results.

Design	Top Layer	h in. (cm)	Second Layer	h in. (cm)	Third Layer	h in. (cm)	Fourth Layer	h in. (cm)	Avg. falling rate ft/d (m/d)
A	Topsoil	10 (25.4)	Fill sand	12 (30.5)	#57 Stone + Geotex.	8 (20.3)	-	-	0.31 (0.09)
B	Amended Topsoil	10 (25.4)	Fill sand	12 (30.5)	#57 Stone + Geotex.	8 (20.3)	-	-	2.25 (0.69)
C	Amended Topsoil	6 (15.2)	Fill sand	16 (40.6)	#57 Stone + Geotex.	8 (20.3)	-	-	1.32 (0.40)
D	Amended Topsoil	6 (15.2)	Fill sand	15 (38.1)	Pea Gravel	1 (2.54)	#57 Stone	8 (20.3)	0.92 (0.28)
E	Amended Topsoil	6 (15.2)	Pea Gravel	4 (10.2)	#57 Stone + Geotex.	18 (45.7)	-	-	1.6 (0.49)

Note: h = Height of the layer

After this, Designs A-1G and Design F underwent three falling head infiltration rate tests, with an initial water column of 2.0 ft (0.6 m), and 3 constant head infiltration rate tests lasting 6 hours each, with a constant head of 2.0 ft (0.6 m). Table 2.29 summarize the characteristics of these designs and their results.

Table 2.29. Designs A-1G and F: Characteristics and Results

Design	Top Layer	h in. (cm)	Second Layer	h in. (cm)	Third Layer	h in. (cm)	Fourth Layer	h in. (cm)	Avg. falling rate ft/d (m/d)	Avg. constant rate ft/d (m/d)
A-1G	Topsoil	10 (25.4)	Fill sand	12 (30.5)	#57 Stone	8 (20.3)	-	-	0.62 (0.19)	0.46 (0.14)
F	Amended Topsoil	10 (25.4)	Fill sand	12 (30.5)	Pea Gravel	6 (15.2)	#57 Stone	8 (20.3)	5.99 (1.83)	7.66 (2.33)

Note: A-1G represents the ALDOT design with a single layer of geotextile separating the fill sand from the #57 stone. h = Height of the layer.

This test was important because the specimen A-1G, which was similar to specimen A except that it had a single layer of geotextile (separating the #57 stone from the fill sand) instead of two like A, averaged 0.62 ft/d (0.19 cm/d) in falling head infiltration rate tests, twice as much as Design A, which obtained 0.31 ft/d (0.09 cm/d). This finding led the team to explore other alternatives to replace the use of geotextile.

At this point in the research, the testing process was reversed. Therefore, the three constant head infiltration tests, which simulate the prolonged use of infiltration media, were conducted first. Subsequently, the three falling head infiltration tests were performed to determine how long water remains pooled in the infiltration swale after it stops receiving water runoff. The specimens tested in this phase were A*, B*, F*, F1, F2, F3, ALDOT + Grass, and F3 + Grass.

The specimens marked with an asterisk, A*, B*, and F*, are the same specimens A, B, and F, respectively, with a correction in the weight of their top layers. In the previous tests, the final densities of each layer of the specimens were checked more accurately thanks to the transparency of the infiltrometers. It was revealed that the final density reached by the Topsoil was 96.8 lb/ft^3 (1.55 g/cm^3), not 88.6 lb/ft^3 (1.42 g/cm^3) as estimated before. Additionally, the final density reached by the Amended topsoil was 68.7 lb/ft^3 (1.10 g/cm^3), not 61.2 lb/ft^3 (0.98 g/cm^3) as previously estimated.

In the final stage of the small-scale phase of the project, the F3 design was reached, which ultimately achieved the best infiltration rate results. To arrive at this design, it started with Design B*, which is similar to A* (representing the current ALDOT design), with the only difference being that the topsoil was replaced by amended topsoil. Making this change resulted in significant improvements in infiltration rates. In the falling head test, specimen B* achieved 1.1 ft/d (0.33 cm/d), 2.2 times more than specimen A*, which obtained 0.49 ft/d (0.15 cm/d).

To further enhance the performance of the engineered media, F-type designs were proposed. Similar to Design B*, these designs included amended topsoil instead of topsoil. Additionally, they introduced a layer of pea gravel as a transition and separation medium between the fill sand and #57 stone, eliminating the need for geotextile, which causes a reduction in the long-term infiltration rate of engineered media.

Finally, the F3 design was achieved, which showed the second-highest infiltration rate in constant head tests and the highest in falling head tests. Subsequently, the ALDOT + Grass Design and the F3 + Grass Design were tested to compare the performance of the current ALDOT engineered media design with the F3 design proposed by the AU Stormwater team as a result of this research, including in both the upper layer of Bermuda grass sod. Table 2.30 summarizes the characteristics of the designs tested in this phase of the project and their results.

Table 2.30. A*, B*, F*, F1, F2, F3, ALDOT + Grass, and F3 + Grass: Characteristics & Results

Design	Top Layer	h in. (cm)	Second Layer	h in. (cm)	Third Layer	h in. (cm)	Fourth Layer	h in. (cm)	Avg. falling rate ft/d (m/d)	Avg. constant rate ft/d (m/d)
A*	Topsoil	10 (25.4)	Fill sand	12 (30.5)	#57 Stone + Geotex.	9.5 (24.1)	-	-	1.73 (0.53)	0.49 (0.15)
B*	Amended Topsoil	10 (25.4)	Fill sand	12 (30.5)	#57 Stone + Geotex.	9.5 (24.1)	-	-	5.38 (1.64)	1.10 (0.33)
F*	Amended Topsoil	10 (25.4)	Fill sand	12 (30.5)	Pea Gravel	6 (15.2)	#57 Stone	4 (10.2)	5.31 (1.62)	1.26 (0.38)
F1	Amended Topsoil	6 (15.2)	Fill sand	16 (40.6)	Pea Gravel	6 (15.2)	#57 Stone	7 (17.8)	4.75 (1.45)	1.11 (0.34)
F2	Amended Topsoil	8 (20.3)	Fill sand	14 (35.6)	Pea Gravel	6 (15.2)	#57 Stone	7 (17.8)	6.73 (2.05)	1.58 (0.48)
F3	Amended Topsoil	6 (15.2)	Fill sand	10 (25.4)	Pea Gravel	6 (15.2)	#57 Stone	9 (22.9)	5.75 (1.75)	2.24 (0.68)
ALDOT +Grass	Topsoil	10 (25.4)	Fill sand	12 (30.5)	#57 Stone + Geotex.	9.5 (24.1)	-	-	0.91 (0.28)	0.31 (0.09)
F3 +Grass	Amended Topsoil	6 (15.2)	Fill sand	10 (25.4)	Pea Gravel	6 (15.2)	#57 Stone	9 (22.9)	13.73 (4.18)	11.66 (3.54)

Note: h = Height of the layer

Finally, in the intermediate-scale phase, the ALDOT Design and the F3 Design were tested in the infiltration swale chamber. The results obtained by both designs in the tests conducted in the infiltration swale chamber are shown in Table 2.31.

Table 2.31. ALDOT and F3 Designs Results in Infiltration Swale Chamber.

Design	Constant head – Avg.	Falling head – Avg.
ALDOT (Chamber)	6.51 ft/d (1.98 m/d)	4.96 ft/d (1.51 m/d)
F3 (Chamber)	87.06 ft/d (26.54 m/d)	75.79 ft/d (23.10 m/d)
Ratio: $\frac{F3\ Rate\ (Chamber)}{ALDOT\ Rate\ (Chamber)}$	13.37	15.28

Table 2.32 shows the results obtained in the transparent infiltrometers for ALDOT and the F3 Designs.

Table 2.32. Infiltration Rate Test Results for ALDOT + Grass and F3 + Grass Designs.

Design	Constant head – Avg.	Falling head – Avg.
ALDOT + Grass	0.91 ft/d (0.28 m/d)	0.31 ft/d (0.09m/d)
F3 + Grass	13.73 ft/d (4.18 m/d)	11.66 ft/d (3.55 m/d)
Ratio: $\frac{F3 + Grass\ Rate}{ALDOT + Grass\ Rate}$	15.09	37.61

Table 2.33 shows the comparison of the results obtained in the infiltration chamber and the infiltrometers between similar designs.

Table 2.33. Ratios Between Infiltration Chamber and in the Infiltrometers.

Ratio	Constant head – Avg.	Falling head – Avg.
$\frac{F3\ Rate\ (Infiltration\ chamber)}{F3 + Grass\ Rate\ (Infiltrometers)}$	$\frac{87.06\ ft/day}{13.73\ ft/day} = 6.3$	$\frac{75.79\ ft/day}{11.66\ ft/day} = 6.5$
$\frac{ALDOT\ Rate\ (Infiltration\ chamber)}{ALDOT + Grass\ Rate\ (Infiltrometers)}$	$\frac{6.51\ ft/day}{0.91\ ft/day} = 7.2$	$\frac{4.96\ ft/day}{0.31\ ft/day} = 16.0$

There is certainly a difference in infiltration rate when comparing the 6 in. (15.2 cm) column experiments to the chamber experiments. A hypothesis is that in the infiltration chamber, water flows faster through the contact surface between the plastic lining and the materials than through the pores of the materials themselves.

The calculations shown in Table 2.34 that the infiltration chamber has 13.4 times more perimeter and 7.1 times more contour area than the infiltrometer columns. Despite both plastic layers covering the interior of the chamber being installed as carefully as possible to prevent wrinkles, it is possible that irregularities along the installation cause opportunities for water to short-circuit and flow more rapidly than through the inherent porosities of the materials composing the infiltration media. In the case of the 6 in. (15.2 cm) infiltrometer columns, the infiltration media materials are in contact with the homogeneous internal surface of the tubing, which prevents water from flowing more rapidly through the contact surface between the materials and the tubing. This fact could be visually confirmed during the saturation of the samples, thanks to the transparency of the used infiltrometers.

Table 2.34. Geometric Calculations of the Infiltrometers and the Chamber

Infiltrometers		
Di	Internal diameter	0.50 ft (0.15 m)
Hi	Height of the samples	2.63 ft (0.80 m)
Ai	Surface area	0.20 ft^2 (0.02 m^2)
Pi	Surface perimeter	1.57 ft (0.47 m)
Cai	Contact area: Pi*Hi	4.12 ft^2 (0.38 m^2)
Infiltration Swale Chamber		
W	Width	2.50 ft (0.76 m)
L	Length	8.00 ft (2.23 m)
Hi	Height of the samples	2.25 ft (0.68 m)
Aisc	Surface area	20.00 ft^2 (6.10 m^2)
Pisc	Surface perimeter	21.00 ft (6.40 m)
Caisc	Contact area	47.25 ft^2 (4.38 m^2)
Comparison		
Areas Ratio	$\frac{Aisc}{Ai}$	$\frac{20.00\ ft^2}{0.20\ ft^2}$ = 101.86
Perimeters Ratio	$\frac{Pisc}{Pi}$	$\frac{21.00\ ft}{1.57\ ft}$ = 13.37
Contact area Ratio	$\frac{Caisc}{Cai}$	$\frac{47.25\ ft^2}{4.12\ ft^2}$ = 11.46

Additionally, the moisture content sensors analysis allowed to confirm that the F3 Design has a better infiltration rate than the current ALDOT Design.

2.6 DISCUSSION

This research assessed the infiltration rate of various designs for infiltration swale media under both constant and falling head conditions. The methodology employed allowed for the identification of the causes behind the low infiltration rate of the current design, including the low permeability of the topsoil and the reduction in infiltration rate caused by the presence of geotextile, whose pores begin to be blocked by the smaller particles of the specimen, permanently reducing the permeability of the system.

With the identified weaknesses, different solutions were considered until the F3 Design was obtained. The F3 Design (Figure 2.12) ensures an infiltration rate 15 times higher than that of the current design, without significant and permanent reduction issues in the infiltration rate like the previous design. Additionally, it has the ability to dry much faster than the previous design, allowing for a greater available storage volume in the face of another rainfall event.

2.7 KEY FINDINGS

To optimize the efficiency of infiltration swale media, it is essential to understand how key aspects such as hydraulic conductivity, thickness, and compaction of each material layer influence their infiltration rate. Additionally, understanding how material consolidation reduces performance over time is crucial. These considerations are vital to maximize their efficiency in infiltrating water and prevent excess water runoff generated by impermeable road surfaces from causing higher peak flows, sediment transport, and the transport of contaminants that may deposit in the surrounding environment and receiving water bodies.

The previous study has demonstrated that the presence of the geotextile layer wrapped around the #57 stone as in ALDOT's current design reduces the infiltration rate of the matrix. This reduction occurs because the geotextile pores gradually become clogged by the finer particles of the sand. Infiltration tests demonstrated that replacing the geotextile layer surrounding the #57 stone with a layer of pea gravel as a separation and transition medium between the fill sand and the #57 stone improves the infiltration rate of the matrices and prevents the permanent decrease caused by the implementation of geotextile.

Permeability and infiltration rate tests conducted on samples composed solely of topsoil showed that this material has very low permeability, preventing infiltration swale media containing it as the top layer from meeting the minimum required infiltration rate of 1 ft/d. Infiltration tests have revealed that amended topsoil, composed of 80% topsoil and 20% pine bark fines by weight, has a higher infiltration rate than topsoil. Furthermore, when replacing topsoil with amended topsoil in infiltration swale media, the tests also demonstrated a significant increase in the infiltration rate of the entire matrix.

2.7.1 COMPARISON TO CURRENT ALDOTIS MEDIA

The results of the infiltration rate tests conducted on the clear infiltrometers to ALDOT design and F3 design, represented by the samples ALDOT + Grass and F3 + Grass respectively, are shown in Table 2.35.

Table 2.35. Infiltration Rate Test Results for ALDOT + Grass and F3 + Grass

Design	Constant head – Avg.	Falling head – Avg.
ALDOT + Grass	0.91 ft/d (0.28 m/d)	0.31 ft/d (0.09 m/d)
F3 + Grass	13.73 ft/d (4.18 m/d)	11.66 ft/d (3.55 m/d)
Ratio: $\frac{F3 + Grass\ Rate}{ALDOT + Grass\ Rate}$	15.09	37.61

The results of the constant head infiltration rate test showed that Design F3 + Grass yielded 13.73 ft/d, 15.09 times more infiltration rate than ALDOT + Grass Design. In the falling head infiltration rate test the Design F3 + Grass yielded 11.66 ft/d, 37.61 times more infiltration rate than ALDOT + Grass Design.

In the intermediate-scale phase, the ALDOT Design and the F3 Design were tested in the infiltration swale chamber. The results obtained by both designs in the tests conducted in the infiltration swale chamber are shown in **Table 2.36**.

Table 2.36. Comparison of ALDOT and F3 Design in the Infiltration Swale Chamber

Design	Constant head – Avg.	Falling head – Avg.
ALDOT (Chamber)	6.51 ft/d (1.98 m/d)	4.96 ft/d (1.51 m/d)
F3 (Chamber)	87.06 ft/d (26.54 m/d)	75.79 ft/d (23.01 m/d)
Ratio: $\frac{F3\ Rate\ (Chamber)}{ALDOT\ Rate\ (Chamber)}$	13.37	15.28

Table 2.37 shows the comparison of the results obtained in the infiltration chamber and the infiltrometers between similar designs.

Table 2.37. Comparison of Ratios Between Similar Designs Tested in the Infiltration Chamber and in the Infiltrometers.

Ratio	Constant head – Avg.	Falling head – Avg.
$\frac{F3\ Rate\ (Infiltration\ chamber)}{F3 + Grass\ Rate\ (Infiltrometers)}$	$\frac{87.06\ ft/day}{13.73\ ft/day} = 6.3$	$\frac{75.79\ ft/day}{11.66\ ft/day} = 6.5$
$\frac{ALDOT\ Rate\ (Infiltration\ chamber)}{ALDOT + Grass\ Rate\ (Infiltrometers)}$	$\frac{6.51\ ft/day}{0.91\ ft/day} = 7.2$	$\frac{4.96\ ft/day}{0.31\ ft/day} = 16.0$

There is certainly a difference in infiltration rate when comparing the 6 in. (15.2 cm) column experiments to the chamber experiments. A hypothesis is that in the infiltration chamber, water flows faster through the contact surface between the plastic lining and the materials than through the pores of the materials themselves.

The calculations shown in Table 2.38 that the infiltration chamber has 13.4 times more perimeter and 7.1 times more contour area than the infiltrometer columns. Despite both plastic layers covering the interior of the chamber being installed as carefully as possible to prevent wrinkles, it is possible that irregularities along the installation cause opportunities for water to short-circuit and flow more rapidly than through the inherent porosities of the materials composing the infiltration media. In the case of the 6 in. (15.2 cm) infiltrometer columns, the infiltration media materials are in contact with the homogeneous internal surface of the tubing, which prevents water from flowing more rapidly through the contact surface between the materials and the tubing. This fact could be visually confirmed during the saturation of the samples, thanks to the transparency of the used infiltrometers.

Table 2.38. Geometric Calculations of the Infiltrometers and the Chamber

Infiltrometers		
Di	Internal diameter	0.50 ft (0.15 m)
Hi	Height of the samples	2.63 ft (0.80 m)
Ai	Surface area	0.20 ft^2 (0.02 m^2)
Pi	Surface perimeter	1.57 ft (0.47 m)
Cai	Contact area: Pi*Hi	4.12 ft^2 (0.38 m^2)
Infiltration Swale Chamber		
W	Width	2.50 ft (0.76 m)
L	Length	8.00 ft (2.23 m)
Hi	Height of the samples	2.25 ft (0.68 m)
Aisc	Surface area	20.00 ft^2 (6.10 m^2)
Pisc	Surface perimeter	21.00 ft (6.40 m)
Caisc	Contact area	47.25 ft^2 (4.38 m^2)
Comparison		
Areas Ratio	$\frac{Aisc}{Ai}$	$\frac{20.00\ ft^2}{0.20\ ft^2}$ = 101.86
Perimeters Ratio	$\frac{Pisc}{Pi}$	$\frac{21.00\ ft}{1.57\ ft}$ = 13.37
Contour area Ratio	$\frac{Caisc}{Cai}$	$\frac{47.25\ ft^2}{4.12\ ft^2}$ = 11.46

Additionally, the moisture content sensors analysis allowed to confirm that the F3 Design has a better infiltration rate than the current ALDOT Design. **Table 2.39** shows a summary of the results obtained from the moisture content data analysis.

Table 2.39. Analysis of Moisture Content Sensors Data.

Design	Layer	Maximum moisture content (%)	Moisture content at 9-hours (%)	Moisture content at 21-hours (%)	Drying ratio (%/hour)	Sensors' response time
ALDOT	Topsoil	31.7	31.7	31.6	0.0083	20 to 25 min
	Fill sand	18.3	18.2	13.7	0.37	20 to 25 min
F3	Amended topsoil	42.4	39.8	28.7	0.92	0 to 5 min
	Fill sand	26.8	25.6	15.6	0.83	0 to 5 min

The data results obtained from the moisture content curves analysis allowed to conclude the following:

1. The amended topsoil of the F3 Design reaches a maximum moisture content of 42.4%, equivalent to 1.33 times the maximum moisture content reached by the topsoil of the ALDOT Design, which was 31.7%.

2. The Fill sand of the F3 Design reaches a maximum moisture content of 26.8%, equivalent to 1.46 times the maximum moisture content reached by the fill sand of the ALDOT Design, which was 18.3%. The reason for this is that in the ALDOT design, topsoil retains so much water that a flow capable of saturating this material does not reach fill sand.
3. The time it takes for water to travel from the surface of the F3 Design to the moisture sensors located in the fill sand is between 0 and 5 minutes, and the time it takes for water to travel from the surface of the ALDOT Design to the moisture sensors located in the fill sand is 20 to 25 minutes. This indicates that the water flow, and consequently the infiltration rate of the F3 Design, is higher than the infiltration rate of the ALDOT Design.
4. The drying rate of the amended topsoil and fill sand of the F3 Design is higher than the drying rate of the topsoil and fill sand layers of the ALDOT Design. The drying rate of the amended topsoil in the F3 Design is 0.92% per hour, which is 111 times greater than the drying rate of the topsoil in the ALDOT Design, which is 0.0083% per hour. The drying rate of the fill sand in the F3 Design is 0.83% per hour, 2.24 times greater than the drying rate of the fill sand in the ALDOT Design, which is 0.37% per hour.

CHAPTER 3. FIELD-SCALE EVALUATION

This chapter outlines the ALDOT and modified infiltration swale (MIS) designs that are implemented/constructed for the field-scale study and based on the findings made from small-scale testing in Chapter 2. Figure 3.1 shows AU-SRF facilities with infiltration swale project/installation area and water supply ponds.

This chapter will also delve into the construction process for the field-scale infiltration swale testing. The construction process consists of a site selection process, swale layout, excavation, filling materials, installing sensors, grading, sodding, and placing the introductory system. The construction phase of the infiltration swale project served as the foundation for subsequent performance evaluation. This critical stage comprised a series of planned and executed steps, ensuring a strong platform for data collection and analysis.

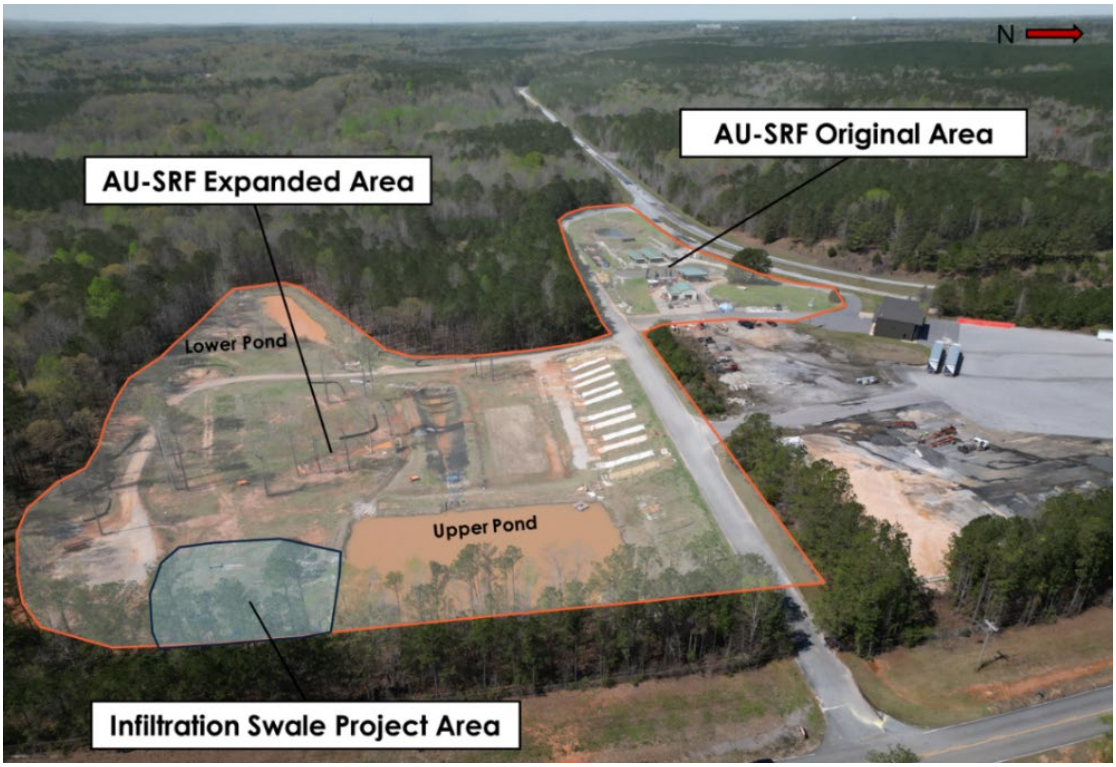

Figure 3.1. AU-SRF Facility

3.1 INFILTRATION SWALE DESIGNS

This section outlines the ALDOT and modified infiltration swale designs and presents a detailed comparison discussing the rationale behind the changes made to the existing ALDOTIS design to create the modified infiltration swale through findings made from small-scale testing described in Chapter 2.

The function of the engineered soil media matrix is to manage the infiltration rate of stormwater runoff and to promote infiltration of runoff back to the native soil and groundwater table. Figure 1.1(b) shows the profile view of the ALDOTIS which is designed for

a 1% longitudinal slope. Also, there are 6 in. (15 cm) earthen check dams that are spaced out at a maximum of every 100 linear ft (30.5 m). The check dams are added to the design to help infiltration by slowing the channelized runoff and creating water impoundment. This increases the infiltration by providing more pressure from a higher water head height from the impoundment at each check dam and slows the channelized water down to give it time to infiltrate rather than flow on the surface.

The MIS design, i.e., design F3 depicted/described in Figure 2.12 and Table 2.17, developed through small-scale testing was used to develop a field-scale swale with a media matrix depth of 5 ft (1.5 m). MISThe final field-scale MIS design is shown in Figure 3.2.

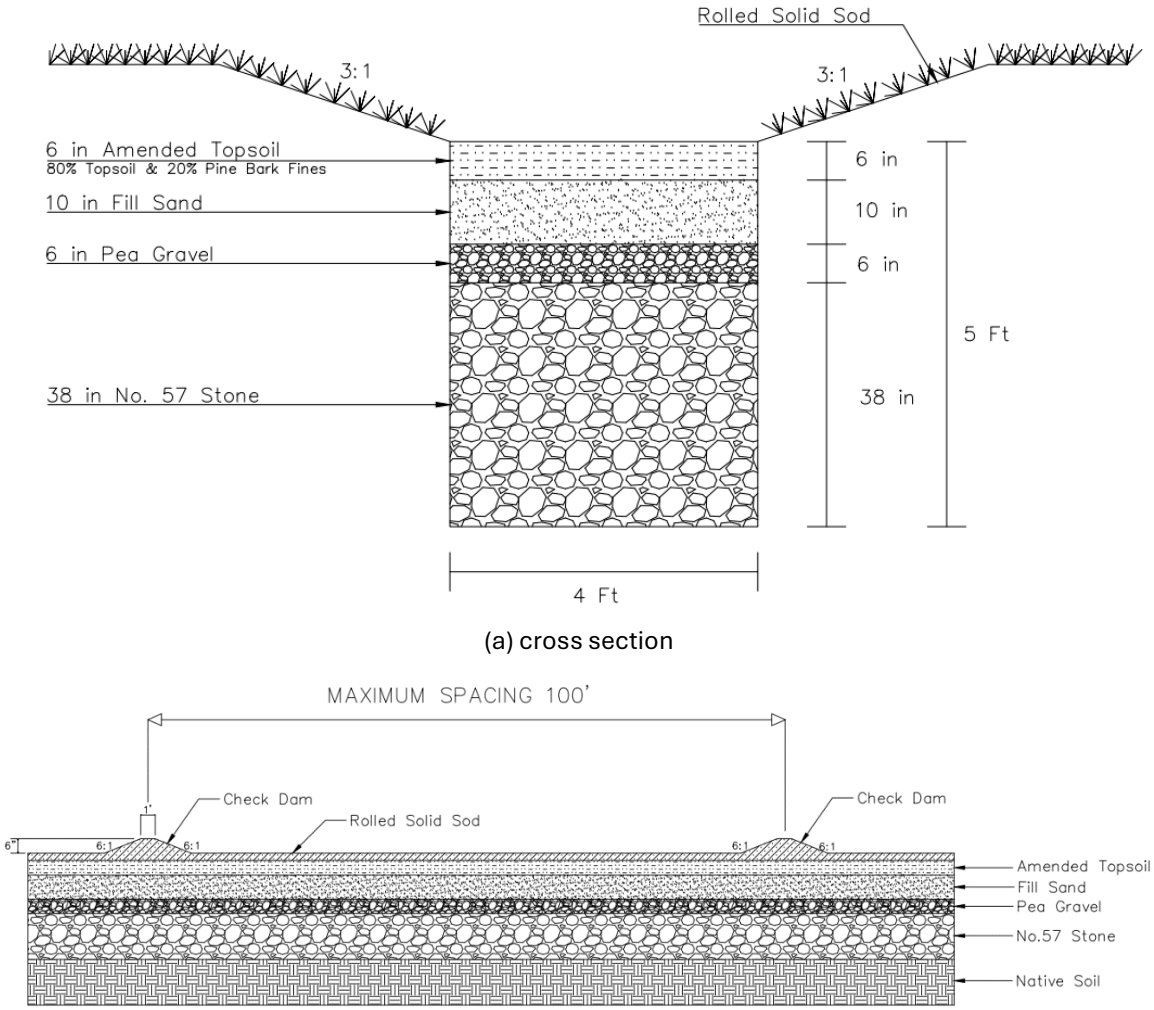

(a) cross section

(b) profile view

Figure 3.2. MIS Field-Scale Drawing

Figure 3.2 shows the modified swale design through both cross section and profile view. Focusing on the cross section view, the field-scale design of the MIS starts with a 6 in.

(15 cm) of amended topsoil (mix of 80% pine bark fines and 20% topsoil). The next layer consists of 10 in. (25 cm) of fill sand material. Then, for the geotextile replacement, it is the 6 in. (15 cm) of pea gravel and increased #57 stone layer that is 38 in. (97 cm). Figure 3.2(b) shows the profile view of the MIS at a 1% longitudinal slope and shows the 6 in. (15 cm) earthen check dams that are spaced out at the maximum of every 100 linear ft (30.5 m).

3.2 Infiltration Swale Construction

The construction of the infiltration swales at the AU-SRF site followed a sequential approach. The ALDOTIS was built first, serving as a valuable pilot project. This initial construction phase provided essential field data and performance insights that ultimately informed a more effective build of the MIS.

The MIS was the second and final swale to be built at the AU-SRF. While the ALDOT swale was being built, the MIS alternative media designs were still undergoing small-scale testing. However, once the modified media design was selected, the construction encompassed the same procedure as the ALDOTIS. This included channel shaping and layout, excavation, filling materials, moisture content sensor installation, grading, sodding, and introductory system set-up. Two infiltration swale designs specifically for research and for construction are shown in Figure 3.3.

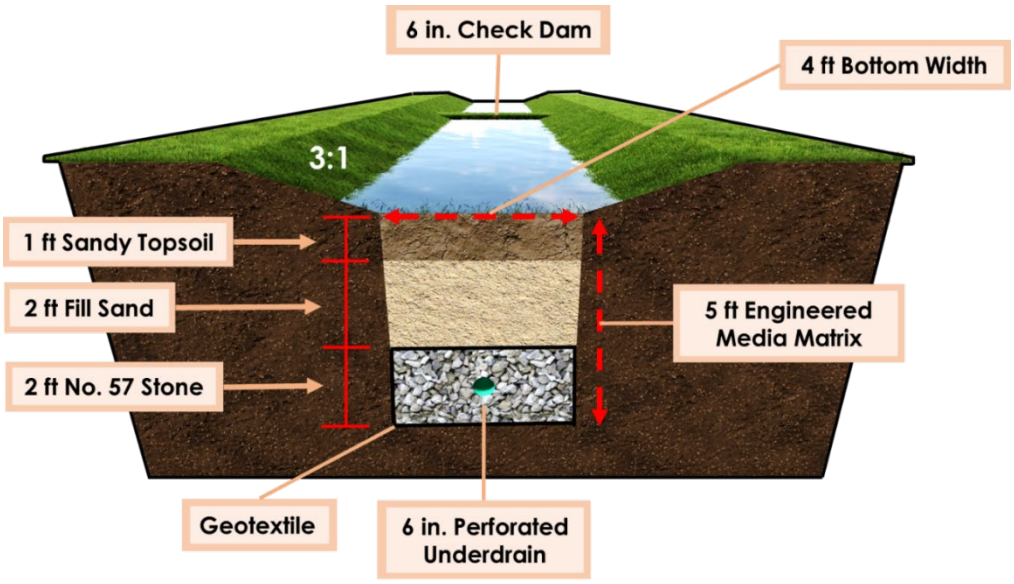

(a) ALDOTIS with underdrain

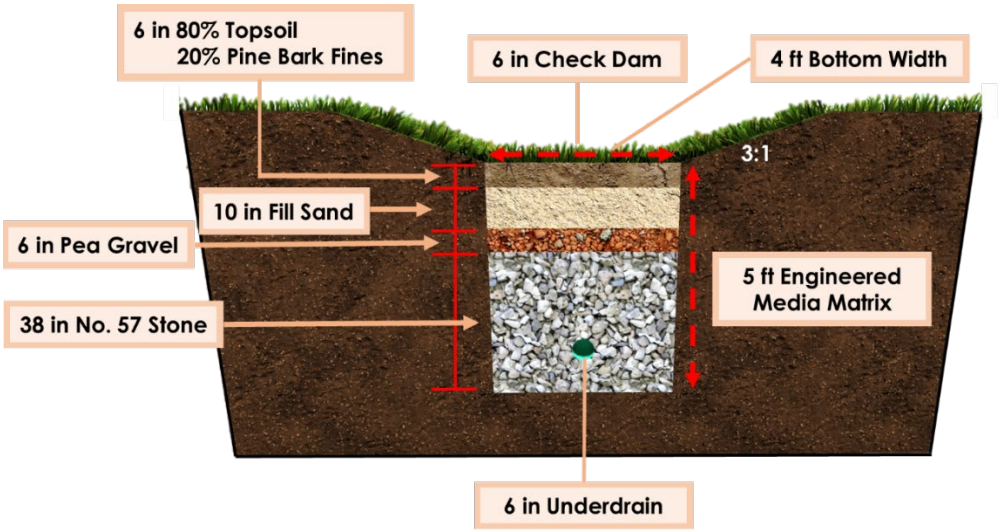

(b) MIS with underdrain

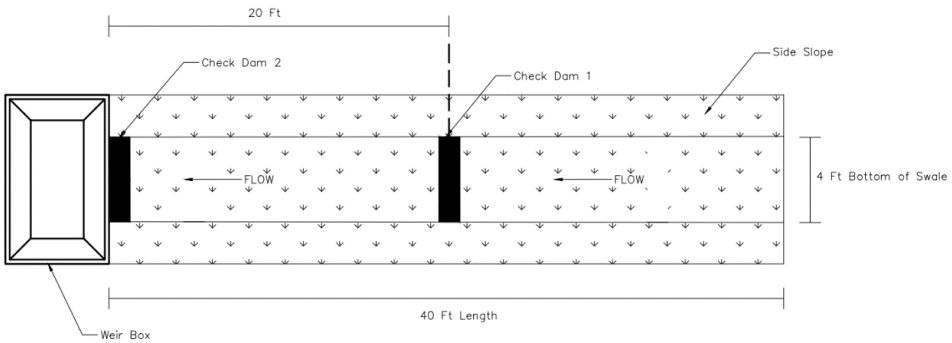

(c) plan view for both swales

Figure 3.3. Research Swale Construction Drawings

For the construction of the swales at the AU-SRF, the length chosen for both infiltration swales was 40 ft (12 m) with check dams of 6" height at the 20 ft (6.1 m) and 40 ft (12 m) mark. The check dam heights are larger than the design standard of 1% longitudinal slope over 100 ft. Another change made from the original design is the addition of a 6 in. (15 cm) perforated underdrain pipe placed in the #57 stone layer shown in Figure 3.3(a) and Figure 3.3(b). This underdrain is not included in the ALDOT design, and the purpose for adding it is to be able to measure the flow and volume of water infiltrated for simulated and natural rainfall events.

3.2.1 GEOTECHNICAL INVESTIGATION

Prior to initiating construction of the infiltration swales at the AU-SRF, a thorough geotechnical pre-investigation is crucial. Figure 3.1 depicts the designated areas at the AU-SRF used for infiltration swale construction. These areas served as the location for extracting and conducting field and laboratory soil tests. This investigation serves to confirm the suitability of the underlying native soils for optimal infiltration swale performance. The subsurface exploration will encompass both field and laboratory testing of the native soils. The primary area of interest is the deepest section of the engineered media matrix, where infiltration will predominantly occur between the final layer of the matrix and the in-situ soils.

Conducting field and laboratory soil testing for infiltration-based SCMs is essential. If a site has slow infiltration rates, it can lead to extended drainage times exceeding 48 hours. This timeframe often represents a critical threshold during which regulatory agencies may require alternative stormwater management solutions. Verifying the adequacy of in-situ soil infiltration is paramount for also optimizing the overall long-term performance of the infiltration swales. This ensures efficient drainage of the engineered media matrix, allowing for exfiltration into the native soil and ultimately, the local groundwater table.

Following the Minnesota Department of Transportation (MnDOT) guidelines, a soil boring and excavation pit were employed within the boundaries of the planned infiltration-based SCMs. These procedures facilitate the classification of native soil types and the determination of their infiltration rates. Notably, MnDOT recommends one boring and one excavation pit for projects with a surface area of less than 1000 ft^2 (92.9 m^2), which aligns perfectly with the size of the planned infiltration swales, which are approximately 160 ft^2 (14.9 m^2) each (Ramirez Florez 2024).

3.2.1.1 AU-SRF Field Boring Sample Collection

The geotechnical investigation at the AU-SRF employed a two-phased approach for collecting soil samples within the designated infiltration swale construction area.

Phase 1: Shallow Soil Sampling (0-4 ft): A handheld soil auger with a 6 in. (15 cm) increment collection capability was utilized to extract soil samples from the surface down to a depth of 4 ft (1.2 m). This method provides a safe and efficient means of collecting samples from shallow depths.

Phase 2: Deep Soil Sampling (4-9 ft): To access soil samples beyond the reach of the handheld auger, a mini excavator was used to create a 4 ft (1.2 m) deep excavation pit. This depth falls within the Occupational Safety and Health Administration (OSHA) guidelines for safe excavation without requiring additional shoring or trench boxes (typically required at depths exceeding 5 ft (1.5 m). Soil samples were then retrieved from the bottom of the excavation pit.

Final Depth Increment (8-9 ft): The final foot of the soil profile 8-9 ft (2.4-2.7 m) was accessed by extending the mini excavator pit by an additional foot. This allowed for the collection of a complete soil profile up to the depth of 9 ft (2.7 m). Figure 3.4 visually depicts the boring process, the 4 ft (1.2 m) deep excavation pit used for deeper sample collection, and the resulting soil profile at the selected site.

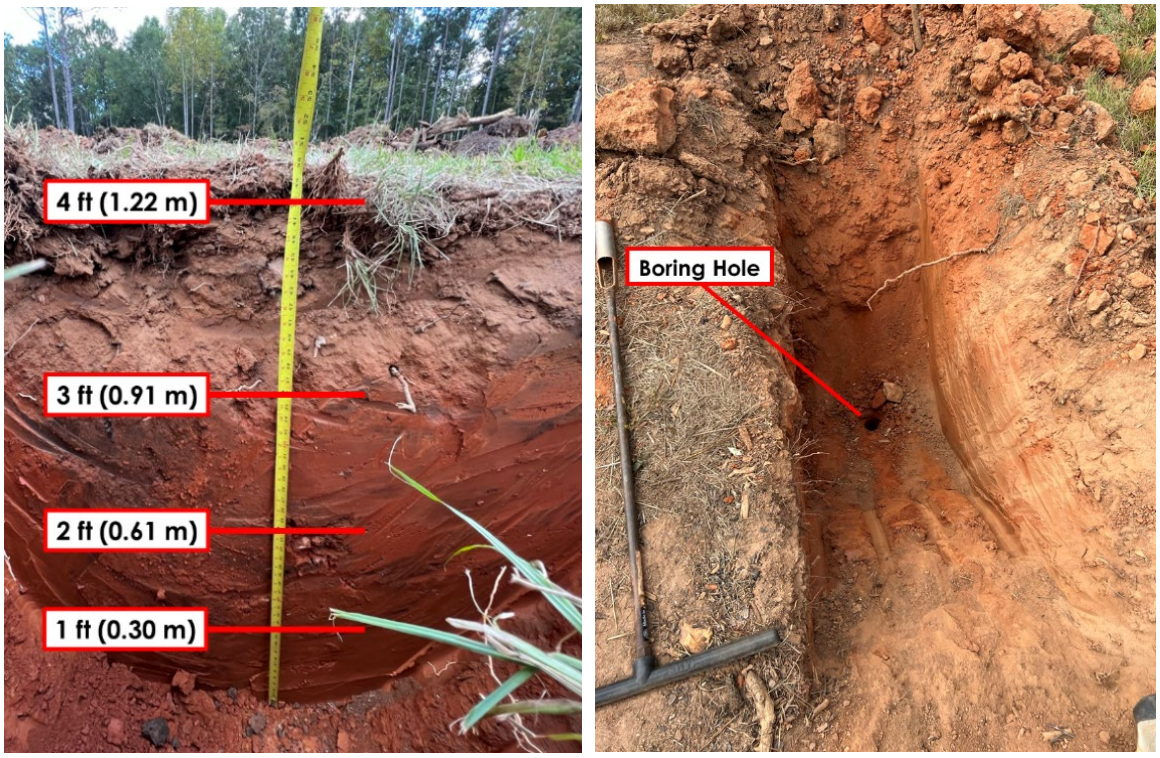

(a) soil profile and soil horizon (b) 4 ft (1.22 m) pit boring

Figure 3.4. Soil Collection and Soil Profiling

3.2.1.2 Soil Laboratory Testing

A critical component of soil classification for the infiltration swales is grain size analysis. This standard test method, conducted in accordance with ASTM C136, measures the distribution of particle sizes within a soil sample. The resulting data provides essential information for estimating infiltration rates within the swale system. Grain size distribution significantly impacts a soil's permeability, which directly influences how quickly water can infiltrate through the material. Soils with a higher proportion of coarse particles (sands, gravels)

generally exhibit faster infiltration rates compared to those dominated by finer particles (silts, clays). The native soil results are found in Chapter 5.

3.2.1.3 Infiltration Field Testing

To obtain a more accurate representation of field conditions compared to laboratory samples, a double-ring infiltrometer test (ASTM D3385) was employed. This standardized field test method measures the infiltration rate of the in-situ soil, minimizing disturbances that may occur during sample collection.

While infiltration testing at various depths is valuable, the most critical location for testing is the interface between the engineered media matrix and the native soil. This zone is where infiltrated water exits the engineered media and enters the underlying native soil profile. Figure 3.5 visually depicts the double-ring infiltrometer field test performed at the surface and the interface boundary.

(a) surface test (b) pit test

Figure 3.5. Double-Ring Infiltrometer

Once the geotechnical investigation results of the site were confirmed, construction of the infiltration swales commenced. Geotechnical investigations for site selection for infiltration-based SCMs are vital and are required to ensure long-term infiltration performance as poor or no soil testing is one of the main factors hindering the infiltration performance. Other important tests to consider for optimal performance are percolation

tests, establishing the groundwater table, and falling and constant head lab testing. Infiltration results are found in section 4.6.2.

3.2.1.4 Site Layout and Preparation

The construction process for both infiltration swale systems commenced with site preparation and layout. This initial stage involved using wooden stakes, tape measures, strings, and spray paint to delineate both of the swale's length of 40 ft (12 m), bottom width of 4 ft (1.2 m), and 3:1 side slope. The spray-painted lines in Figure 3.6 show the boundary of the engineered media matrix component and is where the exaction commenced. Prior to excavation, an automatic laser level was employed to measure the surface elevations at the upstream and downstream ends of the swale's layout. This ensured a longitudinal slope of 1% for optimal flow.

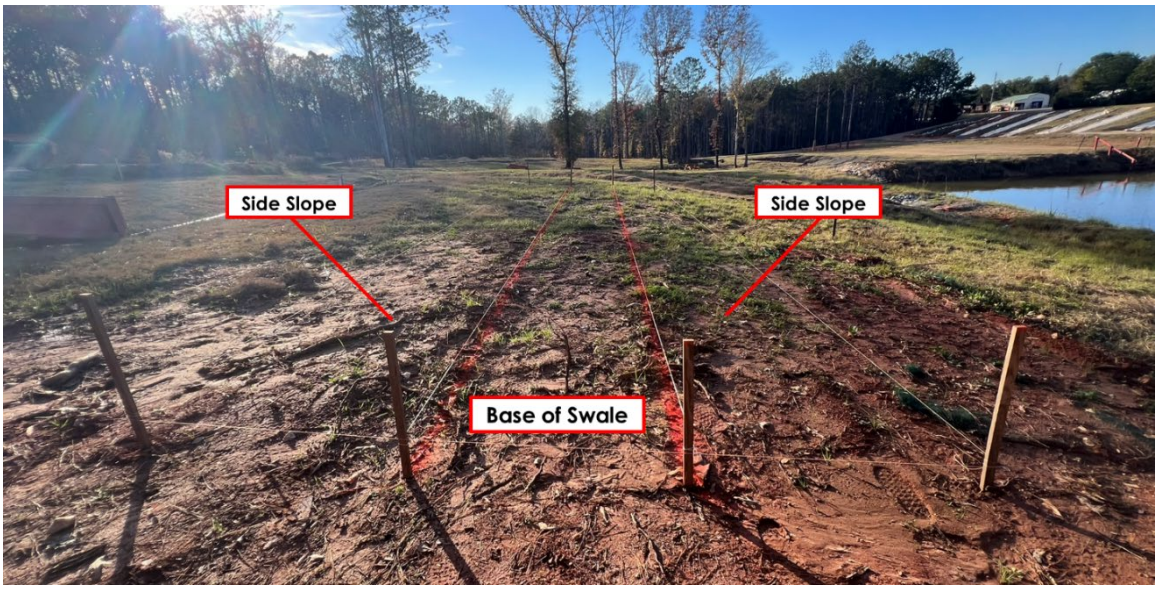

Figure 3.6. Swale Layout

Another important aspect of quality assurance during the construction process was to build a diversion berm to route run-on from surrounding areas away from the infiltration swale to reduce the risk of clogging the practice. The diversion berm layout is shown in Figure 3.7.

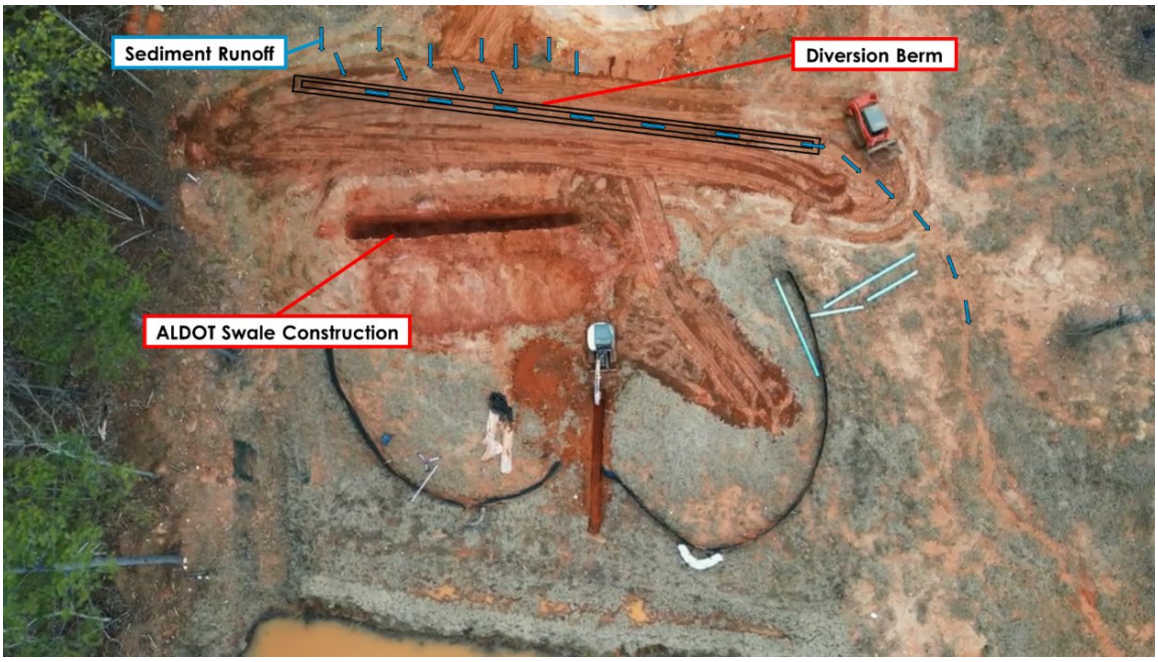

Figure 3.7. Diversion Berm to Divert Surface Runoff after a Rainfall Event

3.2.2 EXCAVATION

Following site preparation, a 6.5 ft (1.9 m) deep trench for the engineered media matrix (5 ft) and grass channel above (1.5 ft) was excavated, starting from the downstream end, and progressing upstream. Next, utilizing a pre-established reference point on the surface, the downstream's final base surface elevation in the excavated pit was established by measuring 1 ft (0.30 m) below the pre-established datum. This elevation served as the base for the downstream channel surface. The upstream surface elevation was marked with spray paint by calculating a 4.8 in. (12 cm) difference from the downstream elevation line to achieve the desired 1% slope over the 40 ft (12 m) length. A string was then used to connect the upstream and downstream elevation lines and subsequently spray painted to mark the entire channel's bottom surface. Once the channel bottom elevation was established, the mini excavator was used to create side slopes with a 3:1 inclination. An automatic laser level was used to verify and mark the side slope measurements on the surface. Lastly, a trench for the underdrain pipe was excavated for the pipe to daylight and allow water to drain away from the swale, ensuring a 1% to 2% downward slope for proper drainage. Figure 3.8 shows the excavation process.

(a) excavated media body (b) trench for underdrain

Figure 3.8. Excavation Process and Installed Underdrain

3.2.3 Engineered Media Matrix and Underdrain Placement

The next phase of construction focused on the placement of the engineered media matrix and underdrain installation. Reference elevations for each media layer were marked based on the surface datum to ensure a 1% slope during filling within the excavation pit. The ALDOTIS's first fill material was the geotextile fabric, following filling the first foot (0.30 m) off the bottom of the excavation pit with #57 stone, forming a foundation for the underdrain pipe positioned in the center of this stone layer. After the underdrain was positioned, the rest of the #57 stone was filled forming a total fill of 2 ft (0.61 m). The geotextile fabric was sealed on all four sides of the #57 stone per ALDOT specifications. The next layer was to then fill in the 2 ft (0.61 m) of fill sand. The last layer to install was the 1 ft (0.30 m) of topsoil. Figure 3.9 shows the fill process for the ALDOT swale.

(a) pipe and #57 stone

(b) sealed geotextile

(c) sand layer

(d) topsoil layer

Figure 3.9. ALDOT's Engineered Media Matrix Installation Process

The MIS's first fill material was 1 ft (0.30 m) of #57 stone, forming a foundation for the underdrain. The underdrain is installed in the exact same location for both swales. After the underdrain was positioned, the rest of the #57 stone was filled forming a total fill of 3.2 ft (0.97 m) or 38 in. (97 cm). The next layer was to then fill 6 in. (15 cm) of the pea gravel layer which was replacing the geotextile. The next fill layer was 10 in. (25 cm) of fill sand, and the last layer to install was 6 in. (15.2 cm) of amended topsoil. Figure 3.10 shows the filling process for the MIS.

(a) pipe and #57 stone

(b) pea gravel layer

(c) sand layer

(d) amended soil layer

Figure 3.10. Modified Swale's Engineered Media Matrix Installation Process

3.2.4 WEIR BOXES INSTALLATION

While installing the engineered media matrix, a surface weir box at the downstream end for both swales was installed. Also, an underdrain weir box for both swales was installed at the underdrain outlet point. The surface weir box installation process entailed excavating pits adjacent to the downstream of each swale. The surface weir box was then placed inside the hole using the mini excavator and was then leveled and backfilled with the native soil. The same process was conducted for the underdrain box for each swale's underdrain outlet. This construction installation process is shown in Figure 3.11.

(a) surface box placed

(b) backfilled

(c) underdrain box

(d) backfilled

Figure 3.11. Weir box Installation

3.2.5 Moisture Content Sensor Installation

Before any materials were filled into the exaction pit for the engineered media matrix, five moisture content sensors were installed in both infiltration swales. The moisture content sensors are to be used for testing once the infiltration swales are fully constructed. More information on moisture content sensor locations and methodology is available elsewhere by Austin (2024). The method to install the sensors included using a handheld auger to dig a boring hole. Next was to use a specific installation tool that allowed for the sensor to be installed perpendicular to the inside of the boring walls and makes sure to eliminate air gaps for installation. Once installed the sensor inside the boring was then backfilled and compacted. Installation for sensors at higher elevations was installed in the media by hand and backfilled with the excavator using the next fill material. Each sensor has a wire attached and connects to a single control box where data is stored and exported for testing. Figure 3.12 shows this process of moisture content sensors installation.

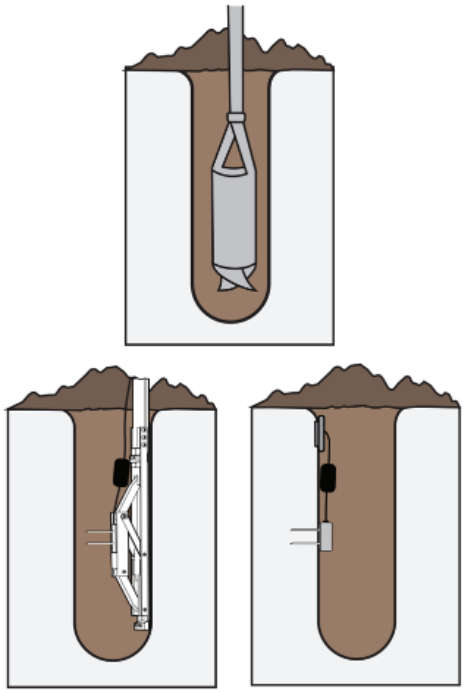

(a) installation [51]

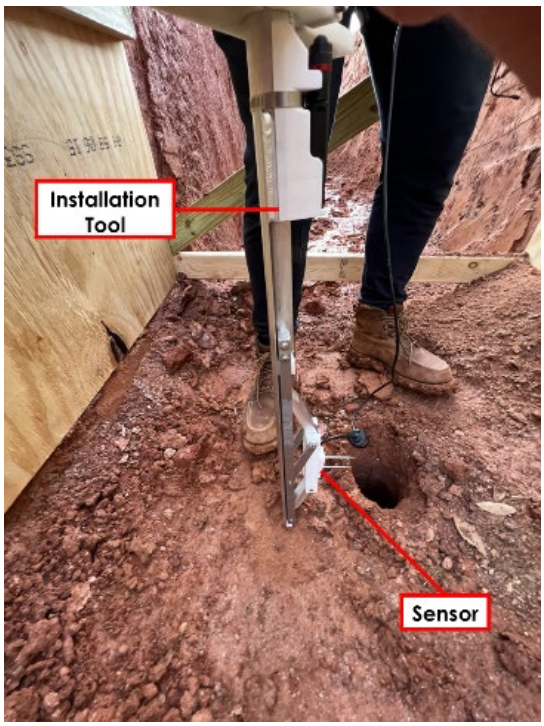

(b) installation set-up

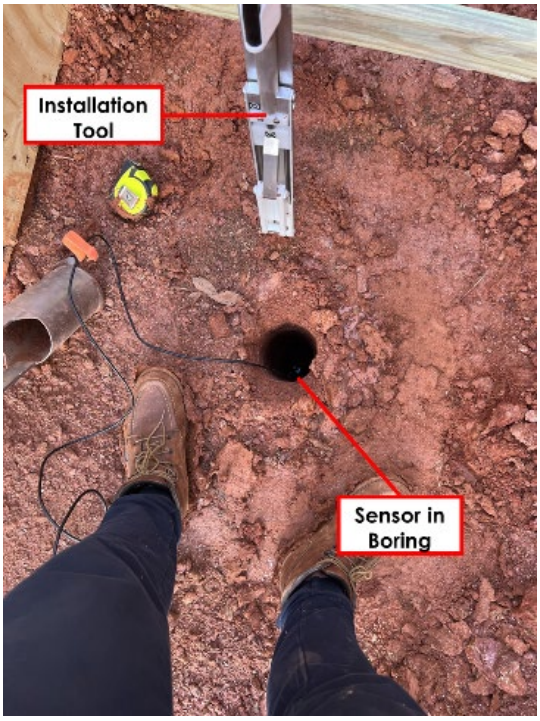

(c) sensor installed

(d) control box

Figure 3.12. Moisture Content Sensor Installation

3.2.6 FINAL GRADING AND SODDING

Upon completion of the engineered media matrix installation, the construction process focused on final touches and vegetation establishment. A final touch to add was the earthen check dams. Using topsoil, two earthen check dams were constructed: one at the 20 ft (6.1 m) midpoint and another at the downstream end (40 ft or 12 m) for both swales. The remaining topsoil was used to create final grading across the side slopes and shoulders of the swale, facilitating sod establishment. Subsequently, Bermuda Tifway sod was used to cover both swales. The sod was compacted and rolled only on the side slopes and shoulders.

(a) final grading

(b) sodding

(c) rolled sod

(d) stabilized sod

Figure 3.13. Final Grading and Sodding

3.2.7 FLOW INTRODUCTION SYSTEM

Two blue plastic introductory flow tanks, each with a 300-gal. (1,136 L) capacity, were used for the corresponding infiltration swale being tested. These tanks facilitated the introduction of water into each swale for evaluation and testing. The two flow tanks are comprised of four key components: inlet ports, a wooden baffle dissipater, rectangular weir opening, and a pumping system.

There are six 4 in. (10 cm) inlet ports on the backside of the introductory flow tub that are openings that can be connected to a flexible hose through PVC and steel attachments. The six inlet ports can be capped and sealed depending on the number of hoses and flow needed for testing. For purposes of this project, only one inlet port with its associated hose and pump was required to reach the adequate flow rates for both infiltration swales.

The wooden baffle is a perforated thin board placed inside the center of the tank and is the length of the inside diameter of the tank. The perforated wooden baffle functions as a hydraulic energy dissipater, mitigating the high-velocity flow and intense water pressure originating from the supply hose. The baffle effectively reduces the flow velocity and intensity within the influent flow tank, ensuring a steady and uniform outflow through the weir opening located on the front side.

The rectangle weir opening on the frontside of the tank faces the infiltration swale and is the component of the tank that controls the amount of flow entering the infiltration swale channel. The weir opening plate is accompanied by a scalar flow control ruler. This ruler facilitates the direct measurement of discharge based on the observed water level within the introductory flow tank. This correlation is established through a 0.25 in. (0.64 cm) clear plastic standpipe connected to the tank's bottom. The water level observed in the standpipe reflects the flow rate produced by the pumping system feeding the blue introductory flow tank.

The last main component of the introductory flow system for the infiltration swale test channels is the pump set-up. Water is pumped from the upper pond from the AU-SRF expanded area (shown in Figure 3.1) into the introductory flow tub by a DuroMax portable engine pump (Model No. XP650WP). There is one pump used per infiltration swale and its corresponding introductory blue tank. The pumps use a 4 in. (10 cm) inlet port to connect to a single 4 in. (10 cm) hose**.** Figure 3.14 shows the four main components of the water introduction system used to add accurate flow amounts to the infiltration swales for tests.

The flow calibration process for the introductory flow tank included filling the inside of the tank up with water until just below the weir opening. This water level inside the tub should correspond to 0 ft^3/s (0 m^3/s) on the scaled flow control ruler. Any deviation from a perfectly level introductory flow tank would result in inaccurate flow readings on the scaled flow control ruler, potentially indicating values below or exceeding 0 ft^3/s (0 m^3/s). Ensuring a level introductory blue flow tank was, therefore, crucial for the functionality of the water introduction system prior to testing.

(a) introductory flow tub (front)

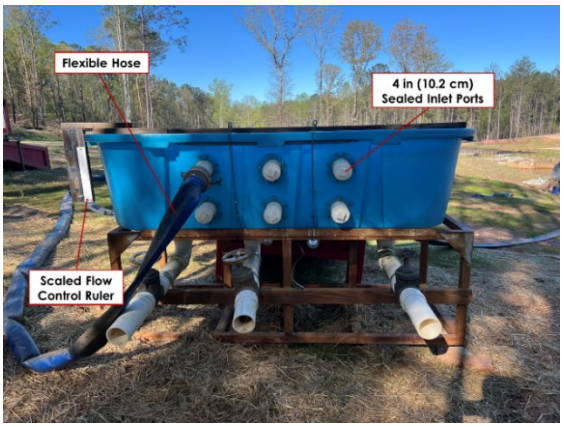

(b) introductory flow tub (back)

(c) pump

(d) wooden perforated baffle

Figure 3.14. Components for Introductory Flow System

3.3 CALIBRATION

To ensure the calibration of the surface weir boxes and introductory flow tanks were correct, plastic fabric was used to cover the entire length and width of the infiltration swales. The impermeable plastic fabric lining served to prevent infiltration of influent water into the underlying soil media. Instead, all influent water was directed to flow over towards the surface weir box for collection and measurement. Figure 3.15(b) shows the ALDOTIS lined with plastic and water flowing into the surface weir box.

(a) scalar flow ruler (b) plastic liner

Figure 3.15. Plastic Liner Calibration

A flow rate of 0.55 ft^3/s (0.02 m^3/s), established using the scaled flow ruler on the water introduction system, was pumped into the swale for a duration of 30 minutes. A levelogger positioned within the surface weir box continuously recorded the water height over the weir crest throughout the test. This ensured continuous monitoring of water inflow to the swale and outflow through the weir box. With the predetermined flow rate and duration of the pumping process known, the total volume of water introduced into the system could be accurately calculated. Once the introduced flow volume was found, the levelogger data was extracted to find the amount of water volume that exited the infiltration swale. Figure 3.16 shows the water level of the surface weir box during this test.

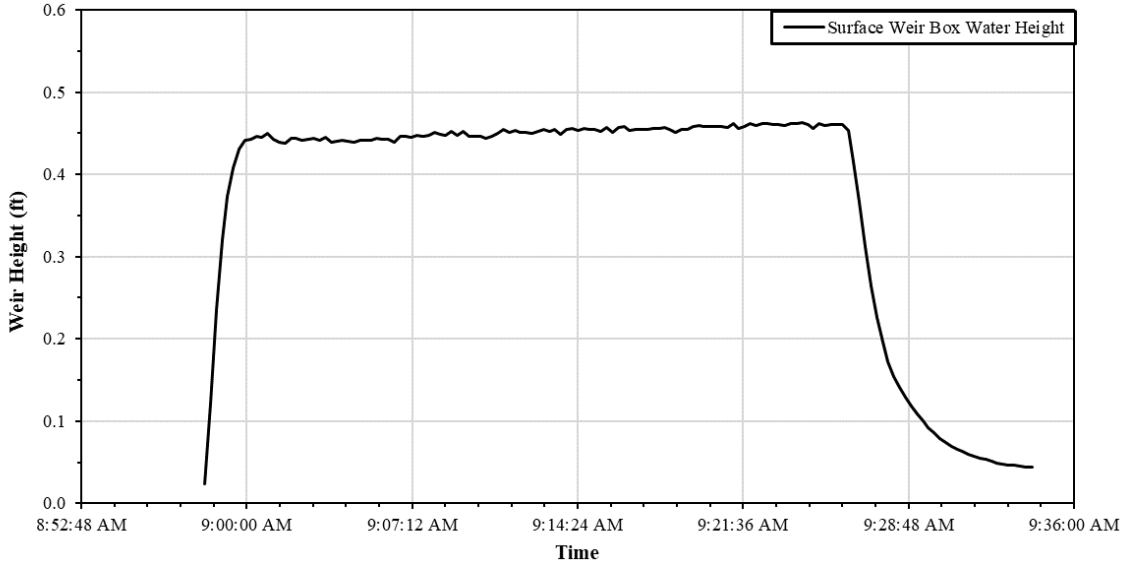

Figure 3.16. Surface Weir Box Water Height

The water level in the weir box was then subtracted from the crest height to solely get the value of water level over the crest. This value was then plugged into the fitted weir flow equation (Austin 2024) to obtain the flow amount for that water level over the crest every 15 seconds. The water level data collected by the Levelogger was processed at 15-second intervals to determine the incremental volume exiting the weir box throughout the test. The sum of these incremental volumes yielded the total outflow volume. The experiment measured an inflow volume of 1039 ft^3 (29.4 m^3) to the infiltration swale, while the total outflow volume exiting the surface weir box was 987 ft^3 (27.9 m^3). The difference of 52.5 ft^3 (1.49 m^3) represents the volume of water retained within the swale as surface storage. According to this calibration 95% of the water was bypassed intro the surface weir box and 5% was captured in the swale's surface. This test confirmed the accuracy of the water introductory system flow amount, and the accuracy of the surface weir boxes for both infiltration swales.

3.3.1 SURFACE STORAGE VOLUME

Building upon the observation in the previous section that both swales, while lined with an impermeable geomembrane, reached their maximum storage capacity without overflowing into the surface weir boxes, a procedure was devised to quantify the precise volume of water the infiltration swales can retain at the surface. To determine the volume of surface water storage within the infiltration swales, a manual pumping system was employed. This system utilized a pump and a calibrated container with a known volume of approximately 5 ft^3 (0.14 m^3). The number of full containers required to empty the surface water was then used to calculate the total volume of water stored. This was performed for both infiltration swales which were both made up of two storage surfaces called zone one and zone two. Figure 3.17 shows the work conducted to measure the volume for the surface storage volume, which is used in Chapter 5.

(a) dewatering surface water (b) 5 ft^3 (0.14 m^3) drum

Figure 3.17. Measuring Surface Storage Volume

3.4 Infiltration and Drawdown Experiments

The infiltration and drawdown experiments are a critical component of the infiltration swale evaluation process. This test quantifies two key parameters: infiltration rates and drawdown times. Infiltration rates indicate the swale's capacity to accept influent water, while drawdown times reflect the rate at which the stored water drains from the system. By analyzing these parameters, we can determine which infiltration swale exhibits superior performance in terms of water infiltration efficiency. Infiltration and drawdown experiments all use the same procedure for testing and are divided into different tests to evaluate the performance: (1) one-day versus three-day dry periods, (2) open versus closed valve for underdrains, (3) colder versus warmer months, (4) wet versus drier soils test, (5) overall performance. These different experiments were performed to help better understand how the infiltration swales perform under different scenarios that may happen in practical situations when implemented. For instance, infiltration swales located in areas with high or low frequency of rainfall, agencies that use underdrains with infiltration swales, and infiltration swales performance present with pre-wetted soils or drier soils. Furthermore, this section will discuss the set-up process and methodology of the infiltration and drawdown testing.

3.4.1 EXPERIMENTAL SET-UP

Figure 3.18 shows the modified and ALDOTIS experimental set-up in an aerial view. In Figure 3.18, the MIS area is denoted by the red boxes and callouts, while the ALDOTIS area is represented by the orange boxes and callouts. Even though the MIS has a different engineered media matrix design than the ALDOTIS design, all other components of the experiment are kept the same. For example, the swale channel length of 40 ft (12 m), swale bottom width of 4 ft (1.2 m), side slopes of 3:1, and both earthen check dam heights. Other factors that are kept the same are the water introductory flow systems, surface weir boxes, and the underdrain weir boxes.

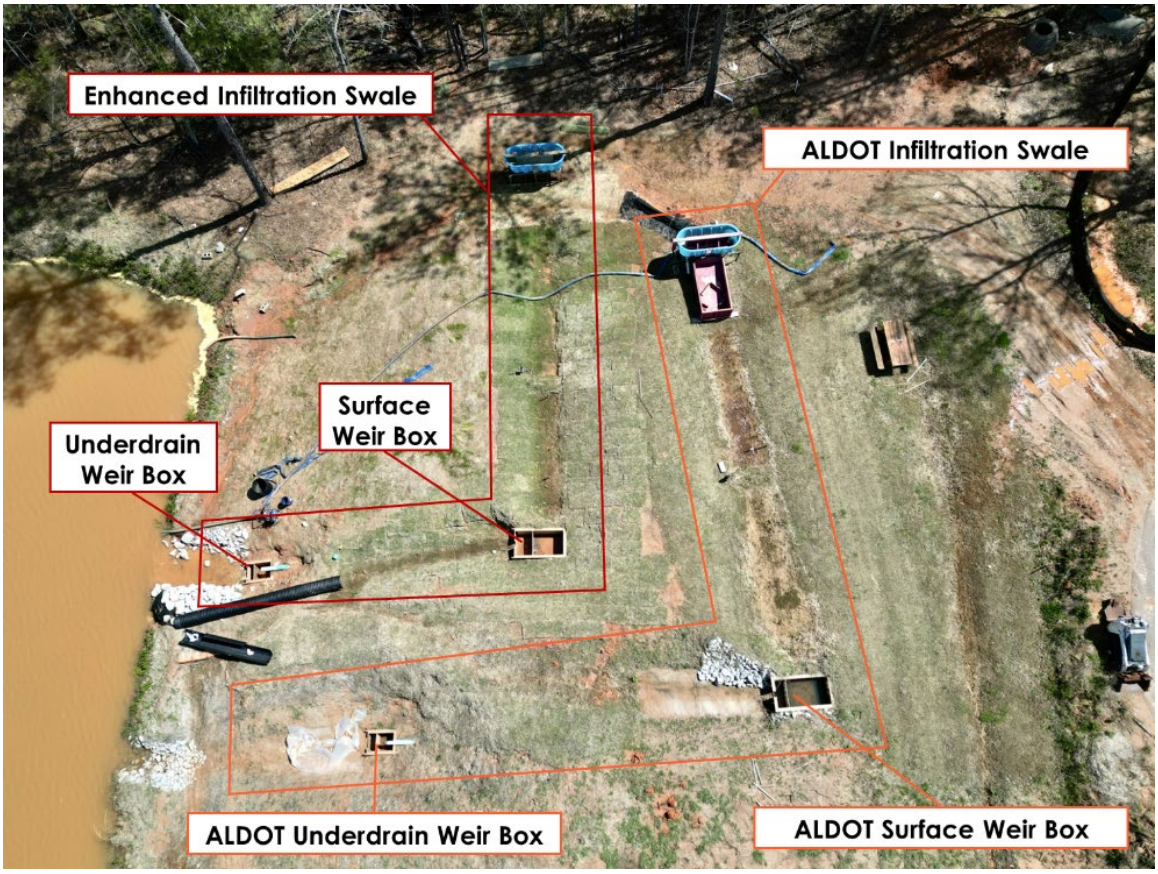

Figure 3.18. Aerial View of Infiltration Swale Set-Up

3.4.2 EXPERIMENTAL PROCEDURE

The experimental procedure for infiltration rate and drawdown time testing starts with the introductory flow systems at the upstream part of the swale. This system introduces a constant, predetermined flow rate of approximately 0.38 ft^3/s (0.01 m^3/s) into the first zone of the infiltration swale. The flow rate of 0.38 ft^3/s (0.01 m^3/s) was chosen because it represents the maximum capacity of the water it can pump. Zone one represents the first body of water the swale holds before checking dam one shown in Figure 3.19.

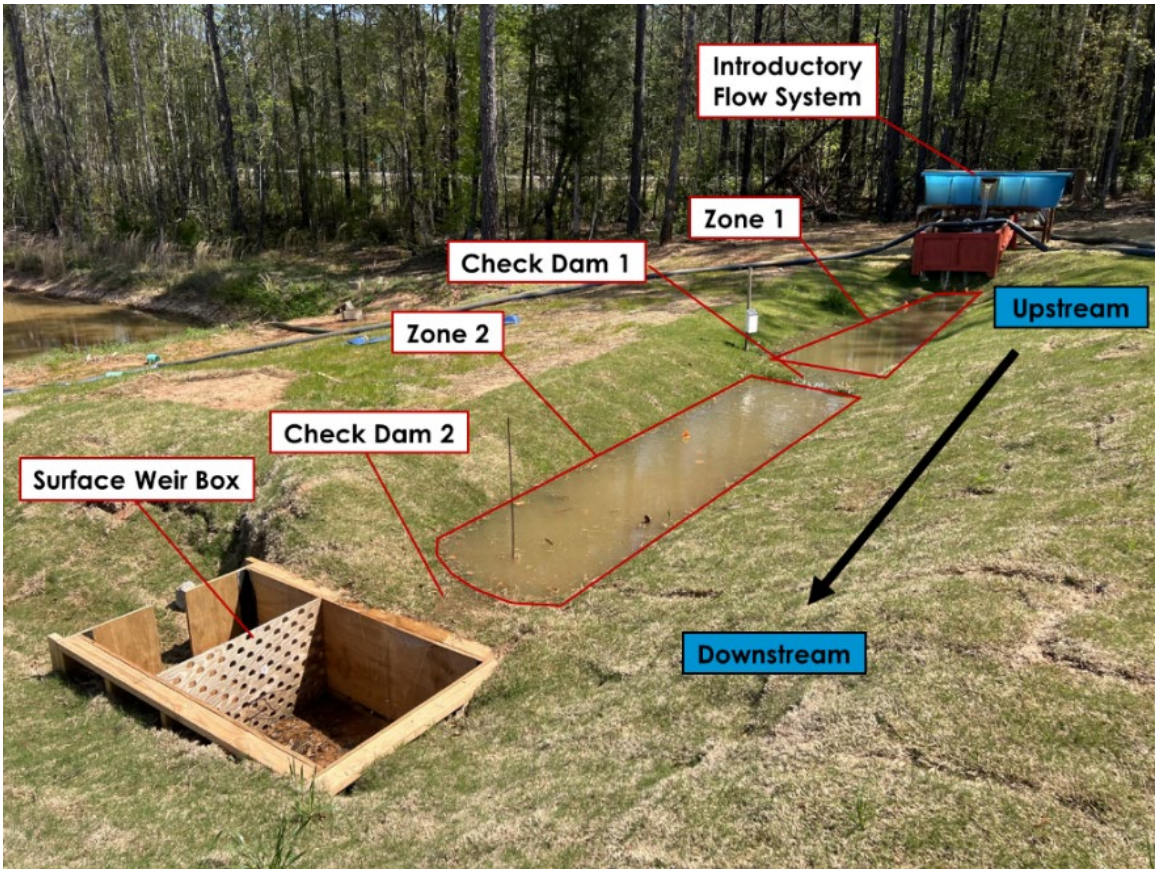

Figure 3.19. Infiltration Swale Set-Up

Infiltration rate testing for each infiltration swale followed a prescribed protocol. The inlet flow system was activated, introducing a constant flow rate of 0.38 ft^3/s (0.01 m^3/s) into zone one of the swales. The test proceeded as water accumulated within zone one. Once the water level surpassed the designated height of check dam one, excess water overtopped the dam and entered zone two, the second designated water storage zone.

The key measurement points for initiating flow shutoff occurred when Zone 2 achieved complete water storage capacity, signified by the absence of overflow into the surface weir box. While minimal overflow into the weir box might occasionally occur during testing, the protocol prioritized minimizing such occurrences. This emphasis stemmed from the critical need for accurate infiltration rate determination.

Infiltration rates are calculated based on the volume of water infiltrated through the swale media, not including water overflowing into the weir box. Overflow would lead to faster and inaccurate infiltration rate calculations. Consequently, infiltration rate testing commenced only after overflow into the surface weir box ceased entirely, indicating zone two had reached its maximum water depth.

Figure 3.20 illustrates two scenarios within the infiltration swale. Figure 3.20(a) depicts an overflow event, where the swale holds excessive water that spills into the surface weir box. Figure 3.20(b) portrays the optimal scenario for initiating the test, where the water level remains within the swale and does not overflow into the weir box.

(a) overflow into the weir box (b) no overflow into the weir box

Figure 3.20. Overflow into Surface Weir Box

Once zone two within each infiltration swale achieved complete water storage capacity, as established above, the infiltration rate testing commenced. During this phase, continuous water level measurements were collected at 15 second intervals using a levelogger positioned at the deepest point (downstream end) of zone two in each swale. This strategic placement ensured that infiltration rates were captured at the location with the maximum water depth and the longest anticipated drainage time. Consequently, this approach yielded the most accurate infiltration rate data, reflecting the behavior of a completely-filled swale throughout the drainage process. Figure 3.21 shows the location in zone two of the levelogger placement and close-up images of the perforated PVC casing that holds the levelogger.

(a) levelogger in PVC casing

(b) levelogger

(c) levelogger location

Figure 3.21. Levelogger Location in Infiltration Swales

To facilitate a robust comparison of infiltration rates and drawdown times between the infiltration swales, both test procedures were initiated simultaneously. This synchronized approach aimed to minimize the influence of external factors that could

potentially skew the results and compromise the evaluation of individual swale performance. Environmental conditions, such as variations in cloud cover, can impact infiltration rates. For example, sunny days often lead to increased evaporation and heating of the surface water storage, while cloudy days experience considerably less evaporation. By conducting the tests concurrently, the impact of these external factors on the performance of both the ALDOT and modified swales was effectively mitigated, yielding more reliable data for comparative analysis. Figure 3.22 shows both infiltration swales side-by-side during an infiltration and drawdown test.

(a) view from the downstream

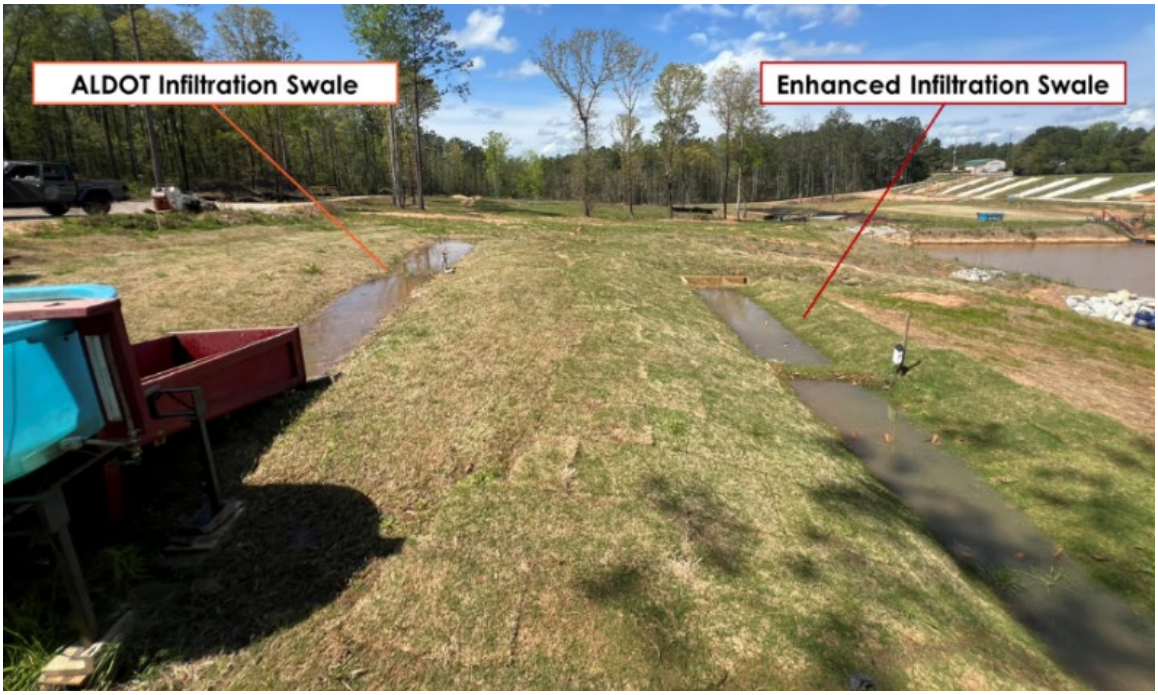

(b) view from the upstream

Figure 3.22. Infiltration and Drawdown Experiment

3.4.3 Infiltration Rate and Drawdown Data Collection

Upon complete drainage of the infiltration swales, signifying the test's conclusion, the leveloggers were retrieved from each swale. The data collected during the testing period was then downloaded and transferred to Excel spreadsheets for further analysis. The

downloaded data encompassed three key parameters for each time point: date, time of measurement, and corresponding water height within the swale.

The primary objective of this analysis was to determine the total drawdown time (time taken for complete drainage) and the associated infiltration rate for each infiltration swale test. To calculate the average infiltration rate for an individual test, the following steps were undertaken:

Initial Water Height: The initial water height, representing a completely full swale (approximately 0.70 ft or 0.21 m), was identified from the downloaded data set.

Final Water Height: A water height of 0 ft (0 m), signifying an empty swale, was designated as the final data point.

Water Height Difference: The difference between the initial and final water heights was calculated.

Drawdown Time: The total time it took for the swale to drain from the initial water height (0.70 ft or 0.21 m) to the final water height (0 ft or 0 m) was extracted from the downloaded data. This value served as the drawdown time for the specific test.

Infiltration Rate Calculation: Finally, the average infiltration rate (I) was determined using the following equation (4-2) formula:

$$I = \frac{(inital\ water\ height - final\ water\ height)}{drawdown\ time} \quad (4\text{-}2)$$

This formula calculates the average infiltration rate throughout the entire drawdown process because the infiltration rate is higher at the initial water height when the soil is dryer and the water height is larger to create a pressure. The drawdown time obtained in step 4 is directly incorporated into the infiltration rate calculation (step 5).

3.4.4 ONE-DAY VERSUS THREE-DAY DRY PERIOD INFILTRATION TEST

This infiltration and drawdown experiment is the one-day dry period versus the three-day dry period testing. The one-day dry period represents filling up both swales at the same time each day and letting them drain one day so that the start times of two filling events (mimicking two rainfall events) have a gap or dry period of 24 hours (one day). For instance, the swales were filled up completely with water once at the same time on Monday, Tuesday, Wednesday, and Thursday for the one-day dry period. For the three-day dry period, the swales were filled up at the same time but were filled every three days. For instance, both swales were filled up on Monday and the next time they were filled was on that Thursday and so on. The one-day dry period experiment represents a higher frequency of rainfall events. This represents dramatic rainfall events that would mimic a worst-case scenario if it rained every day for four to five days in a row. The three-day dry period experiment represents a normal rainfall frequency. The duration of three days in between filling the swales up was chosen because historical rain data from Montgomery, AL, on average showed rainfall events occur every three days. The one-day set-up will showcase both infiltration swale's

performance for an extreme rainfall event week while the three-day setup will showcase a more practical representation of performance if the infiltration swale was implemented in Central Alabama.

It is noteworthy to mention that these tests were performed in trying to avoid actual rainfall from interrupting or skewing the infiltration rates and drawdown times. The timing of these tests included monitoring the weather and finding a forecast that had no rain for days or weeks which were difficult to find living on the east coast. Lastly, all tests were conducted with the underdrain valve open unless mentioned otherwise.

3.4.5 Open versus Closed Valve Underdrains

A set of experiments comparing an open vs. closed underdrain was conducted to analyze the performance of both infiltration swales under varying underdrain configurations. Specifically, the comparison investigates the impact of a closed underdrain valve (no underdrain functionality) on infiltration rates and drawdown times compared to an open underdrain valve (functioning underdrain). This evaluation aims to determine the influence of the underdrain system on the swale's ability to infiltrate stormwater and achieve acceptable drawdown times without the underdrain's active contribution. According to established principles, open underdrain valves allow infiltrated water to readily enter the underdrain system and discharge quickly, facilitating faster drawdown and potentially higher infiltration rates. Conversely, closed valves restrict underdrain discharge, forcing water to infiltrate solely into the native soil, potentially leading to slower drawdown and infiltration.

3.4.6 Colder versus Warmer Months

Infiltration rates and drawdown times can be influenced by various environmental factors, including temperature. To assess the potential impact of seasonal variations, this section analyzes the infiltration data from the two infiltration swales with respect to the corresponding test months in Auburn, Alabama. By categorizing the data into colder and warmer months, we aim to investigate whether seasonal temperature fluctuations have a significant influence on the infiltration performance of the swales.

3.4.7 Wet versus Drier Underlying Soils

This section examines the influence of initial media and native soil moisture conditions on the performance of infiltration swales for all open valve tests. The analysis compares the swales' behavior under two scenarios: one with pre-wetted underlying media and soil, and another with drier underlying media and soil. Tests were classified as drier if it was the first day for each of the one-day dry period test, while subsequent days within that period were classified as wet. All tests within the three-day dry period tests were considered drier due to the three-day interval between rain (filling) events. All other tests were classified based on the presence of rainfall before the test commenced.

3.5 Overall Infiltration Performance Comparison

This section presents a comprehensive analysis of infiltration performance data collected from both the ALDOT swale and the modified swale. Given that the majority of infiltration tests were conducted with open underdrain valves, this analysis will exclusively focus on this configuration to maximize the sample size and ensure a more robust comparison between the ALDOT swale and the modified swale. By comparing the infiltration rates and drawdown times observed in these tests, we aim to establish a clear understanding of the relative performance of each swale design.

This comparative analysis is crucial for drawing definitive conclusions about the overall effectiveness of each swale. Ultimately, the results will help us determine which swale design exhibits superior infiltration capabilities and achieves faster drawdown times. This information is vital for guiding future design and implementation decisions for infiltration swales in stormwater management applications.

3.5.1 Settlement Measurement Points

In addition to infiltration rate and drawdown testing, an evaluation of the infiltration swales' settlement characteristics was undertaken. This assessment aimed to track the vertical displacement (settlement) of both infiltration swales over an extended period following construction.

Monitoring settlement is crucial because it can impact infiltration rates over time. Consolidation and settlement processes within the engineered media matrix can lead to a reduction in the overall volume of air voids. As these air voids decrease in size and quantity, the available storage capacity for infiltrating water diminishes. Furthermore, excessive settlement can contribute to clogging of the engineered media, further hindering infiltration. Therefore, settlement measurements for both swales were recorded throughout the project duration.

Settlement measurements for the infiltration swales needed an established network of fixed reference points throughout the length of each swale's bottom channel. Given the swale dimensions of 40 ft (12 m) in length and 4 ft (1.2 m) in bottom channel width, reference points were installed in cross-sections spaced at 5 ft (1.5 m) intervals along the channel. Each cross-section comprised three reference points: one at the center and one offset by 2 ft (0.6 m) to either side (left and right). The specific locations of these points are illustrated in Figure 3.23.

(a) wooden stakes and strings installation

(b) string crossing for point location

(c) orange steel nail installation

(d) settlement set-up completion

Figure 3.23. Settlement Point Set-Up

To establish the reference points, the following procedures were implemented. A tape measure was used to mark and install wooden stakes every 5 ft (1.5 m) along the longitudinal direction (parallel to the channel length) on both sides of the swale channel. The center point of the channel bottom width was identified and marked using wooden stakes placed at both the upstream and downstream ends of the swale. Wooden stakes were installed at an offset of 2 ft (0.6 m) to the left and right of the center point to establish the remaining two points within each cross-section. Strings were used to connect corresponding wooden stakes across the channel width, ensuring all points within a cross-section were aligned. The intersection points of the strings were marked with orange spray paint for improved visibility. Steel nails with bright orange markers were driven into the ground at each spray-painted location (refer to Figure 3.23[c]). These permanent markers facilitated easy visual identification during subsequent settlement measurements and allowed the nails to settle along with the swale bottom over time.

3.5.2 SETTLEMENT TEST

Following the establishment of the settlement measurement points (Section 2.5.1), monthly elevation measurements were obtained at each point for both infiltration swales. An automatic level laser survey instrument was employed to precisely measure the elevation of each reference point. A total of 24 points were installed and subsequently measured on a monthly basis commencing from the completion of swale construction.

It is important to note that the automatic level was not positioned at the same location for each monthly measurement. To address this, two permanent, external reference points were established outside the swale perimeter at locations unaffected by settlement. These fixed points served as the benchmark for all subsequent monthly settlement measurements. Figure 3.24 presents an aerial view of the ALDOTIS, illustrating the distribution of the 24 settlement points and the two external benchmark points.

Figure 3.24. Settlement Points

Elevation at each reference point was measured sequentially using the automatic level laser. The measured elevations were then documented in an Excel spreadsheet for further analysis. This process facilitated the pairing of corresponding points across each month's data set, enabling the identification of any elevation changes over time.

Following data transcription, the recorded elevations were converted from their original units to feet (meters) for consistency. Furthermore, an average elevation was calculated for each cross-section by averaging the individual elevations of the three points within that section. To determine the settlement at each cross-section, the average cross-section elevation was subtracted from the corresponding elevation measured at one of the two external fixed reference points.

Finally, the calculated settlement values for each cross-section were plotted on a monthly basis to visualize the settlement trends over time.

This section details and compares the infiltration performance of the traditional ALDOT swale to the modified swale. The lists below summarize different sections and results that are evaluated and discussed in this chapter:

- **Geotechnical and Native Soil Testing:** this section characterizes and classifies the underlying native soil and its infiltration properties to ensure the site is proper for infiltration swales.
- **Infiltration and Drawdown Evaluation:** explores how factors including simulated rainfall frequency (one-day vs. three-day dry period), underdrain configuration (open vs. closed valve), seasonal variation (colder vs. warmer months), initial moisture content (wet vs. drier), and overall performance comparison affect infiltration rates and drawdown times in both swales.
- **Overall Performance:** this section compares the overall infiltration efficiency of the two swales.
- **Statistical Analysis:** explores the MLR results and what factors had the most effect on infiltration rates.
- **Surface Storage Volumes:** assess the surface storage volume capacity and any discrepancies between the ALDOT and modified swales.
- **Moisture Content Sensor Evaluation:** data from moisture sensors installed within the swales provide insights into water movement patterns through the media layers.
- **Settlement Evaluation:** this section examines potential changes in surface elevation over time due to media compaction, which can impact infiltration capacity.

By analyzing these results, valuable insights into the effectiveness of each swale design and identify areas for potential improvement.

3.6 GEOTECHNICAL AND NATIVE SOIL CLASSIFICATION

This section integrates the findings from the construction phase (Section 4.2) with laboratory soil testing results and field infiltration data to evaluate the suitability of the native soil for an infiltration-based SCM. Determining site suitability for infiltration practices is crucial for ensuring the long-term effectiveness and functionality of infiltration swales. By carefully considering these factors and integrating the data from laboratory analysis and field testing, an informed decision can be made about the suitability of the site, for an alternative SCM may be needed for poor native soils.

3.6.1 SOIL LABORATORY TESTING

Figure 3.25 presents the collected soil profile from 0 to 9 ft (2.7 m) depths displayed in transparent plastic bags. The figure additionally incorporates the corresponding grain size results for each sample depth up to 7 ft (2.1 m). This combined visualization aids in comprehending the relationship between soil texture (as determined by grain size) and depth within the profile.

(a) boring profile

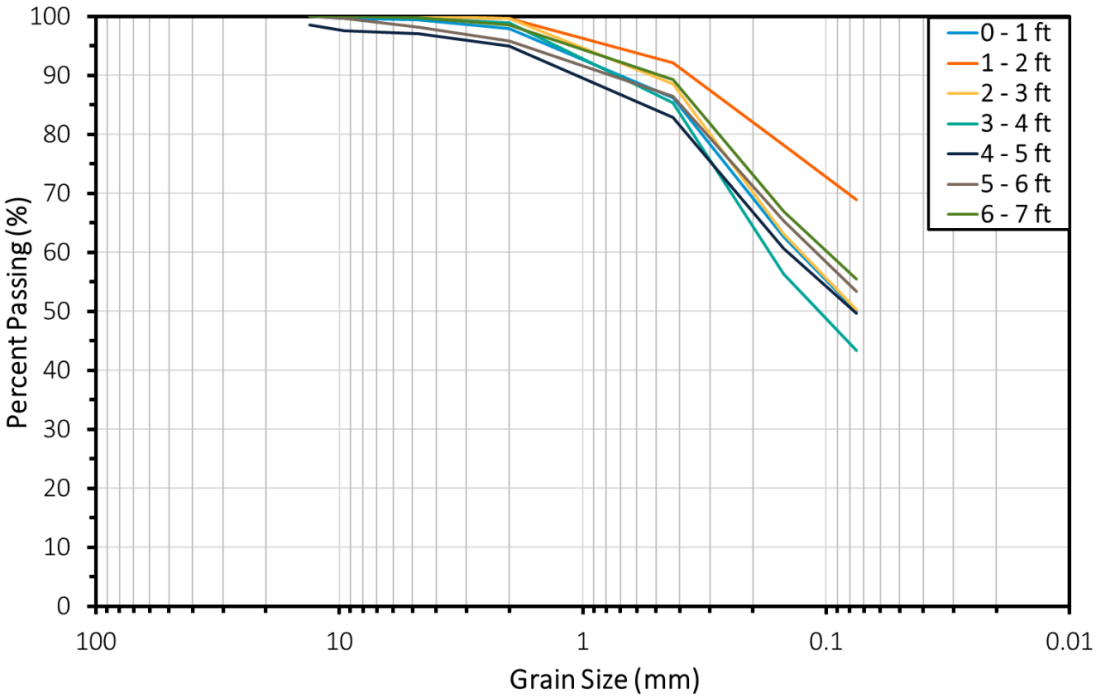

(b) grain size results

Figure 3.25. Native Soil Results

This analysis revealed that the in-situ soil at the AU-SRF site can be classified as a silty loam based on its particle size distribution and usage of a laser-induced spectroscopy. Knowledge of the soil texture (silty loam) allows us to leverage the Minnesota Department of Transportation (MnDOT) HSG classification system Table 3.1. This system categorizes soils based on their infiltration rate and drainage characteristics. Table 3.1 presents the MnDOT HSG table, listing soil groups A through D, their corresponding infiltration rates, and associated soil textures.

The classification of the soils at the site were silty loam soils as identified through the grain size analysis. Using Table 3.1, silty loam soils fall within the HSG B classification. This indicates the location is suitable for constructing infiltration swales, as HSG groups A and B are recommended by most DOTs across the country. HSG C soils may also be acceptable if they can achieve complete drainage within 48 hours.

Table 3.1. Hydrological Soil Table for MnDOT (MPCA 2022)

Hydrologic soil group (HSG)	Infiltration rate (in./hr)	Infiltration rate (cm/hr)	Soil textures
A	>1.63	> 4.14	Gravel, sandy gravel
	1.63a	4.14	silty gravels, gravelly sands, sand
	0.8	2.03	Sand, loamy sand, sandy loam
B	0.45	1.14	silty sands
	0.3	0.76	loam, silt loam
C	0.2	0.51	Sandy clay loam, silts
D	0.06	0.15	clay loam, silty clay loam, sandy clay, silty clay, clay

3.6.2 Field Infiltration Soil Testing

While the laboratory analysis classified the in-situ soil as a silty loam, potentially corresponding to an HSG B, field testing is crucial for verifying the actual infiltration rate at the designated infiltration swale construction site. This approach ensures long-term performance by confirming the suitability of the native soil for optimal infiltration. The infiltration rate for the deepest soil layer averaged approximately 0.55 in./hr (1.4 cm/hr). To account for potential variations and ensure long-term infiltration performance, a safety factor of two is often applied to field-measured infiltration rates. Dividing the raw infiltration rate by two results in a safety factor infiltration rate of. 0.28 in/hr. (0.7 cm/hr.). It is confirmed that the in-situ soil at the AU-SRF site sits between HSG B and C; however, 0.28 in/hr. (0.7 cm/hr.) sits closer to the HSG B class according to Table 3.1. This finding is close to the preliminary classification based on the soil texture classification (silty loam) determined through grain size analysis.

3.7 Infiltration And Drawdown Evaluation

A series of tests were conducted on both swales, focusing on two parameters infiltration rates and drawdown times. These two parameters are key findings in evaluating the performance of the infiltration swales. This section is divided into four different result sections to evaluate the performance: (1) one-day dry period versus three-day dry period, (2) open versus closed valve underdrains, (3) wet versus drier underlying soil, (4) overall infiltration performance comparison. These four different experiments were performed to help better understand how the infiltration swales perform under different scenarios that

may happen in practical situations when implemented. For instance, (1) infiltration swales located in areas with high or low frequency of rainfall, (2) agencies that use underdrains with infiltration swales, and (3) infiltration swales performance present with pre-wetted soils or drier soils. The testing methodology for all three experiments is the same as mentioned in Section 4.4, which entailed filling both swales up completely with water simultaneously and using the levelogger to record water depths at the deepest points and drawdown times till both swale's surfaces drained fully.

3.7.1 One-Day vs Three-Day Dry Periods

The experiment compared infiltration and drawdown performance under two simulated rainfall frequencies: one-day and three-day dry periods. The one-day scenario represents frequent rainfall events, while the three-day scenario reflects a more typical pattern based on historical Montgomery rain data. All tests were conducted under drier conditions to avoid real rain interference and used open underdrains unless otherwise specified.

Figure 3.26 illustrates the results collected from performing the one-day dry period versus the three-day dry period tests. This figure shows the surface water depth of the infiltration swales on the y-axis and time on the x-axis. The orange line represents the data collected from the ALDOT swale and the dark blue line represents the data collected from the MIS. Figure 3.26(a) shows the results collected from the three-day dry period tests and Figure 3.26(b) shows the results for the one-day dry period. Figure 3.26(b) had four tests performed because the last day for the one-day tests was a natural rainfall event that was not simulated and was excluded. Recorded water depths on Figure 3.26 do not decrease linearly with time, and that indicates the infiltration rates (slopes at any time of those drawdown curves) were not constant but changed with time: much larger infiltration rates at earlier hours and smaller in later hours. That is why *I* calculated using Equation (4-2) is an average infiltration rate for each drawdown experiment/testing.

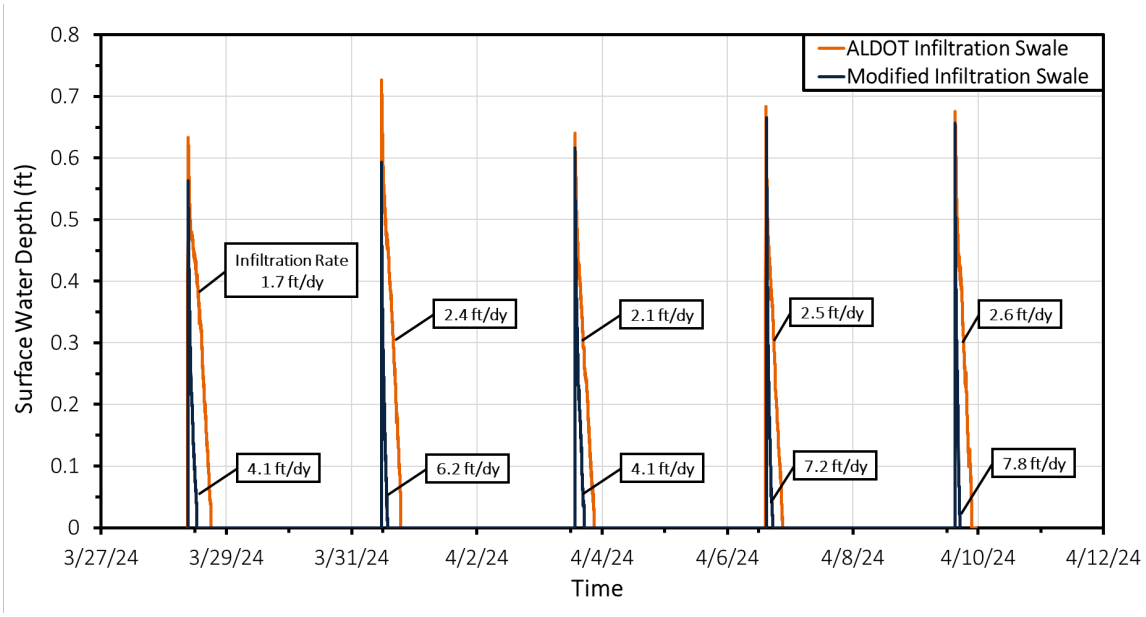

(a) three-day dry period

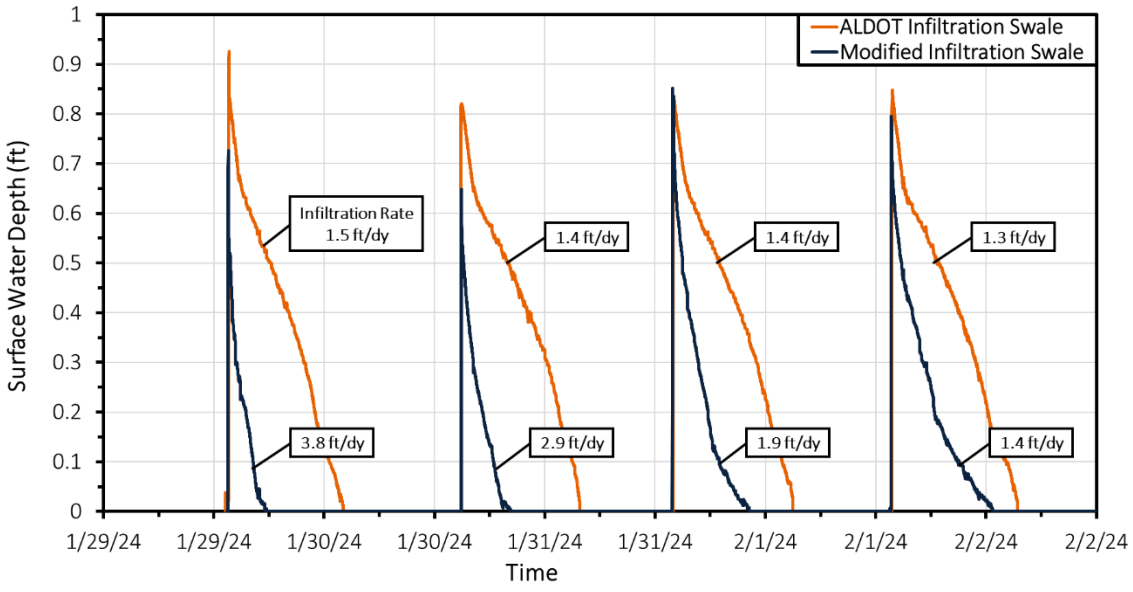

(b) one-day dry period

Figure 3.26. Dry Period Infiltration Rate Comparison

Focusing on the three-day interval infiltration rates first in Figure 3.26(a), the ALDOT swale exhibited an average infiltration rate of 2.26 ft/d (0.69 m/d), while the modified swale demonstrated a significantly higher rate of 5.88 ft/d (1.79 m/d), representing an approximately 2.6-fold increase. A two-sample t-test with pooled variance confirmed a statistically significant difference (p = 0.0008807) between the infiltration rates of the two swales, rejecting the null hypothesis at the 95% confidence level. Figure 3.26(a) three-day dry period test results showed that the modified swale outperformed the ALDOT swale. Focusing on the ALDOT swale, the infiltration rate recorded for the first test was 1.7 ft/d (0.52 m/d) while the following infiltration rates increased and stayed consistent within the range of 2.1 ft/d (0.64 m/d) to 2.6 ft/d (0.79 m/d). This consistent infiltration rate showed that the ALDOTIS can recover and maintain high infiltration rates for rain events that occur every three days. The infiltration rate recorded for the first MIS test was 4.1 ft/d (1.2 m/d) while the following days were also consistently high infiltration rates. Even though it decreased on the third test, this infiltration rate was almost double the infiltration rates recorded from the ALDOTIS. The MIS maintained high infiltration rates and showed it can recover and maintain high infiltration rates for rain events that occur every three days. Comparing them side by side, the MIS had infiltration rates that were 2.6 times faster than the ALDOTIS on average; however, both showed adequate infiltration rates that are acceptable. The three-day results show that both infiltration swales were able to fully drain and even maintain a consistent or increased infiltration rate through the testing duration.

Focusing on Figure 3.26(b), one-day dry period test results showed that the modified swale had faster infiltration rates, with averages of 2.5 ft/d (0.76 m/d) for the modified and

1.4 ft/d (0.43 m/d) for ALDOT, respectively, representing an approximate 1.8-fold increase. A two-sample t-test with pooled variance confirmed a statistically significant difference between the two swales (p = 0.04285), rejecting the null hypothesis at the 95% confidence level. The one-day dry period test represents a more extreme rainfall event to show how well the infiltration swales can recover. The ALDOTIS recorded an infiltration rate of 1.5 ft/d (0.46 m/d) for the first test and the following rates were close and consistent. This shows that the ALDOTIS infiltration rates did not decrease with increased soil moisture content from water being infiltrated every day. The infiltration rates are barely just above the required 1 ft/d (0.3 m/d) required by most DOTs across the country. This is cutting it close to the threshold and literature shows that over time the infiltration rates will slow down further from use. The modified infiltration rate recorded for the first test was 3.8 ft/d (1.2 m/d) and the following infiltration rates decreased after each day. The first three infiltration rates are high infiltration rates; however, the last infiltration rate of 1.4 ft/d (0.43 m/d) is around the consistent infiltration rate for the ALDOT swale. This means the performance of the modified swale matches the ALDOT swale when the fourth day of rain occurred. The one-day dry period test showed that the MIS outperformed the ALDOTIS for the first three days, but on the fourth day matched the performance of the ALDOTIS. Again, both swales drained within the 1 ft/d (0.3 m/d) and showed acceptable performance; however, the ALDOT infiltration rates were cutting it close.

Summarizing Figure 3.26, the ALDOT swale's infiltration rates on average increased from the one-day interval to the three-day interval by a factor of approximately 1.6. The modified swale's infiltration rates on average increased from the one-day interval to the three-day interval by a factor of approximately 2.3. The main take away from comparing infiltration swales from the three-day test to the one-day test is that increased rainfall frequency decreased infiltration rates for both swales. Lasty, the test shows that both swales can sustain infiltration performance for the three-day interval while for the one-day interval the infiltration performance decreases after each test.

Figure 3.27 presents the same three-day and one-day tests shown in Figure 3.26, but instead of the infiltration rates, it represents the drawdown times to empty from being full of water. Figure 3.27(a) shows the results from the three-day dry period tests and Figure 3.27(b) shows the results from the one-day dry period test. The infiltration rate of each test is above each bar.

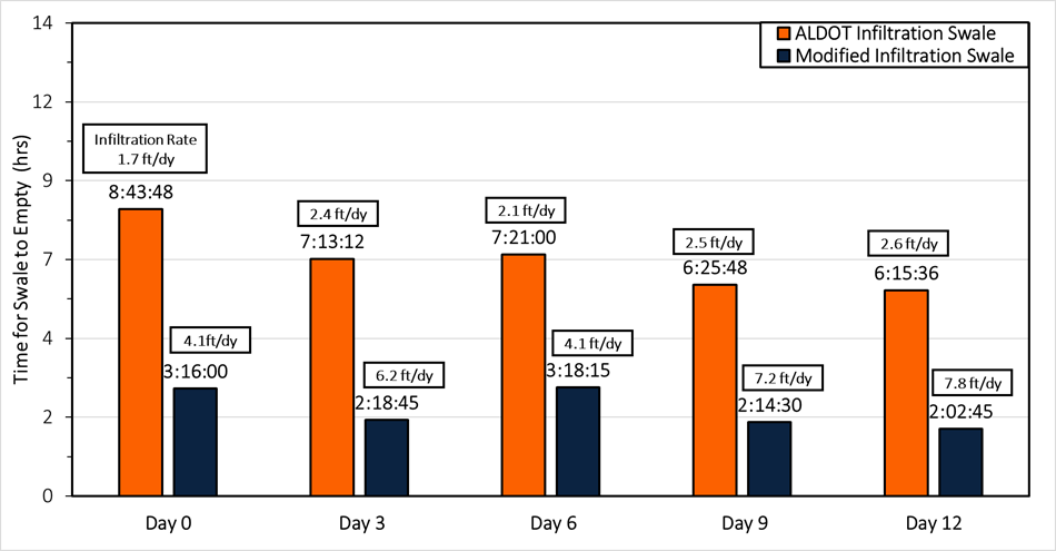

(a) three-day dry period

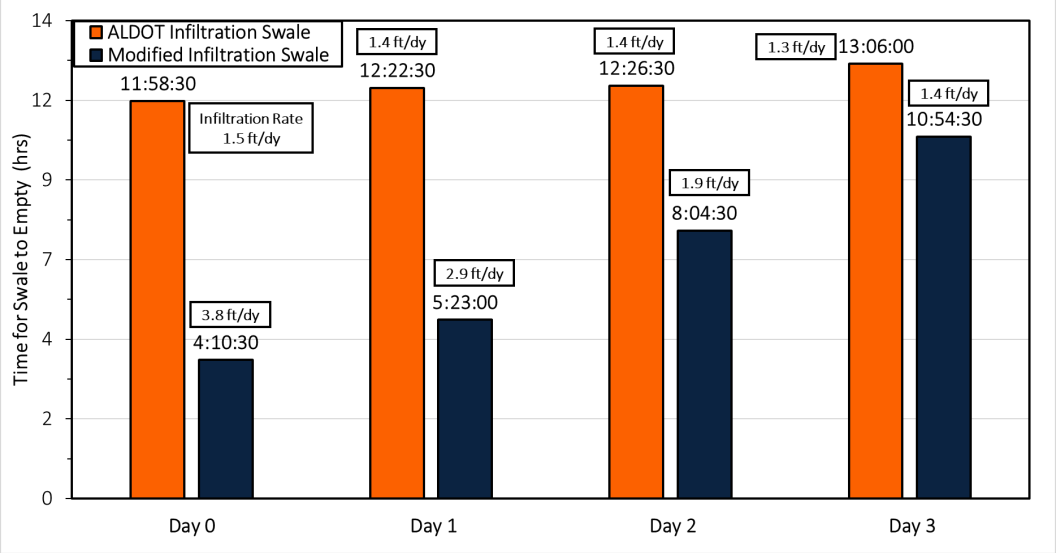

(b) one-day dry period

Figure 3.27. Dry Period Drawdown Time Comparison

Observing Figure 3.27(a), the three-day dry period bar graph, the ALDOT swale achieved complete drainage in an average of approximately 7 hours. The modified swale achieved complete drainage in an average of approximately 2.6 hours. The modified swale drained roughly 2.7 times faster than the ALDOT swale and both swales showed consistent times across each test. The ALDOT swale drawdown times were consistent for each test varying from 6.3 hours to 7.35 hours. These drawdown times are considered fast times and represent adequate performance. However, the MIS significantly outperformed the ALDOT swale with consistent drawdown times varying from 2.03 hours to 3.3 hours which is almost triple the speed of the ALDOT swale. Once again Figure 3.27(a), shows that both swales can recover and keep consistent performance for the three-day interval.

Observing the Figure 3.27(b), the one-day dry period bar graph, the ALDOT swale achieved complete drainage in an average of approximately 12.5 hours. The modified swale achieved complete drainage in an average of approximately 7.1 hours. The modified swale drained roughly 1.8 times faster than the ALDOT swale, and drawdown times remained consistent for the ALDOT swale and increased for modified. The ALDOT swale drawdown times, similar to the infiltration rates, were consistent for each test varying from 11.97 hours to 13.1 hours even though the times were predicted to be longer after each test since the rainfall frequency increased. These drawdown times are still considered fast times and represent adequate performance since they are less than 24 hours. The MIS outperformed the ALDOT swale with drawdown times increasing after each rainfall event varying from 4.17 hours to 10.9 hours. This increase in rainfall frequency to one day affected the MIS more than the ALDOT swale; however, the modified swale still showed enhanced performance. The ALDOT times staying consistent, for the one-day dry period is explained in the underdrain influence section in 5.3.1.1.

Overall, despite the longer drawdown times under more frequent rainfall, it's important to note that both swales achieved complete drainage within 24 hours for all test scenarios. A key takeaway is the clear impact of rainfall frequency on drawdown times. When subjected to more frequent rainfall events, e.g., with one-day dry periods, both swales exhibited longer drawdown rates and reduced infiltration rates compared to the three-day day period. This is expected as the soil has less time to dry between rain events. Results also provide evidence that both swales recover infiltration performance for the three-day dry period which is the average historical time interval for rainfall events in central Alabama.

3.7.2 Underdrain Influence Discussion

Noteworthy mentions from Figure 3.26(b) and Figure 3.27(b), the one-day dry period tests, the ALDOT infiltration rates and drawdown times were consistent over the four testing days while the modified infiltration rates and drawdown times slowed after each test.

The distinct discharge patterns observed between the ALDOT and modified swales under identical underdrain conditions suggest potential differences in media performance. While the modified swale demonstrated consistent underdrain discharge after each test, the ALDOT swale exhibited no discharge. This disparity may be attributed to media infiltration rates and seepage into the native soil. It is predicted that ALDOT's low infiltration rates from the topsoil and sand layers into the gravel layer, coupled with the relatively low seepage rate of the native soils, did not allow infiltrated water to impound within the gravel layer to the level sufficient to flow into the underdrain. The addition of the geotextile fabric between the sand and the gravel layer is another obstacle that may cause slow infiltration into the gravel layer. Geotextiles clogging was found in the small-scale testing (MPCA 2022) and is backed by evidence from literature reporting clogging occurs most at the geotextile fabric layer (MPCA 2021).

The above test series were conducted with both valves on the underdrain closed. This ensured the swales function as designed, allowing for a more accurate assessment of their infiltration rates and drawdown times under real-world conditions.

3.7.3 OPEN VS CLOSED VALVE UNDERDRAIN

This section examines the impact of underdrain valve configuration (open versus closed) on infiltration swale performance. The analysis focuses on how the underdrain system influences infiltration rates and drawdown times without its active contribution (closed valve). Open underdrains likely promote faster drawdown and potentially higher infiltration rates by allowing infiltrated water to readily discharge. Conversely, closed underdrains may hinder these processes by restricting water discharge.

Figure 3.28(a) depicts the results from the ALDOT swale tests and Figure 3.28(b) shows the results from the modified swale tests. Yellow lines represent the valve was closed during the test and the blue line represent the valve was open during the test.

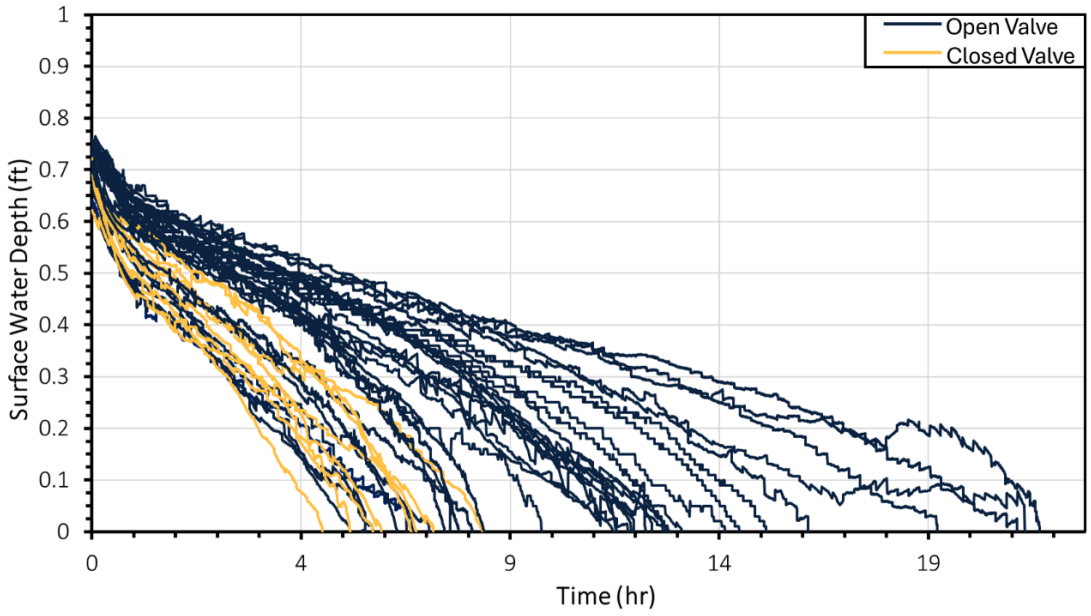

(a) ALDOT swale

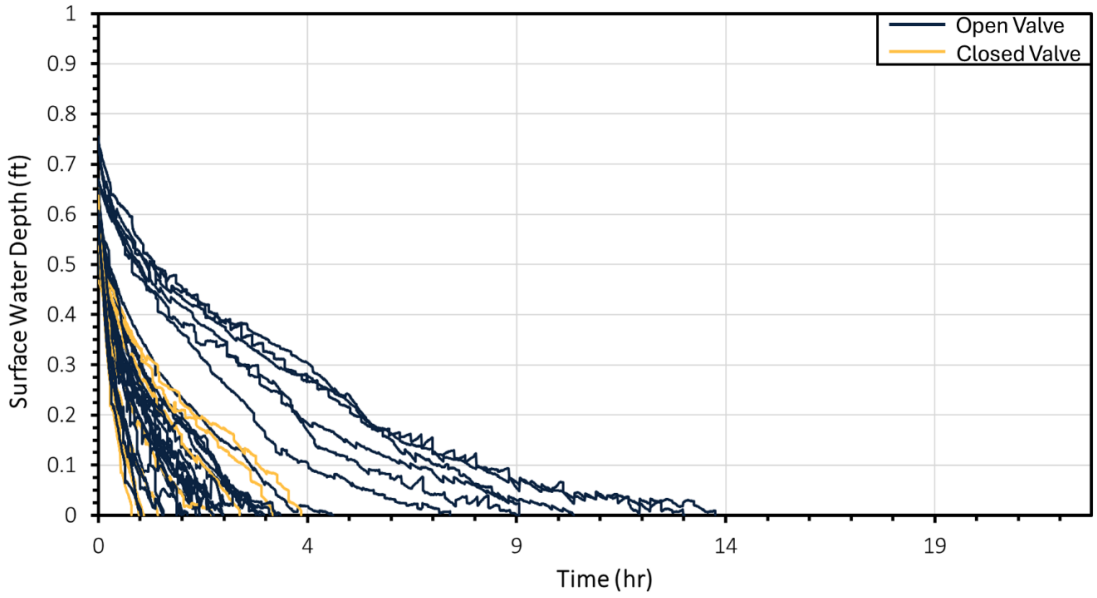

(b) modified swale

Figure 3.28. Open vs. Closed Valve Underdrains Comparison

The ALDOT swale, Figure 3.28(a), for the open valve configuration (n=32), an average infiltration rate of 1.6 ft/d (0.49 m/d) and an average drawdown time of 12 hours were observed. Conversely, the closed valve configuration (n=8) demonstrated a higher average infiltration rate of 2.5 ft/d (0.76 m/d) and a shorter average drawdown time of 6.97 hours. A Welch's t-test revealed a statistically significant difference (p=0.0002279) between the two conditions, with the closed valve configuration exhibiting superior performance.

Contrary to the prediction, the open underdrain valve configuration did not demonstrate improved infiltration rates or drawdown times compared to the closed valve configuration. As previously mentioned, the ALDOT underdrain system exhibited no observable discharge during tests with an open valve. Consequently, the data collected from the ALDOT swale for open and closed valve tests cannot be definitively used to isolate the influence of the underdrain on the swale's performance. Also, most of the open valve tests were performed in the winter with colder temperatures. Further investigation of seasonal variation on the open valve and closed valve comparison is shown further below where the open and closed valve tests were performed in the same month in Figure 3.29.

The modified swale, Figure 3.28(b), exhibited significantly higher performance metrics compared to the ALDOT swale. Under the open valve condition (n=27), it achieved an average infiltration rate of 5.2 ft/d (1.6 m/d) and an average drawdown time of 5 hours. When the underdrain valve was closed (n=8), performance was further enhanced, with an average infiltration rate of 9.5 ft/d (2.9 m/d) and a reduced drawdown time of 2.3 hours. A Welch's t-test indicated a no statistical significance difference in infiltration rates between the open and closed valve conditions for the modified swale ($p=0.01112$). The sample average of open valve infiltration rates is smaller than the sample average of closed valve, but not small enough to be statistically significant.

The results for the modified swale, Figure 3.28(b), deviate from the anticipated trend, similar to the findings from the ALDOT swale. The modified swale exhibited slower infiltration performance on average with an open underdrain valve compared to a closed valve. Unlike the ALDOT swale, the modified swale's underdrain system functioned as designed, with significant discharge observed during open valve tests.

A potential explanation for this unexpected outcome in the modified swale results may lie in the seasonal timing of the tests. As Figure 3.28(b) indicates, open valve tests were primarily conducted during the winter months (January to March) in Auburn, AL, when temperatures are lower. Lower winter temperatures can lead to increased water viscosity, and fluids with higher viscosity tend to infiltrate slower than those with lower viscosity. Conversely, the closed valve tests were conducted in April and June, coinciding with warmer temperatures and higher sunlight exposure. Warmer temperatures are associated with decreased water viscosity, potentially contributing to the faster infiltration observed in these closed valve tests. The next group of tests presented below was performed under open or closed valves within the same month to investigate any changes in performance of the valve within the same season.

Figure 3.29 shows a one-day dry period testing over four days for an open valve and for closed valve. The closed valve test was performed from 6/7/2024 to 6/10/2024 and the open valve the week after from 6/13/2024 to 6/16/2024.

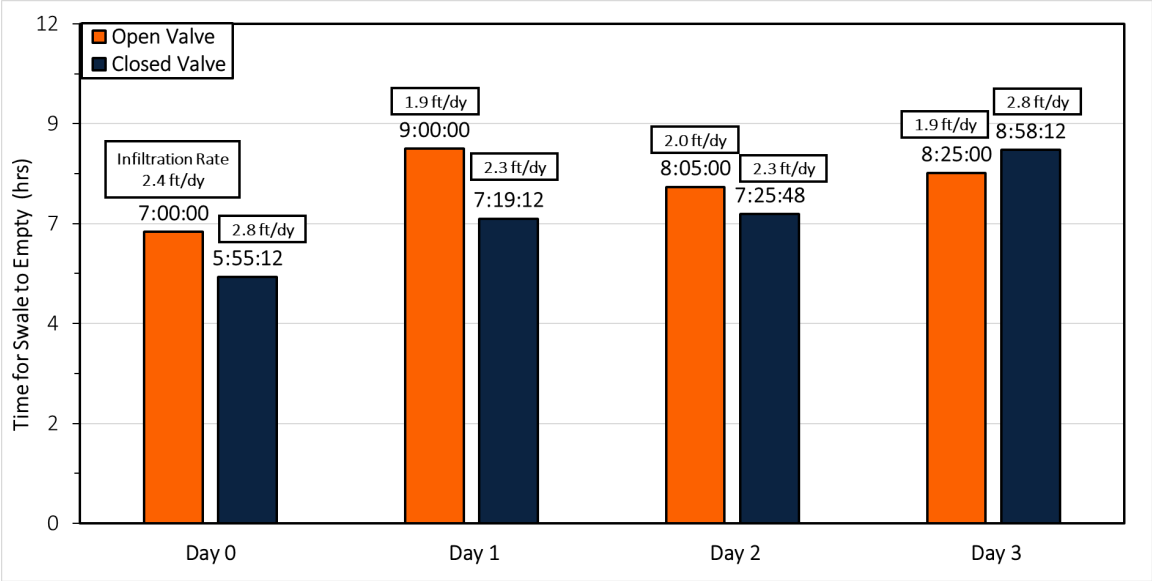

(a) ALDOT swale

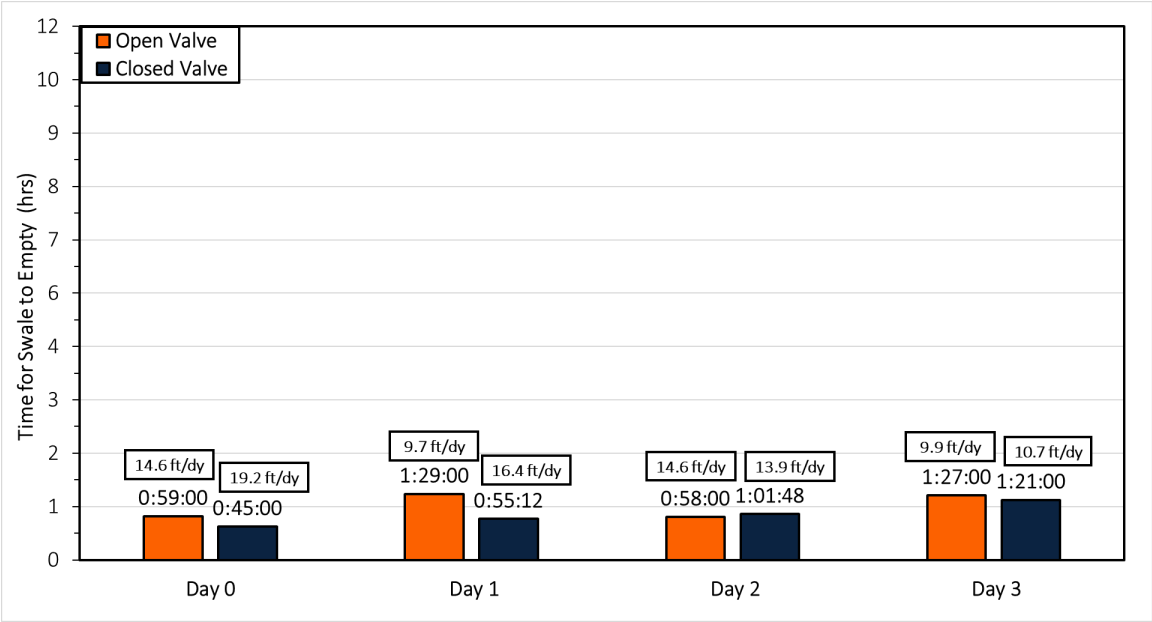

(b) modified swale

Figure 3.29. Open vs. Closed Valve One-Day Dry Period Comparison

A closer examination of the open and closed valve test results for the ALDOT swale (Figure 3.29[a]) reveals a narrower range of performance between the two configurations compared to previous observations. The difference between the sample average of open valve and closed valve is not big enough to be statistically significant. The p-value equals 0.3502, this means that the chance of type I error, rejecting a correct H_0, is too high: 0.3502 (35.02%). While the closed valve again exhibited slightly faster performance with an average drawdown time of 7.4 hours and an average infiltration rate of 2.3 ft/d (0.7 m/d), these values are closer to those achieved by the open valve with average drawdown time of 8.1 hours and

average infiltration rate of 2.1 ft/d (0.64 m/d). Notably, the open valve tests were conducted only two days following the completion of the closed valve tests. This temporal proximity raises the possibility that residual soil moisture from the closed valve tests may have influenced the performance of the open valve tests, potentially leading to slower infiltration rates in the latter case.

Overall, the findings suggest that the underdrain system in the ALDOT swale does not function as intended. The observed results likely represent a scenario where both configurations essentially performed under closed valve conditions due to the lack of observed discharge from the underdrain.

Observing Figure 3.29(b), the modified swale's valve comparison, similar to the ALDOT swale, the closed valve configuration exhibited marginally superior performance with an average drawdown time of 1 hour and an average infiltration rate of 15 ft/d (4.6 m/d) compared to the open valve (average drawdown time: 1.2 hours, average infiltration rate: 12.3 ft/d (3.7 m/d). The difference between the sample average of open valve and closed valve is not big enough to be statistically significant. The p-value equals 0.2749, this means that the chance of type I error, rejecting a correct H_0, is too high: 0.2749 (27.49%). The test statistic T equals -1.2014, which is in the 95% region of acceptance: [-2.4469: 2.4469]. As observed in the ALDOT swale tests, the open valve tests were conducted shortly after the completion of the closed valve tests (two days). This temporal proximity might have influenced the open valve results, with residual soil moisture from the preceding closed valve tests potentially leading to slightly slower infiltration rates.

However, unlike the ALDOT swale, the modified swale underdrain system appears to function as designed. This is evidenced by the observed decrease in infiltration rates and drawdown times following each test in the closed valve configuration, which aligns with the expected trend of reduced performance over subsequent tests due to increased soil moisture. Interestingly, the open valve tests do not exhibit a clear pattern, with Day 2 even showing slightly better performance compared to other days. This might be due to the two tests performed before Day 2, potentially leading to a temporary increase in effective porosity within the media.

Notably, the performance metrics (infiltration rate and drawdown time) for both open and closed valve tests conducted in June are relatively similar. This suggests that the underdrain may not have had a significant impact on infiltration performance during this specific month. It is important to acknowledge the limitations of this study, particularly the lack of data from closed valve tests conducted in colder months. Future investigations exploring the influence of the modified swale's underdrain on performance could benefit from incorporating additional environmental factors such as water temperature, soil temperature at various depths, and sunlight exposure at the swale surface. Analyzing these additional parameters alongside infiltration data might provide more conclusive evidence regarding the influence of seasonal variations on infiltration performance in the modified swale.

3.7.4 SEASONAL VARIATION

Figure 3.29 explores the potential influence of seasonal temperature variations on infiltration rates. To investigate this concept further, the infiltration data obtained from the existing ALDOT and MIS open/closed valve tests (Figure 3.28) were utilized. In Figure 3.30, each data curve is linked to a specific calendar month, and the curves are categorized based on the corresponding season in Auburn, Alabama (colder vs. warmer). The teal-colored curves represent infiltration tests conducted during the colder months (late November to mid-March), while the red-colored curves depict tests performed during the warmer months (late March to June).

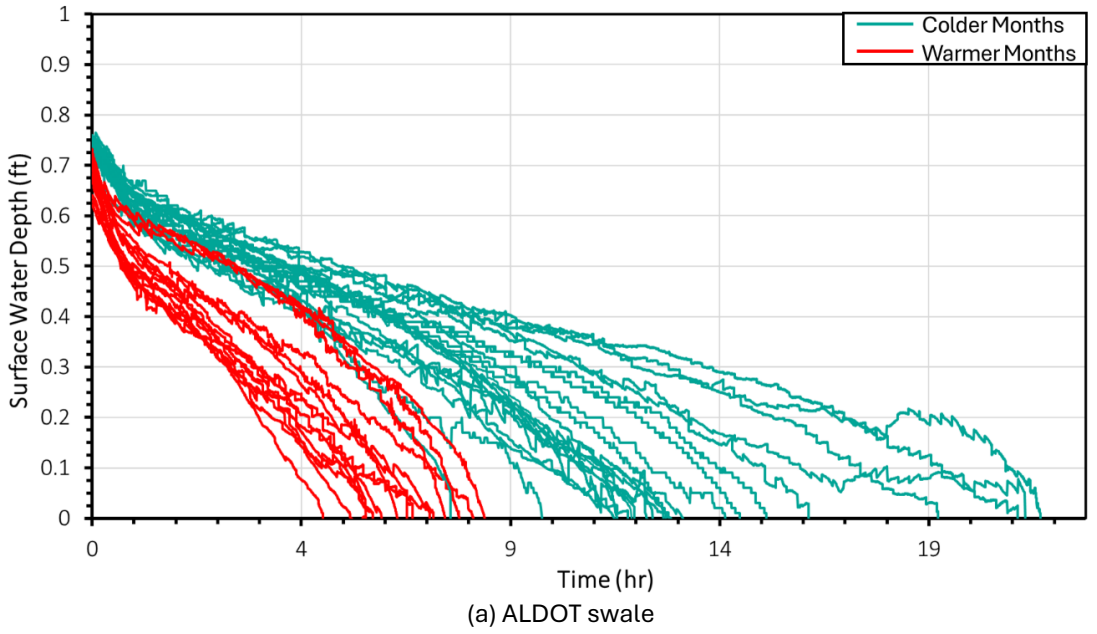

(a) ALDOT swale

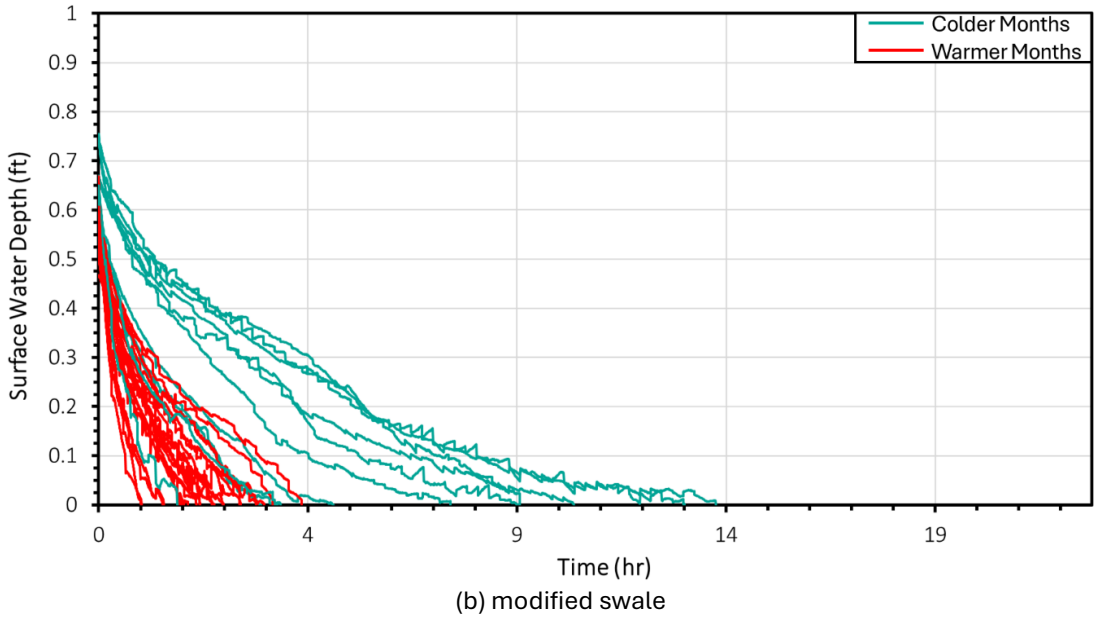

(b) modified swale

Figure 3.30. Seasonal Variation Comparison

The ALDOT swale, Figure 3.30(a), exhibited seasonal variations in infiltration performance. During colder months (n=21), the average infiltration rate was 1.3 ft/d (0.39 m/d) with an average drawdown time of 14.4 hours. Conversely, warmer months (n=11) demonstrated improved performance, with an average infiltration rate of 2.2 ft/d (0.67 m/d) and a reduced drawdown time of 7.5 hours.

The modified swale, Figure 3.30(b), demonstrated a pronounced seasonal influence on its performance. During colder months (n=12), the swale exhibited an average infiltration rate of 2.7 ft/d (0.82 m/d) and an average drawdown time of 8.5 hours. In contrast, warmer months (n=15) saw a significant increase in performance, with an average infiltration rate of 7.2 ft/d (2.2 m/d) and a reduced drawdown time of 2.3 hours.

The results from Figure 3.30 reveal a distinct pattern: colder months are associated with slower infiltration rates and longer drawdown times for both swales. Conversely, warmer months exhibit enhanced infiltration rates and faster drawdown times. The ALDOT swale displayed nearly doubled infiltration rates and drawdown times in warmer months compared to colder months. Notably, the MIS demonstrated a more dramatic seasonal effect. Warmer months yielded nearly four times faster infiltration rates and drawdown times in the modified swale compared to colder months. These findings suggest that while both swales exhibit improved performance in warmer temperatures, the MIS design experiences a greater relative increase in infiltration capacity.

The impact of seasonal variations on swale performance is further evidenced by the drainage time data collected during one-day dry period tests. The modified swale exhibited a clear trend of decreasing drainage times throughout the year, with values ranging from 4.2 to 10.9 hours in January, 2 to 3.8 hours in May, and 0.9 to 1.5 hours in June. The overall pattern indicates faster drainage times from warmer months. To further evaluate seasonal variation, a linear regression was conducted for both swales showing the correlation of water temperature pumped into the swale versus the infiltration rate found when the test was completed. Observing Figure 3.31 illustrates a stronger correlation between water temperature and infiltration rate for the ALDOT swale compared to the modified swale, as indicated by R-squared values of 0.91 and 0.75, respectively.

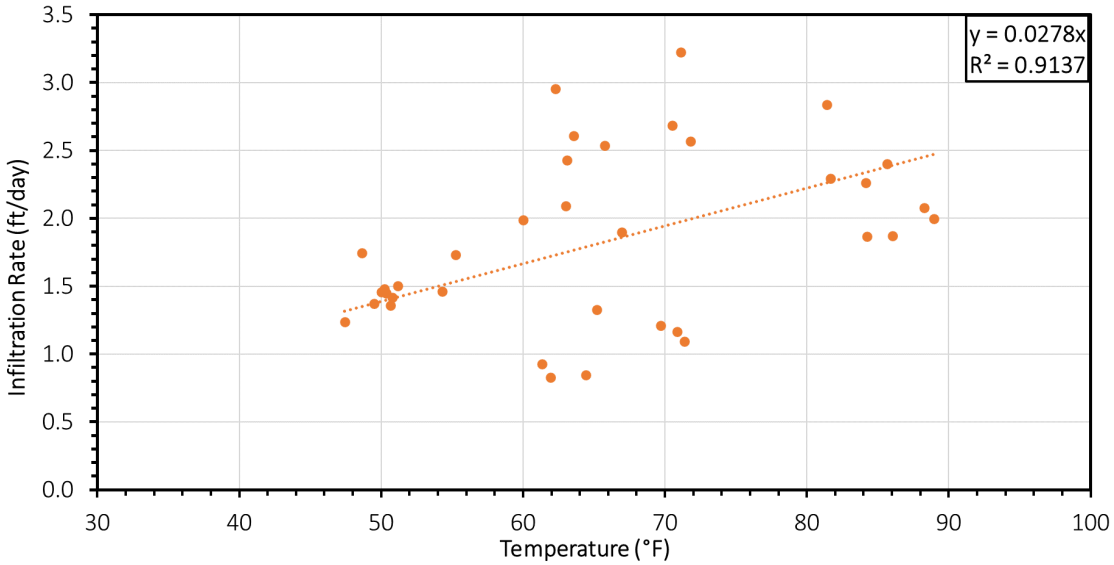

(a) all ALDOT swale tests

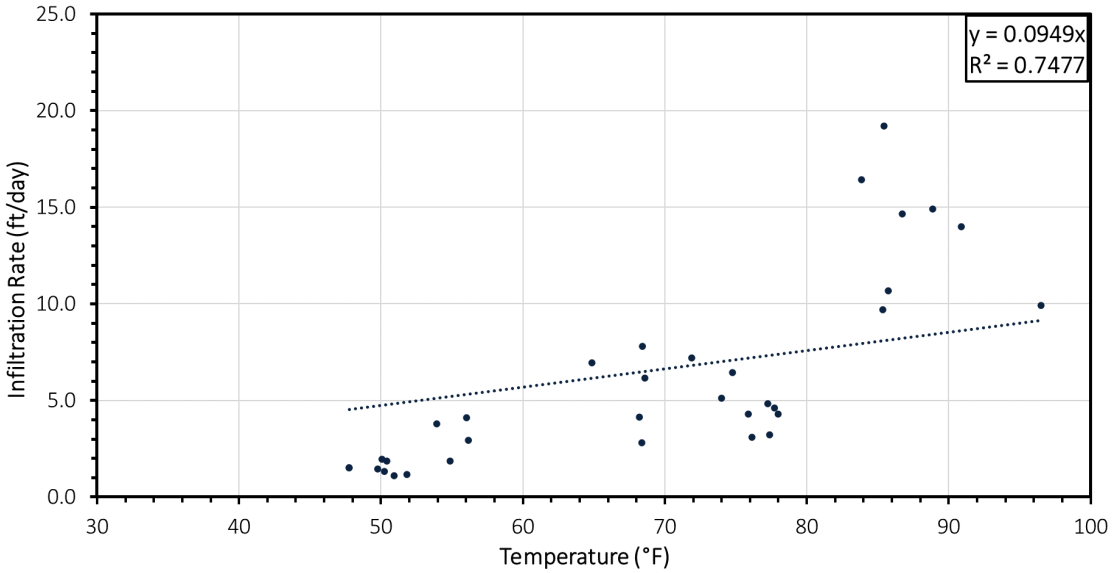

(b) all modified swale tests

Figure 3.31. Water Temperature vs Infiltration Rates

While the R-squared value for the modified swale indicates a moderate correlation, it nonetheless contributes to the overall understanding of seasonal influences on infiltration performance for both swale types. To further elucidate these seasonal patterns, continued data collection throughout the subsequent year is recommended. This would allow for a more robust evaluation of the observed seasonal trends in infiltration rates and drawdown times. By replicating the findings across multiple winter seasons, we can strengthen the confidence in the observed relationship between temperature and infiltration performance.

3.7.5 WET VERSUS DRIER UNDERLYING SOILS

This section analyzes how initial moisture content (wet vs. drier) in the swale media and native soil affects infiltration performance under open valves. It compares pre-wetted scenarios to drier conditions. Notably, only the first day of each one-day dry period is considered drier, while subsequent days are considered wet. All three-day dry period tests are considered drier due to the longer interval between rain events.

Figure 3.32 presents red curves representing the drier test, while blue curves represent the wet test. Established research suggests a negative correlation between infiltration capacity and increased soil moisture (Meter Group 2024). This well-established principle is demonstrably evident in Figure 3.32(a). It reveals a clear trend where tests conducted under initial wetted conditions (presumably corresponding to later days within the testing period) exhibit demonstrably longer drawdown times compared to those with drier initial conditions (likely corresponding to the first day of each testing period). This observation aligns with the established principle, suggesting that soils with increased moisture exhibit a slower infiltration rate, resulting in extended drawdown times. While Figure 3.32(a) aligns with established principles regarding the impact of initial moisture content, Figure 3.32(b) presents a contrasting observation. Notably, Figure 3.32(b) includes wet test data points with drawdown times comparable to those observed in drier tests. This seemingly contradicts the expected negative correlation between infiltration and soil moisture. This unexpected finding warrants further investigation to elucidate potential explanations. One possibility is that the modified swale's design or material composition may mitigate the influence of soil moisture to a greater extent compared to the ALDOT swale. Future research could explore the specific mechanisms by which the modified swale design might achieve this effect.

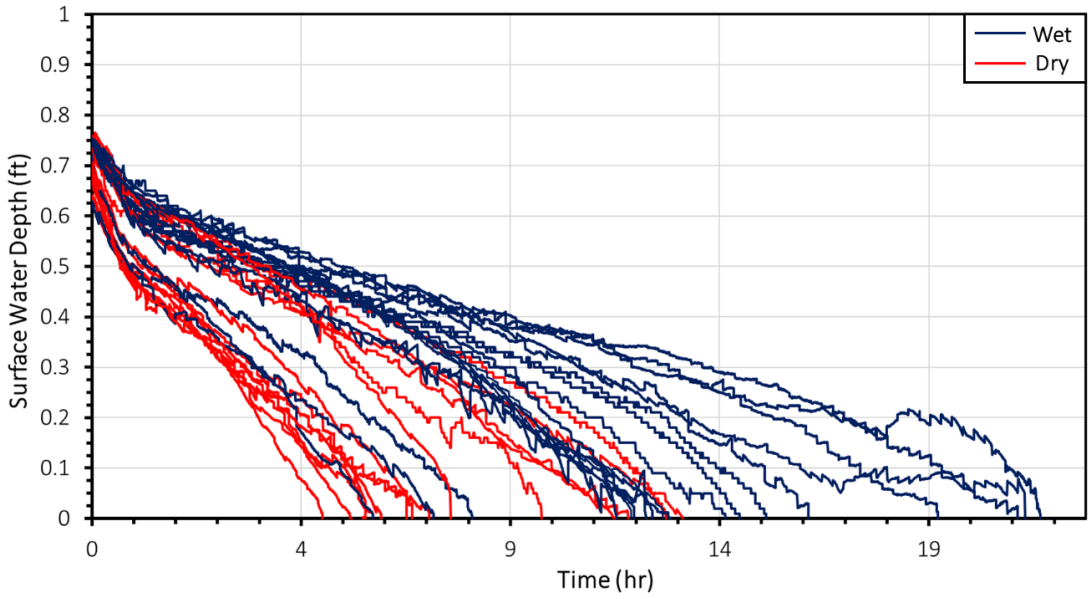

(a) ALDOT swale

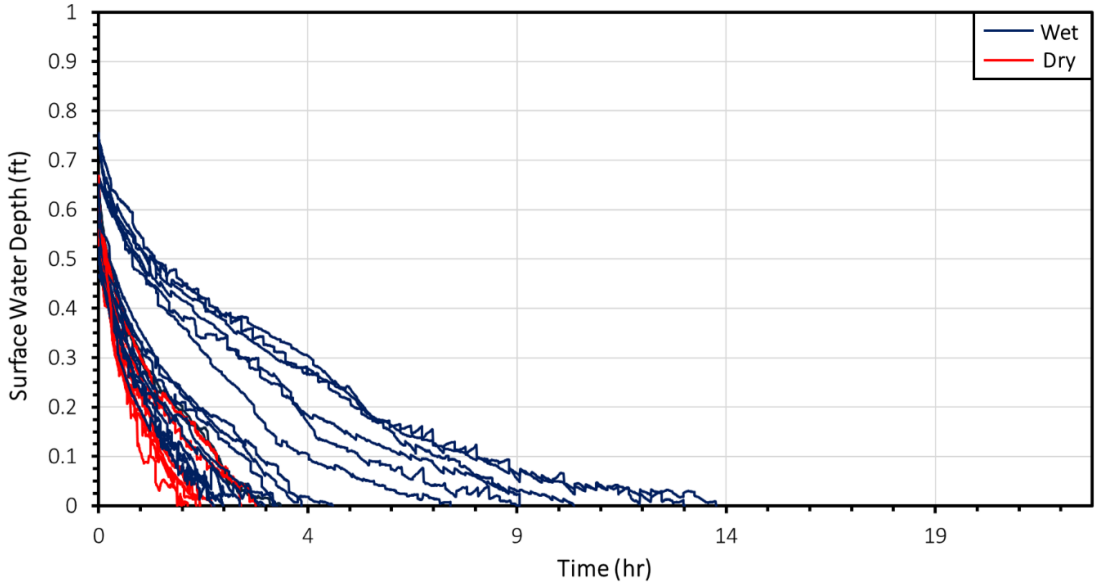

(b) modified swale

Figure 3.32. Wet vs. Drier Soils

The ALDOT swale, Figure 3.32(a), exhibited varying performance under different soil moisture conditions. In wet soil conditions (n=20), the average infiltration rate was 1.4 ft/d (0.43 m/d) with an average drawdown time of 13.7 hours. Conversely, drier soil conditions (n=13) resulted in improved performance, with an average infiltration rate of 2.1 ft/d (0.64 m/d) and a reduced drawdown time of 8.72 hours. A two-sample t-test with pooled variance confirmed a statistically significant difference (p=0.0002872) between the two soil moisture conditions, with drier soils demonstrating superior infiltration characteristics.

Figure 3.32(a) provides compelling evidence regarding the influence of initial soil moisture conditions on the ALDOT swale's performance. The drier test data points cluster in the bottom left corner of the graph, signifying both faster drawdown times and higher infiltration rates. Conversely, the wet test data points tend to concentrate towards the upper right portion of the Figure 3.32(a), indicating slower drawdown times and lower infiltration rates. While outliers exist in both categories, the overall trend suggests a clear separation between the two datasets. The findings are further corroborated by numerical data, demonstrating a statistically significant difference between the average wet soil infiltration rate and the average drier soil infiltration rate. The sample average infiltration rate under wet soil conditions is demonstrably lower than the sample average under drier soil conditions. The data further indicates that drier soil conditions within the ALDOT swale lead to an average drawdown time reduction of approximately 5 hours and an infiltration rate increase of 1.5 times compared to wet soil conditions. These findings highlight the importance of managing soil moisture content to optimize the performance of the ALDOT swale.

The modified swale, Figure 3.32(b), demonstrated a strong sensitivity to soil moisture conditions. Under wet soil conditions (n=13), the swale exhibited an average infiltration rate of 2.5 ft/d (0.76 m/d) with an average drawdown time of 8.1 hours. In contrast, drier soil conditions (n=11) led to significantly improved performance, with an average infiltration rate of 5.8 ft/d (1.8 m/d) and a reduced drawdown time of 2.7 hours. A two-sample t-test with pooled variance confirmed a highly statistically significant difference (p=0.000004164) between the two conditions, with drier soils facilitating superior infiltration capacity.

Figure 3.32(b) reveals interesting insights regarding the impact of initial soil moisture content on the modified swale's performance. Similarly, the ALDOT swale, a trend is evident where drier soil test data points generally cluster towards the bottom left corner of the graph, indicating faster drawdown times and higher infiltration rates. However, a key distinction emerges when compared to the ALDOT swale. The modified swale exhibits a larger number of wet soil test data points that achieve drawdown times comparable to those observed for drier tests. However, the results still demonstrate a statistically significant difference between the average wet soil infiltration rates and the average drier soil infiltration rates. The sample average infiltration rate under wet soil conditions is demonstrably lower than the sample average under drier soil conditions. While drier tests on average demonstrate a performance advantage, with a reduction in drawdown time of approximately 4.6 hours and an infiltration rate increase of 2.1 times compared to wet tests, the modified swale seems to be less susceptible to the negative infiltration consequences from increased soil moisture compared to the ALDOT swale.

3.7.6 Overall Infiltration Performance Comparison

This section presents a comprehensive analysis of infiltration performance data collected from both the ALDOT swale and the modified swale. Given that the majority of infiltration tests were conducted with open underdrain valves, this analysis will exclusively focus on this configuration to maximize the sample size and ensure a more robust comparison between the ALDOT swale and the modified swale. By comparing the infiltration rates and drawdown

times observed in these tests, we aim to establish a clear understanding of the relative performance of each swale design.

Figure 3.33(a) presents a comprehensive comparison of all infiltration tests conducted on both swales. The orange line represents the ALDOT swale test data, while the blue line corresponds to the modified swale test data. A clear distinction is evident between the two swales' performance profiles. Notably, the fastest drawdown times and infiltration rates observed for the ALDOT swale coincide with the slowest drawdown times and infiltration rates exhibited by the modified swale. This indicates an inverse relationship, where peak performance in one swale aligns with the lowest performance in the other. Furthermore, the Figure 3.33(a) demonstrates that the modified swale's fastest infiltration performance surpasses any recorded value for the ALDOT swale.

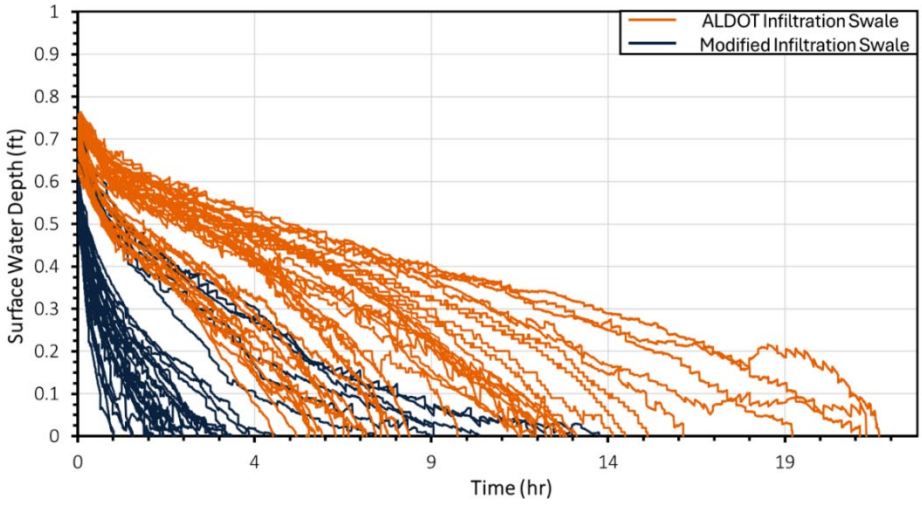

(a) ALDOT swale vs. modified swale tests

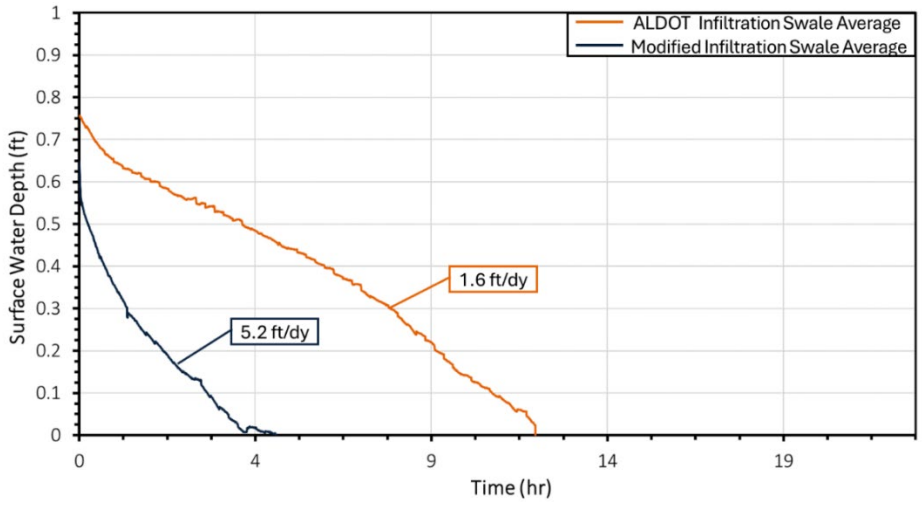

(b) average performances

Figure 3.33. ALDOT and Modified Swale Overall Infiltration Performance

Figure 3.33(b) shows the average drawdown time with its corresponding infiltration rate for both swales. The data reveals a significant difference in performance. The average of ALDOT's infiltration rates is less than the average of the modified's infiltration rates. In

other words, the sample average of ALDOT is less than the sample average of the modified, and the difference is big enough to be statistically significant. The p-value equals 9.974e-7, this means that the chance of type I error (rejecting a correct H_0) is small: 9.974e-7 (0.0001%). The test statistic T equals -5.2936, which is not in the 95% region of acceptance: [-1.672: ∞].

The ALDOT swale exhibits an average drawdown time of approximately 12.25 hours, while the modified swale achieves an average drawdown time of 5.06 hours. This translates to an average drawdown time advantage of 7.19 hours for the modified swale. Similarly, the average infiltration rate for the ALDOT swale is approximately 1.6 ft/d (0.49 m/d), whereas the modified swale displays an average infiltration rate of 5.2 ft/d (1.6 m/d). This represents an improvement in infiltration rate of approximately 3.25 times for the modified swale compared to the ALDOT swale.

To quantify the water storage capacity of each swale, a topographic survey was conducted to determine the volume-depth relationship. This analysis enabled the calculation of potential water storage for both swales. The ALDOT and modified swales were capable of storing an average of 96.1 ft^3 (2.7 m^3) and 134 ft^3 (3.8 m^3) of water per day, respectively. These findings underscore the superior water storage capacity of the modified swale, contributing to its enhanced overall performance.

3.7.7 Infiltration Media Mechanics Analysis

After analyzing the overall performance of both swales, the drawdown curves reveal distinct patterns for the two swale designs. The ALDOT swale exhibited a generally linear and concave downward trend, indicating a relatively consistent infiltration rate over time. In contrast, the modified swale displayed a steeper, concave upward curve, suggesting a more rapid infiltration rate during the initial stages of the drawdown process. These patterns, visualized in Figure 3.33(a), highlight the differential infiltration behaviors of the two swale designs. This indicates that both swales are not made up of just one infiltration rate but multiple infiltration rates at different times.

Figure 3.34 presents representative drawdown curves for the ALDOT and modified swales. The ALDOT swale drawdown curve, Figure 3.34(a), exhibits two distinct phases: an initial rapid drawdown phase (slope 1) followed by a prolonged, slower phase (slope 2). Slope 1 has an infiltration rate of 2.4 ft/d (0.73 m/d) and slope 2 has an infiltration rate of 1.2 ft/d (0.37 m/d). The modified swale drawdown curve, Figure 3.34(b), demonstrates a pattern with three discernible phases: a rapid initial drawdown (slope 1), an intermediate phase (slope 2), and a final phase of slower drawdown (slope 3). Slope 1 has an infiltration rate of 19.1 ft/d (5.82 m/d), slope 2 is 6.4 ft/d (1.9 m/d), and slope 3 is 2.4 ft/d (0.73 m/d). These patterns suggest that infiltration rates decreased over time for both swale types, likely due to increasing soil saturation and decreasing hydraulic head.

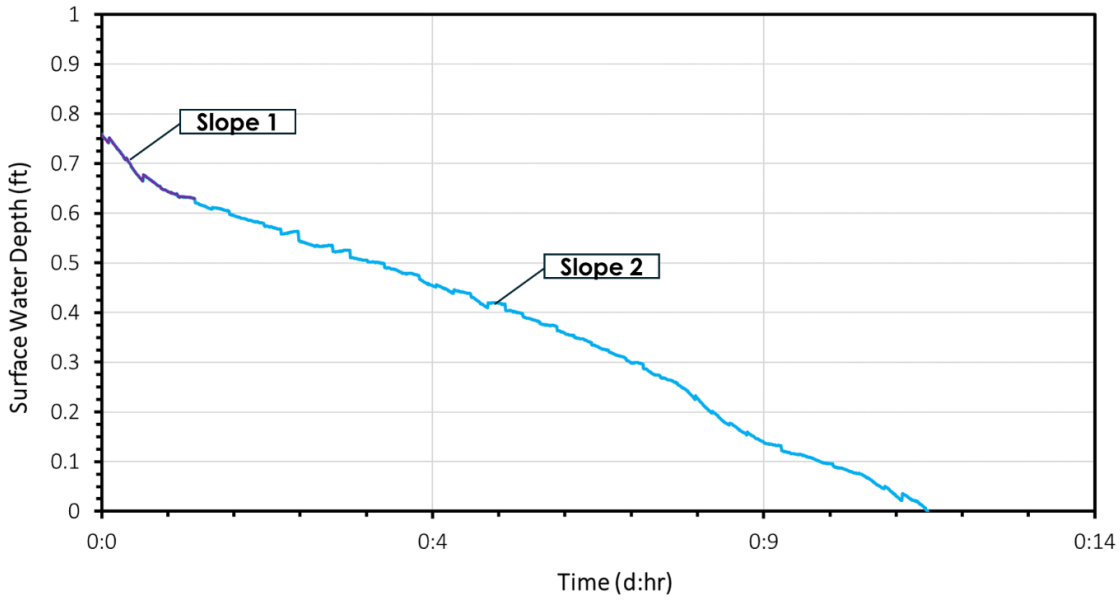

(a) ALDOT swale

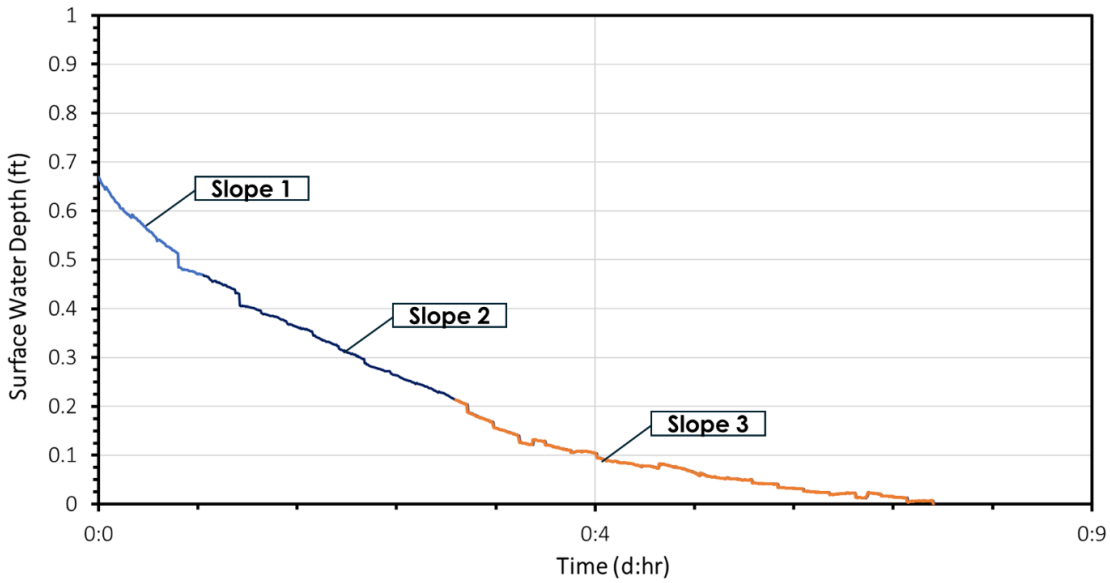

(b) modified swale

Figure 3.34. Swale Infiltration Rates Change Over Time

The calculation of average infiltration rates was based on initial and final depths over drainage time. This method assumes a linear drawdown, which is not representative of the observed data. While the ALDOT swale exhibited a more linear drawdown pattern, the modified swale demonstrated a nonlinear behavior with multiple drawdown phases. This highlights the dynamic nature of infiltration processes and shows that infiltration rates change over time and are not made up of a single infiltration rate.

To get a better understanding of the drawdown process in constructed infiltration swales, we closely reexamined the drawdown curves that were recorded every 30 seconds. Figure 3.35 shows four examples (Day 1 and Day 4) of the recorded and simulated ponding depth over time for MIS and ALDOTIS in January-February infiltration and drawdown experiments. The orange lines give the average infiltration rates (initial ponding depth divided by the drawdown time). For MIS, the infiltration rates changed with time in different periods: higher early and smaller later. The recorded ponding time curve was separated into several periods, and a regression line to fit the ponding depth over time with a high R^2 value (>0.95) was used to determine the infiltration rate for each period. Table 3.2 summarizes the average infiltration rate and fitted infiltration rates over several periods for all infiltration and drawdown experiments conducted by Austin (2024). Typically, infiltration rates decrease with time, with very high infiltration (much larger than the average infiltration rate) at the beginning of the drawdown process.

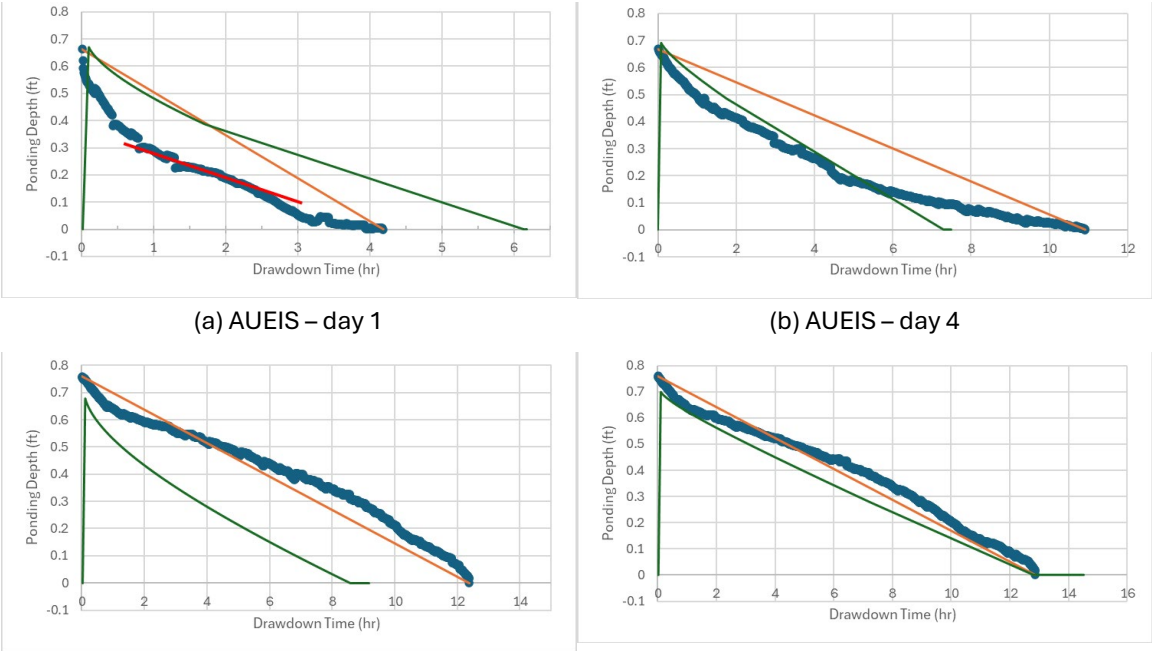

(a) AUEIS – day 1

(b) AUEIS – day 4

(c) ALDOTIS – day 1

(d) ALDOTIS – day 4

Figure 3.35 Examples (Day 1 and Day 4) of the recorded and simulated ponding depth over time for MIS and ALDOTIS in January-February infiltration and drawdown experiments

Table 3.2 Average and fitted infiltration rates over different periods (in./hr) from recorded ponding depth data for two infiltration swales in different drawdown tests by Austin (2024)

Infiltration Swale Tests	Event 1	Event 2	Event 3	Event 4	Event 5
MIS (Jan, one dry day)	1.9 (41.3, 4.2, 2.2, 1.4, 0.5)	1.4 (19.1, 2.9, 1.3, 1.1, 0.4, 0.3)	1.0 (2.7, 1.0, 0.4)	0.7 (2.7, 1.0, 0.4)	0.6 (2.1, 0.7, 0.2)
ALDOTIS (Jan, one dry day)	0.7 (1.2, 0.5, 0.8)	0.7 (1.2, 0.5, 0.8)	0.7 (2.0, 0.5, 0.7)	0.7 (1.1, 0.5, 0.8)	N/A
MIS (Apr, one dry day)	2.5 (10.6, 6.4, 2.6, 1.7, 1.5, 0.3, 0.5)	2.4 (24.6, 3.0, 1.4)	1.4 (13.2, 2.1, 1.8, 1.5, 0.8, 0.5,1.4)	1.5 (11.7, 2.2, 0.9, 0.6, 1.4, 0.8, 1.1, 2.1, 0.8,0.7)	N/A
ALDOTIS (Apr, one dry day)	1.5 (3.4, 1.1, 1.5)	1.3 (12.2, 2.3, 0.9, 1.1, 1.5, 1.0, 1.5)	1.0 (2.9, 0.9, 0.8)	1.3 (2.9, 0.9)	N/A
MIS (Jun, one dry day)	9.5 (14.9, 5.6, 3.5)	8.2 (13.3, 6.4, 3.1, 3.5)	6.7 (15.4, 8.3, 3.1)	5.3 (9.2, 4.0, 2.7, 4.0)	N/A
ALDOTIS (Jun, one dry day)	1.5 (3.3, 0.8, 1.1, 2.1)	1.2 (7.7, 2.7, 0.8, 0.9, 1.9)	1.2 (2.1, 0.9, 1.4, 3.8)	1.0 (2.2, 1.4, 0.7, 0.8, 2.1)	N/A
MIS Open (Jun, one dry day)	9.2 (47.4, 13.4, 5.2, 1.9)	5.5 (46.1, 11.3, 4.2, 1.6 1.8)	8.4 (19.8, 9.9, 5.0, 5.7)	4.8 (9.5, 3.2, 0.2, 1.3)	N/A
ALDOTIS Open (Jun, one dry day)	1.5 (12.1, 3.3, 0.9, 2.1)	1.1 (11.7, 2.3, 0.5, 1.0, 2.6)	1.3 (10.4, 1.9, 0.5, 1.0, 2.7)	1.2 (13.3, 2.8, 0.6, 1.0, 2.6)	N/A

Note: the number outside the brackets is the average infiltration rate (in./hr), and the numbers inside the brackets are the fitted infiltration rates over different periods (in./hr).

In October 2024, five additional infiltration and drawdown tests were performed for two field-scale infiltration swales to understand any impact from the seasonal effect. The drawdown time of the event 2 on October 23 was not recorded. There were four dry days between events 3 and 4 during the weekend and two dry days between other events. The detailed results are given in Table 3.3. The average measured drawdown time of ALDOTIS was 1.33 hours (±0.11), indicating relatively consistent performance across the four events. The average measured drawdown time of MIS was 0.27 hours (±0.04), demonstrating a much faster infiltration rate than ALDOTIS and MIS in previous tests (Table 3.2). These drawdown times are very different from other measurements performed by Austin (2024). October 2024 was part of a dry period in Auburn, AL, and successive droughts may increase the soil infiltration rates, resulting in shorter drawdown times. October 2024's time series of observed ponding depth was also analyzed to determine average infiltration rates (in./hr) and fitted infiltration rates over different periods for each event and two infiltration swales. Results are summarized in Table 3.3, and average infiltration rates for MIS ranged from 19.2 to 33.0 in./hr and 5.1 to 7.2 in./hr for ALDOTIS. The fitted infiltration rates over early periods were much higher and less for later periods than the average infiltration/drawdown rates.

Table 3.3 Average and fitted infiltration rates over different periods (in./hr) from recorded ponding depth data for two infiltration swales in October's drawdown tests

Infiltration Swale Tests	Event 1	Event 2	Event 3	Event 4	Event 5
MIS (October, 2-4 dry days)	31.5 (61.6, 15.4, 10.3)	31.1 (43.6, 21.5)	33.0 (48.6, 20.0)	19.2 (30.8, 20.0, 6.8)	N/A
ALDOT (October, 2-4 dry days)	7.2 (17.8, 4.3, 6.9)	6.4 (11.3, 4.7, 6.6)	6.1 (20.8, 4.6, 4.9)	5.1 (8.1, 4.0)	N/A

Note: the number outside the brackets is the average infiltration rate (in./hr), and the numbers inside the brackets are the fitted infiltration rates over different periods (in./hr).

3.7.8 STATISTICAL ANALYSIS

To identify the factors influencing infiltration rates, a MLR analysis was performed on both swale's dataset. The model incorporated soil moisture content, underdrain valve status (open or closed), and water temperature as independent variables. Results, Table 3.4, indicate that both water temperature (p-value = 1.23E-09) and soil moisture content (p-value = 1.57E-05) significantly influenced infiltration rates. Conversely, the underdrain valve status (open or closed) did not exhibit a statistically significant effect on infiltration performance. This finding may be attributed to the inherently high infiltration capacity of the modified swale media, which minimized the impact of underdrain conditions.

Table 3.4. Modified Swale MLR Results

Variables	Coefficients	p-value
Intercept	21.3	<0.001
Temperature Range (°F)	0.279	<0.001
Moisture Content (%)	-1.09	<0.001
Valve Condition	-0.202	0.861

[a] *Comparison to effects of base at 95% confidence level and p-value <0.05*

A MLR analysis was also performed on the ALDOT swale's dataset. Results, Table 3.5, indicate that both soil moisture content (p-value = 7.53E-07) and valve condition (p-value = 0.002) significantly influenced infiltration rates. Conversely, the water temperature did not exhibit a statistically significant effect on infiltration performance. This finding may be attributed to the inherently slower infiltration capacity of the modified swale media, which may have minimized the impact of water temperature.

Table 3.5. ALDOT Swale MLR Results

Variables	Coefficients	p-value
Intercept	3.83	<0.001
Temperature Range (°F)	0.005	0.351
Moisture Content (%)	-0.249	<0.001
Valve Condition	0.565	0.002

[a] *Comparison to effects of base at 95% confidence level and p-value <0.05*

3.7.9 GRASS SWALE VS INFILTRATION SWALE PERFORMANCE COMPARISON

A comparative analysis was conducted to assess the infiltration performance of infiltration swales relative to traditional grass swales. This analysis involved comparing the average infiltration rates reported in the literature for grass swales to those measured for the infiltration swales in this study. The infiltration rates reported for the five grass swale studies were as following five studies: (1) 0.709 ft/d (0.22 m/d) (Bäckström 2002), (2) 1.57 ft/d (0.48 m/d) (Abida and Sabourin 2006), (3) 1.36 ft/d (0.41 m/d) (Barrett 2005), (4) 5.6 ft/d (1.71 m/d) (Ackerman and Stein 2008), and (5) 1.40 ft/d (0.43 m/d) (Davis et al. 2012).

The ALDOT and MIS designs exhibited infiltration capacities exceeding those observed in all the reviewed grass swale studies except for study four. This study reported an average infiltration rate of 5.6 ft/d (1.7 m/d), which surpassed the performance of the ALDOTIS but yielded comparable results to the MIS. Also, the ALDOT swale infiltration rate showed similar results to study two. Study one, two, four, and five employed infiltrometer tests from smaller-scale methodologies, such as the modified Philip Dunne infiltrometer and the double ring infiltrometer. In contrast, the study three utilized a methodology more closely resembling the approach adopted in this study. This method involved completely filling the swales with water and recording the infiltration rate as the water drained. Consequently, focusing on studying three's infiltration rate average and comparing it to the infiltration swales tested in this study offers a more accurate comparison due to the shared methodological foundation. Study three reported an average infiltration rate of 1.36 ft/d (0.42 m/d), which aligns closely with the performance of the ALDOT swale. However, the modified swale's significantly higher average of 5.6 ft/d surpasses the infiltration rate observed in study three.

These findings suggest that infiltration swales, particularly those incorporating the modified media design, may offer a superior solution for stormwater runoff management. In comparison to traditional grass swales, which primarily function to capture smaller storm events, both the ALDOT and, more significantly, the MIS demonstrate the potential to infiltrate a greater volume of runoff, even from larger storm events.

3.8 SURFACE STORAGE INFLUENCE

The observed disparity in drawdown times and infiltration rates between the ALDOT and modified swales can likely be attributed, at least in part, to a difference in water storage

capacity within zone two. Table 3.6(a) shows the data collected for the surface storage volume of the MIS zone 2 and Table 3.6(b) for the ALDOTIS zone 2.

Table 3.6. Surface Storage Volumes of Infiltration Swales

MIS Surface Storage Volume (Zone 2)			
#	**Depth (in)**	**Depth (ft)**	**Volume (ft^3)**
1	21.5	1.79	4.9
2	21.5	1.79	4.9
3	21.5	1.79	4.9
4	21.5	1.79	4.9
5	21.5	1.79	4.9
6	10	0.83	2.2
	Volume (ft^3) =		26.7
ALDOTIS Surface Storage Volume (Zone 2)			
#	**Depth (in)**	**Depth (ft)**	**Volume (ft^3)**
1	21.5	1.79	4.9
2	21.5	1.79	4.9
3	21.5	1.79	4.9
4	21.5	1.79	4.9
5	21.5	1.79	4.9
6	21.5	1.79	4.9
7	4	0.33	0.8
	Volume (ft^3) =		30.2

The total surface storage for the MIS is about 49.3 ft^3 (1.40 m^3) and 57.2 ft^3 (1.62 m^3) for the ALDOTIS. However, data collection for infiltration and drawdown measurements was exclusively conducted within zone 2, which is what Table 3.6 represents. The ALDOT swale zone two possesses an increased storage capacity of 3.5 ft^3 (0.08 m^3) compared to the modified swale. The percentage difference between the zone's two surface volumes is about 10.6%.

Ideally, the surface storage volumes of the infiltration swales would prefer minimal variation. However, on-site slope constraints encountered during construction limited the ability to create exact replicas. Nonetheless, the measured surface storage volumes demonstrate acceptable. This highlights the inherent variability encountered during real-world construction projects, where achieving perfect uniformity in infiltration swales can be difficult.

3.9 Moisture Content Sensor Evaluation

This section analyzes the data collected from the moisture content sensors installed within both infiltration swales. While the sensor responses confirm activation upon water introduction and subsequent infiltration into the soil layers, the absolute moisture content values appear unreliable. Inconsistencies are observed in the numeric data between

sensors positioned within the same soil media which potentially represents that infiltrated water was moving through the media through paths of least resistance which could be at various locations in the media that did not intercept where the sensors were located. This is evidenced by the need for separate y-axes in Figure 3.36 to visualize the responses from the ALDOT and modified swale sensors. If the sensors shared the same y-axis, it would be hard to visualize the response in the sensors from infiltrated water since the moisture content sensors percentage fluctuations are at completely different ranges and scales.

3.9.1 One-Day Dry Period

Figure 3.36 presents the recorded volumetric moisture content (%) for the ALDOT swale and modified swale during one-day dry period tests. The data from these moisture content sensors provides valuable insights into the temporal dynamics of water infiltration within the swale media and native soils at various depths. The figure depicts the moisture content profiles for both swales, segmented by sensor location: topsoil, sand layer, #57 stone layer, side native soil, and deep native soil. The specific depths and placements of each sensor were detailed in Chapter 4. The vertical red lines on the time axis indicate the start of each test. The peaks observed in Figure 3.36 represent the maximum volume of water detected by the sensor. The time difference between the vertical red line and the corresponding peak on the sensor data curve represents the time lag for that sensor. In essence, the time lag signifies the duration it takes for water to infiltrate and fully saturate the sensor. This time lag analysis can provide valuable insights into the amount of time it takes water to infiltrate to specific layers. The time lag is represented as double sided red arrows in the Figure 3.36.

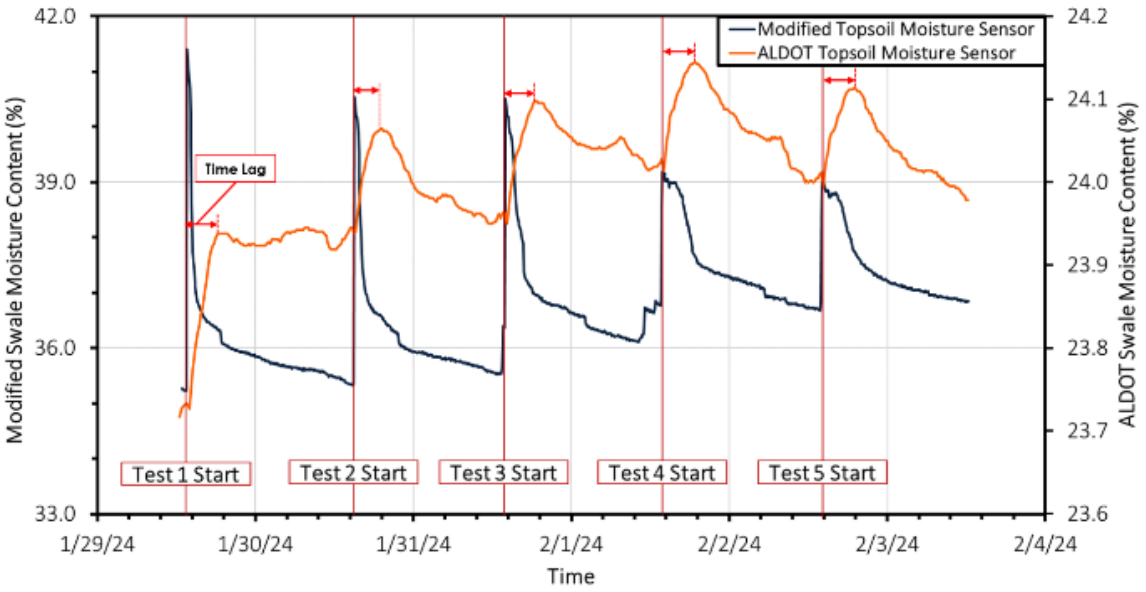

(a) topsoil layer moisture content

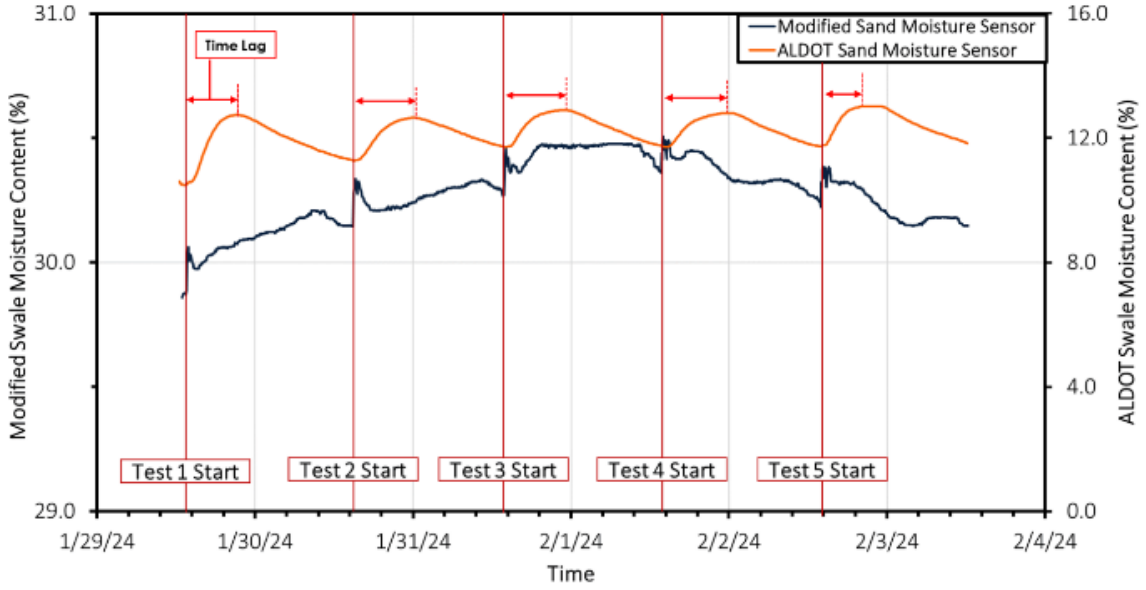

(b) sand layer moisture content

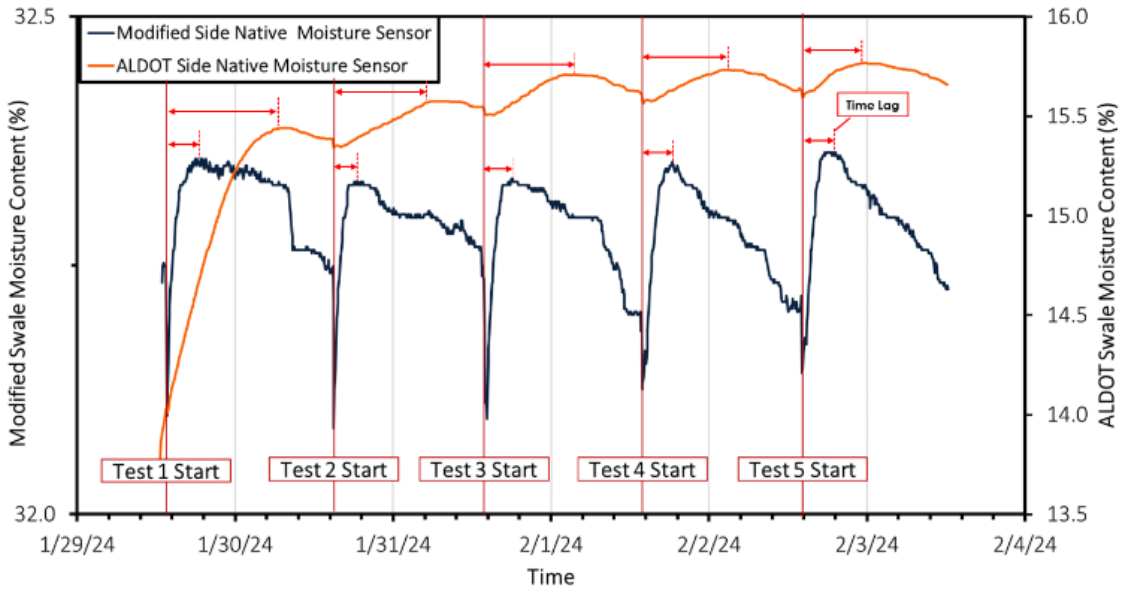

(c) side native soil moisture content

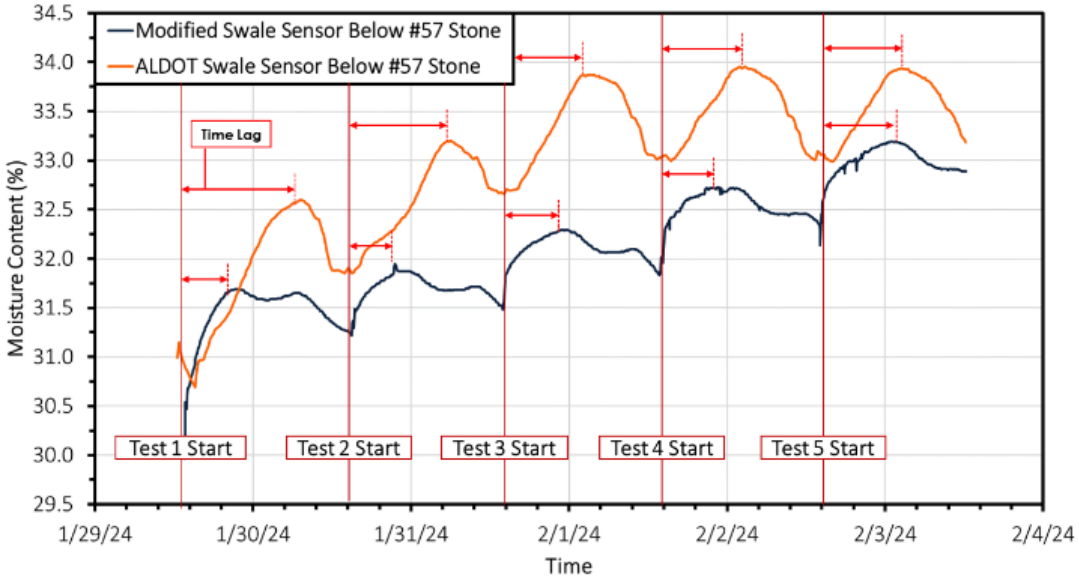

(d) sensor below #57 stone

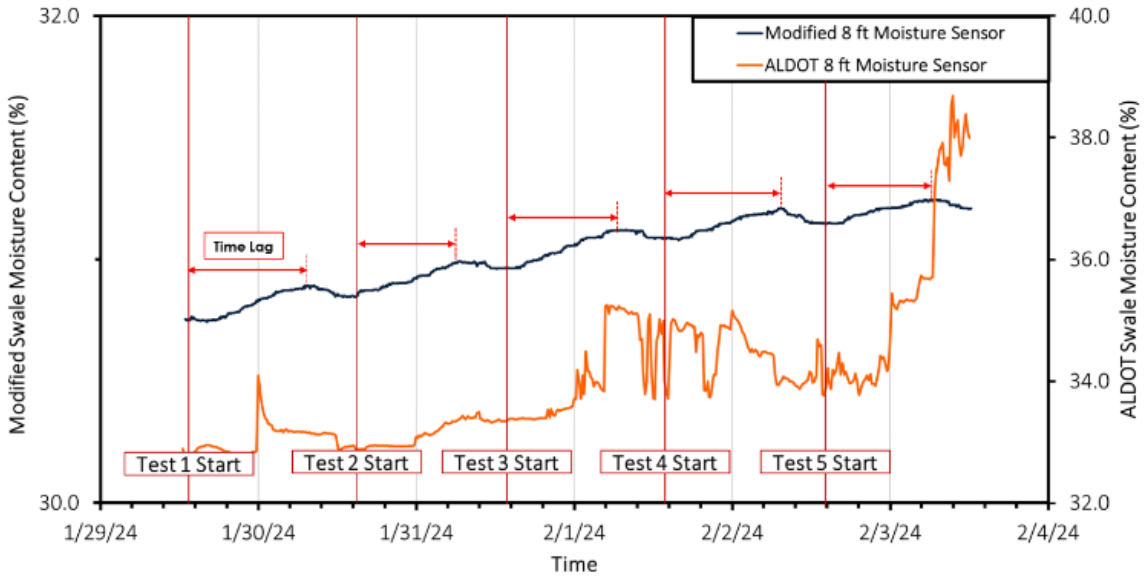

(e) 8 ft deep layer

Figure 3.36. Moisture Contents Between ALDOT and Modified Swale Media Layers

From Figure 3.36, moisture content sensors were installed at various depths to monitor water movement in the ALDOT swale. A sensor placed at a depth of 6 in. (15.2 cm) within the topsoil registered a water travel time of 4.75 hours. At a depth of 24 in. (60.9 cm) within the sand layer, the travel time increased to 8.6 hours. Within the native soil, a sensor located at a depth of 4.5 feet (1.4 meters) showed travel time of 14.4 hours. The sensors placed below the #57 stone layer at a depth of 5 feet (1.5 meters) recorded a travel time of 14.6 hours. The deepest sensor, situated at 8 feet (2.4 meters), did not record a measurable water arrival time.

From Figure 3.36, the modified swale, demonstrated faster travel times at each sensor's location. A sensor at a depth of 3 in. (7.6 cm) within the topsoil recorded a travel time of just 0.2 hours. At a depth of 11 in. (27.9 cm) within the sand layer, the travel time increased to 0.68 hours. Within the native soil, a sensor located at a depth of 4.5 feet (1.4 meters) measured a travel time of 4.42 hours. The sensors placed below the #57 stone layer at a depth of 5 feet (1.5 meters) recorded a travel time of 9.13 hours. The deepest sensor at 8 feet (2.4 meters) registered a travel time of 17.67 hours.

The analysis of time lag data for each sensor layer verifies the findings from the infiltration rates and drawdown section, supporting the notion of higher infiltration efficiency and overall performance in the modified swale compared to the ALDOT swale. Examining each layer individually, the modified swale's topsoil sensor recorded the maximum infiltrated water volume 4.55 hours earlier than the ALDOT swale sensor. Similarly, the modified swale's sand layer sensor detected peak infiltration 7.92 hours ahead of the corresponding sensor in the ALDOT swale. The topsoil and sand moisture content sensors in the modified swale exhibit a rapid response to infiltrated water. This is evident from the peak

readings in moisture content data, which appear to coincide with (or immediately follow) the red vertical lines representing the start time of each test. The side native soil and #57 stone layer sensors in the modified swale also exhibited earlier responses, reaching peak infiltration volumes of 9.98 and 5.47 hours sooner, respectively, compared to their counterparts in the ALDOT swale. However, data from the 8 ft (2.24 m) deep sensor are excluded from the comparative analysis due to malfunctioning in the ALDOT swale at that location, rendering infiltration times for that layer unreliable.

It's important to note that due to design modifications in the modified swale, the depths of the topsoil and sand layer sensors differ between the two swales, despite being installed centrally within their respective layers. This difference arises from the reduced media depth in the modified swale design. Consequently, direct comparisons of sensor data for these two layers are not feasible.

In contrast, the side native soil and #57 stone layer sensors in both swales occupy identical locations and depths. Examining Figure 3.36(d), the #57 stone layer which shares the same y-axis, shows a consistent pattern that emerges in the modified swale's moisture content profiles following each test. These profiles exhibit a steeper concave shape compared to the milder concave shape observed in the ALDOT swale profiles. This steeper initial rise in moisture content for the modified swale suggests that infiltrated water transits pass the sensors more rapidly compared to the ALDOT swale. The gentler slope in the ALDOT profiles indicates a slower movement of infiltrated water through the media.

The #57 stone in both swales are the best sensors for comparison since they are at the same depth, location, and are at the bottom of the media. Figure 3.37 reflects the same tests from Figure 3.36(d) of the #57 stone sensors in both swales; however, Figure 3.37 shows the time lag between the start of the one-day dry period test to the time the sensor recorded the first initial rise in moisture content. This time presented represents the time it takes the #57 stone sensor to sense the first of the infiltrated water that passed through all the different layers of the media and made it to the bottom of the media.

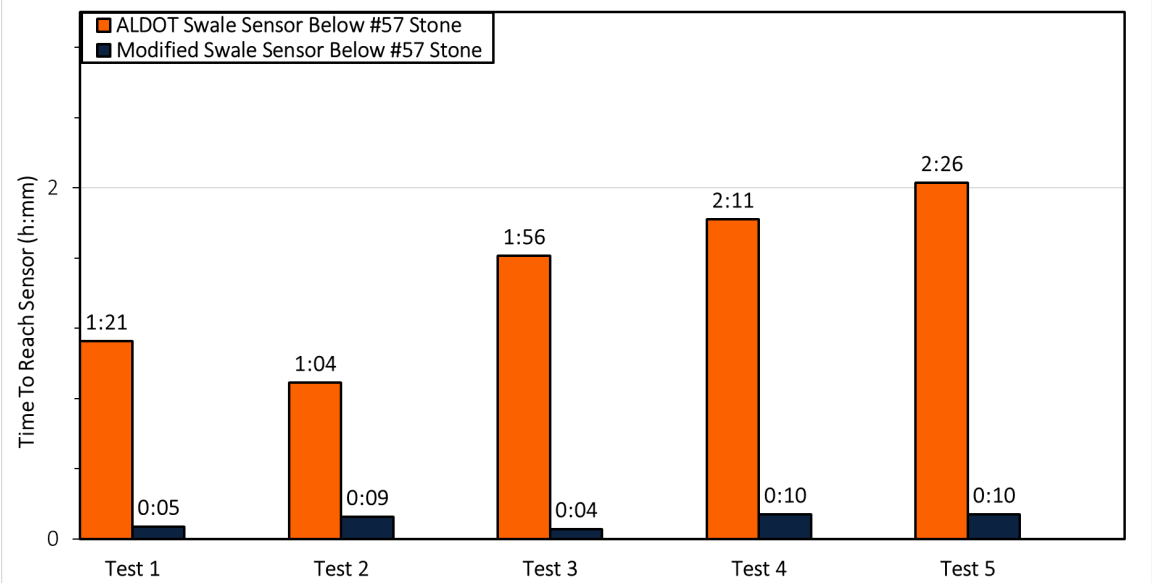

Figure 3.37. Sensor Below #57 Stone Times

Figure 3.37 shows the modified #57 stone sensor in blue and the ALDOT sensor in orange. The MIS shows times averaging 0.13 hours while ALDOT swale shows an average time of 1.8 hours. These findings provide evidence that the modified swale media demonstrates superior infiltration efficiency. Notably, despite having a reduced surface storage capacity (3.5 ft^3 or 0.08 m^3 less than the ALDOT swale), the modified swale allows infiltrated water to pass through the media and reach the bottom of the #57 stone layer more quickly than the ALDOT swale by 1.67 hours faster. The sample average of the modified swale is less than the sample average of the ALDOT swale, and the difference is big enough to be statistically significant. The p-value equals 0.0000941, this means that the chance of type I error (rejecting a correct H_0) is small: 0.0000941 (0.0094%). This suggests that the modified swale design promotes faster infiltration despite a smaller storage volume. Another interesting pattern shown in Figure 3.37 is that the ALDOT sensor time increases after each test, except test one, which represents that the underdrain for the ALDOT swale was not functioning as designed since both swales were open valved.

3.9.2 Moisture Content Sensor Limitations

The observed discrepancies in the numerical data between sensors positioned within the same soil media warrant consideration of potential spatial variability in infiltration patterns. Infiltrating water may preferentially exploit pathways of least resistance within the media. These flow paths could deviate from the specific locations where the sensors are installed. Consequently, sensors might not always capture the peak infiltration events at a particular depth, leading to inconsistencies in the recorded moisture content values. The moisture content sensors seemed to be unreliable and further investigation with more sensors installed within a cross-section and throughout the length of the swale's media is needed for confirmation of results.

3.10 SETTLEMENT EVALUATION

Settlement testing was conducted on both the ALDOT and modified swales to assess potential surface elevation changes following media installation and sod stabilization. Monitoring settlement is crucial as media compaction can decrease infiltration capacity. Figure 3.38 presents the settlement data collected throughout the first year after installation for each swale (ALDOT installed in 2023, modified swale installed in 2024). The x-axis represents the longitudinal distance along the swale bed in 5 ft (1.5 m) increments, moving from upstream (left) to downstream (right). Each colored line on Figure 3.38 depicts the settlement measurements for a specific month.

The results from both swales consistently show negligible settlement across the entire swale surface at each 5 ft increment throughout the monitoring period. All data points for each month in both swales cluster closely around a common baseline, indicating minimal changes in surface elevation. This finding suggests that neither swale experienced significant settlement within the first six months following installation.

While this initial data is promising, further monitoring is recommended to determine if settlement might occur at a later stage. Nonetheless, the current results indicate that both the ALDOT and modified swale designs effectively maintained their initial surface elevations during the first six months after construction.

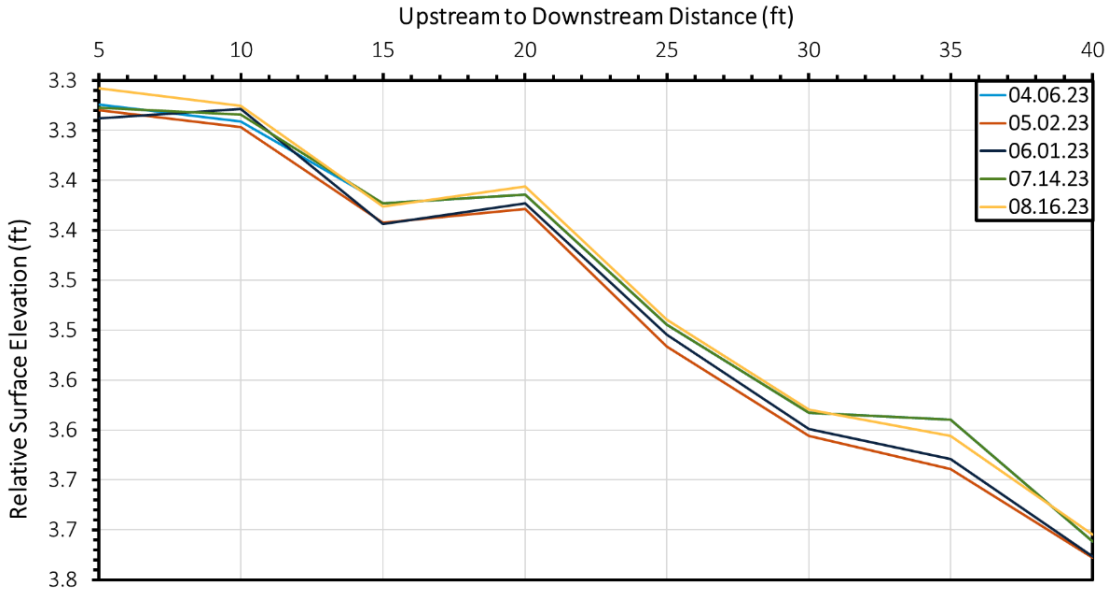

(a) ALDOT swale settlement

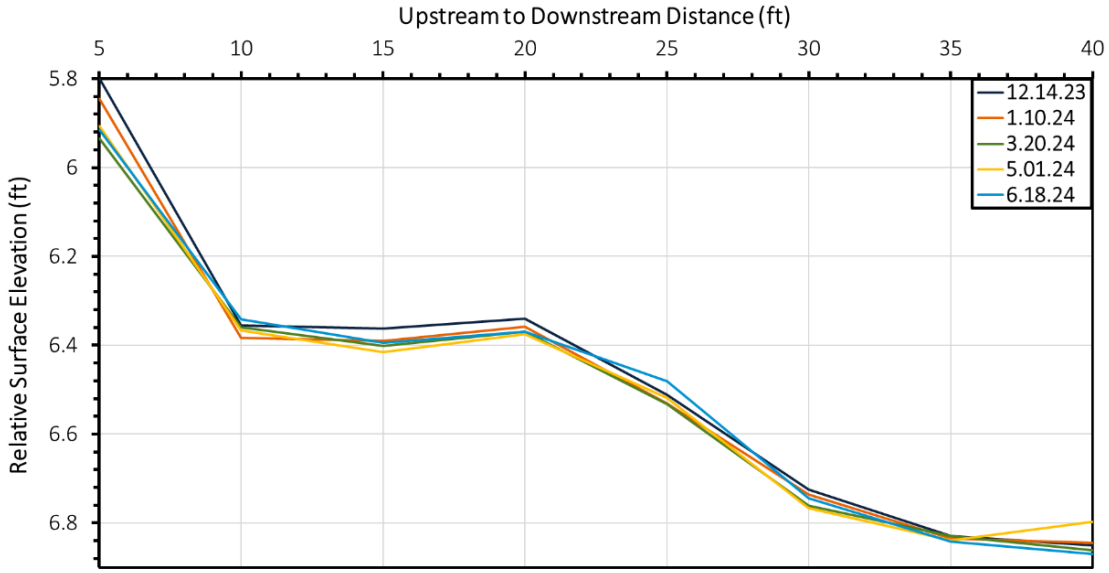

(b) modified swale settlement

Figure 3.38. Swale Settlement Comparison

CHAPTER 4. MODELING RUNOFF CONTROL PERFORMANCE

This chapter summarizes the modeling efforts and results on the infiltration swales (ISs) using different models. The infiltration swales differ from swales or grass swales previously studied by other researchers (Abida and Sabourin 2006; Ahmed et al. 2014; Ahmed et al. 2015; Davis et al. 2012; Kirby et al. 2005). The swale is a vegetated open channel and typically has ditch checks or check dams to slow or pond stormwater runoff to promote infiltration through native soil with a vegetative cover. Because of the infiltration through native soils, the grass swales were also called the infiltration swales in some previous studies. In this study, the infiltration swales are the bio-retention basins at the bottom of a grass swale/channel. The ALDOTIS cross-sectional view (Figure 4.2) has an engineered media matrix or three layers (topsoil, sand, and gravel) beneath the vegetative cover. For comparison, the ALDOTIS would be called a bio-swale by NCDOT (Ekka and Hunt 2020). Bio-retention basins and bio-swales performance in controlling stormwater runoff can be modeled using several modeling tools, such as the EPA National Stormwater Calculator (SWC) (Rossman and Bernagros 2019), the EPA Storm Water Management Model (SWMM) (Rossman and Huber 2016), and the Bentley's CivilStorm . These modeling tools can be used to simulate hydrological performance on runoff control from several types of Low Impact Development (LID) facilities.

4.1 USING BIO-RETENTION CELL TO MODEL INFILTRATION SWALES

The EPA SWMM can model the following 8 types of LIDs (Table 5.1): BRCs, Rain Garden, Green Roof, Infiltration Trench, Permeable Pavement, Rain Barrel, Rooftop Disconnection, and Vegetative Swale. The ALDOTISs are quite different from rain barrels and rooftop disconnection and should not be modeled as these two LID types. The modeling schematic diagrams in Figure 4.1 show the key features of each LID, which are modeled by SWMM, SWC, and CivilStorm. The rain garden only has an engineered soil layer above the native soil but no storage layer between the two soil layers. The infiltration trench has a storage or gravel layer to hold the runoff. The green roof has three thin layers (in in. or mm): vegetation, soil, and drain mat. The permeable pavement consists of two or three relatively thin layers: pavement, soil, and storage because the soil layer is optional. The vegetative swale is a grass trapezoidal channel and does not have a storage layer (gravel), and its soil infiltration capability is modeled by one of its subcatchment infiltration methods (e.g., CN, Horton, Modified Horton, Green Ampt, Modified Green Ampt). Therefore, the infiltration swales also differ from green roofs, permeable pavement, rain gardens, infiltration trenches, and vegetative swales, and should not be modeled by the above five LID types. The BRCs are the most similar to an ALDOTIS or bio-swale. A BRC in SWMM is modeled in three layers: surface, soil, and storage with an optional drainpipe or drain (Figure 4.2). The description of the LID module's parameters is listed and summarized in Table A.7 (Appendix A).

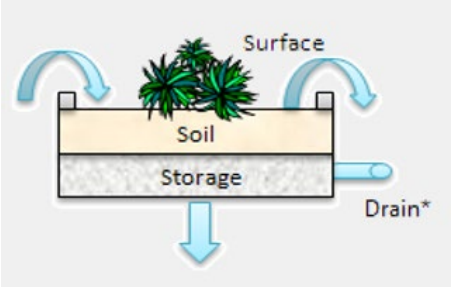

(a) Bio-Retention Cell

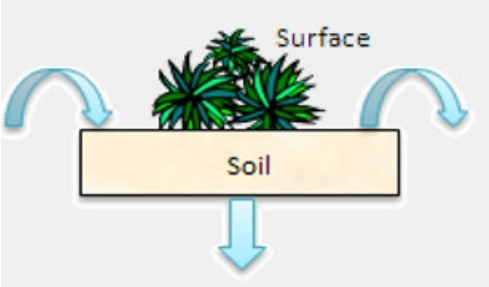

(b) Rain Garden

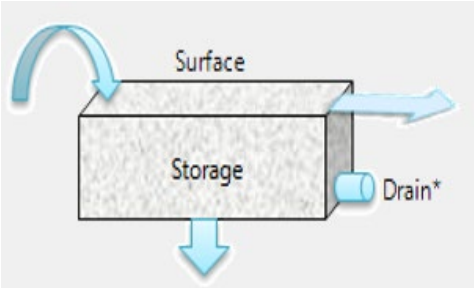

(c) Infiltration Trench

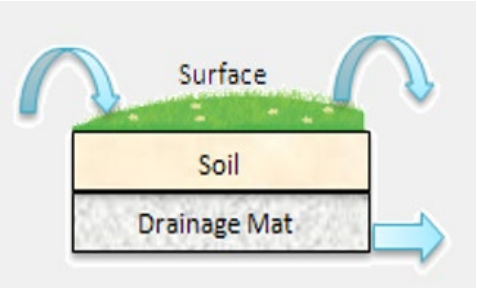

(d) Green Roof

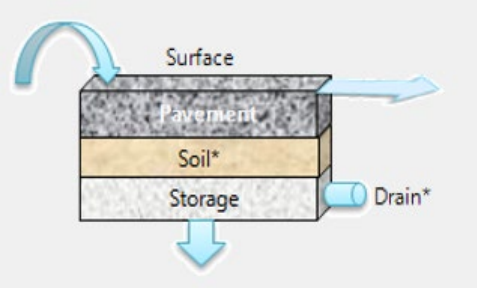

(e) Permeable Pavement

(f) Rain Barrel

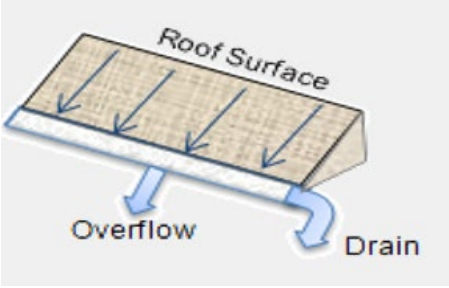

(g) Rooftop Disconnection

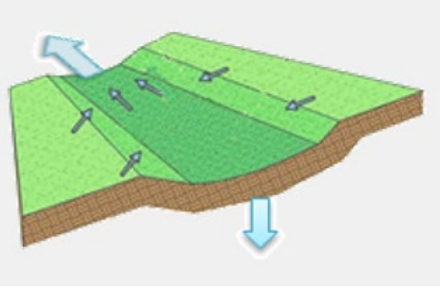

(h) Vegetative Swale

Figure 4.1 Modeling schematic diagrams for 8 LID types in SWMM LID Control Editor.

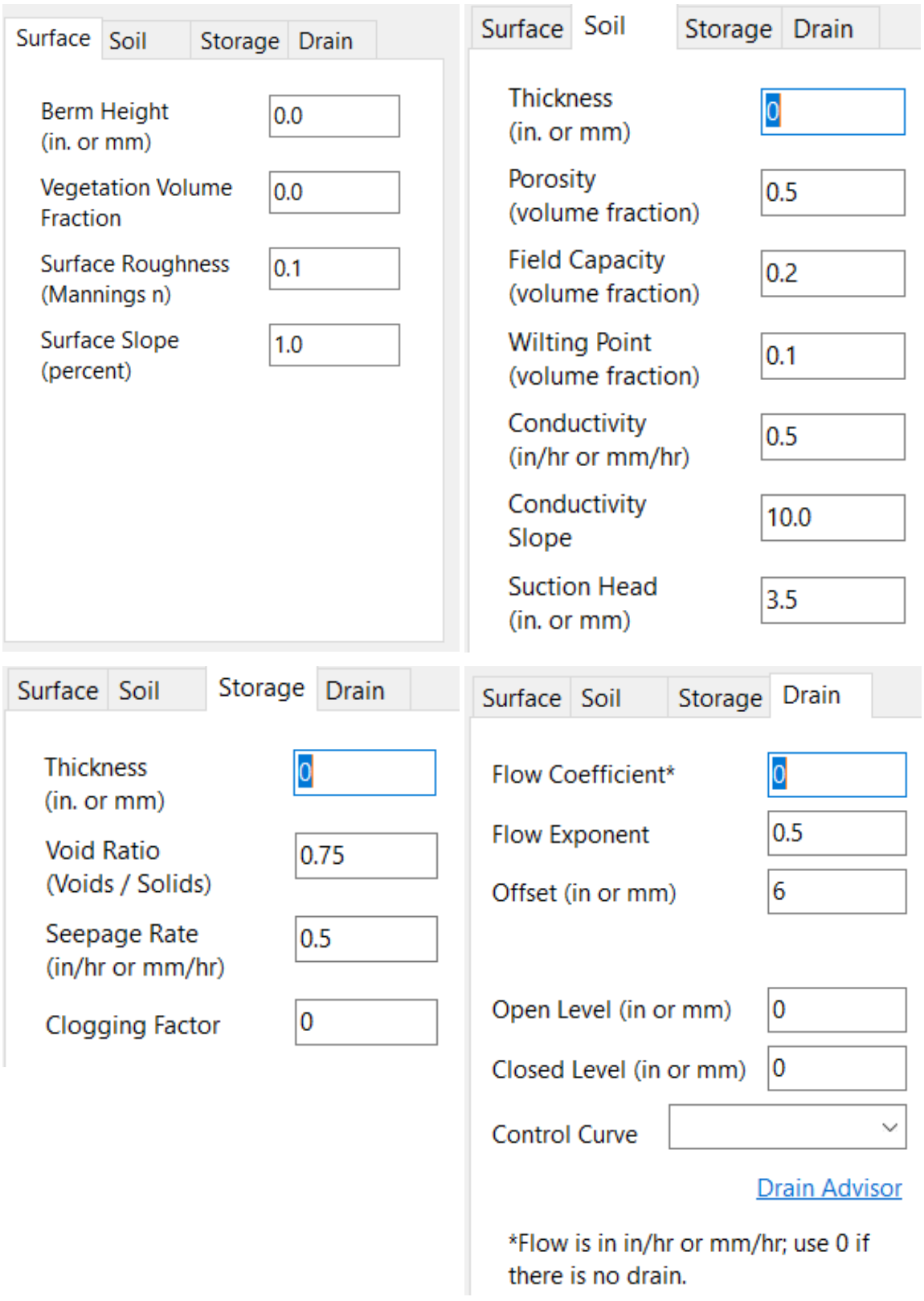

Figure 4.2 SWMM modeling parameters for surface, soil, storage, and drain layers in a bio-retention cell.

4.1.1 SOIL LAYER PROPERTY FOR SBC MODELING

The LID's soil layer is typically filled with sand or engineered (bio-retention) media that is a mixture manufactured from soil (sand, silt, clay) and other components (e.g., compost, organic matter, iron/chemicals, etc.) in specific proportions to improve soil properties, such as infiltration rate and fertility, or remove certain pollutants in stormwater runoff by adsorption to improve water quality of outflow from the drain. Many states in the USA require or suggest a specified range of sand (30–60%), compost (20–40%), and topsoil (20–30%) for planting soil mix in rain gardens or BRCs (Carpenter and Hallam 2010). Carpenter and Hallam (2010) studied two planting soil mix designs: (1) 20% compost, 50% sand, 30% topsoil, and (2) 80% compost and 20% sand in the laboratory and field to determine various mix properties (hydraulic conductivity, field capacity, density, porosity).

The ALDOTIS design (Figure 4.3) is not a soil mix but a layered system comprised of 1 ft of topsoil, 2 ft of fill sand, and 2 ft of #57 stone. ALDOTISs are supposed to be constructed/implemented at the roadside channel bottom and vegetated with grass; therefore, a layer of topsoil is used to support the growth of grass sod (providing nutrients, organics, and moisture retention). However, the SWMM LID module (Figure 4.3 (a)) includes only one homogeneous soil layer. Therefore, two soil layers for infiltration swales are combined for modeling purposes into an equivalent soil layer for the SWMM LID model. The seven soil property parameters (Table 4.1) can be determined experimentally in the laboratory (column test) or estimated if soil properties for each layer are known or determined separately. The equivalent soil thickness is the sum of two soil layers, e.g., 3 ft for ALDOTIS design. The equivalent soil porosity, field capacity, wilting point, and/or suction head can be weighted by soil volume or thickness. Table 4.1 lists some properties of topsoil, fill sand, #57 stone, and Evergreen topsoil (e.g., pine bark fines) measured by Ramirez Florez (2024) using the falling head permeability test. The equivalent soil porosity for ALDOT design is 39.3% for 12 in. of topsoil (38.5% porosity) and 24 in. of fill sand (40.9%).

The MIS design, that is design F3 depicted/described in Figure 2.12 and Table 2.17 for the small-scale column testing (Chapter 2) and constructed for the field-scale study (Figure 3.2, Chapter 3). The MIS has 6 in. of the soil mix that is composed of 50% topsoil and 50% pine bark fines by volume (80% topsoil by weight) and 10 in. fill sand. The porosity of the mix is 57.2% (average of two porosities because of equal volume); therefore, the soil layer of MIS has a porosity of 45.5% for 6 in. of the mix and 10 in. of fill sand. The fill sand used for the study is similar to packed sand (with a porosity of 38.5%) and has a lower porosity than natural sand (with a porosity of 43%), but the not compacted, loose sand may have a porosity of 0.46.

Ramirez Florez (2024) used a standard permeameter apparatus to determine permeabilities at 20°C (Table 4.1) of loose samples of topsoil, fill sand, #57 stone, and pea gravel. The constant head permeability test determines the flow rate (in./min or in./hr) of water through a column of cylindrical soil sample under the constant pressure difference and calculates the permeability based on Darcy's law. The 3-ft fill sand was tested under different compaction and under constant head over 9 or 72 hours. The permeability or

saturated hydraulic conductivity of fill sand decreased over time when the compaction was less than 95%. The initial permeability ranged from 0.19 to 2.11 in./min (11.4 in./hr to 126.6 in./hr), and the final permeability from 0.17 to 1.26 in./min (10.2 in./hr to 75.6 in./hr) after 9 hours. Ramirez Florez (2024) also developed and constructed the infiltration rate columns to perform the constant head (2 ft water) and the falling head (starting with 2 ft of water) infiltration rate tests to determine the infiltration rate (in./hr) of water through a column of a cylindrical sample. The samples included single soil samples (e.g., topsoil and a mixture of topsoil and pine bark fines) and layered samples for various configurations (e.g., 10 in. topsoil, 12 in. fill sand, and 8 in. #57 stone). All soil samples were completely saturated during tests before the infiltrated water volume was collected over a time interval to calculate the infiltration rate, which is supposed to equal the soil's saturated hydraulic conductivity. These infiltration rates were summarized in Chapter 2. Permeabilities measured by the modified constant head tests were typically larger than infiltration rates measured by the modified falling head tests. The falling head permeability tests are recommended/used for fine-grained soils with a low discharge.

Table 4.1 Properties of topsoil, fill sand, #57 stone, and Evergreen topsoil (from Ramirez Florez, 2024).

Sample	Bulk density (g/cm^3)	Porosity (%)	Permeability at 20 °C (constant head)	Infiltration rate (falling head)
Fill sand	1.43	38.5	10.2–126.6 in./hr, 35.8 in./hr*	/
Topsoil	1.30	40.9	0.34±0.05 (0.30–0.41) in./hr, 0.96 in./hr*	0.31±0.12 (0.14–0.69) in./hr
#57 stone	1.22	52.4	2403.0 in./min*	/
Pea gravel	1.62		215.3 in./min*	/
Pine bark fines	0.17	73.5	/	/
Mixture	0.98	57.2%	0.91±0.17 (0.72–1.06) in./hr	2.8±1.07 (1.7–3.8) in./hr

*Note: 1 in./hr = 2 ft/d. 1 in./hr = 60 in./min. The mixture is 80% by-weight topsoil and 20% pine bark fines. * stands for loose samples.*

Under steady conditions, the effective or equivalent saturated hydraulic conductivity of two soil layers (e.g., topsoil and sand) can be calculated using Equation 4.1 based on Darcy's law for each layer.

$$k_s = \frac{h_1+h_2}{\frac{h_1}{K_{s1}}+\frac{h_2}{K_{s2}}} \quad (4.1)$$

For example, Ramirez Florez (2024) experimentally determined saturated hydraulic conductivity or falling-head permeability for topsoil to be 0.315 in./hr (0.63 ft/d) (average from three samples, each tested three times) and for the fill sand used to construct the infiltration swale in the Auburn University – Stormwater Research Facility (AU-SRF) to be 35.86 in./hr (71.72 ft/d), which is more than 110 times faster infiltration in comparison to topsoil. Therefore, one foot of topsoil becomes a major limiting factor for surface runoff infiltrating into the soil layer of the infiltration swale. Using 1 ft of topsoil was originally

recommended to promote the healthy growth of grass sod. For the ALDOTIS design (h_1 = 1 ft and h_2 = 2 ft), the equivalent saturated hydraulic conductivity of the soil layer is 0.93 in./hr (much smaller than the saturated hydraulic conductivity of the fill sand) and has almost no change when the hydraulic conductivity of the fill sand changes.

The MIS contains 6 in. of the mixture of topsoil and pine bark fines and 10 in. of fill sand, a total of 16 in. of the soil layer in the SWMM LID module. Ramirez Florez (2024) measured the mixture's infiltration rates by the falling head tests, and the mixture's percent of pine bark fines ranged from 5% to 100%. The mixture was also called amended topsoil. The infiltration rate increased from 0.76 ft/d (0.38 in./hr) to 1840 ft/d (920 in./hr). The mixture with 20% pine bark fines and 80% topsoil by weight had 2.8 in./hr (5.6 ft/d) of infiltration rate (about 9 times higher infiltration than the topsoil) and was used to construct the field-scale infiltration swale, that is the MIS. For the MIS design (h_1 = 6 in. and h_2 = 10 in.), the equivalent saturated hydraulic conductivity of the soil layer is 6.61 in./hr (13.22 ft/d) if the mixture's infiltration rate of 2.80 in./hr (5.6 ft/d) under falling head conditions is used or 2.33 in./hr (4.66 ft/d) if the mixture's average permeability (constant-head permeameters) of 0.91 in./hr (1.82 ft/d) was used.

The infiltration rate of various layered samples, e.g., F3 design for MIS, were measured under the 2-ft constant head and the falling head (from 2 to 0 ft). The infiltration rate of layered samples under the constant head was 2–5 times larger than that under the falling head (Table 2.2 and Table 2.6). Since pea gravel and #57 stone have very large permeability (Table 4.1), the infiltration rates measured for the F3 design (four layers) should be the same as the two soil layers (6 in. amended topsoil and 10 in. fill sand). The average infiltration rate of the F3 design from three constant head tests was 5.75 ft/d (2.87 in./hr) and 2.24 ft/d (1.12 in./hr) for three falling head tests, which are slightly smaller than the theoretically calculated values from Equation 5.1. Further data analysis for the F3 design constructed in AU-SRF is necessary to recommend what hydraulic conductivity of the soil layer should be used in the SWMM model.

4.1.2 Governing Equations Modeling the Infiltration Swales

A typical BRC modeled by SWMM with three horizontal layers along its depth is given in Figure 4.3(a) a graphical representation of its vertical profile and Figure 4.3(b) a conceptual representation of the BRC SWMM model. Figure 4.3(b) shows all related variables (defined through Equations 4.2, 4.3, and 4.4) and hydrological processes: rainfall, runon from upstream sub-catchments, surface infiltration, soil percolation, exfiltration to native soil, evapotranspiration (ET), surface runoff, and outflow from underdrain. To model the hydrologic performance of the BRC unit, the following assumptions are made in SWMM to simplify BRC hydrologic/hydraulic behavior (Rossman and Huber 2016): 1) the cross-sectional or horizontal area of the unit remains constant throughout its depth, 2) flow through the unit is one-dimensional in the vertical direction, 3) inflow to the unit is distributed uniformly over the top surface, 4) moisture content is uniformly distributed throughout the soil layer, and 5) matric forces of water/runoff within the storage (gravel) layer are negligible

(i.e., ignore surface tension effects), so as to act as a simple reservoir that stores water from the bottom up.

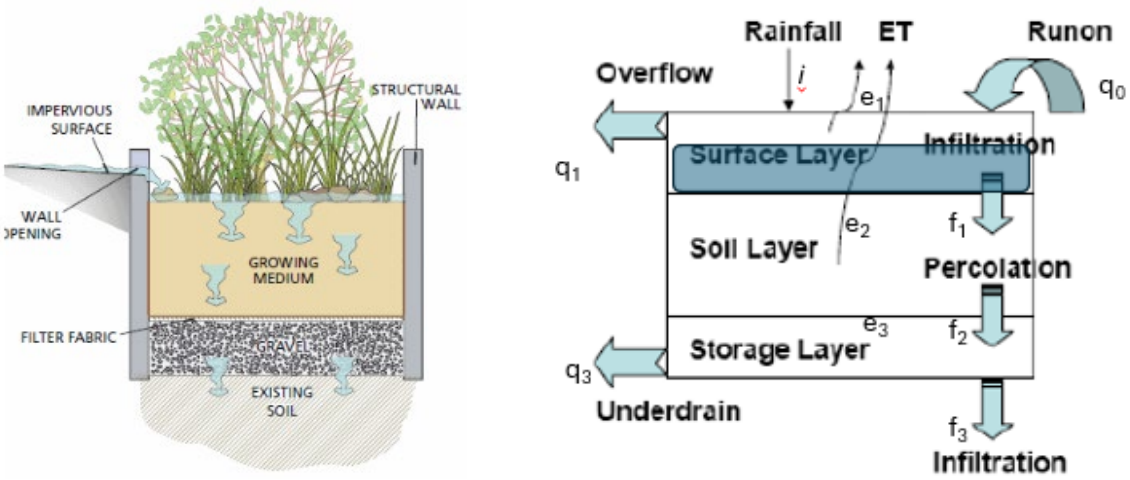

(a) graphical depiction of vertical profile (b) concept of BRC SWMM model

Figure 4.3 A typical BRC modeled by SWMM: (A) vertical profile and (B) three-layer conceptual model showing the related processes and variables.

SWMM uses three governing (differential) equations 4.2, 4.3, and 4.4 to model and solve three LID variables: surface depth d_1, soil layer moisture content θ_2, and depth of water in the storage layer d_3. Other variables in Figure 4.3(b) and these three equations are either input data (e.g., rainfall intensity i and seepage or exfiltration rate f_3 of water from the storage layer into native soil) or pre-calculated from other SWMM modules (e.g., infiltration rate f_1 of surface water into the soil layer). Each mass-balance or continuity equation describes the change in water content/depth in a particular layer over time after considering the possible inflow and the outflow water flux rates to the layer, and each term is expressed as volume per unit area per unit time (ft or m per second). For design rainfall simulations, evapotranspiration (ET) rates (e_1, e_2, and e_3) were not simulated; for long-term simulations, the potential ET was modeled in SWMM's runoff module using air temperature time series as a part of input data.

$$\phi_1 \frac{\partial d_1}{\partial t} = i + q_0 - e_1 - f_1 - q_1 \qquad \text{Surface layer} \qquad (4.2)$$

$$D_2 \frac{\partial \theta_2}{\partial t} = f_1 - e_2 - f_2 \qquad \text{Soil Layer} \qquad (4.3)$$

$$\phi_3 \frac{\partial d_3}{\partial t} = f_2 - e_3 - f_3 - q_3 \qquad \text{Storage Layer} \qquad (4.4)$$

where: d_1 = depth of water stored on the surface (ft),

θ_2 = soil layer moisture content (volume of water / total volume of soil),

d_3 = depth of water in the storage layer (ft),

i = precipitation rate falling directly on the surface layer (ft/sec),

q_0 = inflow to the surface layer from runoff captured from other areas (ft/sec),

q_1 = surface layer runoff or overflow rate (ft/sec),

q_3 = storage layer underdrain outflow rate (ft/sec),

e_1 = surface ET rate (ft/sec),

e_2 = soil layer ET rate (ft/sec),

e_3 = storage layer ET rate (ft/sec),

f_1 = infiltration rate of surface water into the soil layer (ft/sec),

f_2 = percolation rate of water through the soil layer into the storage layer (ft/sec),

f_3 = exfiltration rate of water from the storage layer into native soil (ft/sec),

ϕ_1 = void fraction of the surface layer (i.e., the fraction not filled with vegetation)

ϕ_2 = porosity (void volume / total volume) of the soil layer (Equation 4.5),

ϕ_3 = void fraction of the storage layer (void volume / total volume),

D_1 = freeboard height for surface ponding (ft) (Equation 4.5),

D_2 = thickness of the soil layer (ft),

D_3 = thickness of the storage layer (ft)

For BRCs, the berm height and vegetation volume fraction (1 - ϕ_1) are the only two parameters that directly affect the surface runoff or an overflow rate q_1 (Equation 5.5) when ponding depth d_1 is greater than D_1.

$$q_1 = \max\left[(d_1 - D_1)/\Delta t, 0\right] \tag{4.5}$$

The infiltration of surface water into the soil layer, f_1 (ft/sec), is modeled with the Green-Ampt equation (an optional infiltration method in SWMM):

$$f_1 = K_{2s}\left(1 + \frac{(\phi_2 - \theta_{20})(d_1 + \psi_2)}{F}\right) \tag{4.6}$$

Where:

K_{2s} = soil's saturated hydraulic conductivity (ft/sec),

θ_{20} = moisture content at the top of the soil layer (fraction),

ψ_2 = suction head at the infiltration wetting front formed in the soil (ft), and

F = cumulative infiltration volume per unit area over a storm event (ft).

The rate f_1 is limited by the amount of empty pore space available $[(\phi_2 - \theta_2)D_2/\Delta t]$ plus the volume removed by drainage divided by percolation, f_2, and evapotranspiration e_2 over the time step. When the soil layer is saturated (i.e. $\theta_2 = \phi_2$), f_1 is limited by the percolation rate, f_2, which is equal to the saturated hydraulic conductivity K_{2s}, when ET is not considered.

The rate of percolation (e.g., drainage) of water through the soil layer into the storage layer below it, f_2, is modeled using Darcy's Law in the same manner used in SWMM's existing groundwater module (Rossman and Huber 2016).

$$f_2 = \begin{cases} K_{2s} exp\left(-HCO(\phi_2 - \theta_2)\right), & \theta_2 > \theta_{FC} \\ 0, & \theta_2 \leq \theta_{FC} \end{cases} \quad (4.7)$$

HCO is a decay constant derived from moisture retention curve data that describes how conductivity decreases with decreasing moisture content. When the soil moisture content θ_2 in the soil layer is less or equal to the soil's field capacity θ_{FC}, f_2 is zero or no drainage from the soil layer to the storage layer; otherwise, the soil hydraulic conductivity K_{2s}, soil porosity ϕ_2, soil moisture content θ_2, and *HCO* affect the percolation rate as shown in Figure 4.4 when θ_{FC} = 0.17 and K_{2s} = 0.43 in./hr. Typical percolation decay constant HCO ranges from 30 to 55 (Rossman and Huber 2016) and can be considered as a SWMM model calibration parameter. Figure 4.4 shows that when *HCO* = 48, soil percolation rate f_2 is basically zero when θ_2 is less than 0.34 (65.4% saturation for ϕ_2 = 0.43).

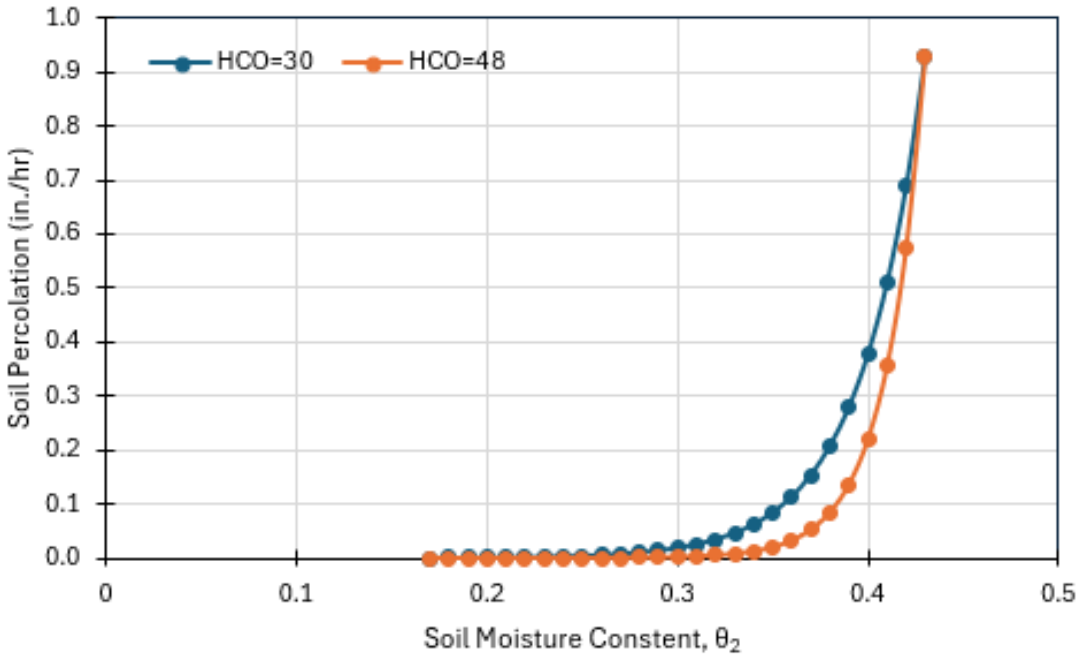

Figure 4.4 Soil percolation rate f_2 as a function of the soil moisture content and parameter HCO using Equation (4.7).

For the storage layer, if the drainpipe is not used, the water depth, d_3, depends on the percolation rate, f_2, the seepage/exfiltration rate, f_3, into the native soil, and the initial saturation condition. When the storage layer is not saturated, the maximum f_2 is the soil's saturated hydraulic conductivity K_{2S} (Equation 4.7); when it is saturated, f_2 is limited by the seepage rate f_3 of the native soil. If the storage depth is not zero, the exfiltration rate, f_3, is equal to the seepage rate as a LID model input parameter (Figure 4.2). When f_2 is less than the seepage rate, f_3 (exfiltration) equals f_2 when the storage level is zero.

4.2 EVALUATING ISS USING THE NATIONAL STORMWATER CALCULATOR (SWC)

To quantitatively evaluate the performance of the designed infiltration swales in controlling surface runoff, numerical models were also used in addition to performing the field-scale tests presented in Chapter 4. This is because numerical models can be set up for different model scenarios and run under long-term historical rainfall data (events). Therefore, these models can help us understand (1) the swale's performance when varying different model parameters (reflecting various swale configuration or physical property changes) and (2) the long-term performance of the designed infiltration swales. In this section, simulations were first conducted using the National Stormwater Calculator (SWC) developed by the United States Environmental Protection Agency (EPA). By integrating the data of specific sites into the model, the infiltration capacity and runoff reduction potential of the basin were systematically evaluated. This analysis provides crucial insights into the effectiveness of the designed infiltration swales, which are also called Low Impact Development (LID) strategy, proposed in specific regions.

4.2.1 INTRODUCTION OF SWC

The National Stormwater Calculator (SWC) (Rossman and Bernagros 2019) is a user-friendly tool from the United States Environment Protection Agency (USEPA), and its computational engine is the advanced EPA Storm Water Management Model (SWMM). The SWC has a desktop version, which is no longer supported by the USEPA, and a mobile web-based application, which is continuously updated and can be accessed at https://swcweb.epa.gov/stormwatercalculator/. The web-based SWC can be used on desktop devices (Microsoft Edge, Google Chrome, Mozilla Firefox, and Apple Safari) and mobile devices (smartphones and tablets), and is compatible with all operating systems. The SWC is a simple-to-use tool for computing small-site hydrology with or without green infrastructure as LID controls for any location within the USA. It estimates the amount of stormwater runoff generated from a site under different development and control scenarios over long-term historical and future rainfall. Each SWC project or case study can be saved as an XML file and reopened later. Each SWC run needs to access and set up six to nine web pages: Location, Soil Type, Soil Drainage, Topography, Precipitation/Temperature, Climate Change, Land Cover, LID Controls, Project Cost, and Results, since Climate Change, LID Controls, and Project Cost are optional depending on the situation of a study.

On the Location page, one should find or search the study site by entering an address or a zip code and then input the site area in acres. The map from the SWC can be used to pan and zoom to navigate and mark the site-specific location by selecting it with the cursor. The map offers different views, such as standard road, aerial, bird's eye, and streetside, and the site area can be defined up to a maximum of 12 acres. The SWC can access several national databases to provide the site's local soil, meteorological, and potential evaporation data with a specific address.

On the Soil Type page, one can identify the soil type at the present site, represented by its Hydrologic Soil Group (HSG), which indicates the soil's physical characteristics and

runoff potentials such as sand (low runoff), sandy loam (moderately low runoff), clay loam (moderately high runoff), and clay (high runoff). The soil type can be selected by local knowledge or by automatically retrieving the information (default option when the Soil Type page is selected) from the U.S. Department of Agriculture's Natural Resources Conservation Service (NRCS) Soil Survey Geographic Database (SSURGO) database, which is organized into map units that define specific soil survey areas and is displayed in the SWC map, which is selected to choose in the SWC. However, the SSURGO does not cover all parts of the country, and the calculator will show a warning if there is no data for the site.

On the Soil Drainage page, one should identify the soil infiltration rate, known as saturated hydraulic conductivity. This can be achieved by selecting the study site location from the calculator's SSURGO database map or manually entering a known rate for the site, whose unit is in. per hour. The SSURGO database is derived from the soil texture and groundwater depth but not based on the field measurements, which may lead to some locations lacking specific soil conductivity.

On the Topography page, one should identify the site's surface slope, which impacts the runoff rate of excess stormwater. The calculator categorizes slopes into four levels: flat (≤ 2%), moderately flat (≤ 7%), moderately steep (≤ 15%), and steep (> 15%). SSURGO slope data is displayed on the map and can be directly selected, but selections can also be changed based on local site knowledge.

On the Precipitation/Temperature page, one should select a rain gage location to supply rainfall data to model runoff and a weather station for temperature data to model evaporation. The calculator uses long-term hourly rainfall records and 24-hour extreme event storms for runoff modeling. It automatically identifies the five nearest rain gauges from a catalog of over 2,600 of the National Oceanic and Atmospheric Administration's (NOAA) National Centers for Environmental Information (NCEI) stations, displaying their location, record period, and average annual rainfall, which provide many choices to select the most suitable rain gauge for the site. The page also allows for selecting a weather station from Oregon State University's PRISM Climate Group for daily minimum and maximum temperature data to estimate evaporation using the Hargreaves Equation. All the data on precipitation and temperature can be downloaded to support the long-term SWMM modeling (section 4.4.6) besides SWC.

On the Climate Change page (optional), one can select a future climate change scenario for the site. The scenarios, derived from the World Climate Research 23 Program's Coupled Model Intercomparison Project (https://www.wcrp-climate.org/wgcm-cmip), Phase 5 (CMIP5) multi-model dataset, and EPA's Climate Resilience Evaluation and Awareness Tool (CREAT) tool (https://www.epa.gov/crwu/), adjust monthly average rainfall, temperature, and extreme storm events for each rain gauge and weather station location (Rossman and Bernagros 2019). The calculator simulates potential future conditions based on the changes from historical data. Four climate scenarios are "No change (Historical)", "Hot/Dry", "Central", and "Warm/Wet", and three storm scenarios are "No change (Historical)", "Stormy", and "Less Stormy". It helps to explore a range of possible future

conditions, including changes in storm intensity and runoff. Climate projections are available for two periods: near term (2035) and far term (2060).

On the Land Cover page, one needs to describe the site's land cover for the development scenario and provide the site's percentages for four pervious areas: Forest, Meadow, Lawn, and Desert, then the percent impervious area for the site is calculated by SWC (100% - Sum of four pervious areas). Each land cover has SWC pre-defined depression storage depths and roughness coefficients for SWMM modeling. Impervious areas are the calculated percentages by the calculator and are considered to drain directly off-site but can be partially disconnected using LID. It is worth mentioning that the total runoff is highly dependent on the amount of impervious areas on the site and is less sensitive to how impervious areas are divided between different land cover categories. Using the land cover categories for the site can reflect the specific situation: pre-development, current, or post-development.

On the LID Controls page (optional), one needs to specify the percentage of the site's impervious area that would be treated by a list of LID controls: disconnection, rain harvesting, rain gardens, green roofs, street planters, infiltration basins, and permeable pavement. SWC's rain harvesting systems collect runoff from rooftops and convey it to a cistern tank where it can be used for non-potable water uses and on-site infiltration. Therefore, SWC's rain harvesting is the same as rain barrels in SWMM. SWC's street planters consist of concrete boxes filled with engineered soil that supports vegetative growth, and beneath the soil is a gravel bed that provides additional storage equaling BRCs in SWMM. SWC also includes an infiltration basin as one of the LID controls but excludes the infiltration trench and vegetative swale because these two LIDs depend on more information, which is unavailable from SWC input.

On the optional Project Cost page, one can select regional cost adjustment factors based on Bureau of Labor Statistics (BLS) data to estimate project costs. The default option is National, which applies if the site is over 100 miles from the 17 BLS Regional Centers across the Northeast, Midwest, South, and West regions. This part can be selected from the three nearest BLS Regional Centers listed by proximity to the site. The other option allows users to input their cost adjustment factor for advanced customization. The map on this page shows the BLS Regional Centers, where areas within a 100-mile radius of a center are assigned regional multipliers, with regions beyond that radius defaulting to a national multiplier of 1. Users can also override the default by choosing from the three closest centers in the Cost Region dropdown. Regional multipliers larger than 1 increase costs, while those less than 1 decrease costs relative to the National average.

On the Results page, the calculator performs a hydrologic site analysis (running the SWMM model in the background) and displays results, including estimates for capital and maintenance costs. The Site Description report provides a review and an option to modify input data before running the analysis. This page has three sections: options, actions, and reports. For option, the calculator can set parameters for the rainfall analysis, including the number of years of rainfall data to use, moving back from the latest available year, and event threshold, which defines the minimum daily rainfall or runoff to be considered measurable.

An option to exclude consecutive wet days from runoff statistics is often used to exempt extreme storm events, such as hurricanes, from retention requirements. For action, the calculator includes commands to control the simulation and results, such as refresh Results, which runs a long-term hydrologic simulation and updates the display if input data changes; use as Baseline Scenario, which marks the current data and results as a reference for comparison with future runs; and remove Baseline Scenario, which deletes any previously set baseline from the reports. The Reports section allows users to select how the rainfall/runoff results generated for the site should be displayed; various report options can be chosen as discussed in the next section 4.3.1, and the graphic analysis results can be exported to PDF files.

4.2.2 Example Results for an Infiltration Swale in Southern Alabama

A construction project in Southern Alabama was selected to model and understand the runoff control of infiltration swales using SWC. Precipitation and air temperature data from Mobile, AL Downtown Airport were used with available data from 1/1/2005 to 12/31/2019 (15 years). Three scenarios, pre-construction, post-construction without LID, and post-construction with LID, are modeled using SWC. As a general term, LID was used to represent infiltration swales for the following three scenarios. These three scenarios have 10%, 27%, and 27% of impervious areas, respectively. SWC uses four land covers (forest, meadow, lawn, and desert) to represent pervious areas. Only lawn land cover along roadways was used in this study site. The percent of lawn area subtracts the percent of impervious areas from 100%, (e.g., 73% lawn = 100% - 27%) for post-construction with LID. SWC input parameters are summarized in Table 4.2. SWC summary results (Table 4.4) were developed using 15 years (2005–2019) of the available precipitation and air temperature data, with 0.1in. for the rainfall event threshold.

The SWC consists of a series of LID controls that manage stormwater on-site by controlling the percentage of impervious areas treated by each LID. These controls are critical to converting stormwater into resources, minimizing stormwater runoff, and reducing the risk of pollution of waterways, wear and tear on infrastructure, flooding, and overburdened treatment systems. Each LID practice has preset design parameters, which can be modified by selecting the control type. The LID practice used here is the street planter, which can almost mimic an infiltration swale and is an urban rain garden consisting of vertical walls and an open or closed bottom that collects and absorbs runoff from sidewalks, parking lots, and streets, making them ideal for densely populated urban areas with limited space. A user can change four parameters of the street planter for specific LID design. The ponding height is the wall of a planter above the soil bed to allow for ponding within the unit; the soil media thickness is concrete boxes filled with an engineered soil that supports vegetative growth; the soil media conductivity is the hydraulic conductivity of the soil media; and the gravel bed is beneath the soil to provide additional storage. Parameter values for street planters to model two infiltration swale designs (ALDOTEI and MIS) are given in Table 4.3. The percent capture ratio is the ratio of its area to the impervious area whose runoff it captures and is equal to 5.84% for both swales since infiltration swales have a total surface

area of 4,020 ft^2. Table indicates there are more input parameters for SWMM to model a LID control; therefore, other parameters are internally fixed by SWC.

Table 4.2 SWC Input Data for Three Modeling Scenarios in Southern Alabama Study Site.

Parameter	Pre-construction	Post-construction without LID	Post-construction with LID
Area of Site	5.41 ac	5.85 ac	5.85 acr
Site Soil Type	Sandy Loam (Moderately low)		
Site Soil Drainage	0.108 in./hr (Saturated hydraulic conductivity)		
Site Topography	Flat (~2% slope)		
Site Precipitation /Temperature	2005/01/01 to 2019/12/31 from Mobile Downtown Airport		
Land Cover	10% impervious area & 90% lawn/forest	27% impervious area & 73% lawn/forest	
LID Control	No	No	Street Planters

Table 4.3 Parameter Values for Street Planters to Model Two Infiltration Swale Designs

Parameters	ALDOTIS	MIS
Ponding Height	6 in.	6 in.
Soil Media Thickness	36 in.	16 in.
Soil Media Conductivity	0.93 in./hr	2.33 in./hr
Gravel Bed Thickness	12 in.	32 in.

Since the same rainfall data were used, the average annual rainfall over 15 years (57.4 in.) did not change with the scenarios (Table 4.4). The annual average runoff could substantially be increased by about 31.6% (from 16.62 in. to 21.89 in.) for the post-construction scenario without LID, indicating that the increase in surface runoff was caused by the increase of impervious area (10% to 27%). However, after the use of LID (infiltration swales), the annual average runoff was not only reduced by about 31.6 percent compared to the post-construction value without LID (from 21.89 in. to 14.97 in.), but also by about 9.9% compared to the pre-construction value (from 16.62 in.in. to 14.64 in.in.). This result shows the strong effectiveness of LID in reducing runoff.

When LID is not used after construction, evaporation increases by about 82.7% (from 0.81 in.in. to 1.48 in.in.), while when LID is used, evaporation further increases by 32.4% (from 1.48 in.in. to 1.96 in.in.), which indicates that LID can help increase evaporation, e.g., due to ponding.

After construction without LID, the average annual infiltration decreased by 14.7% (from 40.17 in.in. to 34.25 in.in.), which means that conventional construction reduces water infiltration into the ground, thereby increasing surface runoff. After the use of LID, the infiltration volume not only increased by 18.5% (from 34.25 in.in. to 40.58 in.in.) compared with that of traditional construction, but also slightly increased by 1% (from 40.17 in.in. to 40.58 in.in.) compared with that before construction, which indicates that LID can not only improve the water absorption capacity of the ground after traditional construction, but also improve the water absorption capacity of the ground. It can also help maintain or slightly improve the water absorption capacity of the original site.

Table 4.4 Summary Results from SWC for Four Modeling Scenarios for Southern Alabama.

Statistic	Pre-Construction	Post-Construction w/o LID	Post-Construction with ALDOTIS	Post-Construction with MIS
Average Annual Rainfall (in.)	57.4	57.4	57.4	57.4
Average Annual Runoff (in.)	16.62	21.89	14.97	14.64
Average Annual Evaporation (in.)	0.81	1.48	1.96	2.13
Average Annual Infiltration (in.)	40.17	34.25	40.58.	40.76
Days per Year with Rainfall	70.97	70.97	70.97	70.97
Days per Year with Runoff	20.99	35.45	18.93	17.99
Percent of Wet Days Retained	70.42	50.05	73.33	74.65
Smallest Rainfall w/ Runoff (in.)	0.13	0.13	0.13	0.13
Largest Rainfall w/o Runoff (in.)	1.1	0.56	1.68	1.78
Max Rainfall Retained (in.)	3.02	2.57	2.74	2.63

Without LID, the number of days with runoff per year after construction increased by 69% (from 20.99 days to 35.45 days), indicating that runoff events became more frequent due to traditional construction. By using LID, the number of runoff days is not only reduced by about 87.2% compared with traditional construction (from 35.45 days to 18.93 days) but also by about 9.9% compared with pre-construction (from 20.99 days to 18.93 days), indicating that LID can effectively reduce the frequency of runoff events to a level lower than preconstruction.

Without LID, the maximum rainfall without runoff after traditional construction was reduced by 49% (from 1.1 in.in. to 0.56 in.in.), which indicates that the traditional construction site has a lower ability to infiltrate/retain relatively large rainfall without producing runoff. However, after using LID, this capability is significantly increased by 52.7%

(from 1.1 in.in. to 1.68 in.in.) compared with that before the construction, indicating that using LID can improve the management of heavy rainfall events at the construction site.

In the absence of LID, the maximum retained rainfall after traditional construction was reduced by 15% (from 3.02 in.in. to 2.57 in.in.) compared with that before construction, but in the presence of LID, the maximum retained rainfall was only slightly reduced by 9.3% (from 3.02 in.in. to 2.74 in.in.). This indicates that LID can reduce the influence of construction on the maximum retained rainfall.

In summary, both LID designs substantially reduce the negative hydrological impact of traditional construction by reducing runoff, maintaining or increasing infiltration, and improving water retention capacity.

Figure 4.5 shows the SWC's Rainfall/Runoff (in.in.) scatter plots of the daily runoff depth associated with each daily rainfall depth over the simulation period (e.g., 15 years, 2005–2020). Only days with rainfall above the event threshold (i.e., >0.1 in.) are plotted, but the runoff can be zero or above zero. In SWC, a user can hover the cursor over any data points or bars on the graph, and SWC will show its corresponding *x* and *y* values.

The pre-construction scatter plot data points are tightly grouped at lower daily rainfall and runoff levels. It can be seen from Figure 4.5 that with the increase in daily rainfall, the daily runoff increases gradually. Very few events have high daily rainfall or runoff, which were extreme heavy rainfall events in the upper right corner of the graph. From the scatter plots with and without LID after construction, it can be seen that there are more high-runoff events without LID than with LID. This is obvious because compared with the data without LID, more data with LID appear at a higher level of daily runoff. Under the same rainfall level, events with LID have a lower degree of aggregation on the runoff axis than those without LID, indicating that LID effectively reduces runoff. It is worth noting that the LID scenario after construction is closer to the event distribution before construction, which indicates that LID reduces the influence of construction on runoff.

Figure 4.5 shows the SWC's Rainfall/Runoff frequency plots in three scenarios to indicate how many times (days, y axis) per year, on average, a given daily rainfall depth or runoff depth (x axis) will be exceeded. In Mobile (South Alabama), there are 6 days per year where it rains more than two in., but only two days per year where there is more than this amount of runoff. Daily rainfall with more than 4 in. of rain occurs only once every three years (1/0.33). The frequency plots are useful in comparing the complete range of daily rainfall/runoff results among three development scenarios. It helps us to determine how close a post-development condition with LID comes to meeting pre-development hydrology or see what effect future changes in precipitation due to climate change might have on LID control effectiveness.

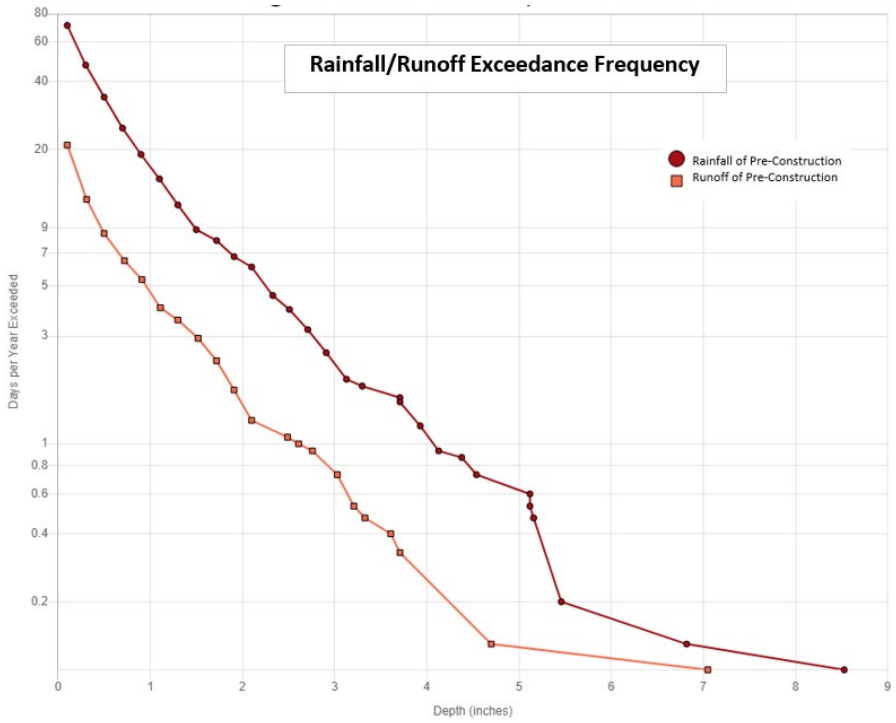

(a) Pre-construction runoff conditions

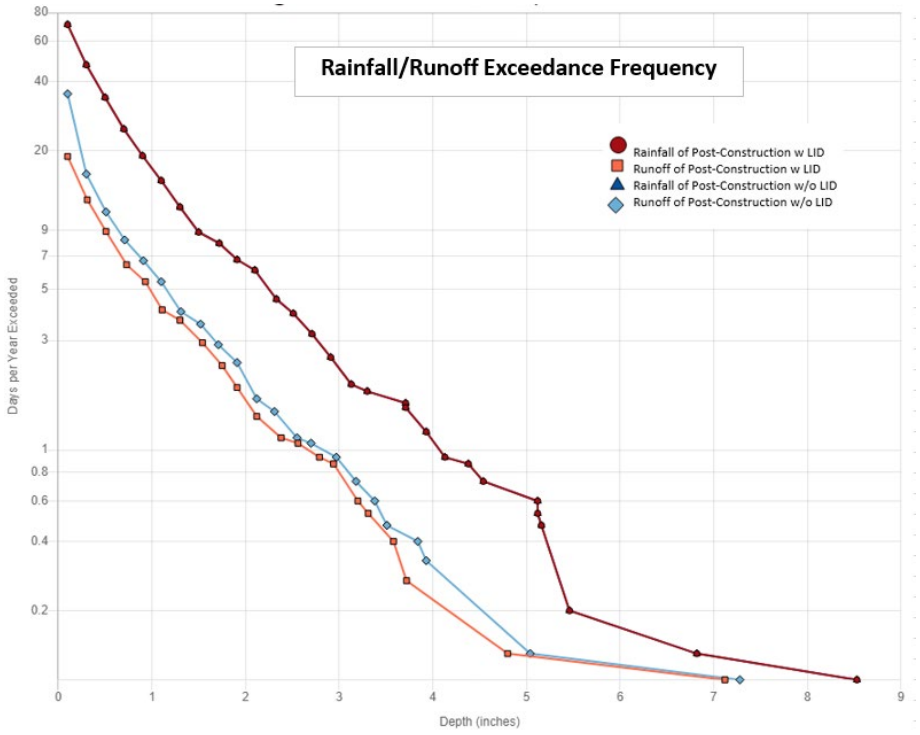

(b) Post-construction runoff conditions

Figure 4.5 Rainfall/Runoff Exceedance Frequency of Pre-Construction, Post-Construction with LID, and Post-Construction w/o LID.

Figure 4.5 for Pre-construction shows the frequency with which rainfall and runoff at a given depth equal or exceed. The lines of rainfall and runoff frequency are relatively apart from each other, indicating that runoff is less closely related to rainfall patterns in the pre-construction environment due to large infiltration losses. The figure of post-construction shows that the frequency of rainfall remains constant, represented by overlapping lines of rainfall before and after construction, which is expected because construction does not affect weather patterns. After the construction without LID, the runoff line is always higher than that with LID, indicating that without LID, the higher runoff depth will be exceeded more frequently. The runoff line using LID is closer to the runoff line before construction, which indicates that LID practice helps to maintain the runoff frequency level similar to the natural or pre-development conditions.

Pre-construction plots (Figure 4.6) show that for very small rainfall events, the retention rate starts at 100% and decreases as the size of the event increases. The retention rate drops sharply when rainfall increases to about 0.5 in., after which the retention curve gradually flattens out, suggesting that most of the rainfall above that amount is not fully retained (only 70.5%). A large proportion of rainfall events retain about 1 inch of daily rainfall, after which almost all events result in runoff. The plot with and without LID after construction shows that for the smallest events, the lines without LID and with LID start with 100% retention, just like the scenes before construction. Through comparison, without LID after construction, the retention will decline faster (to ~51% retention as rainfall > 2 in.) than with LID, and the retention percentage will decrease as the daily rainfall increases but less than 2.0 in. This suggests that construction without LID results in less water being absorbed or retained by the ground. Under all rainfall levels, the retention rate of LID after construction is much higher than that without LID except for 100% retention, just slightly higher than the retention rate before construction, especially under minor rainfall events.

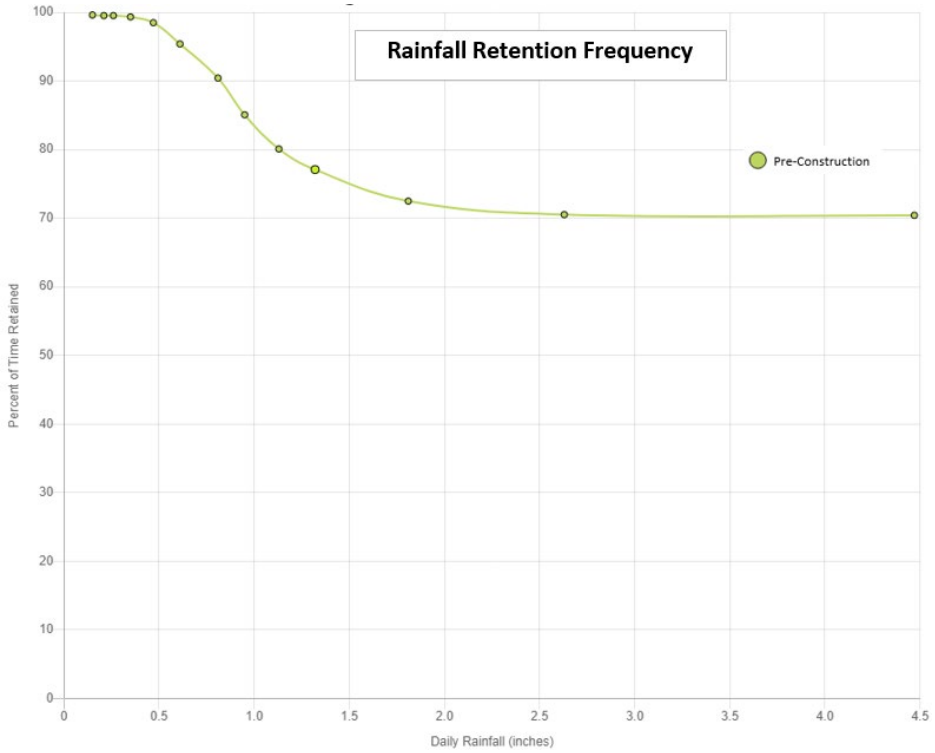

(a) Pre-construction runoff conditions

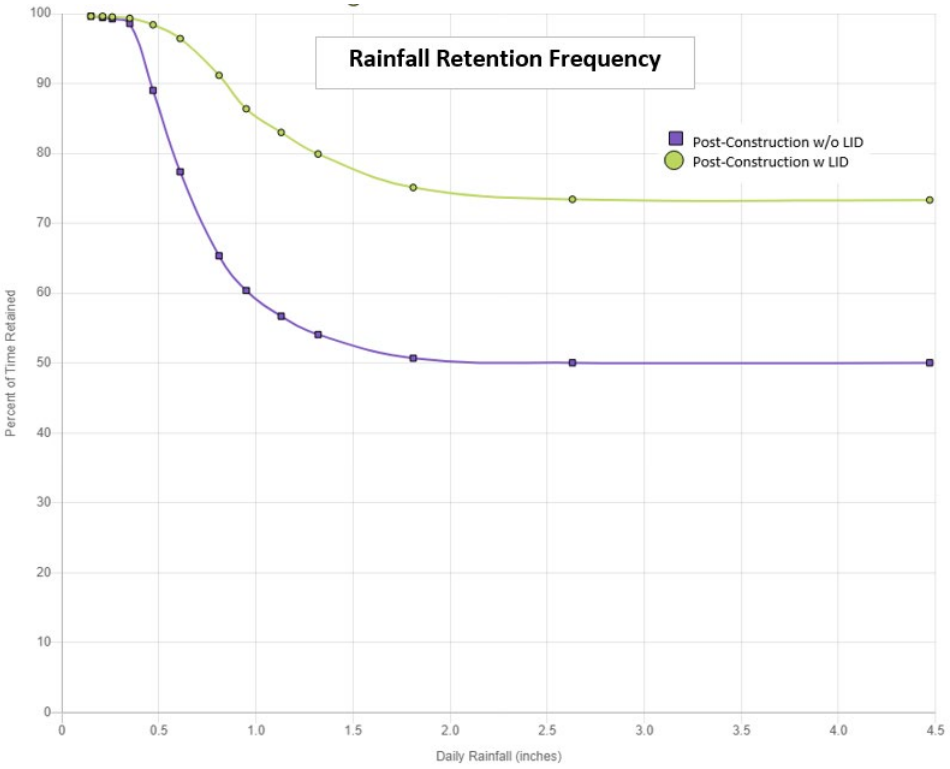

(b) Post-construction runoff conditions

Figure 4.6 Rainfall Retention Frequency versus daily rainfall of Pre-Construction, Post-Construction with LID, and Post-Construction site w/o LID scenarios.

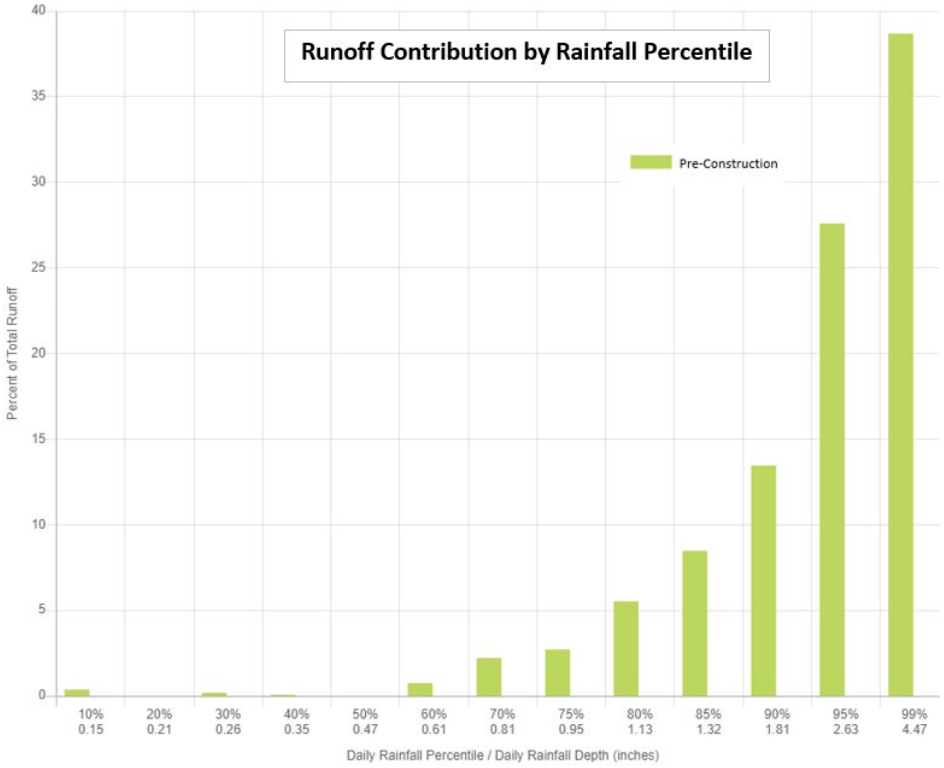

(a) Pre-construction runoff conditions

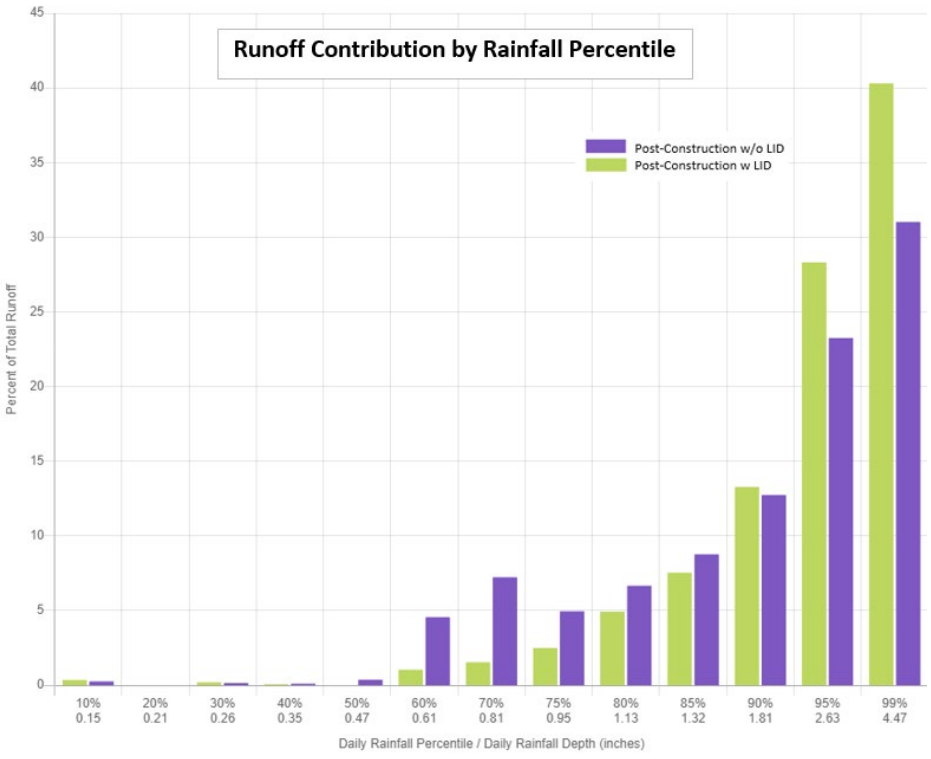

(b) Post-construction runoff conditions

Figure 4.7 Runoff Contribution by Rainfall Percentile of Pre-Construction, Post-Construction with and without (w/o) LID.

The pre-construction histogram (Figure 4.7) shows the contribution of different rainfall percentiles to total runoff. Figure 4.7 shows that smaller, more frequent rainfall events contribute less to runoff. As the rainfall percentiles increase, the contribution of runoff increases significantly, peaking at the 95th and 99th percentiles. This suggests that the most significant portion of runoff is due to infrequent but heavy rainfall events. Histograms with and without LID after construction show a significant increase in runoff contributions for all percentiles after construction without LID compared to the pre-construction situation. This suggests that construction activity without LID generally increases runoff from all types of rainfall events. The LID after construction shows that the runoff contribution is usually closer to the pre-construction level, especially in the middle and high percentiles. However, even with LID, the runoff contribution is still slightly higher than the highest percentile pre-construction scenario. Both cases show higher percentiles but are more pronounced in post-construction without LID.

The pre-construction bar chart in Figure 4.8 shows the rainfall depth and the corresponding runoff in different return periods. These extreme event (high intensity) rainfalls are the annual maximum daily rainfall generated using a statistical extrapolation technique (Rossman and Bernagros 2019). To simulate each extreme storm, the SWC uses the NRCS 24-hour distributions (USDA 1986) to disaggregate the event's total rainfall depth into a series of rainfall intensities (in./hr) at six-minute intervals. It can be seen from Figure 4.8 that both rainfall and runoff depth increase with the increase of the return period. Rainfall is always higher than runoff depth because not all rainfall becomes runoff. The bar charts with and without LID after construction show that under the same rainfall depth, the runoff depth after construction without LID is 0.42–0.65 in. higher than before construction, higher increase at a long return period. Compared with no LID, the depth of runoff with LID is reduced at 0.45–0.47 in. from post-construction without LID, although most runoff with LIDs is still slightly higher (~0.15 in.) than before construction. Figure 4.8 and Figure 4.9 use stacked vertical bars, so it is difficult to do a graphic comparison, but a user can hover the cursor over any bars to get its *x* and *y* values.

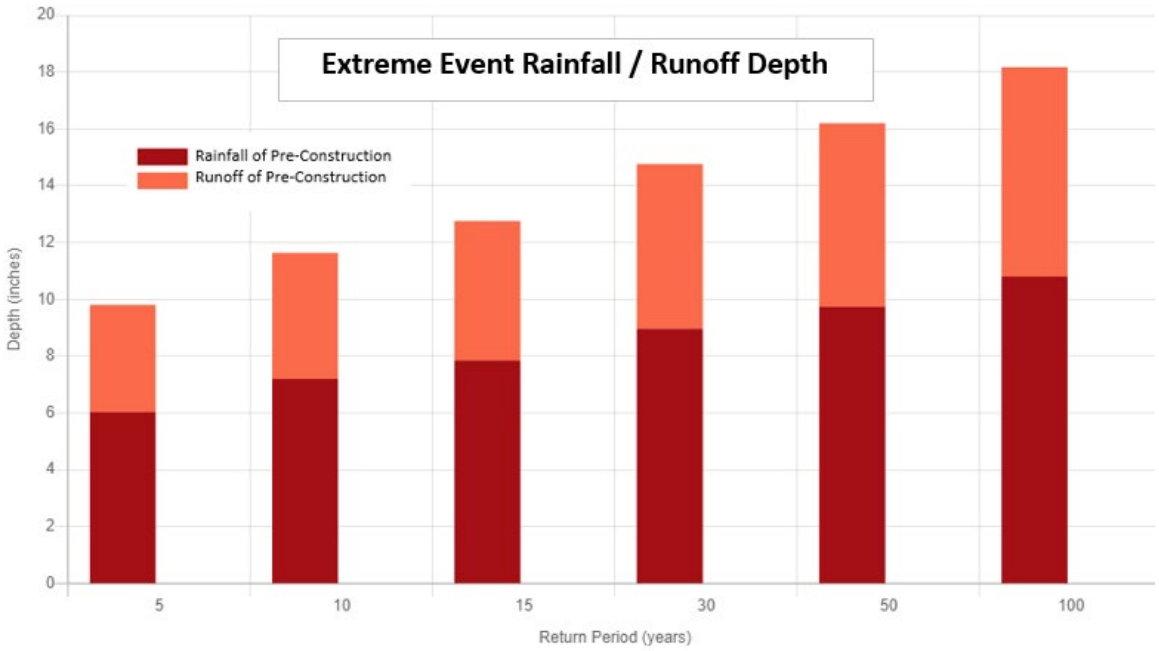

(a) Pre-construction runoff conditions

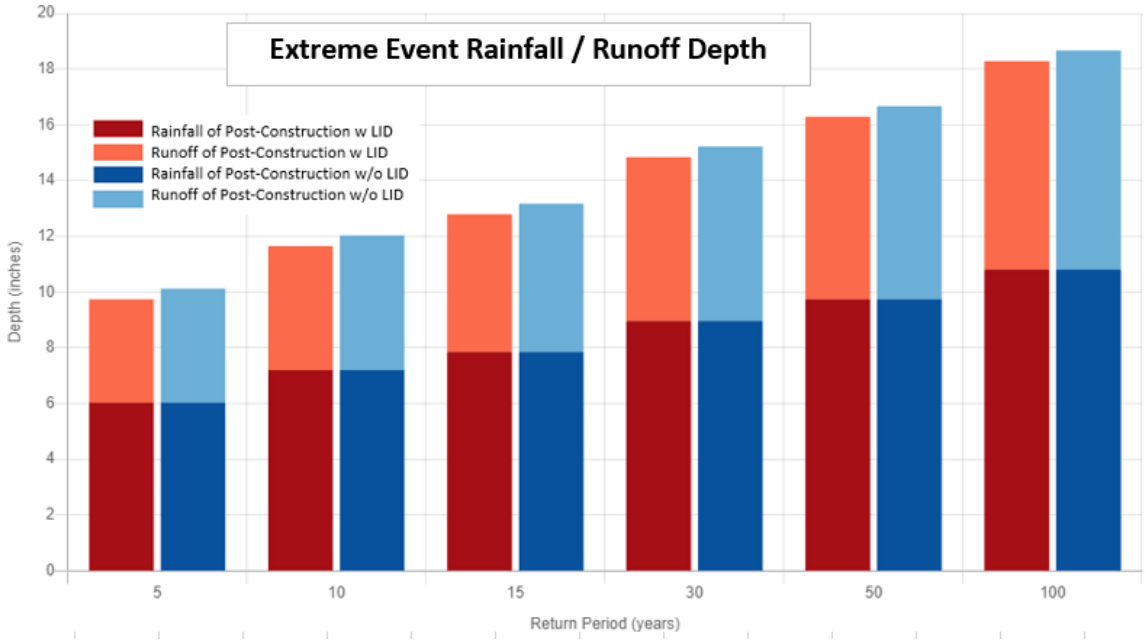

(b) Post-construction runoff conditions

Figure 4.8 Extreme Event Rainfall/Runoff Depth (in.) versus Return Period (years) of Pre-Construction, Post-Construction with LID, and Post-Construction without LID.

The pre-construction histogram (Figure 4.9) shows that the peak rainfall intensity (in./hr) from NRCS distributions (USDA 1986) and related peak runoff intensity (in./hr, peak discharge divided by area) increase with the increase of the return period. Peak runoff intensity is typically larger than the peak rainfall intensity for the study catchment. Moreover,

the differences between runoff and rainfall intensity also increase with the increase in the return period. The bar charts with and without LID after construction show that in all return periods, the post-construction conditions without LID show a slightly higher peak runoff intensity (0.01–0.03 in./hr) than those with LID, which indicates that LID is somewhat effective in reducing the peak runoff depth.

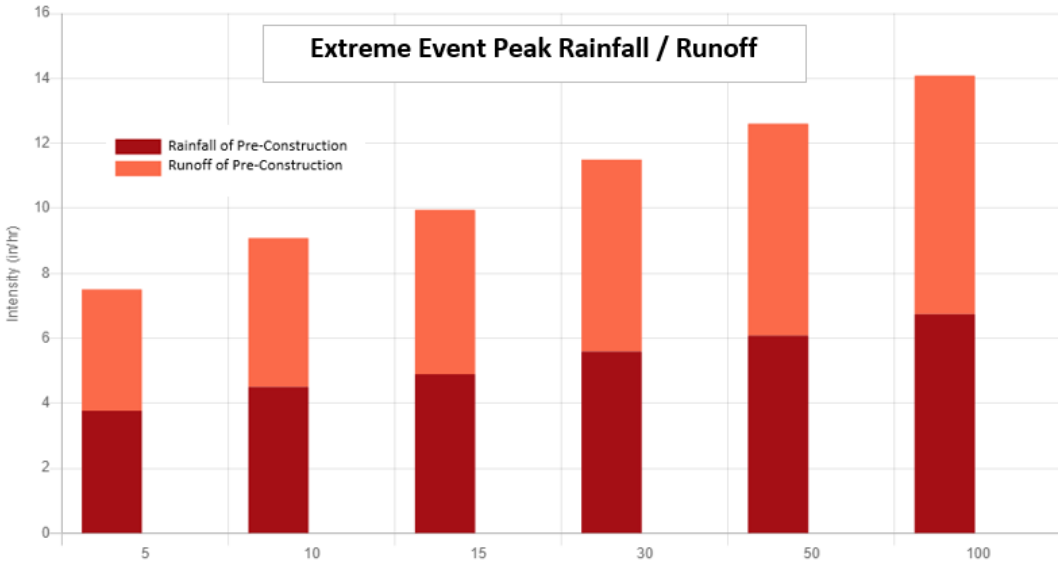

(a) Pre-construction runoff conditions

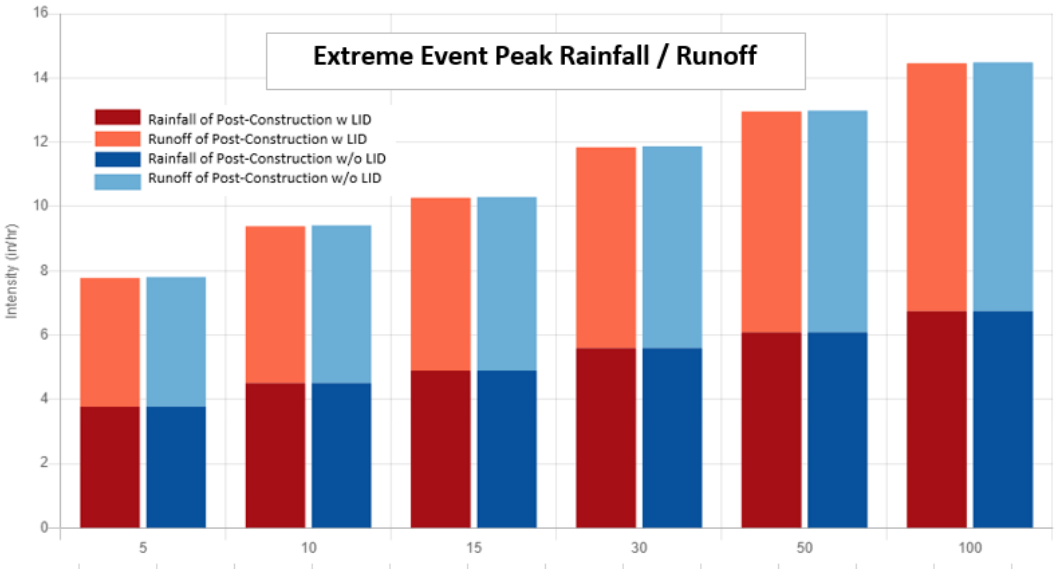

(b) Post-construction runoff conditions

Figure 4.9 Extreme Event Peak Rainfall/Runoff Intensity (in./hr) as a function of the return period (years, x axis) of Pre-Construction, Post-Construction with and without LID.

4.2.3 PREDICTION RESULTS AT OTHER LOCATIONS IN ALABAMA

A hydrologic analysis was conducted for three hypothetical construction project sites in Alabama (Auburn, Birmingham, and Huntsville, Table 4.5) to assess runoff control using infiltration swales in the SWC. Precipitation and air temperature data from Auburn No. 2, Birmingham International Airport, and Huntsville Intl/C.T. Jones FIE stations were used with available data over a 20-year analysis period. Three scenarios—pre-construction, post-construction without LID, and post-construction with LID—were modeled for each site. The same two infiltration swale designs (Table 4.3) were modeled in SWC for three study sites, and different capture ratios for Auburn and Birmingham sites are given in Table 4.5.

Table 4.5 Summary Information from SWC for Three Modeling Sites.

Parameter	Auburn	Birmingham	Huntsville
Address	Lee Road 151, Opelika, AL 36830	Sunrise Ln, Birmingham, AL 35242	AL Hwy 20, Madison, AL 35756
Pre-development Area (ac)	5.41	5.41	5.41
Post-development Area (ac)	5.85	5.85	5.85
Soil Type	Sandy Loam (Moderately Low)	Clay (High Runoff)	Sandy Loam (Moderately Low)
Soil Drainage (in./hr)	0.108	0.108	0.108
Topography	Moderately Flat (5% Slope)	Moderately Steep (10% slope)	Flat (2% Slope)
Pre-construction Land Cover	25% Forest, 65% Lawn, 10% Impervious	90% Forest 10% Impervious	90% Forest 10% Impervious
Post-construction Land Cover	25% Forest, 52% Lawn, 23% Impervious	77% Forest 23% Impervious	73% Forest 27% Impervious
Rainfall/weather station	Auburn NO.2	Birmingham International Airport	Huntsville Intl/C.T.Jones FIE
Years to Analyze	20	20	20
Percent capture ratio	6.86%	6.86%	5.84%

Each scenario exhibits varying impervious area percentages: for Auburn, 10%, 23%, and 23%; for Birmingham, 10%, 23%, and 23%; and for Huntsville, 10%, 27%, and 27% in the pre-construction, post-construction without LID, and post-construction with LID scenarios, respectively. SWC models the pervious areas using four land covers (forest, meadow, lawn, and desert), with only the lawn cover along roadways used for this analysis. For example, in Auburn, the lawn cover in the post-construction with LID scenario was 77% (100% - 23%). The SWC input parameters for each site, including soil type, topography, and drainage rates, are summarized in the table above. A 20-year precipitation data with a 0.1 in. rainfall event threshold was used to simulate long-term hydrologic impacts.

For post-construction without LID in Auburn, the runoff increases significantly from 6.47 in. to 12.61 in. (approximately 95% increase). However, with LID, the runoff reduces to

4.76 in., which is even lower than the pre-construction condition, showing the effectiveness of infiltration swales in reducing runoff. Without LID, infiltration decreases from 46.74 in. to 39.96 in. due to the increase in impervious surfaces. With LID, infiltration rises to 47.24 in., slightly improving over pre-construction conditions, indicating the ability of LID to store/hold/infiltrate more runoff. Post-construction without LID, the number of days with runoff increases to 36.68 (a rise of 131% compared to pre-construction). With LID, the days with runoff decrease to 11.74, showing a reduction in runoff frequency. Post-construction with LID also increases evaporation from 0.56 to 1.80 in., indicating that LID can contribute to water loss through evaporation and reduce runoff.

Table 4.6 Summary Results from SWC for Four Modeling Scenarios in the Auburn area.

Statistic	Pre-Construction	Post-Construction w/o LID	Post-Construction with ALDOTIS	Post-Construction with MIS
Average Annual Rainfall	53.69 in.	53.69 in.	53.69 in.	53.69 in.
Average Annual Runoff	6.47 in.	12.61 in.	4.16 in.	3.14 in.
Average Annual Evaporation	0.56 in.	1.25 in.	1.89 in.	1.71 in.
Average Annual Infiltration	46.74 in.	39.96 in.	47.74 in.	48.95 in.
Days per Year with Rainfall	73.36	73.36	73.36	73.36
Days per Year with Runoff	15.84	36.68	10.09	6.50
Percent of Wet Days Retained	78.41	50.00	86.24	91.14
Smallest Rainfall w/ Runoff	0.56 in.	0.28 in.	0.56 in.	0.56 in.
Largest Rainfall w/o Runoff	1.27 in.	0.54 in.	2.16 in.	2.57 in.
Max Rainfall Retained	3.67 in.	3.13 in.	3.59 in.	3.65 in.

Birmingham shows a higher initial runoff compared to Auburn. Without LID, runoff increases from 12.77 in. to 17.93 in. (approximately 40% increase) (Table 4.7). With LID, it reduces to 10.63 in., indicating LID's ability to partially mitigate the increase in runoff. Without LID, infiltration decreases from 39.49 in. to 33.75 in.. With LID, it increases to 40.45 in., slightly exceeding pre-construction levels. The number of days with runoff almost doubles without LID (19.89 to 36.68 days). With LID, the days with runoff drop to 16.79, bringing it closer to pre-construction levels. With LID, the largest rainfall without runoff increases from 0.58 in. (without LID) to 1.83 in., showing how LID controls can reduce runoff for more substantial rainfall events.

Table 4.7 Summary Results from SWC for Four Modeling Scenarios in the Birmingham area.

Statistic	Pre-Construction	Post-Construction w/o LID	Post-Construction with ALDOTIS	Post-Construction with MIS
Average Annual Rainfall	52.88 in.	52.88 in.	52.88 in.	52.88 in.
Average Annual Runoff	12.77 in.	17.93 in.	9.96 in.	9.29 in.
Average Annual Evaporation	0.87 in.	1.47 in.	2.03 in.	1.88 in.
Average Annual Infiltration	39.49 in.	33.75 in.	41.04 in.	41.85 in.
Days per Year with Rainfall	73.46	73.46	73.46	73.46
Days per Year with Runoff	19.89	36.68	15.84	14.84
Percent of Wet Days Retained	72.93	50.07	78.44	79.80
Smallest Rainfall w/ Runoff	0.28 in.	0.13 in.	0.28 in.	0.28 in.
Largest Rainfall w/o Runoff	1.05 in.	0.58 in.	2.00 in.	2.00 in.
Max Rainfall Retained	2.58 in.	2.21 in.	2.62 in.	2.66 in.

In the Huntsville area, without LID, the runoff increases from 8.36 in. to 15.50 in., nearly doubling. With LID, the runoff drops to 7.01 in., lower than the pre-construction condition, indicating effective runoff control through LID. Without LID, infiltration drops from 41.77 in. to 33.79 in. With LID, it returns to 41.61 in., essentially restoring pre-construction infiltration conditions. Without LID, the number of days with runoff increases from 15.34 to 39.88, reflecting the rise in impervious surface area. With LID, the days with runoff are reduced to 13.54, showing the effectiveness of the swales in reducing the frequency of runoff events. Like Auburn, Huntsville increases evaporation with LID (2.23 in. compared to 0.80 in. pre-construction), suggesting that more water is retained and lost to evaporation rather than contributing to surface runoff.

Across all three sites, LID practices significantly reduce the runoff compared to the post-construction without LID scenario. Huntsville shows the most substantial reduction, achieving lower runoff than pre-construction levels. LID helps restore infiltration levels that are otherwise diminished due to increased impervious surfaces. In Auburn and Huntsville, infiltration levels with LID exceed or nearly match pre-construction values, showing that infiltration swales effectively promote groundwater recharge. Post-construction with LID consistently increases evaporation across all three sites, indicating that LID practices encourage water retention and evapotranspiration, which help reduce runoff. The frequency of runoff events increases significantly post-construction without LID but decreases with LID implementation. This is critical in managing stormwater in urbanized areas as it reduces the strain on drainage systems and lowers the risk of flooding.

Table 4.8 Summary Results from SWC for Four Modeling Scenarios in the Huntsville area.

Statistic	Pre-Construction	Post-Construction w/o LID	Post-Construction with ALDOTIS	Post-Construction with MIS
Average Annual Rainfall	50.78 in.	50.78 in.	50.78 in.	50.78 in.
Average Annual Runoff	8.36in.	15.50 in.	7.01 in.	6.38 in.
Average Annual Evaporation	0.80 in.	1.64 in.	2.23 in.	2.07 in.
Average Annual Infiltration	41.77 in.	33.79 in.	41.61 in.	42.39 in.
Days per Year with Rainfall	75.86	75.86	75.86	75.86
Days per Year with Runoff	15.34	39.88	13.54	12.04
Percent of Wet Days Retained	79.78	47.43	82.15	84.12
Smallest Rainfall w/ Runoff	0.13 in.	0.13 in.	0.13 in.	0.13 in.
Largest Rainfall w/o Runoff	1.11 in.	0.47 in.	1.83 in.	2.05 in.
Max Rainfall Retained	3.02 in.	2.46 in.	2.83 in.	2.87 in.

The SWC tool, leveraging historical rainfall data, soil characteristics, and land cover information, provides a clear framework for comparing pre-construction, post-construction without LID, and post-construction with LID scenarios. The use of the SWC to evaluate the performance of infiltration swales for stormwater management demonstrates the significant impact of LID practices on mitigating runoff, improving infiltration, and enhancing water retention across different geographic locations in Alabama.

4.2.4 Limitations Using the National Stormwater Calculator

While the SWC is a valuable tool for modeling stormwater management and the impacts of LID practices, several limitations can affect the accuracy and applicability of results. For users' convenience, the SWC directly provides data from several national databases on soil type, topography, and weather according to the study location. However, it cannot directly input detailed information like the catchment's width and slope. The study site is for a relatively small area and cannot be divided into different sub-catchments, such as the road, natural area, channel, and so on. It is not a good representation of the site with different sub-areas impacting the runoff because of their hydrologic properties. The SWC is most appropriate for performing screening level analysis of small footprint sites up to several dozen acres in size with uniform soil conditions. It includes only five land cover types with default or pre-selected depression storage depths and surface roughness coefficients. The SWC uses an area-weighted average of depression storage depths and roughness coefficients for the previous area in one catchment.

The SWC uses the long-term historic rainfall as the precipitation in the stormwater modeling, it summarizes results as the annual averages or daily values. Grouping rainfall data and simulated runoff as daily values may result in the wrong information when some of the rainfall crosses midnight and is grouped into two days. For a more accurate analysis of

rainfall and runoff, they should be separated by an appropriate inter-event dry period (e.g., 6 hours).

The SWC allows a user to set an event threshold (e.g., 0.1 in.), which is the minimum amount of rainfall (or runoff) that must occur over a day for that day to be counted as having rainfall (or runoff). Rainfall (or runoff) above the threshold is referred to as "observable" or "measurable". For example, a 10-acre site with 0.1 in. of runoff has 3,630 ft^3 of runoff volume, which most of the management agencies would not consider as not measurable runoff. Later (section 5.4.6) we will find out that there are many events producing runoff less than or equal to 0.1 in. for the Southern Alabama study site under the post-construction without LID scenario.

The SWC can simulate the impacts of LIDs, but only limited LID property parameters (e.g., Table 4.3 for infiltration swales) can be inputted by a user. All other LID parameters are pre-selected and cannot be altered by a SWC modeler.

Therefore, although SWC is a widely useful tool for stormwater management, it still has some limitations and cannot provide enough information for runoff analysis. In the next part, we will use the EPA's Stormwater Management Model, which can provide more details for our research.

4.3 Evaluating the Infiltration Swales Using SWMM

The EPA Storm Water Management Model (SWMM) was used to study the performance of infiltration swales in controlling the surface runoff from contributing watersheds. Two field-scale infiltration swales (ALDOTIS and MIS) were constructed and tested at the Auburn University - Stormwater Research Facility (Austin 2024), as presented in Chapter 3. The data collected from these two infiltration swales were used to examine/calibrate the SWMM models developed for them. SWMM was also used to study the performance of an infiltration swale (both ALDOTIS or MIS designs) in a South Alabama construction site under the design rainfall and long-term historical rainfall events. Then, we studied how the infiltration swale controls the runoff under the central (Birmingham) and north (Huntsville) Alabama climatic conditions. Model results are analyzed and discussed.

4.3.1 Introduction of SWMM Model

The SWMM is a dynamic hydrologic and hydraulic simulation tool developed by the USEPA for modeling stormwater runoff, water quality, and the performance of stormwater control measures in urban and rural areas. SWMM is widely used for designing, analyzing, and managing stormwater drainage systems, including evaluating various LID techniques like infiltration swales, rain gardens, and permeable pavements.

SWMM models the rainfall-runoff process for pervious and impervious surfaces in each subcatchment, considering factors such as rainfall intensity, soil infiltration rates, and surface storage. This enables accurate estimation of stormwater generation during rain events. The model replicates the movement of stormwater through drainage networks, encompassing pipes, channels, and detention ponds. SWMM can analyze both steady-state

and unsteady flows, aiding in comprehending water movement through intricate drainage systems. In addition to hydrologic and hydraulic processes, SWMM can simulate pollutant buildup and wash-off, modeling stormwater quality as it progresses through the system. This is crucial for assessing the environmental impact of stormwater runoff on water bodies. SWMM allows for integrating LID techniques to mimic natural hydrology and decrease runoff by encouraging infiltration, evaporation, and storage; the BRC in Figure 4.3 is an example. LID controls can be simulated within SWMM to evaluate their effectiveness in managing stormwater and reducing flood risks. SWMM is employed in various applications, from small-scale site-specific studies to large-scale watershed management projects. It supports long-term (e.g., over many years) continuous simulations and short-term event-based modeling for design storms and historical events.

The SWMM is a link and node model system. Links represent the transport components, such as pipes, orifices, weirs, and outlets, in a drainage system. Nodes represent the transport compartments, such as junctions and storage units (detention ponds, reservoirs, etc.). Each SWMM model includes one or more subcatchments that receive precipitation and generate runoff and pollutant loads, rain gauges that specify the rainfall events for simulation, nodes, and links. There are many parameters (Table A.1) to consider when setting up a subcatchment in SWMM.

The USEPA SWMM can simulate eight types of LID controls: BRC, Rain Garden, Green Roof, Infiltration Trench, Permeable Pavement, Rain Barrel, Rooftop Disconnection, and Vegetative Swale. Infiltration swales differ from most LID types (green roofs, rain gardens, permeable pavements, infiltration trenches, and vegetative swales). However, they closely resemble bio-retention cells. In SWMM, bio-retention cells are modeled with three main layers: surface, soil, and storage, with an optional drainpipe (Figure 4.3 and Figure 4.10), making this the most appropriate LID type for simulating infiltration swales. Normally, a BRC receives all or a part of the runoff from the impervious areas of a watershed to reduce the runoff flowing downstream. However, infiltration swales are placed in a drainage channel that receives all runoff from all pervious and impervious areas of the study area.

4.3.2 SWMM Model for ALDOTIS

Appendix A provides detailed steps to set up a SWMM model, and section A.6 provides the necessary steps to create a “LID Control” in SWMM for configuring infiltration swales. First, go to “Hydrology” under the Property browser panel to access/click “LID Controls” and click “+” site (Figure A.1) to add a LID object for opening the LID Controls Editor window, as shown in Figure 4.10. Then specify the Control Name, e.g., “AULID” for the MIS, and select/define the “LID Type” as “Bio-Retention Cell”, which is the best fit to describe the infiltration swale as discussed in section 5.2. The third step is to access and input all the necessary property parameters for the LID surface, soil, storage, and drain layers shown in Figure 4.2 and Figure 4.10. The last step is to connect LIDs to a subcatchment by clicking the “LID Controls” property (three dots button on the right) for editing under the LID subcatchment. Figure 4.11 shows sub-windows of “LID Controls” for a subcatchment and “LID Usage Editor” to connect a LID to the subcatchment. Even though Figure 5.11 only shows one LID connecting to the

subcatchment for the current study, in general, many predefined LIDs can be added and connected to a subcatchment. Therefore, it is also called “LID Group Editor”. The SWMM’s LID Group Editor is a tool for managing the placement and configuration of one or multiple LID controls within a subcatchment. It defines a set of preconfigured LID controls to be implemented within the sub-catchment, specifies their dimensions, and allocates the percentage of runoff from the without LID portion of the subcatchment that each LID control will manage/treat runoff.

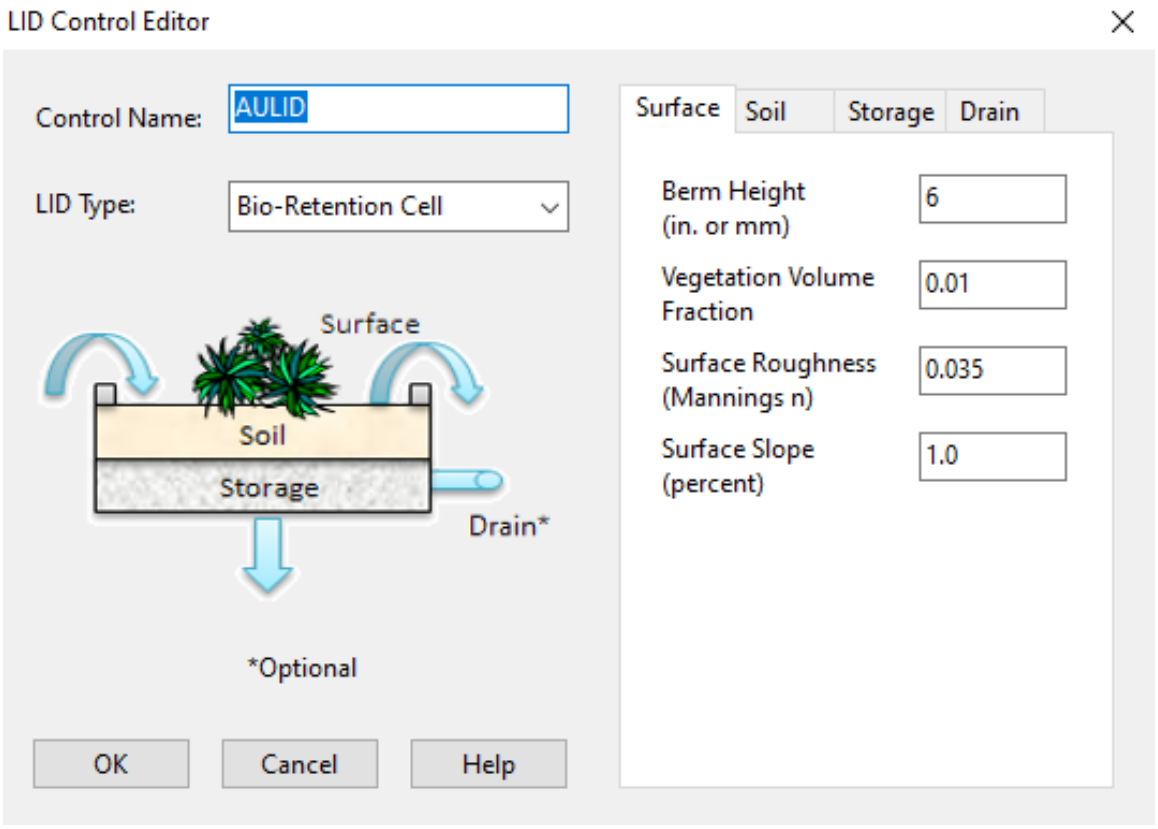

Figure 4.10 SWMM’s LID Control Editor after adding an LID object under the “LID Controls” category of “Hydrology” in the Project browser panel.

The “LID Usage Editor” is accessed through the “Edit” option of the “LID Controls” for a subcatchment (Figure 4.11) after selecting an existing LID control or using the “Add” option when no LID controls have been added yet. It defines how a specific LID control will be applied within the subcatchment. Table provides detailed descriptions for all parameters under the “LID Usage Editor.” In this study, “LID Occupies Full Catchment” is checked, and then % of Impervious or Pervious Area Treated is ignored (no input data is needed). However, when a LID facility does not occupy full catchment, one must specify them, which are very important LID design parameters to determine how much runoff flows to the LID for retention/storage/infiltration and water quality improvement. The total area allocated to all LID units within the subcatchment must not exceed 100% of the subcatchment's total area.

Similarly, the percentages of runoff treated from impervious and pervious surfaces must not exceed 100%.

LID Usage Editor's "% Initially Saturated" parameter allows SWMM to determine/calculate the initial soil moisture in the soil layer and the water level in the storage layer (multiplied by the storage layer thickness). The percent saturation for the soil layer is 0% at the wilting point and 100% at the porosity. The "% Initially Saturated" will affect how the soil moisture and storage water level change with time after rainfall events, which will be shown in section 5.4.5 (e.g., Figure 4.13, Figure 4.15, and Figure 4.17). The same "% Initially Saturated" is applied to both the soil and the storage layers. The simulation results in section 5.4.5 show that these two % saturations can be quite different at the following events, e.g., the soil has 77–81% saturation, but the storage is dry, 0% saturation (Figure 4.13). Therefore, using the same "% Initially Saturated" for both layers may not allow SWMM to model/duplicate the results/observations for some LID facilities under certain rainfall events. This impact could be larger for a short-term simulation (a few rainfall events) and much less for the long-term simulations of LID facilities or no effect after the model warming-up or spin-up period. SWMM molders may not have the data for "% Initially Saturated" so it can be estimated or considered a calibration parameter.

The "Detailed Report File" in the LID Usage Editor is optional but could be an important output file that contains detailed time-series data about the performance of the LID unit. It includes a time series of total inflow from subcatchment to LID (including the direct rainfall), total evaporation, surface infiltration to the soil layer, soil or pavement percolation to the storage layer, storage exfiltration or seepage to the native soil, surface runoff, underdrain outflow, surface-layer water level, pavement water level, soil moisture content, and storage-layer water level. The first eight variables are in./hr over (normalized by) the LID surface area, the three water levels are in., and the moisture content is dimensionless. These valuable data can help modelers/engineers better understand the performance of LID under different rainfall or upstream runoff conditions as shown in section 5.4.5. They can help identify potential problems, such as too small storage thickness or insufficient soil infiltration rate, and find out why LID may not be able to reduce runoff or meet design objectives effectively. This may lead to adjusting LID parameters such as surface area, storage-layer thickness, or soil characteristics to achieve better performance of LID in controlling/ retaining/storing the surface runoff for stormwater management.

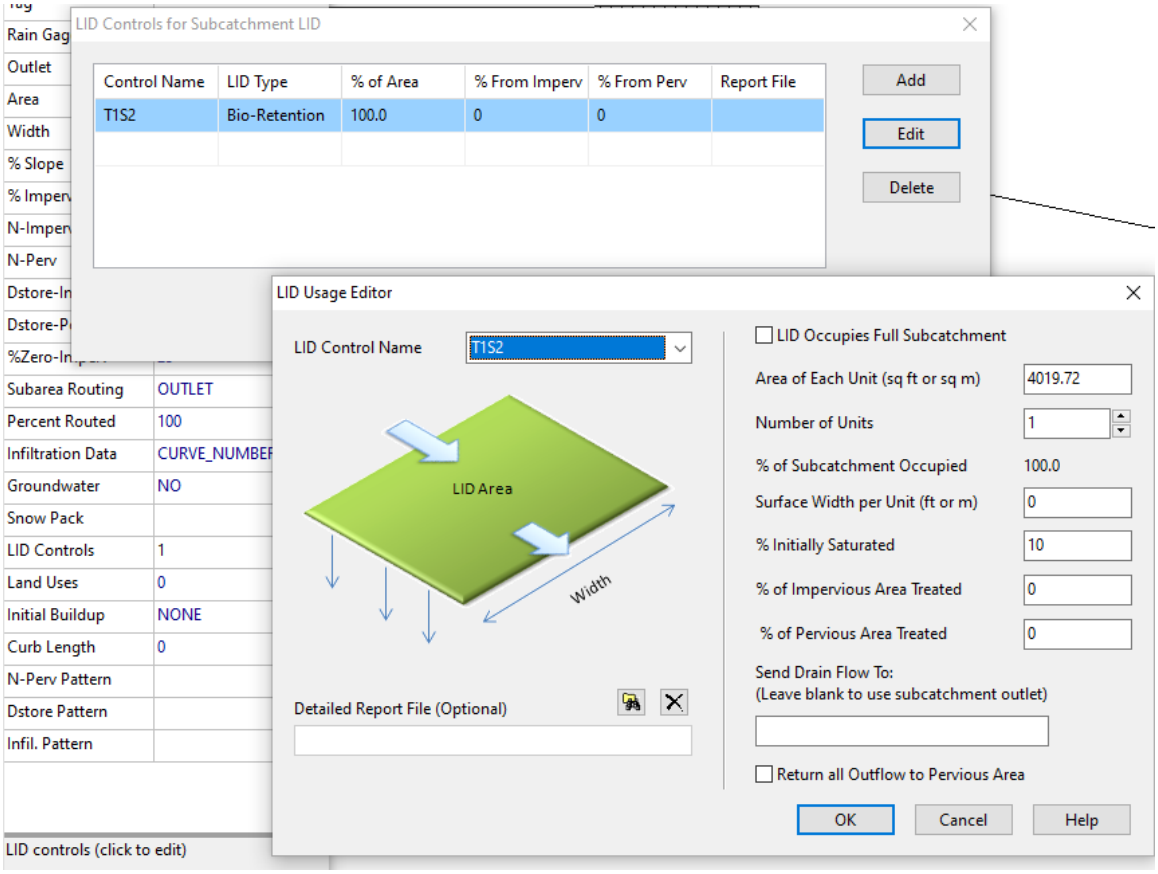

Figure 4.11 Sub-windows of "LID Controls" for a subcatchment and "LID Usage Editor" to connect a LID to the subcatchment.

4.3.3 How to use the CN Method to Mimic the Runoff Coefficient Method

ALDOT's GFO 3-73 suggests using the 95th percentile rainfall as a design storm to size infiltration swales or other green infrastructures to capture the runoff volume increase from pre- to post-development conditions. Runoff volumes and peak discharges for the pre- to post-development conditions are determined using ALDOT internal procedure for small storm events, i.e., the 95th percentile daily rainfall that ranges from approximately 2.0 to 2.8 in. for Alabama. For the ALDOT drainage design or stormwater management study, each contributing watershed to an outlet (or stormwater inlet) is often divided into several sub-areas (ALDOT calls "source areas" meaning contributing areas) under 8 categories: roof areas, parking and storage areas, driveway or sidewalks, streets or alley areas, highway areas, undeveloped or pervious areas, residential areas, and other areas (commercial/industrial, high traffic urban paved areas, high traffic urban pervious areas, excavation or embankment construction). Each type of these sub-areas has further sub-categories with assigned volumetric runoff coefficients R_v from rainfall depths of 2, 2.2, 2.4, 2.6, and 2.8 in. The volumetric runoff coefficient R_v is used to convert design rainfall depth into rainfall excess or runoff depth in in. and may increase slightly with rainfall depth, for

example, streets with smooth textures have R_v of 0.88 at 2 in. (runoff of 1.76 in.) and 0.91 at 2.8 in. design rainfall (runoff of 2.55 in.).

The SWMM model considers the infiltration process, i.e., rainfall penetrating the ground surface into the unsaturated soil zone, with five modeling options: classical Horton method (five model parameters), modified Horton method, Green-Ampt method (three model parameters), modified Green-Ampt method, and Curve Number (CN) method. The CN method in SWMM has one model parameter for design event modeling and uses one more parameter (drying time, the number of days it takes a fully saturated soil to dry) for long-term simulations with many rainfall events. The ALDOT method of determining runoff for small storm events (95th percentile rainfall depth P) is also based on the NRCS CN method and uses Equation 4.8 to calculate CN from runoff Q that is equal to design rainfall P times runoff coefficient R_v ($Q = P \times R_v$). Therefore, the CN method in SWMM is used to model the rainfall-runoff process in contributing areas to the infiltration swales.

$$CN = \frac{1000}{10+5P+10Q-10\sqrt{Q^2+1.25QP}} \tag{4.8}$$

In the SWMM model, runoff from a rainfall event depends on not only the infiltration method for the previous area but also several other modeling parameters: percent of impervious area, depression storages (in. or mm, Dstore) for impervious and pervious areas. First, one should understand that the CN method in SWMM does not directly include the initial abstraction (I_a) in the NRCS CN method: $I_a = r\,S$, where S is the potential maximum soil retention and a function of CN (S = 1000/CN -10), and r is user-defined ratio typically between 0.05 to 0.2 (the standard NRCS method uses r = 0.2). Therefore, it is proposed that depression storage in SWMM of previous areas is set to be 0.1S (r = 0.1) to mimic the initial abstractions I_a. For ALDOT source areas with CN < 99, the percent of impervious areas in SWMM is set to be 0% since CN is a lumped rainfall loss parameter for both impervious and pervious areas of a source area. SWMM model (Figure 4.12) also reports the runoff coefficient (total runoff divided by total precipitation) for each subcatchment; therefore, we can verify whether the proposed method works well or not, i.e., comparing the simulated runoff and reported R_v by SWMM with them from ALDOT spreadsheet.

Further study on SWMM code on CN method finds that SWMM set two limits for CN: $10 \le CN \le 99$. When the CN specified by the user/modeler is greater than 99, the SWMM code resets the CN to 99. ALDOT drainage design R_v table has several source areas with R_v = 0.99, and the calculated CN from Equation 4.8 is 99.8 (greater than 99). The initial SWMM tests indicate that using CN = 99 and 0% impervious area cannot produce the needed runoff for the source areas with runoff coefficient R_v = 0.99. From test trials, it was found that using CN = 99, 99% impervious area, Dstore = 0.01in. for the impervious area can produce needed runoff (i.e., 0.99P) in SWMM. For source areas with hydrologic soil group (HSG) A, R_v is quite small (<0.15), the calculated CN is less than 70, the calculated Dstore (*0.1S*) becomes too large (>0.5 in., Table 4.8), the simulated runoff and corresponding R_v from SWMM are too

small. Through test trials, it was found that Dstore should be calibrated for each case, and Dstore is 0.07S to 0.09S for hydrologic soil group (HSG) A soil in SWMM.

SWMM models were systematically set up to test the proposed method to model different ALDOT source areas under different design rainfall (2.0 to 2.8 in.). Figure 4.12 shows subcatchment runoff summary results from an SWMM model with four different source areas: undeveloped, road, roof area, and driveway for a design storm of 2.6 in. from the ALDOT construction project in Southern Alabama. These four source areas have volumetric runoff coefficients, R_v, (from ALDOT drainage design R_v table) of 0.21 (for HSG B), 0.91, 0.99, and 0.99, respectively. Figure 4.12 shows SWMM runoff coefficients for these four source areas match well with ALDOT R_v values. Table 4.8 lists calibration test results of the SWMM CN method for various source areas, including ones with R_v = 0.99 or less than 0.15, as discussed previously. For R_v < 0.15, Table 4.8 lists the calculated Dstore as *0.1S*, calibrated Dstore (0.07S to 0.09S), corresponding R_v values, and their errors (difference in R_v values). In summary, one can use the SWMM CN number method and appropriate Dstore value (0.07S–0.1S) to reasonably reproduce runoff from different contributing/source areas along roadways.

Summary Results

Topic: Subcatchment Runoff Click a column header to sort the column.

Subcatchment	Total Precip in	Total Runon in	Total Evap in	Total Infil in	Imperv Runoff in	Perv Runoff in	Total Runoff in	Total Runoff 10^6 gal	Peak Runoff CFS	Runoff Coeff
Undeveloped	2.60	0.00	0.00	1.60	0.00	0.56	0.56	0.06	0.45	0.215
Road	2.60	0.00	0.00	0.19	0.00	2.38	2.38	0.10	2.31	0.916
RoofArea	2.60	0.00	0.00	0.00	2.57	0.02	2.59	0.00	0.07	0.998
Driveway	2.60	0.00	0.00	0.00	2.57	0.02	2.59	0.01	0.17	0.998
LID	2.60	68.57	0.00	5.66	0.00	0.00	42.62	0.11	2.48	0.599

Figure 4.12 Subcatchment runoff summary results (snapshot) from a SWMM model with four different source areas (not including LID)

Table 4.8 Calibration test results of SWMM CN method for various source areas.

Source Areas	Rainfall (inches)					Rainfall (inches)					Rainfall (inches)					Rainfall (inches)				
	2	**2.2**	**2.4**	**2.6**	**2.8**	2	2.2	2.4	2.6	2.8	2	2.2	2.4	2.6	2.8	2	2.2	2.4	2.6	2.8
Roof Areas	**Rv**					**CN/Dstore-Perv**					**Rv from SWMM**					**Error (Difference in Rv)**				
Flat, Connected	0.90	0.91	0.91	0.92	0.93	98.2/0.018	98.3*/0.017	98.1/0.018	98.2/0.019	98.3/0.018	0.901	0.914	0.912	0.923	0.931	-0.001	-0.004	-0.002	-0.003	-0.001
Pitched, Connected	0.99	0.99	0.99	0.99	0.99	99/0.010	99/0.010	99/0.010	99/0.010	99/0.010	0.995	0.996	0.996	0.997	0.997	-0.005	-0.006	-0.006	-0.007	-0.007
Flat or Pitched, Unconnected, A Soil	0.07	0.09	0.10	0.12	0.13	65.3/0.531 (0.400)	65.2/0.534 (0.450)	64.2/0.558 (0.470)	64.2/0.558 (0.500)	63.4/0.577	0.002 (0.068)	0.041 (0.082)	0.060 (0.100)	0.095 (0.120)	0.115	0.068 (0.002)	0.049 (0.008)	0.040 (0.000)	0.025 (0.000)	0.015
Flat or Pitched, Unconnected, B Soil	0.16	0.18	0.19	0.21	0.22	73/0.370	72.5/0.380	71.4/0.401	71.1/0.406	70.2/0.425	0.160	0.189	0.202	0.231	0.241	0.000	-0.009	-0.012	-0.021	-0.021
Flat or Pitched, Unconnected, C or D Soil	0.26	0.28	0.29	0.31	0.32	78.9/0.267	78.4/0.276	77.4/0.292	77/0.299	76.3/0.311	0.288	0.313	0.324	0.346	0.359	-0.028	-0.033	-0.034	-0.036	-0.039
Driveways or Sidewalks																				
Connected	0.99	0.99	0.99	0.99	0.99	99/0.010	99/0.010	99/0.010	99/0.010	99/0.010	0.995	0.996	0.996	0.996	0.970	-0.005	-0.006	-0.006	-0.006	0.020
Unconnected, A Soil	0.07	0.09	0.10	0.12	0.13	65.3/0.531 (0.515)	65.2/0.534 (0.432)	64.2/0.558 (0.450)	64.2/0.558 (0.460)	0.577	0.001 (0.070)	0.041 (0.088)	0.058 (0.106)	0.093 (0.134)	0.114	0.069 (0.000)	0.049 (0.002)	0.042 (-0.006)	0.027 (-0.014)	0.016
Unconnected, B Soil	0.16	0.18	0.19	0.21	0.22	73/0.370	72.5/0.380	71.4/0.401	71.1/0.406	70.2/0.425	0.158	0.187	0.200	0.227	0.239	0.002	-0.007	-0.010	-0.017	-0.019
Unconnected, C or D Soil	0.26	0.28	0.29	0.31	0.32	78.9/0.267	78.4/0.276	77.4/0.292	77/0.299	76.3/0.311	0.286	0.311	0.322	0.346	0.356	-0.026	-0.031	-0.032	-0.036	-0.036
Highway Areas																				
Paved Lane and Shoulder	0.88	0.89	0.90	0.91	0.91	0.021	0.021	0.021	0.020	0.022	0.888	0.898	0.906	0.916	0.915	-0.008	-0.008	-0.006	-0.006	-0.005
Undeveloped or Pervious Areas																				
Undeveloped or Pervious Areas, A Soil	0.07	0.09	0.10	0.12	0.13	65.3/0.531 (0.380)	65.2/0.534 (0.420)	64.2/0.558 (0.440)	64.2/0.558 (0.480)	63.4/0.577 (0.520)	0.000 (0.071)	0.029 (0.088)	0.048 (0.105)	0.083 (0.121)	0.100 (0.129)	0.070 (-0.001)	0.060 (0.002)	0.050 (-0.005)	0.040 (-0.014)	0.030 (0.001)
Undeveloped or Pervious Areas, B Soil	0.16	0.18	0.19	0.21	0.22	73/0.370	72.5/0.380	71.4/0.401	71.1/0.406	70.2/0.425	0.147	0.177	0.190	0.220	0.229	0.013	0.003	0.000	-0.010	-0.009
Undeveloped or Pervious Areas, C or D So	0.26	0.28	0.29	0.31	0.32	78.9/0.267	78.4/0.276	77.4/0.292	77/0.299	76.3/0.311	0.274	0.299	0.311	0.332	0.346	-0.014	-0.019	-0.021	-0.022	-0.026

4.3.4 BIO-RETENTION CELL MODEL PARAMETERS TO SIMULATE INFILTRATION SWALES

For the SWMM models, BRC is used as the LID type in the LID Control Editor to simulate the hydrologic performance of the ALDOTIS and MIS. Table 4.9 lists key model parameters that are different between ALDOTIS and MIS. For the surface layer of the BRC, the berm height is 6 in., and the vegetation volume fraction is 0. Surface slope and roughness are not used for the BRC. Since the field capacity and wilting point were not measured in our study, we used the corresponding property values of sand (since most of the soil layer is sand) from the Minnesota Stormwater Manual's soil water storage properties found on the website given below:
https://stormwater.pca.state.mn.us /index.php?title=Soil_water_storage_properties.

Table 4.9 Key Model Parameters for Bio-retention Cells Used to Simulate Two Infiltration Swale Designs.

Parameter	ALDOTIS Design	MIS Design
Surface Berm height	6 in.	6 in.
Soil thickness	36 in. (12 in. topsoil and 24 in. fill sand)	16 in. (6 in. topsoil and 10 in. fill sand)
Soil porosity (volume fraction)	0.39	0.46
Field Capacity (volume fraction)	0.17	0.17
Wilting Point (volume fraction)	0.06	0.06
Conductivity (in./hr)	0.93	2.33
Conductivity Slope	30	30
Suction Head (in.)	3.3	2.45
Storage thickness (in.)	12 (24)	32 (44)
Void Ratio (Voids/Solids)	0.85	0.85
Seepage Rate (in./hr)	0.43	0.43

Note: The storage layer thickness inside brackets is for a 5-ft infiltration swale constructed in the Auburn University - Stormwater Research Facility (AU-SRF).

How much runoff each infiltration swale can hold or retain depends on the swale design (thickness of each layer), median porosities, and whether each layer can reach the saturation condition. For a 5-ft ALDOTIS design (constructed at AU-SRF), it can hold a maximum of 31.1 in. (surface 6 in. + soil layer 0.39*36 + storage layer 0.46*24 in.) of runoff if each layer is saturated. If the model runs for 48 hours, the maximum seepage (exfiltration) to the native soil is 20.64 in. (48 hrs*0.43 in./hr) if the storage layer depth does not go to zero. Therefore, the maximum amount of runoff that ALDOTIS design can retain in 48 hours could be 51.7 in., and 53.9 in. for MIS after performing the same calculation. The following modeling studies will explore the potential performance of runoff control for these two designs under various conditions, which can be compared with maximum runoff retentions.

4.3.5 Modeling Constructed Large-Scale Infiltration Swales at AU-SRF

Austin (2024) constructed two infiltration swales at the AU-SRF based on ALDOTIS and MIS designs, as presented in Chapter 3. Austin (2024) conducted several infiltration and drawdown experiments/tests to critically evaluate the performance of ALDOTIS and MIS in controlling runoff. For these experiments, a fixed amount of water (~70 ft^3) was introduced into the surface layer of two infiltration swales with two 6 in. height check dams (one in the middle and another at the end) and with a channel bottom of 4 ft (width) by 40 ft (length) (Figure 3.19) over a short period (~5 minutes) without creating flow overtopping at the downstream check dam.

The water depth near the downstream check dam (deepest point) was monitored using a level logger and the drawdown time was determined when water depth became zero. The initial water depth divided by the drawdown time gave an average infiltration rate that was reported and summarized in Chapter 3 (section 3.5). Infiltration and drawdown experiments were repeated with one-day or three-day dry periods between the water-filling events.

Two SWMM models were developed for these two infiltration swale designs and included a direct high rainfall to generate the needed runoff to fill the surface layer in 5 minutes. Figure 4.13 plots simulated surface depth d_1, soil moisture content θ_2, and storage level d_3 with measured surface depth for four infiltration and drawdown experiments to ALDOTIS design from January 29 at 2 pm (0 hour on the *x*-axis) to February 1, 2024. Water was filled into the infiltration swale with one dry day interval (~24 hours with small variations, 23.1–25.3 hours). Water was added after 24 hours (a dry period) in the SWMM model, and the starting time of measured surface depth in Figure 4.13 was aligned with the water introduction time. The surface berm height used in the BRC was set to 9 in. to prevent surface runoff from the infiltration swale after considering side slopes (3:1) of the trapezoidal channel above LID, but the SWMM model assumes a vertical side wall above LID. The simulated time series of surface depth matches with measured one reasonably well (Figure 4.13) when the equivalent saturated hydraulic conductivity of soil of 0.6 in./hr was used for the calibration run. It was less than 0.93 in./hr calculated using Equation 4.1 and data from Ramirez Florez (2024) infiltration column tests.

Austin (2024) measured soil moisture in the soil layer. It was found that the average soil moisture content was ~27% saturation for ALDOTIS and ~54% saturation for MIS. The soil saturation is the soil moisture content with respect to the wilting point (considered 0% saturation) and porosity (considered 100% saturation). Therefore, the initial saturation of 27% for ALDOTIS and 54% for MIS was used in the SWMM models.

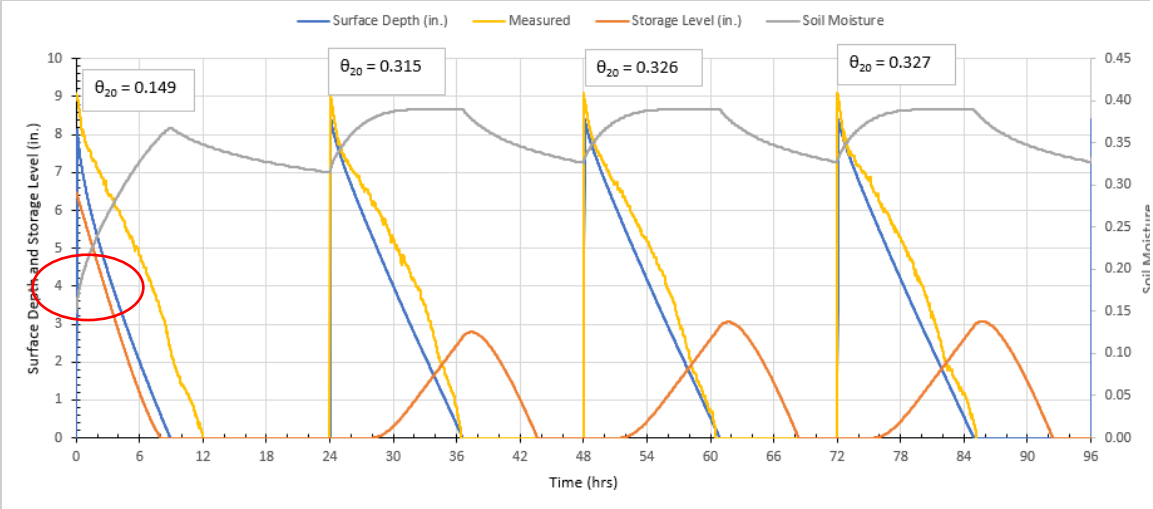

Figure 4.13 Simulated surface depth d_1, soil moisture θ_2, and storage level d_3 with measured surface depth for four infiltration and drawdown experiments with one dry day interval from January 29 at 2 pm (0 on the x axis) to February 1, 2024, for ALDOTIS design.

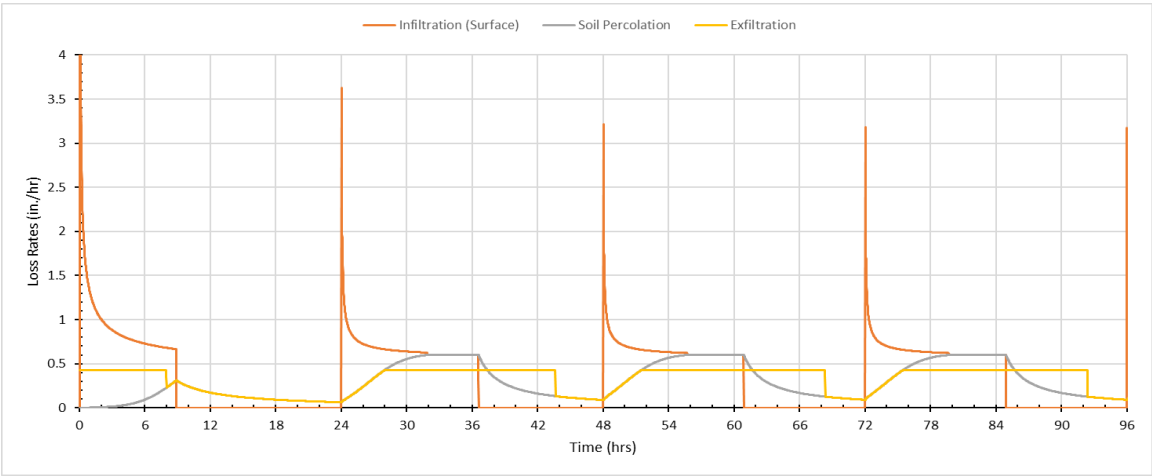

Figure 4.14 Simulated surface infiltration rate, soil percolation, and exfiltration (seepage) (in./hr) for four infiltration and drawdown experiments with one dry day interval from January 29 at 2 pm (0 on the x axis) to February 1, 2024, for ALDOTIS design

Table 4.10 summarizes measured and simulated drawdown time (hours) for infiltration swales. For ALDOTIS, the average measured drawdown time for four experiments with one dry day was 12.47 hrs with a small standard deviation of 0.42 hrs. The simulated drawdown time using k_s = 0.6 in./hr and 27% initial saturation (section 4.9) is 8.9 hrs for the first experiment and then increases to 12.58 hrs for the second experiment (event). The simulated drawdown time for the third event is 12.88 hrs (a small increase), but there is almost no change for the fourth event (12.92 hrs). This is because the simulated soil moisture

content starts at the initial value of θ_{20} = 0.149 for the first event (27% initial saturation with a porosity of 0.39 and wilting point of 0.06), does not reach saturation (maximum of 0.37 when the surface depth becomes zero), and becomes 0.315 (77.2% saturation), 0.326 (80.6% saturation), and 0.327 (80.9% saturation) after 24 hrs for the second, third, and fourth events, respectively (Figure 4.13) since the dry time was one day (24 hours). The simulated soil moisture content reaches saturation (0.39) and lasts several hours for the second, third, and fourth events (experiments) since the drawdown time was approximately 12 hours. The simulated water level in the 24 in. storage layer starts 6.48 in. (27%*24 in.), decreases with time, and becomes zero at 8:00 hrs for the first event since the simulated exfiltration rate is equal to either the seepage rate of the native soil (0.43 in./hr) or the simulated soil percolation rate, whichever is smaller (Figure 4.14). The simulated water level in the storage layer is zero over a number of hours for each of the four experiments when the simulated exfiltration rate and soil percolation rate are the same (Figure 4.14). For the second, third, and fourth events, the simulated water level in the storage layer increases from zero to 2.79 in., 3.05 in., and 3.07 in., respectively, then decreases to zero (Figure 4.13). This indicates that most of the depth and most of the time of the storage layer is not utilized to store the runoff under the experimental condition. Figure 4.14 shows that the simulated infiltration rate is high at the beginning of each experimental event, decreases with time, and becomes the soil's saturated hydraulic conductivity when the soil is saturated (Equation 4.6). The simulated soil percolation rate reaches its maximum value of the soil hydraulic conductivity when the soil is saturated (Equation 4.7).

Table 4.10 Measured and simulated drawdown time (hours) for infiltration swales with one dry day between water-filling events.

Designs	ks	Event 1	Event 2	Event 3	Event 4	Event 5	Average
ALDOTIS (measured)	/	11.97	12.37	12.43	13.10	/	12.47±0.41
ALDOTIS (simulated)	0.6 in./hr	8.90	12.58	12.88	12.92	/	11.82±1.69
MIS (measured)	/	4.17	5.38	8.07	10.90	14.18	8.54±3.65
MIS (Simulated)	0.9 in./hr	7.43	8.65	8.70	8.70	8.70	8.40±0.54

For MIS, the average measured drawdown time for four experiments with one dry day was 7.13 hrs with a large standard deviation of 2.59 hrs because the drawdown time for the first experiment was 4.17 hrs and increased to 10.9 hrs for the fourth experiment (Table 4.10). This large increase in the drawdown time was unusual and was suspected to be influenced by the groundwater level in the water storage pond at AU-SRF because the bottom elevation of MIS was just 1–4 ft above the pond water level. Simulated results from SWMM are presented in Figure 4.15 and Figure 4.16 using 0.9 in./hr for the soil's saturated hydraulic conductivity and 0.43 in./hr for the seepage rate of the native soil. The average simulated drawdown time for four experiments is 8.40 hrs with a standard deviation of 0.54 hrs. The simulated drawdown time is 7.43 hrs for the first experiment and increases to 8.65 hrs for the

second experiment and then has almost no increase from the third to fifth experiments. The simulated soil moisture content starts at the initial value of θ_{20} = 0.276 for the first event (54% initial saturation with a porosity of 0.46 and wilting point of 0.06) and reaches saturation over several hours (making the surface infiltration and soil percolation rates to be 0.9 in./hr) for all four experiments (events) since the soil layer is only 16 in. with higher infiltration rate. The initial value of θ_{20} becomes 0.400 (73.9% saturation), 0.402 (74.3% saturation), and 0.403 (74.6% saturation) after 24 hrs for the second, third, and fourth events, respectively (Figure 4.15). For each experiment, the simulated storage level increases to a maximum height and then decreases with time until the next event starts. The simulated storage level starts at 23.7 in. for 54% initial saturation and decreases to 5.1 in. at 96 hrs because the seepage rate is 0.43 in./hr for the whole simulation period (Figure 4.15) when the storage level is always greater than zero. When MIS's soil layer allows the runoff to infiltrate fast, the storage layer is used better to store the runoff but not fully used since the thickness is 44 in.

For MIS, using a constant soil's saturated hydraulic conductivity k_s of 0.9 in./hr did not result in a good match between the simulated and measured drawdown times: simulated is either 3.3 hrs more or 5.5 hrs less than measured. Therefore, SWMM models were used to run each experiment over 24 hours by changing the soil's k_s and suction head to match the measured drawdown time. The suction head ψ_s was calculated from k_s, $\psi_s = 3.237 k_s^{-0.328}$ (R^2 =0.9), which is the regression equation from SWMM (Rossman and Huber 2016) and based on average values of k_s and ψ_s using the data from Rawls et al. (1983). When the soil's k_s is 1.55, 1.3, 0.9, and 0.68 in./hr for the first, second, third, and fourth experiments, the simulated drawdown time is 4.2, 5.5, 8.02, and 10.8 hrs, respectively, and the root-mean-square error between the simulated and measured drawdown times is only 0.08 hrs. For these model runs, the seepage rate was set as 0.43 in./hr. Considering the groundwater effects, the seepage rate of the native soil could be reduced; however, the groundwater module in SWMM does not simulate and couple with the seepage rate of LIDs (input data). Several SWMM model runs were made to reduce the seepage rate from 0.43 in./hr to 0.1 in./hr but not change on k_s (=1.55 in./hr) to predict similar drawdown times for these four experiments to MIS. This is because the storage layer of MIS can become saturated when the soil's k_s is 1.55 in./hr, leading to plenty of runoff percolating into the storage layer. When the storage layer is saturated, the surface infiltration rate is limited by the seepage rate of the native soil to increase the drawdown time. However, for ALDOTIS, changing the seepage rate does not affect the simulated drawdown time because the storage layer cannot become saturated when it only adds 70 ft^3 of runoff, so the surface infiltration rate is not affected by the seepage rate.

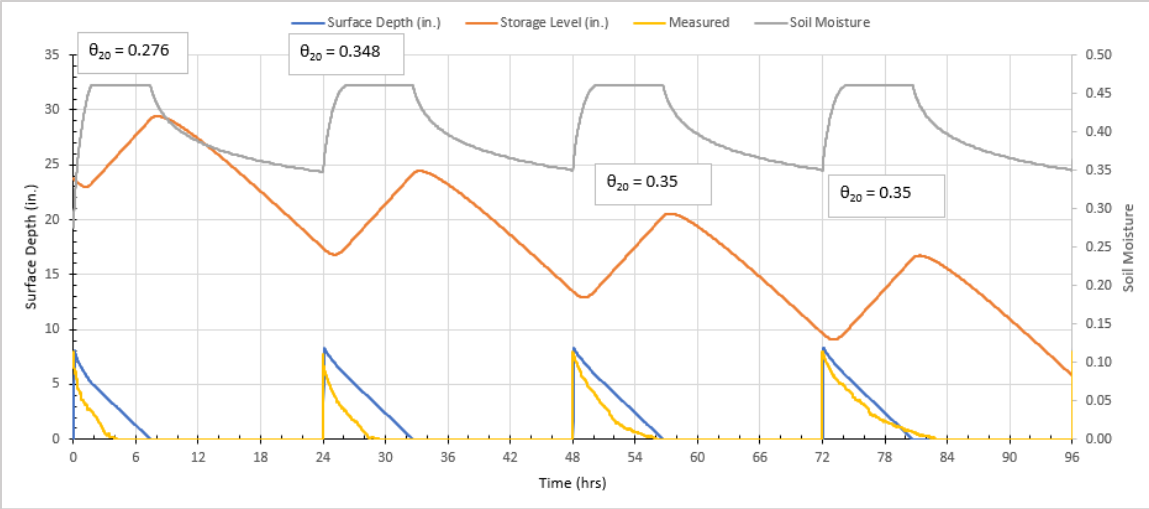

Figure 4.15 Simulated surface depth d_1, soil moisture θ_2, and storage level d_3 with measured surface depth for four infiltration and drawdown experiments with one dry day interval from January 29 at 2 pm (0 on the x axis) to February 1, 2024, for MIS design

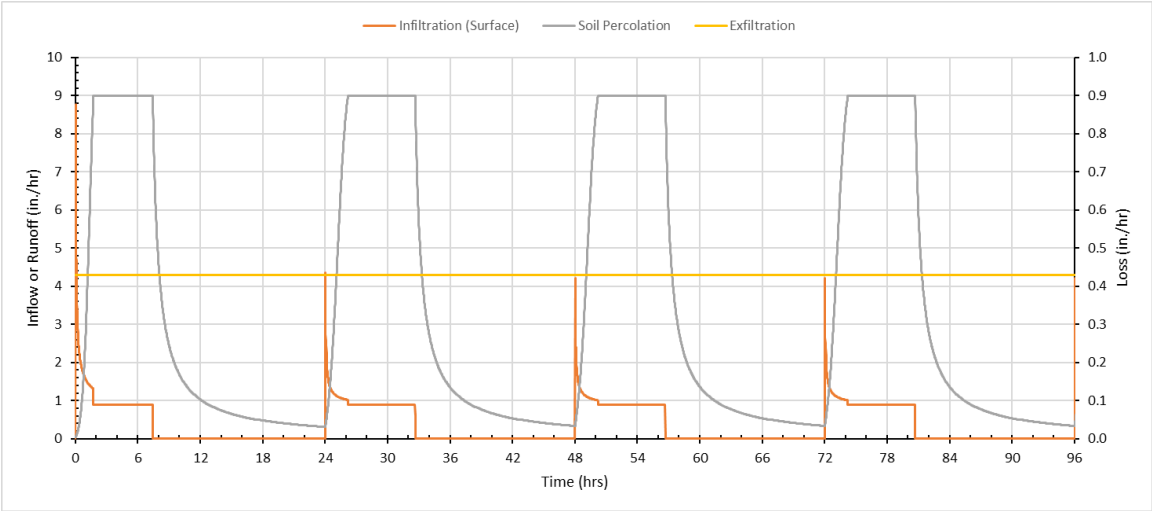

Figure 4.16 Simulated surface infiltration rate, soil percolation, and exfiltration (seepage) (in./hr) for four infiltration and drawdown experiments with one dry day interval from January 29 at 2 pm (0 on the x axis) to February 1, 2024, for MIS design

In late March and early April of 2024, Austin (2024) performed additional infiltration and drawdown experiments for both field-scale infiltration swales with three dry days between experiments since it has a low probability for four rainfall events with one dry day (January experiments). Table 4.11 summarizes the measured and simulated drawdown time for five experiments started on March 29, 2024, with three dry days. The calibrated soil's saturated hydraulic conductivity in the SWMM LID module is 0.8 in./hr for ALDOTIS and 2.33 in./hr for MIS, and then the average simulated drawdown time matches reasonably well with

the average measured drawdown time. When the soil's saturated hydraulic conductivity is 0.8 in./hr for ALDOTIS with three dry days, the simulated drawdown time for the second event is 0.73 hrs longer than for the first event. However, the increase from the first to the second event for one dry day is 3.8 hrs for ALDOTIS (Table 4.10). It means longer dry days between events have less impact on the LID's hydrologic performance. When the soil's saturated hydraulic conductivity is 2.33 in./hr for MIS with three dry days, the simulated drawdown time for all four experiments is basically the same (2.92 hrs). The measured drawdown times for MIS had a variation of 0.54 hours for five events over 17 test days.

Table 4.11 Measured and simulated drawdown time (hours) for infiltration swales under five water-filling (rainfall) events having three dry days between two events.

Type	k_s	Event 1	Event 2	Event 3	Event 4	Event 5	Average
ALDOTIS (measured)	/	8.73	7.22	7.35	6.43	6.27	7.20±0.88
ALDOTIS (simulated	0.8 in./hr	6.77	7.50	7.53	7.53	7.53	7.39±0.30
MIS (measured)	/	3.27	2.30	3.30	2.23	2.03	2.63±0.54
MIS (Simulated)	2.33 in./hr	2.93	2.92	2.92	2.92	2.92	2.92±0.01

Figure 4.17 shows simulated surface depth, d_1, soil moisture, θ_2, storage level, d_3, and measured surface depth versus time for the first three infiltration and drawdown experiments with three dry days from March 28 at 9:23 am (0 on the *x* axis) to April 5, 2024, for (a) ALDOT and (b) MIS designs. The simulated drawdown time for the first experiment is approximately two hours smaller than the measured one for the ALDOTIS, and the simulated ones match reasonably well with the measured ones for the second and third experiments; however, the measured drawdown times for the fourth and fifth experiments decreased by about one hour unexpectedly when the simulated ones remained unchanged (7.53 hours). For MIS, the simulated drawdown times match reasonably well with the measured ones (Table 4.10 and Figure 4.17). The simulated storage level starts at 24 in. for the initial saturation of 54.4%, increases to 35 in. due to the water filling on the first day, and then continuously decreases to zero at approximately 29 hours before the second water filling starts. This is likely due to the seepage rate into the native soil from the storage layer is 0.43 in./hr as long as the storage level is positive. Therefore, for MIS with a 44 in. storage layer, the runoff for the first water-filling takes 44.6 hours (1.9 days) to exfiltrate into the native soil, respectively. Figure 4.17 also shows that, for MIS, the second and third water-filling events only increase the storage water level to 10.7 in. at approximately 3:55 hours and then decrease to zero at 18 hours. With three dry days, MIS's storage layer at the beginning of the later water-filling event (excluding the first one) is completely dry, but the soil is wet. This indicates the saturation of the soil and storage layers could be different.

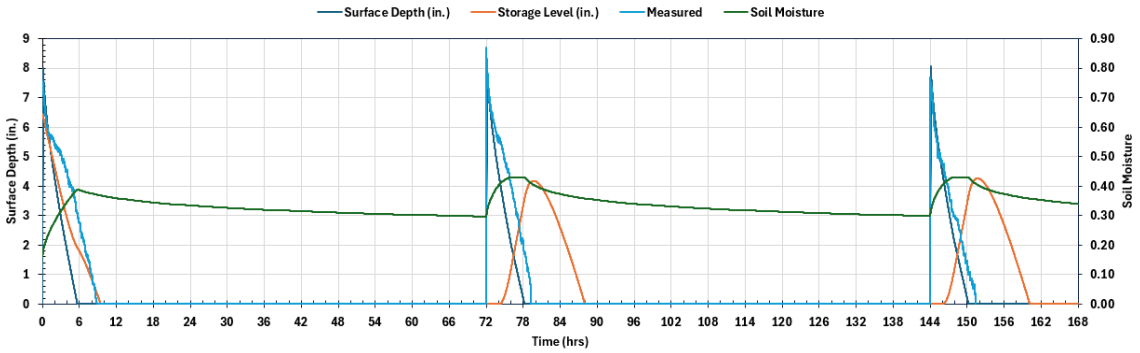

(a) ALDOTIS designs.

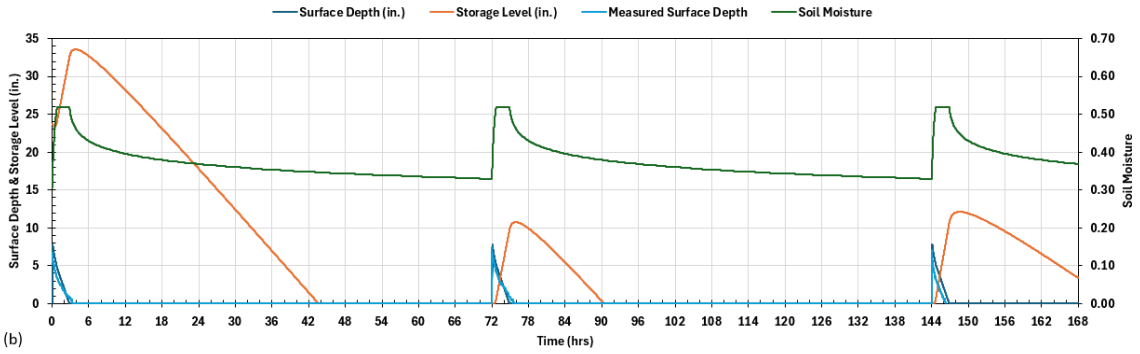

(b) MIS designs.

Figure 4.17 Simulated surface depth d_1, soil moisture θ_2, and storage level d_3 with measured surface depth for the first three infiltration and drawdown experiments with three dry days from March 28 at 9:23 am (0 on the x axis) to April 5, 2024, for (a) ALDOT and (b) MIS designs.

Figure 4.17 also shows simulated soil moisture content in both ALDOTIS and MIS. MIS's soil layer reaches full saturation for about two hours for each water-filling event. It then gradually decreases to a moisture content of 0.27, and ALDOTIS decreases to a moisture content of 0.26 before the next water-filling event.

In April and June 2024, Austin (2024) performed additional infiltration and drawdown experiments for both field-scale infiltration swales with one dry day between experiments to understand any impact from opening or closing the drainage pipe and temperature effects. Table 4.12 summarizes the measured and simulated drawdown time for these experiments. The measured average drawdown time for ALDOTIS ranged from 6.6 hours to 8.4 hours, with standard deviations from 0.8 to 1.2 hours. These drawdown times are similar to one measured in January with relatively colder temperatures. However, for MIS, the average drawdown time was 3.6 hours in April and 1.0 to 1.2 hours in June (not affected by opening the valve of the drainage pipe). These drawdown times were significantly less than the ones measured in January (4.2 to 10.9 hours).

Table 4.12 Measured and simulated drawdown time (hours) for infiltration swales under four water-filling (rainfall) events with one dry day between two events.

Type	Date/k_s	Event 1	Event 2	Event 3	Event 4	Average
ALDOTIS (measured)	15th Apr to 18th Apr	5.338	6.483	7.842	6.68	6.6±0.9
ALDOTIS (simulated)	1.0 in./hr	5.483	7.250	7.250	7.333	6.83±0.8
MIS (measured)	15th Apr to 18th Apr	2.621	3.258	4.000	4.675	3.6±0.8
MIS (Simulated)	1.9 in./hr	3.583	3.583	3.583	3.583	3.6±0.0
ALDOTIS (measured)	7th Jun to 10th Jun	6.125	7.642	7.704	9.425	7.7±1.2
ALDOTIS (simulated)	0.9 in./hr	6.050	8.117	8.233	8.233	7.6±1.0
MIS (measured)	7th Jun to 10th Jun	0.7583	0.925	1.042	1.358	1.0±0.2
MIS (Simulated)	6.45 in./hr	1.100	1.083	1.083	1.083	1.1±0.0
ALDOTIS Open (measured)	13th Jun to 16th Jun	7.246	9.304	8.479	8.754	8.4±0.8
ALDOTIS (simulated)	0.8 in./hr	6.767	9.217	9.367	9.383	8.82±1.0
MIS Open (measured)	13th Jun to 16th Jun	1.004	1.517	0.996	1.463	1.2±0.2
MIS (Simulated)	6.45 in./hr	1.100	1.083	1.083	1.083	1.1±0.0

To get a better understanding of the drawdown process in constructed infiltration swales, we closely reexamined the drawdown curves that were recorded every 30 seconds, and results are presented in Table 3.2. Figure 3.35 shows four examples (Day 1 and Day 4) of the recorded and simulated ponding depth over time for MIS and ALDOTIS in January-February infiltration and drawdown experiments. The simulated surface (ponding) depths from SWMM using constant model parameters (e.g., saturated hydraulic conductivity) may match well with the recorded ones or under- or over-estimated drawdown times in these examples. Figure 3.35 shows four water-filling events when the surface infiltration rate starts with a high value at the beginning of the event, decreases rapidly with time, and reaches a more stable rate. Therefore, the simulated surface depth decreases nonlinearly with time first and becomes more or less a straight line. For MIS, both Day 1 and Day 4 events reach soil saturation with the surface infiltration rate equal to the soil's saturated hydraulic conductivity so that the simulated surface depth decreases linearly with time over those periods. For ALDOTIS, the Day 1 event does not reach soil saturation, but the Day 4 event reaches, so the corresponding simulated surface depth changes with time either nonlinearly or linearly, as shown in Figure 3.35. The red line for the MIS Day 1 event has the same slope as the linear decrease of the simulated surface depth but overlaps with the recorded data for comparison. In SWMM modeling, a 5-minute high-intensity rainfall event produces the simulated surface depth, so it increases from zero to the maximum depth at 5 minutes and then starts to decrease for the drawdown process.

In October 2024, five additional infiltration and drawdown tests were performed for two field-scale infiltration swales to understand any impact from the seasonal effect. The SWMM model for ALDOTIS predicts an average drawdown time of 1.20 hours (±0.00) under an infiltration rate of 5 in./hr, which is a close match with the measured (Table 4.13). The SWMM model for MIS predicts an average drawdown time of 0.26 hours (±0.01) under a very large infiltration rate of 32 in./hr to closely align with the measured values. As the fill sand has a saturated hydraulic conductivity of 35.8 in./hr, the soil equivalent saturated hydraulic conductivity can be 32 in./hr if the mix saturated hydraulic conductivity is 27 in./hr (if the topsoil impact to the mix property is very minor). Otherwise, MIS constructed in the AU-SRF could develop unknown pathways (i.e., cracks) for fast infiltration. These drawdown times are very different from other measurements (Table 4.10, Table 4.11, and Table 4.12). October 2024 was part of a dry period in Auburn, AL, and successive droughts may increase the soil infiltration rates, resulting in shorter drawdown times.

Table 4.13 Measured and simulated drawdown time (hours) for infiltration swales under four water-filling (rainfall) events having two dry days between two events.

Type	Date/ks	Event 1	Event 3	Event 4	Event 5	Average
ALDOTIS (measured)	21st Oct to 31st Oct	1.26	1.23	1.34	1.50	1.33±0.11
ALDOTIS (simulated)	5 in./hr	1.20	1.20	1.20	1.20	1.20±0.00
MIS (measured)	21st Oct to 31st Oct	0.25	0.25	0.24	0.35	0.27±0.04
MIS (Simulated)	32 in./hr	0.27	0.27	0.25	0.27	0.26±0.01

4.3.6 MODELING AN INFILTRATION SWALE SYSTEM IN SOUTHERN ALABAMA

The drainage design for a roadway construction project in Southern Alabama was selected to model and understand the runoff control using infiltration swales by developing SWMM models. Model runs were first conducted under the design rainfall, i.e., the 95th percentile rainfall events, and then under historical long-term rainfall events. Three scenarios, pre-construction, post-construction without LID, and post-construction with LID, are modeled using SWMM. For long-term simulation, precipitation and air temperature data from Mobile Downtown Airport were used with available data from 1/1/2005 to 12/31/2019 (15 years). Those SWMM simulation runs aim to assess how well the swale retains runoff, promotes infiltration, and reduces the frequency and volume of runoff events under the design and historical rainfall conditions. To simulate the operation and effectiveness of the infiltration swale in Southern Alabama, three SWMM models for three scenarios (Table 4.2) were developed.

The SWMM model for the Southern Alabama construction site is shown in Figure 4.18, which includes five subcatchments, one channel, and one outfall (outlet). The information on subcatchments provided by ALDOT includes description or name, area, and runoff coefficients, however, SWMM subcatchments require many model parameters (Table A.). When a subcatchment is added to develop an SWMM model, a set of default model

parameters is provided, but some of the model parameters are not active or used for the specific modeling study. The key and effective parameters for SWMM subcatchments are summarized in Table 4.14 for three modeling scenarios. Both pre- and post-construction scenarios have five subcatchments (Road, Undeveloped, Roof areas, Driveway, and Channel), but three subcatchments have different areas (Table 4.14). Four subcatchments: Road (including paved lanes and shoulders), Undeveloped (HSG B soil), Roof areas, and Driveway, have volumetric runoff coefficients (R_v) of 0.91, 0.21, 0.99, and 0.99, respectively, and the Channel subcatchment is considered as a part of undeveloped land use area and set as a separate subcatchment in SWMM models for simulating channel flow with infiltration swales. The area-weighted runoff coefficient is 0.29 for pre-construction (5.41 acres) and 0.41 for post-construction (5.85 acres) scenario (Table 4.14). The post-construction scenario has a much larger area for the road (almost four times larger) since this is a road expansion construction project and smaller undeveloped and driveway areas. It means a part of an undeveloped area is converted into a road.

Infiltration swales are constructed in drainage channels along the roadway, and for the study site, four infiltration swales are designed and constructed to reduce the runoff volume. The bottom width of the drainage channels is 6 ft, which is the width of the four infiltration swales. The total length of the four infiltration swales is 670 ft; therefore, the total surface area of the LIDs is 4,020 ft^2 (0.09228 acres for SWMM input). The height of these infiltration swales is 4 ft (48 in.) deep: 12 in. of topsoil, 24 in. of fill sand (0.385 porosity), and 12 in. of #57 stones (0.459 porosity). The post-construction with LID scenario is to add the infiltration swales (bio-retention cells) into the Channel subcatchment (4020 ft^2) in the SWMM models.

Based on porosity and depth in the soil layer, one can compute the rainfall depth needed to reach the soil saturation. These depths are 14.04 in. and 7.36 in. for ALDOTIS and MIS, respectively; therefore, the soil layer in the MIS will reach the soil saturation more quickly and under a smaller rainfall depth. When the soil is saturated, the percolation rate is equal to the saturated hydraulic conductivity and adds water to the storage layer. Based on porosities in the soil and storage layers and surface depth, one can compute the total available depths to retain or pond water (in.) in LIDs. These depths are 25.56 in. and 27.86 in. for ALDOTIS and MIS, which are 47.3% and 51.64% of the total depth (54 in.). From the total available depths, both infiltration swales are similar and the MIS is able to store 2.3 in. more. However, the hydraulic conductivity of the soil layer for the MIS is about 2.5 times larger than that for the ALDOT swale. Further modeling analysis will demonstrate how the soil's hydraulic conductivity affects the LID performance in controlling/retaining the runoff under the design rainfall and long-term historical rainfall events.

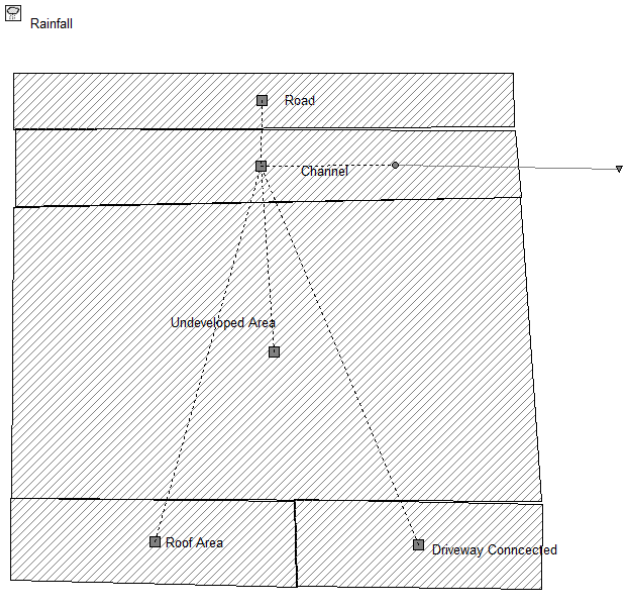

Figure 4.18 The Study Area Map for Pre- and Post-Construction Scenarios in the SWMM Model for a Southern Alabama Construction Site.

According to Austin (2024), the ALDOTIS and MIS inputs for SWMM's LID catchment are summarized in Table 4.15. The 12 in. of topsoil and 24 in. of fill sand are combined into one soil layer of 36 in. thick with equivalent hydraulic conductivity. The 5-ft total height is the standard or normal ALDOTIS design, but the total height for the study site in the Southern Alabama road expansion project is 4 ft. The storage-layer thicknesses in Table 4.15 are given for both 5 ft and 4 ft heights for infiltration swales, and other design parameters are the same.

Table 4.14 SWMM Subcatchment Parameters for Pre- and Post-development Scenarios.

Name	Road	Undeveloped	Roof Area	Driveway	Channel
Area (acre)	0.39 (1.55)	4.728 (4.065)	0.044	0.156(0.099)	0.092
Width (ft)	844	844	44	66	6
% Slope	2.9	0.5	0.5	0.5	0.5
% Imperv	0	0	99	99	0
N-Imperv	N/A	N/A	0.01	0.01	N/A
N-Perv	0.015	0.03	0.015	0.015	0.03
Dstore-Imperv	N/A	N/A	0.01	0.01	N/A
Dstore-Perv	0.02	0.406	0.01	0.01	0.406
% Zero-Imperv	N/A	N/A	25	25	N/A
Subarea Routing	Outlet	Outlet	Outlet	Outlet	Outlet
Percent Routed	100	100	100	100	100
Infiltration Data	CN = 98	CN = 71	CN = 99	CN = 99	CN = 71

Note: The areas inside the brackets are for the post-construction scenario.

Table 4.15 Summary of SWMM's LID Input Data for Two Infiltration Swales.

Layer	Parameter	ALDOTIS	MIS
Surface	Berm Height (or Storage Depth), D_1 (in.)	6	6
	Vegetation Volume Fraction	0	0
	Surface Roughness	N/A	N/A
	Surface Slope	N/A	N/A
Soil	Thickness (in.)	36	16
	Porosity	0.39	0.46
	Field Capacity	0.17	0.17
	Wilting Point	0.06	0.06
	Conductivity (in./hr)	0.93	2.33
	Conductivity Slope	30	30
	Suction Head (in.)	3.30	2.43
Storage	Thickness (in.)	12 (24)	32 (44)
	Void Ratio	0.85	0.83
	Porosity	0.46	* (*)
	Seepage Rate (in./hr)	0.43	0.43
	Clogging Factor	0	0
Total available depths to retain water (in.)		25.56 (32.5)	28.8 (34.3)

Note: "N/A" means the model parameter does not apply to bio-retention cells. The numbers inside the brackets are for the 5-ft height infiltration swales.

4.3.6.1 Runoff Control Performance under Design Rainfalls

ALDOT has developed an isohyetal map for the 95th percentile rainfall depths in Alabama, which range from 2.0 in. to 2.8 in. (Figure 4.19a). For the selected roadway construction project near Mobile, the design rainfall is 2.6 in. over 24 hours (daily) and distributed using NRCS Type III rainfall distribution (Figure 4.19b and Figure 4.19c). To examine the runoff control performance of infiltration swales in Central and Northern Alabama, model runs were also made using NRCS Type II rainfall distribution. The 95th percentile rainfall depths in Northern Alabama range from 2.0 in. to 2.4 in. and in Southern Alabama from 2.0 in. (small areas) to 2.8 in. Therefore, Figure 4.20 shows 5-minute incremental rainfall depths for Type II distribution of 2.0 in. rainfall, Type III distribution of 2.8 in. rainfall, and Type II and III distributions of 2.4 in. rainfall over 24 hours. Type II distributions have higher intensity at 12 hrs as shown for 2.4 in. rainfall, and the highest intensity for 2.8 in. Type III is just slightly larger than the highest intensity for 2.0 in. Type II.

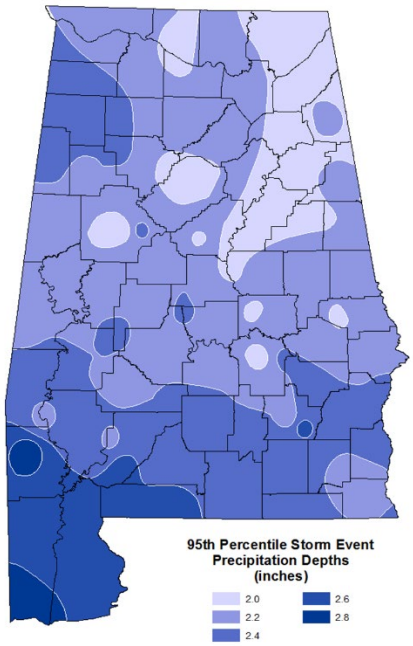

(a) The 95th Percentile Rainfall Depths in Alabama

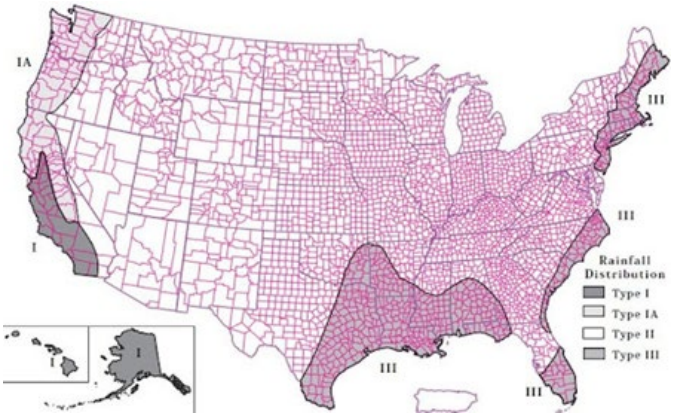

(b) NRCS 24-hr Rainfall Distributions in the USA

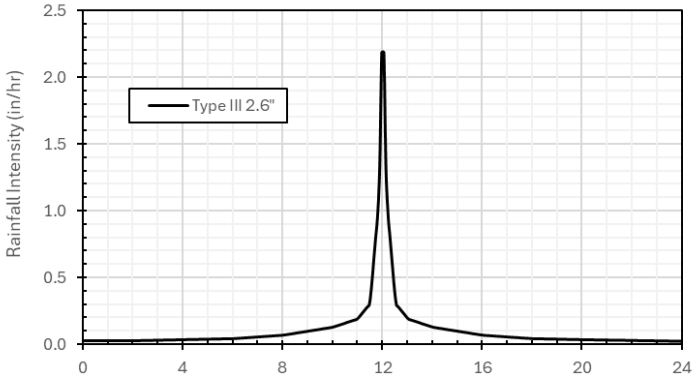

(c) 2.6” Rainfall with NRCS Type III Distribution

Figure 4.19 (a) The 95th Percentile Rainfall Depths in Alabama, (b) NRCS 24-hr Rainfall Distributions in the USA, and (c) 2.6” Rainfall with NRCS Type III Distribution.

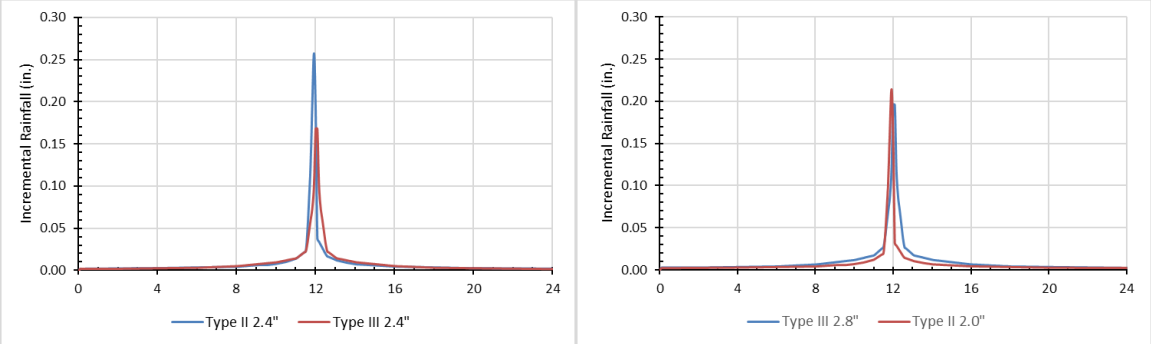

(1) Type II and Type III 2.4 in.

(2) Type III 2.8 in. and Type II 2.0 in.

Figure 4.20 NRCS Incremental Rainfall Distributions Used in SWMM Modeling: (1) Type II and Type III 2.4 in., (2) Type III 2.8 in. and Type II 2.0 in..

A 10% initial saturation was used for the infiltration swales, and simulated outflow hydrographs for pre- and post-construction scenarios at the Southern Alabama study site are shown in Figure 4.19(c) for 2.6 in. Type III rainfall distribution. The two post-construction scenarios have 4-ft deep infiltration swales with different configurations (ALDOTIS and MIS). All four scenarios did not produce the runoff before 4 hours under NRCS Type III rainfall distribution. Pre-construction and post-construction without LID start to have a gradual runoff increase after 4 hours and have a sudden increase at 12 hours when the rainfall intensity increases rapidly. Pre-construction has a peak discharge of 1.38 cfs at 12:35 and post-construction without LID has a peak discharge of 3.61 cfs at 12:15. With LID, the runoff is zero up to 11:50 for ALDOTIS or 12:00 for MIS since the swale holds the runoff up to 6 in. of surface depth and infiltrates the runoff into LID. Then, the runoff rate has a sharp increase to a peak discharge of 3.70 cfs for ALDOTIS and 3.60 for MIS. Peak discharges with LIDs are either slightly larger or smaller than the peak discharge for post-construction without LID. It seems LID does not alter runoff peak discharge under the design rainfall, where the very high rainfall intensities occur over a short period around 12:00 (Figure 4.19 and Figure 4.20). Whether these runoff rates from LIDs are accurate or not is a shortcoming of the SWMM LID module.

The SWMM bio-retention cell module produces an overflow rate of q from the LID unit, and q is equal to the surface depth minus the surface berm height divided by the time step. In this study, the surface berm height was set to 6 in. Based on the water balance of inflow from sub-catchments, runoff infiltration into the soil layer, and evaporation (not simulated here), the surface depth is calculated in the SWMM model. If the simulated/calculated surface depth in a time step is more than the surface berm height, the overflow rate is calculated and reported as the surface runoff rate, and the surface depth is decreased to the surface berm height for the next step of the SWMM modeling. The surface depth remains the surface berm height as long as the surface overflow or runoff rate exists. In SWMM, the overland surface runoff is calculated based on surface roughness, slope, and depression storage depth (d_s), but the overflow is not calculated based on them (berm height

is equivalent to depression storage depth). Therefore, the overflow rate may not represent the runoff rate over a ditch check from an infiltration swale. When the SWMM BRC LID module was used to mimic the infiltration swale hydrologically, the focus should be on the runoff volume reduction, runoff retention in LID, and surface ponding above it as demonstrated in Table 4.16.

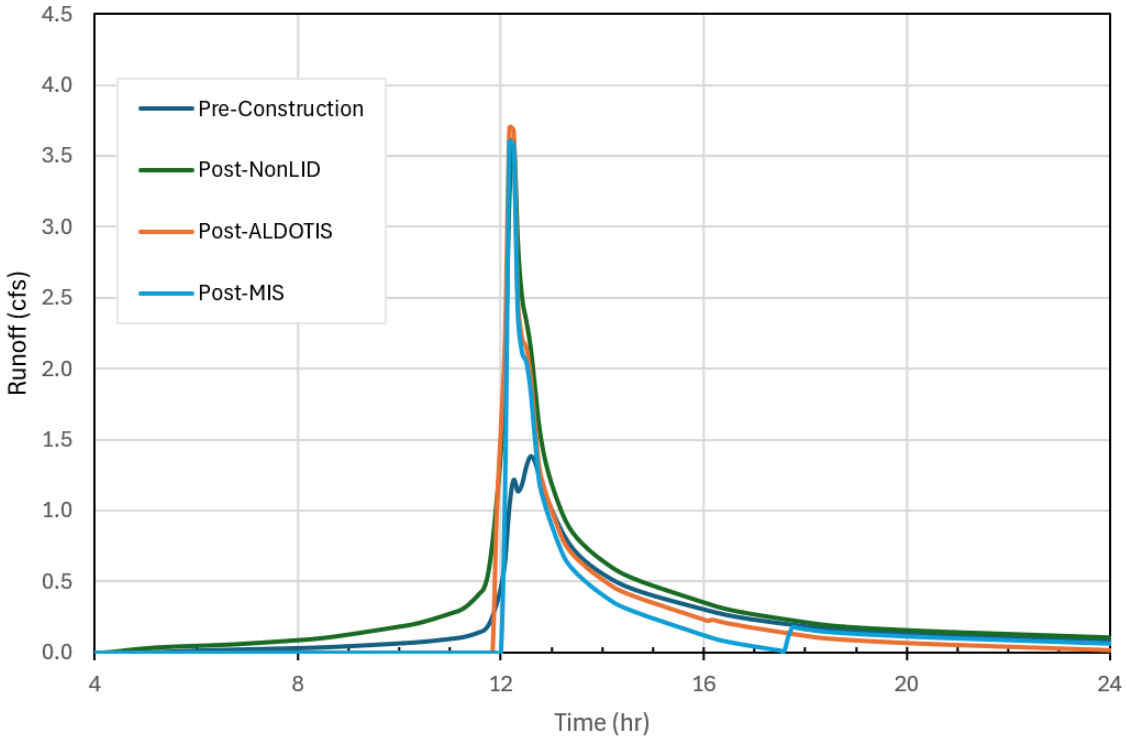

Figure 4.21 Simulated Runoff Hydrographs from SWMM for Type III 2.6 in. 24-hr Design Rainfall for the Construction Site at Southern Alabama Under Four Different Scenarios.

Figure 4.22 shows simulated time series of surface water depth (in.), storage level (in.), and soil moisture content for the post-construction scenarios with (a) ALDOTIS and (b) MIS for Type III 2.6 in. 24-hr design rainfall (Type III, Figure 4.19c) from SWMM models over 48 hours. Surface water depths start to increase from 8:20 and 10:25 for ALDOTIS and MIS, respectively, reaching 6 in. (berm height) at about 12:00 and keeping 6 in. until 24:00 (end of the rainfall event). As explained before, when the BRC (infiltration swale) has an overflow (surface runoff), the surface depth remains at berm height. The simulated surface depth takes about 12 to 15 hours to decrease to zero gradually after the rainfall event.

The storage level has an initial depth (1.1 or 3.1 in.) due to a 10% initial saturation condition and then decreases to zero over ~1–3 hours because of the native soil seepage rate of 0.43 in./hr and without any percolation from the soil layer yet. For the ALDOTIS, the storage level starts to increase from 14:10 and reaches 9.3 in. at 24:00, which is not saturated as the storage layer is 12 in. deep. After the rain stops, the storage level continues to increase to 12 in. (full saturation) at 26:08 (2:05 the following day) because of the continuous soil percolation and then remains at 12 in. up to 38:83 (14:50) when the soil percolation starts to

decrease (Figure 4.23). The storage level decreases to 6.4 in. at 48:00 (end of simulation). Therefore, the storage layer for ALDOTISdoes not reach saturation during the 24-hour storm but gets saturation after it for 10 hours and 40 minutes under 2.6 in. design storm, which is the 95th percentile of daily rainfall. Therefore, over 48 hours of simulation, ALDOTIS has 22.2% of the time for the storage layer to be fully utilized. However, MIS has 47.9% of the time for the storage layer to be fully utilized, as discussed below.

For the MIS, the storage level starts to increase from 9:55 and reaches 32 in. at 17:40, fully saturated as the storage layer is 32 in. deep. After the rain stops, the storage level remains at 32 in. up to 40:92 (16:55 the following day) and then decreases with time when the soil percolation starts to decrease (Figure 4.23). The storage level decreases to 27.5 in. at 48:00 (end of simulation); therefore, the storage layer for MIS reaches saturation early and lasts about 23 hours under a 2.6 in. design storm over 48 hours of simulation. It means that due to higher hydraulic conductivity in the soil layer for MIS, the storage layer below is fully utilized under the design rainfall.

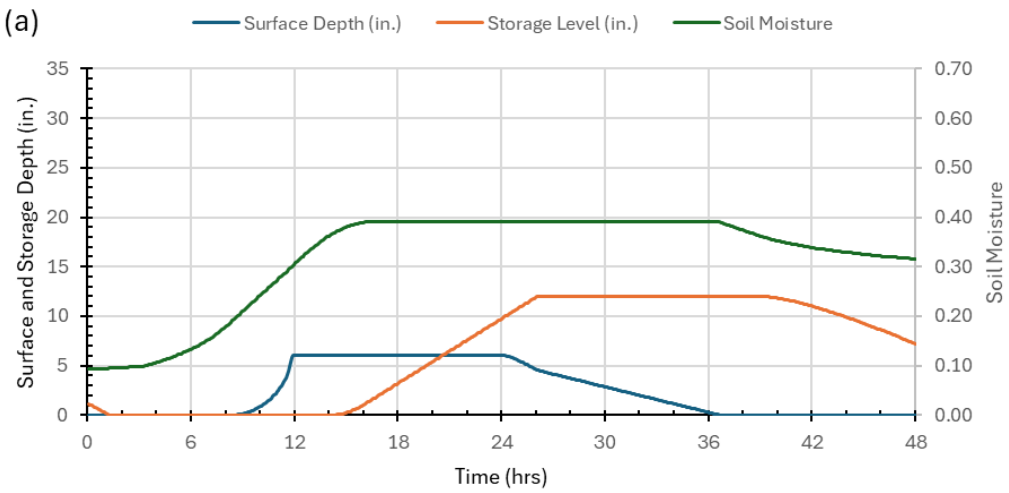

(a) ALDOTISs

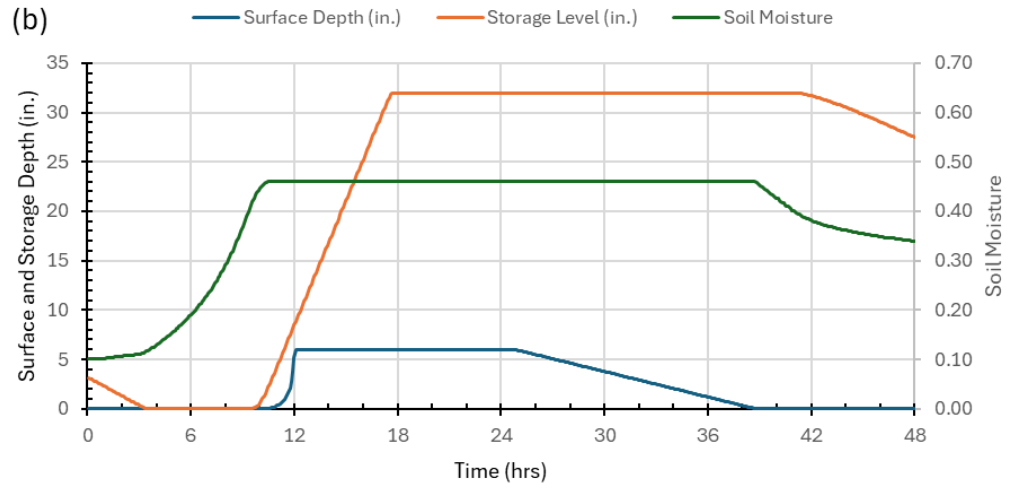

(b) MIS

Figure 4.22 Simulated Surface Water Depth (in.), Storage Level (in.), and Soil Moisture Content for (a) ALDOTIS and (b) MIS for Type III 2.6 in. 24-hr Design Rainfall from SWMM Models over 48 hrs.

Figure 4.23 shows simulated time series of total inflow to LID (in./hr), runoff (in./hr), surface infiltration rate (in./hr), soil percolation rate (in./hr), and exfiltration rate (in./hr) for the post-construction scenarios with (a) ALDOTIS and (b) MIS for Type III 2.6 in. 24-hr design rainfall (Type III, Figure 4.19c) from SWMM models over 48 hours. When the storage layer depth is positive (Figure 4.22), the exfiltration rate is equal to the model seepage rate (0.43 in./hr); otherwise, it is equal to the soil percolation rate (< 0.43 in./hr). ALDOTIS and MIS infiltrate 15.6 and 18.2 in. of runoff into the native soil over 48 hours of the simulation. The maximum surface infiltration rate (determined by using the Green-Ampt method in SWMM) is 1.3 in./hr for ALDOTIS and 2.5 in./hr for MIS due to higher hydraulic conductivity. Over 48

hours, ALDOTIS and MIS have 26.4 in. and 33.1 in. of runoff infiltrated from the surface layer into the soil layer and 18.4 in. and 29.2 in. of runoff percolated from the soil layer into the storage layer, respectively (integration of time series in Figure 4.23). Therefore, there are 9.0 in. and 3.9 in. of runoff stored inside the soil layer, respectively. Figure 4.23 shows when the soil layer becomes saturated, the surface infiltration rate is limited by the soil hydraulic conductivity, which is 0.93 in./hr for ALDOTIS and 2.33 in./hr for MIS. When the storage layer is saturated, the surface infiltration rate and the soil percolation rate are both equal to the seepage rate or exfiltration rate (Figure 4.23). After the rain stops at 24 hours, the surface infiltration continues as long as the surface layer depth is positive and then decreases to zero when the surface depth becomes zero. When the surface infiltration becomes zero, the soil moisture starts to decrease (Figure 4.22), and the percolation rate decreases but stays at the seepage rate if the storage layer is saturated and the calculated percolation rate (Equation 4.7 and Figure 4.4) is larger than the seepage rate. When the soil moisture becomes low/small enough, then the calculated percolation rate at 38.8 hours for ALDOTIS and 41.0 hours for MIS becomes less than the seepage rate, which makes the storage layer unsaturated since the runoff supply from the soil layer is less than the exfiltration rate.

When the surface layer depth becomes larger than 6 in. during a time step, the inflow to LID creates an overflow, i.e., surface runoff (in./hr, Figure 4.23). This surface runoff can be converted to the surface runoff in ft^3/s (flow rate) after multiplying the LID surface area (0.09228 acres). The maximum surface runoff rate is 39.8 in./hr and 38.7 in./hr, and the total runoff volume is 46.5 in. and 39.9 in. for ALDOTIS and MIS, respectively. After multiplying the LID surface area, the total runoff volume becomes 15,590.0 and 13,365.0 ft^3 for ALDOTIS and MIS, respectively, which are the same as the runoff volume reported in Table 4.16. The surface runoff from ALDOTIS increases to its maximum rate rapidly at 12:00 (maximum rainfall) and then decreases with time and becomes zero after 10 minutes of rainfall that stops at 24:00. The surface runoff from MIS decreases faster after the peak runoff and becomes a small runoff (0.12 in./hr) at 17:35 and then increases to 1.9 in./hr at 17:45 and becomes zero after 25 minutes of rainfall. The later increase of runoff from MIS is because both the soil and storage layers become saturated so that the surface infiltration is reduced from the saturated hydraulic conductivity (2.33 in./hr) to the seepage rate (0.43 in./hr, Figure 4.23) and the surface depth increases over time steps become larger to result in larger overflow. Despite the later increase of surface runoff, the total runoff from MIS is still 6.64 in. (or 2,224.7 ft^3) less than the total runoff from ALDOTIS. Both Figure 4.22 and Figure 4.23 provide us with a comprehensive understanding of the performance of LIDs in the runoff control and detailed mechanisms to pond, store/hold, and exfiltrate runoff generated from the upstream sub-catchments.

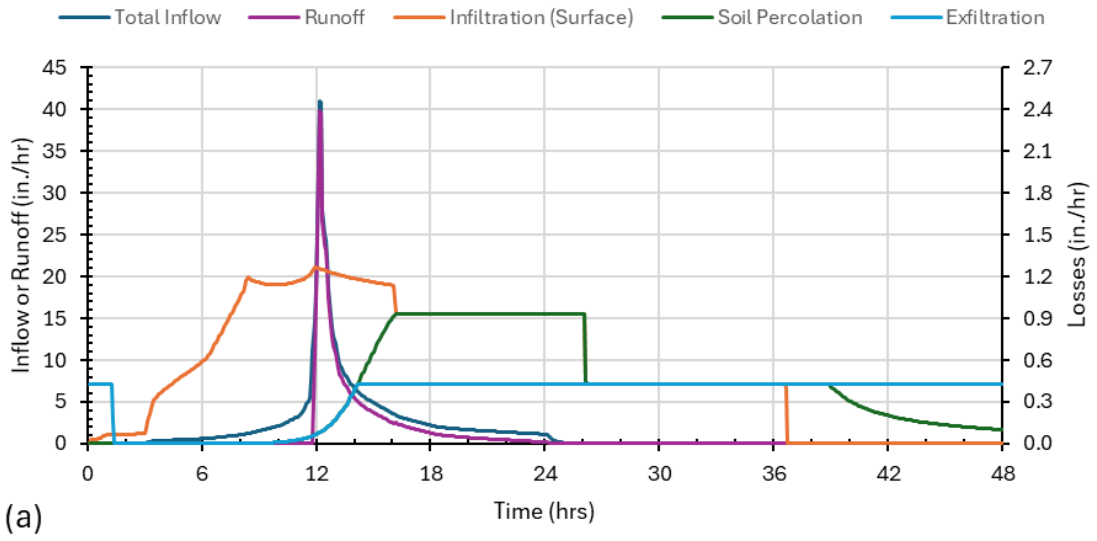

(a) ALDOTIS

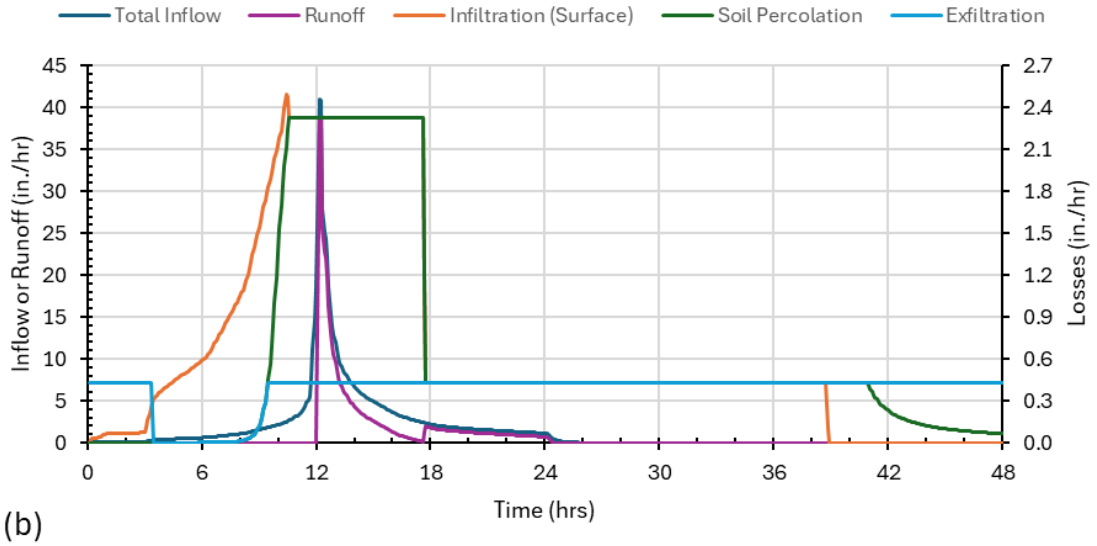

(b) MIS

Figure 4.23 Simulated Total Inflow, Surface Runoff (Overflow), Surface Infiltration, Soil Percolation, and Exfiltration Rates in in./hr for (a) ALDOT and (b) MIS for Type III 2.6 in. 24-hr Design Rainfall from SWMM Models over 48 hrs.

Table 4.16 summarizes and compares the runoff volumes (ft^3) simulated from SWMM models for four modeling scenarios (4-ft swales) under design rainfall (Type III 2.6 in.). The post-construction leads to an 8,300.6 ft^3 increase in the runoff volume when the road area is increased about 4 times, and the undeveloped area is reduced. Both infiltration swale designs lead to a large decrease (-8,445.2 or -10,669.8 ft^3) in the runoff volume from the post-construction scenario. The runoff volumes with infiltration swales are even smaller than the

volume for pre-construction. Therefore, these infiltration swales achieve their purpose of reducing the runoff to the pre-development hydrology. Table 4.16 also clearly shows that the MIS performs much better than the ALDOTIS design in reducing the runoff volume. When ALDOT's PrePost Analysis spreadsheet is used, the runoff volume for pre-construction and post-construction without LID is 14,771 ft^3 and 22,888 ft^3, respectively, and corresponding SWMM results (Table 4.16) are about 5–6.5% larger. The ALDOT's runoff increase for the post-construction is 8,116 ft^3, similar to the SWMM result (only 2.3% larger). The total gross rainfall volume is 51,060 ft^3 and 55,212 ft^3 for pre-construction and post-construction scenarios for 2.6 in. rainfall, respectively. Therefore, the watershed runoff coefficient, R_v, is also calculated and reported in Table 4.16. Post-construction has a larger runoff coefficient than pre-construction does, and adding infiltration swale reduces the runoff coefficient, which is even smaller than pre-construction, R_v.

For the pre-construction scenario, 35,325 ft^3 of rainfall is infiltrated since 89.1% of the area is undeveloped. For the post-construction scenario, 31,177 ft^3 of rainfall is infiltrated since 71.1% of the area is undeveloped. For post-construction with LID scenarios, an additional 8,455.2 ft^3 and 10,669.8 ft^3 of runoff are ponded on the surface or held in the soil/storage layer or infiltrated into the native soil through ALDOTIS and MIS, respectively. Based on the porosity of soil and storage layers plus surface ponding and native soil seepage, the maximum runoff volume that 4-ft ALDOTIS and MIS can hold and infiltrate is 12,452.0 ft^3 and 13,221.1 ft^3 over 27 hours of simulation, respectively. Therefore, the available maximum retention of the 4-ft ALDOTIS and MIS is 77.4% and 82.2% of the swale volume (16,080 ft^3) under 2.6-in. design rainfall, respectively. The ALDOT PrePost Analysis method assumes that the ALDOTIS can use 41.25% of the swale volume to reduce/retain the runoff, which gives a volume reduction of 6,633 ft^3. This is about 21.5% and 37.8% less than the volume reduction (8,455.2 and 10,669.8 ft^3) simulated by SWMM from ALDOTIS and MIS design, respectively. SWMM simulated runoff volume reduction (8,455.2 and 10,669.8 ft^3) is 67.8% and 80.7% of the available maximum retention (12,452.0 ft^3 and 13,221.1 ft^3) under 2.6-in. design rainfall, respectively. Again, MIS has a higher maximum available retention potential and also a higher utilization rate in comparison to ALDOTIS.

For results of post construction scenario with ALDOTIS in Table 4.16, the soil-layer's saturated hydraulic conductivity was tested for four possible values: 0.93 in./hr (Table 4.15), 0.5 in./hr (1.0 ft/d), 0.25 in./hr (0.5 ft/d), and 0.125 in./hr (0.25 ft/d), respectively. The required minimum infiltration rate in the Alabama LID Manual of 1.0 ft/d was used, and half and quarter of it were also used for simulations. The soil's hydraulic conductivity of 0.25 ft/d corresponds the current ALDOT drainage time requirement: <48 hours over 6 in. surface ponding (controlled by ditch check height of 6 in.). Topsoil with variable particle size distributions from different project sites would result in smaller saturated hydraulic conductivity, which is why the SWMM simulation using 0.25 in./h was conducted. For these three assumed soil-layer's saturated hydraulic conductivities, the corresponding topsoil's conductivity is 0.34 ft/d, 0.17 ft/d, and 0.084 ft/d, which are possible based on the column tests in Chapter 2. They produce 17,788 and 19,405.4 ft^3 of runoff from the infiltration swale, respectively, which is 13.1% and 23.3% increase from pre-construction, because they

infiltrate or store (ponding + holding) less runoff by the ALDOT infiltrate swale. With 0.25 in./hr (0.5 ft/d) of soil layer's hydraulic conductivity, which is the maximum soil percolation based on Equation 4.7, ALDOTIS can reduce 4,629.8 ft^3 from post-construction without LID. This volume reduction is equivalent to 1.15 ft (13.8 in.) of runoff above LID (4,020 ft^2) or 0.018 ft (0.22 in.) over the contributing watershed (5.85 acres). The MIS's volume reduction is 10,669.8 ft^3, equivalent to 2.65 ft (31.9 in.) of runoff above LID or 0.042 ft (0.5 in.) over the contributing watershed. Runoff infiltrated or stored by ALDOTIS reduces to 37,495.5 and 35,878.3 ft^3 from 39,622.3 ft^3. Both ALDOTIS and MIS have 28.3 hours of surface ponding over 48 hours of the simulations for 24-hour 2.6 in. Type III design storm. The long ponding time (> 1 day) is due to high rainfall intensity for the design storm and more impervious areas for the post-construction scenario. When ALDOTIS has 1.0, 0.5, and 0.25 ft/d of soil's hydraulic conductivity, the surface ponding time increases to 29.8, 40.2, and 56.7 hours, respectively. Using 0.25 ft/d hydraulic conductivity (its model simulation period was 96 hours because of slow drainage) results in the surface ponding longer than 48 hours (2 days) since the soil layer was never saturated due to the low infiltration rate. Using 0.37 ft/d hydraulic conductivity could result in the surface ponding longer than ~48 hours.

Table 4.16 Simulated Runoff Volumes from SWMM Models for Four Modeling Scenarios under Type III 2.6 in. 24-hr rainfall.

Scenarios	Pre-construction	Post-construction without LID	Post-construction with ALDOTIS [1]	Post-construction with MIS
Volume of Runoff (ft^3)	15,734.6	24,035.2	15,590.0, 17,788.2, 19.405.4, 20,424.0	13,365.4
Change from Pre-construction (ft^3, %)	N/A	8,300.6 (52.8%)	-144.6, 2,053.6, 3,670.8, 4689.4 (-0.9%, 13.1%, 23.3%, 29.8%)	-2,369.2 (-15.1%)
Change from Post-construction without LID (ft^3, %)	N/A	N/A	-8,445.2. -6,247.0, -4,629.8, -3,611.2 (-35.2%, -26.0%, -19.3%, -15.0%)	-10,669.8 (-44.4%)
Watershed Runoff Coefficient R_v	0.308	0.435	0.282, 0.322, 0.351, 0.369	0.242
Infiltrated or stored (ponding + holding) (ft^3)	35,325.0	31,177.1	39,622.3, 37,495.5, 35,878.3, 34,862.0	41,846.9

Note: [1] – Results for the soil-layer's saturated hydraulic conductivity of 0.93, 0.5, 0.25, and 0.125 in./hr (1.86, 1.0, 0.5, and 0.25 ft/d), respectively.

Table 4.17 summarizes simulated runoff volume (ft^3) and watershed runoff coefficient R_v from SWMM models for four modeling scenarios under different design rainfalls. We assumed the construction project in Southern Alabama described in Table 4.14 and Figure 4.18 occurs in other parts of Alabama with different design rainfall depths and time distributions. The infiltration swales are 6 ft in width and 4 ft in depth. The rainfall volumes (ft^3) for pre- and post-construction scenarios are also reported in Table 4.17, so the watershed runoff coefficients R_v can be calculated and reported. The watershed runoff

coefficients R_v have small increases when the design rainfall changes from 2.0 in. to 2.8 in. for all scenarios, and Type II and Type III rainfall distributions do not change the runoff coefficients. The watershed runoff coefficients for post-construction with LIDs are even smaller than the ones for pre-construction scenarios. All watershed runoff coefficients with MIS are always less than ones with ALDOTIS to indicate better performance in the runoff control from MIS. Therefore, the runoff volume for the scenarios with LID is less than one for the pre-development scenarios, except ALDOTIS under 2.8 in. Type III rainfall (because post-construction has a larger area and more impervious surfaces).

For post-construction scenarios with LIDs, the runoff coefficient for each LID is also reported (as bold-font numbers after the watershed runoff coefficients) based on SWMM simulations. The LID runoff coefficients for MIS are always smaller than the ones for ALDOTIS for all four rainfall scenarios. It means that MIS performs better to control/reduce surface runoff than s in different locations in Alabama. The runoff coefficients for each LID under all design rainfalls are larger than the watershed runoff coefficients. It should be noted that the watershed runoff coefficients include effects of runoff reduction inside the watershed by infiltration (e.g., CN = 71 for 4.06-acre undeveloped watershed) and additional runoff reduction through LID. For the Southern Alabama construction site (Figure 4.18), ALDOTIS has a runoff coefficient of 0.446 for 2 in. rainfall and 0.676 for 2.8 in. rainfall. It means ALDOTIS reduces the runoff by 55.4% and 32.4%, respectively. MIS reduces the runoff by 70.9% and 40.3%, respectively, with better performance in runoff reduction.

Table 4.17 Runoff Volume (ft^3) and Watershed/LID's Runoff Coefficient R_v from SWMM Models for Four Modeling Scenarios under Different Design Rainfalls.

Scenarios (Rainfall Volume in ft^3 for Pre- and Post- scenarios)	Pre-construction	Post-construction without LID	Post-construction with ALDOTIS	Post-construction with MIS
2.0 in. Type II (39,277/42,471)	8,231.0 (0.210)	15,157.9 (0.357)	6,845.9 (0.161/**0.446***)	4,471.1 (0.105/**0.291**)
2.4 in. Type II (47,132/50,965)	13,136.9 (0.279)	21,128.4 (0.415)	12,571.8 (0.247/**0.589**)	10,318.7 (0.202/**0.483**)
2.4 in. Type III (47,132/50,965)	13,146.1 (0.279)	21,101.0 (0.414)	12,591.7 (0.247/**0.590**)	10,311.3 (0.202/**0.484**)
2.6 in. Type III (51,060/55,212)	15,734.1 (0.308)	24,035.2 (0.435)	15,559.0 (0.282/**0.638**)	13,365.5 (0.242/**0.547**)
2.8 in. Type III (54,987/59,459)	18,408.9 (0.335)	27,221.4 (0.458)	18,665.0 (0.314/**0.676**)	16,495.6 (0.277/**0.597**)

Note: * - the second R_v is for LID performance output from SWMM modeling.

Table 4.18 reports several LID characteristic parameters for two infiltration swale designs (ALDOTIS and MIS) under different design rainfalls from 2.0 in. to 2.8 in. in Alabama. For each design rainfall, the inflow volume (ft^3) and depth (in.) on LID are calculated. The inflow depth to the LID (0.09228 acres or 4020 ft^2) increases from 45.84 in. to 82.44 in. when the rainfall changes from 2.0 in. and 2.8 in. after considering rainfall loss in all subcatchments except LID. The infiltrated surface runoff, the soil percolation, and the storage exfiltration over 48 hours of SWMM simulation are similar for four design rainfalls

with two time-distributions (NRCS Type II and Type III) despite the increase of rainfall from 2.0 to 2.8 in. with the largest standard deviation of 0.44 in. The infiltrated surface runoff for ALDOTIS (36 in. of soil) increases from 25.41 to 26.72 in. and from 32.50 to 33.20 in. for MIS (only 16 in. of soil) with the increase of rainfall (2.0 to 2.8 in.). Because of only smaller increases in the infiltrated surface runoff from the surface layer to the soil layer, the increase in rainfall results in the surface runoff from 20.44 in. to 55.72 in. for ALDOTIS and 13.35 in. to 49.24 in. for MIS. Overall, MIS has 6.75 in. more surface infiltration and 6.75 in. less surface runoff than ALDOTIS does. With high hydraulic conductivity and small soil depth, MIS has 10.90 in. more soil percolation to the storage layer and further results in 2.55 in. more exfiltration from the storage layer to the native soil. Table 4.18 further shows that MIS performs better than ALDOTIS in controlling (ponding/storing) surface runoff.

Table 4.18 LID Characteristic Parameters from SWMM Models for Two Infiltration Swale Designs under Different Design Rainfalls.

Scenarios (Inflow volume, ft^3 /depth, in.)	ALDOTIS				MIS			
	Surface Infil.	Surface Runoff	Soil Percol.	Storage Exifil.	Surface Infil.	Surface Runoff	Soil Percol.	Storage Exifil.
2.0 in. Type II (15,356/45.84)	25.41	20.44	17.52	15.20	32.50	13.35	28.67	17.69
2.4 in. Type II (21,339/63.70)	26.17	37.53	18.19	15.53	32.90	30.80	29.07	18.06
2.4 in. Type III (21,339/63.70)	26.09	37.59	18.12	15.50	32.90	30.78	29.07	18.06
2.6 in. Type III (24,437/72.95)	26.41	46.54	18.40	15.63	33.05	39.90	29.22	18.20
2.8 in. Type III (27,615/82.44)	26.72	55.72	18.66	15.76	33.20	49.24	29.36	18.33
Average with standard deviation	26.16 (0.44)	39.56 (11.69)	18.18 (0.38)	15.52 (0.19)	33.91 (0.24)	32.82 (11.89)	29.08 (0.23)	18.07 (0.21)

Table 4.19 reports several LID performance parameters (%) for two infiltration swale designs (ALDOTIS and MIS) under different design rainfalls from 2.0 in. to 2.8 in. in Alabama. These parameters are derived from the time series of detailed LID results (Figure 4.22 and Figure 4.23) and normalized by the simulation period (48 hours). All five LID performance parameters have small increases with the increase in rainfall, with the largest standard deviation of 2.2%. The storage saturation gives the percentage of the time when the storage layer is saturated or fully utilized (storage level of 12 in. for ALDOTIS and 32 in. for MIS). It increases from an average of 22.5% to 47.9% from ALDOTIS to MIS. Figure 4.23 shows that storage saturation happens during the rainfall period (24 hours) for ALDOTIS and for MIS. These utilization percentages were simulated under 0.93 in./hr (1.86 ft/d) and 2.33 in./hr (4.33 ft/d) (Table 4.15) as soil-layer's saturated hydraulic conductivity K_s (Equation 4.1). If K_s becomes 0.5 in./hr (1.0 ft/d) for ALDOTIS, the utilization percent for the full saturation in the storage layer is 0%, and the maximum water level in the storage layer is only 2.4 in. and 1.2 in. when the stone layer is 12 in. for a 4-ft swale and 24 in. for a 5-ft swale, respectively. This modeling study shows that lower soil hydraulic conductivity leads to lower utilization rate of the storage layer (stone), which wastes the investment on making the swale deeper with more stone or storage space. When topsoil's particle size distribution can vary a lot with

more fines, topsoil's hydraulic conductivity can be much lower than what was measured by the column tests in Chapter 2 (0.63 ft/d). When soil-layer's saturated hydraulic conductivity (e.g., 0.25 in./hr and 0.125 in./hr) is less than the native soil's seepage rate (e.g., 0.43 in./hr used in this study for HSG B soil), the storage layer is always dry (or does not store/hold any runoff) as percolated runoff from the soil goes into native soil almost immediately.

The percentage with full exfiltration (i.e., 0.43 in./hr) shows that the storage layer has enough water, allowing the full seepage into the native soil; otherwise, the storage layer is dry. Both ALDOTIS and MIS have higher percentages with full exfiltration (72.6% to 86.6%). The soil saturation percentage increases from 41.9% for ALDOTIS to 58.4% for MIS. MIS, with a shallow soil layer and high hydraulic conductivity, can make the soil saturated faster and keep soil saturation longer. The percentage of greater infiltration is reported during the time period when the surface infiltration rate is equal to or larger than the saturated hydraulic conductivity (0.93 in./hr for ALDOTIS and 2.33 in./hr for MIS). When the soil is not saturated yet, the surface infiltration rate can be larger than the saturated hydraulic conductivity, depending on available runoff in the surface layer. The large soil depth for ALDOTIS allows 38.3% of the time with greater infiltration and only 15.5% for MIS. The percentage of both saturations reports the time period when both the soil layer and the storage layer are saturated. This condition limits the surface infiltration and soil percolation to the seepage rate. Figure 4.23 shows those periods when the surface infiltration drops from 0.93 in./hr for ALDOTIS or 2.33 in./hr for MIS to 0.43 in./hr, which is equal to the seepage/exfiltration rate. This is not a favorable condition for infiltration swales because the seepage rate limits the surface infiltration. MIS has 43.3% of the time with both saturations, and ALDOTIS has 20.9% of the time. Even though MIS performs better than ALDOTIS in reducing surface runoff, its performance can be improved if hours with both saturations are reduced. When the storage layer fills with water but is not saturated, then the soil percolation is not limited by the seepage rate but by its hydraulic conductivity.

Table 4.19 LID Performance Parameters (%) from SWMM Models for Two Infiltration Swale Designs under Different Design Rainfalls.

Scenarios	ALDOTIS					MIS				
	Storage Satura.	With full Exifil.	Soil Satura.	Both Satura.	Greater Infil.	Storage Satura.	With full Exifil.	Soil Satura.	Both Satura.	Greater Infil.
2.0 in. Type II	21.7%	71.0%	38.2%	17.2%	37.8%	46.0%	84.7%	56.9%	41.5%	16.0%
2.4 in. Type II	25.5%	72.6%	41.8%	20.8%	37.5%	47.6%	86.5%	58.0%	43.1%	15.3%
2.4 in. Type III	25.2%	72.4%	41.7%	20.7%	38.5%	48.1%	86.6%	58.3%	43.4%	15.5%
2.6 in. Type III	26.6%	73.1%	43.1%	22.0%	38.7%	48.6%	87.3%	59.0%	44.1%	15.3%
2.8 in. Type III	28.3%	73.8%	44.6%	23.6%	38.7%	49.1%	87.8%	59.5%	44.6%	15.3%
Average with STD	25.5% (2.2%)	72.6% (0.9%)	41.9% (2.1%)	20.9% (2.1%)	38.3% (0.5%)	47.9% (1.1%)	86.6% (1.1%)	58.4% (0.9%)	43.3% (1.1%)	15.5% (0.3%)

4.3.6.2 Long-term Simulations to Examine Runoff Control of LIDs

Long-term rainfall simulation using the EPA's SWMM is crucial for assessing the performance of stormwater management systems, such as infiltration swales, over extended periods. These simulations help determine how well a system manages stormwater during different seasonal rainfall patterns and over multiple years, offering a more comprehensive understanding of the system's efficacy compared to single-event simulations.

Table 4.20 shows event (6-hr inter-event dry period) and daily rainfall distributions for 15 years (2005–2019) rainfall data at Mobile Downtown Airport. In this study, when the dry hours between two hourly rainfalls are equal to or greater than 6 hours, they are classified as two events as typical inter-event dry periods for rainfall independence range from 4 to 6 hours (Driscoll et al. 1989). There are, on average, about 127 rainfall events and 130 rainy days per year. First, the events with rainfall less than and equal to 0.1in. are separated since these typically do not produce any measurable runoff (USEPA 2009). For 941 events with rainfall ≤ 0.1in., it has a total of 27.9 in. of rainfall (with an average depth of 0.03 in. per event). There are 49.6%, 75.2%, and 87.0% of events with rainfall less than 0.1 in., 0.5 in., and 1.0 in., respectively. For daily rainfall (midnight to midnight), there are 46.2%, 74.0%, and 87.2% of days with rainfall less than 0.1 in., 0.5 in., and 1.0 in., respectively. The study site in Southern Alabama has many rainfall events/days compared with other locations in the USA, and it also has many events/days with small rainfall depth. For 1427 events with rainfall less than or equal to 0.5 in., it had a total of 155.9 in. of rainfall over 15 years (average 10.4 in. per year), which is 18.1% of total rainfall (860.7 in.).

Table 4.20 Event and Daily Rainfall Distributions for Different Rainfall Ranges.

Rainfall Ranges	Event Rainfall		Daily Rainfall	
	No. Events	Percent Events	No. Days	Percent Days
(0, 0.1][1]	941	49.58%	903	46.17%
(0.1,0.5]	486	25.61%	545	27.86%
(0.5,1.0]	224	11.80%	257	13.14%
(1.0,1.5]	100	5.27%	120	6.13%
(1.5,2.0]	47	2.48%	35	1.79%
(2.0,2.5]	29	1.53%	37	1.89%
(2.5,3.0]	27	1.42%	27	1.38%
(3.0,3.5]	12	0.63%	8	0.41%
(3.5,4.0]	11	0.58%	7	0.36%
(4.0,4.5]	5	0.26%	6	0.31%
(4.5,5.0]	4	0.21%	2	0.10%
(5.0,5.5]	4	0.21%	7	0.36%
(5.5,6.0]	1	0.05%	0	0.00%
(6.0,6.5]	2	0.11%	0	0.00%
(6.5,7.0]	2	0.11%	1	0.05%
(7.0,7.5]	0	0.00%	0	0.00%
(7.5,8.0]	1	0.05%	0	0.00%
(8.0,8.5]	0	0.00%	0	0.00%
(8.5,9.0]	0	0.00%	1	0.05%
(9.0,9.5]	1	0.05%	0	0.00%
(9.5,10.0]	0	0.00%	0	0.00%
(10,10.5]	0	0.00%	0	0.00%
(10.5,11.0]	0	0.00%	0	0.00%
(11.0,11.5]	1	0.05%	0	0.00%
Total	1898	100.00%	1956	100.00%

Note: [1] – (0, 0.1) stands for rainfall greater than 0 using "(" and less than and equal to 0.1 using "]". Some 0.5 in. intervals were not shown when they did not have any rainfall events and days.

SWMM's long-term rainfall simulations require years of continuous precipitation data, which usually comes from NOAA. The historical data includes hourly rainfall records from January 1, 2005, to December 31, 2019, which allows SWMM to simulate the runoff-control performance of two infiltration swales under historical rain events. For historical long-term rainfall data and SWMM simulation results, continuous hourly rainfall records were segmented into individual storm events using 6-hour dry (inter-event) intervals to derive simulation results by events since SWMM results are generated by specifying the output time interval, e.g., 15 minutes, one hour, or one day. This approach helps separate smaller storm events with enough inter-event dry period to the next event and ensures consistency in runoff analysis.

Figure 4.24 plots the daily and event runoff versus rainfall at the Southern Alabama ALDOT construction site under the post-construction with ALDOTIS scenario. There are four watershed scenarios: (a) pre-construction, (b) post-construction without LID, (c) post-construction with ALDOTIS, and (d) post-construction with MIS, but Figure 4.24 plots the scenario (c) for illustration only. The SWMM long-term simulation covers a total of 5,478 days with 1,956 rainy days (the minimum precipitation is reported as 0.01 in.), and the maximum daily rainfall was 8.32 in. Figure 4.24(a) plots the daily runoff versus the daily rainfall, one can find out that there were 34 days with daily runoff greater than the daily rainfall, and this is not acceptable. This is because some rainfall events crossing midnight are divided into two days. Therefore, it is not meaningful or useful to summarize/analyze the long-term daily rainfall-runoff simulation results.

Therefore, Figure 4.24(b) plots the event runoff versus the daily rainfall when 6 hours for a minimum inter-event dry period was used for each event. The maximum event rainfall was 11.31 in., and the maximum runoff for the four scenarios were 8.32, 8.87, 8.64, and 8.38 in., respectively. For this largest rainfall event, the study site infiltrates 2.44–2.99 in. rainfall since there are 69.6% to 87.4% undeveloped areas.

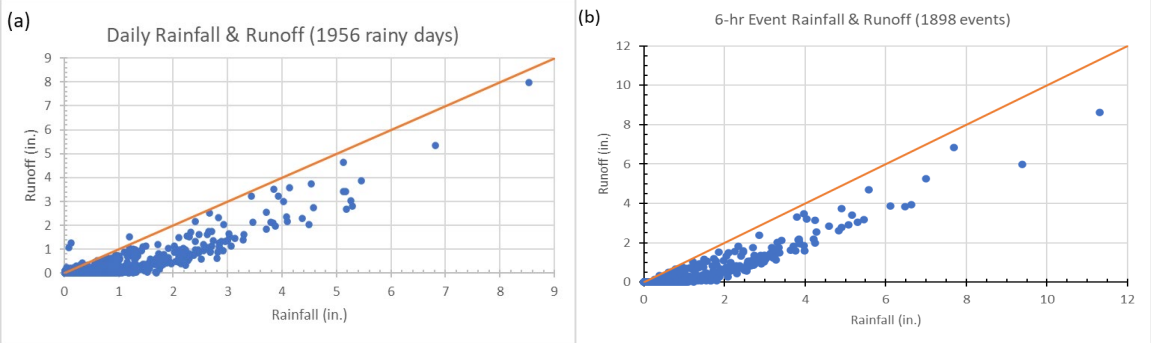

(a) Daily Runoff versus Rainfall (b) 6-hr Event Runoff versus Rainfall

Figure 4.24 Simulated (a) Daily and (b) 6-hr Event Runoff versus Rainfall from Continuous Long-term Rainfall Data (2005–2019) for Post-Construction with ALDOTIS Scenario.

The event runoff from different scenarios is somewhat different for the same rainfall events, e.g., a certain increase in post-construction without LID and then a certain decrease in post-construction with LID. Therefore, we must analyze the event runoff using other methods, e.g., using a histogram, and corresponding results are given in Table 4.21 instead of histogram graphs because of a very high frequency for low runoff values (<0.1in.). Table 4.21 summarizes the number of runoff events for different runoff volume ranges with an increment of 0.1 in. (when the runoff ≤ 1.0 in.) or 0.5 in. (when larger than 1.0 in.) for four modeling scenarios. We specifically list the number of rainfall events that did not produce any runoff, which means all rainfall was either infiltrated or held inside of swales. The post-construction without LID had only 968 events (51.0% of all rainfall events), but both post-construction with LID measures (ALDOTIS and MIS) had 1,546–1,604 events (81.5% or

84.5%) that did not produce any runoff. They even performed much better in controlling runoff than the pre-construction scenario, which had 1,028 (54.2%) no-runoff-producing events. This suggests that both LID designs successfully control runoff from many small rainfall events, closely mimicking pre-development conditions, when the soil-layer's saturated hydraulic conductivity of 0.93 and 2.33 in./hr (1.86 and 4.66 ft/d) were used for ALDOTIS and MIS (Table 4.14), respectively. The pre-construction and the post-construction without LID scenarios still had a relatively large number of events (~110–570) that produced <0.1 or 0.1–0.2 in. runoff. The number of rainfall events that produce runoff of [0.0, 0.5] in. ranges from 1734 to 1771 for four scenarios, which are 91.4% to 93.3% of the total rainfall events over 15 years. The pre-construction scenario has 1,763 events, while the post-development without LID scenario has 29 fewer of these events. There are only a few events (<13) that produced 2 in. or more runoff in those 0.5-in. runoff increments for all scenarios.

When the soil-layer's saturated hydraulic conductivity of 0.5, and 0.25 in./hr (1.0, and 0.5 ft/d) was used for long-term simulations, the number of events producing no runoff decreases to 1510 and 1468 (Table 4.21), but the number of events producing ≤ 0.1 in. of runoff increases.

Table 4.22 lists a set of parameters to summarize event rainfall and simulated event runoff from the long-term (15 years) simulations for four scenarios. Total rainfall over 15 years is 860.7 in. for 1898 events, which is the same for all scenarios. The average rainfall per year is 57.4 in. for all events, but 55.5 in. per year or 0.87 in. per event in Southern Alabama if excluding rainfall less than or equal to 0.1 in. since it had 957 events and 832.8 in. of total rainfall (Table 4.20).

Figure 4.25 shows histograms of no-runoff rainfall events for four modeling scenarios. A lot of small rainfall events, e.g., <0.1 in., do not produce any runoff. With infiltration swales at the end of the watershed for the case study (Figure 4.18), there are some events with relatively large rainfall, e.g., >1.0 in., that do not produce runoff also. This indicates these infiltration swales are very effective in controlling small rainfall events. Additional results for long-term simulations are summarized in Table 4.22 and Table 4.23.

Table 4.21 Number of Events for Different Runoff Ranges (0.1 or 0.5 in. Increment) for SWMM Long-term Rainfall Simulations of Four Scenarios.

Depth of Runoff volume	Pre-construction	Post-construction without LID	Post-construction with ALDOTIS	Post-construction with MIS
0.0	**1028 (54.2%)**	**968 (51.0%)**	**1546, 1510, 1468 (81.5%, 79.1%, 76.9%) [1]**	**1604 (84.5%)**
(0.0,0.1]	569 (30.0%)	410 (21.6%)	55, 76, 90 (2.9%, 4.0%, 4.7%) [1]	43 (2.3%)
(0.1,0.2]	114	173	66, 72, 73	49
(0.2,0.3]	16	95	46, 56, 74	34
(0.3,0.4]	24	60	26, 28, 33	26
(0.4,0.5]	12	28	18, 20, 19	15
(0.5,0.6]	15	16	17, 19, 16	16
(0.6,0.7]	14	17	17, 15, 16	15
(0.7,0.8]	12	14	17, 13, 16	15
(0.8,0.9]	14	16	9	8
(0.9,1.0]	10	6	8	6
(1.0,1.5]	23	40	27	29
(1.5,2.0]	24	21	18	13
(2.0,2.5]	4	13	7	5
(2.5,3.0]	6	3	5	5
(3.0,3.5]	3	7	7	6
(3.5,4.0]	5	3	4	4
(4.0,8.9)	5	8	5	5

Note: [1] – Results for the soil-layer's saturated hydraulic conductivity of 0.93, 0.5, and 0.25 in./hr (1.86, 1.0, and 0.5 ft/d), respectively.

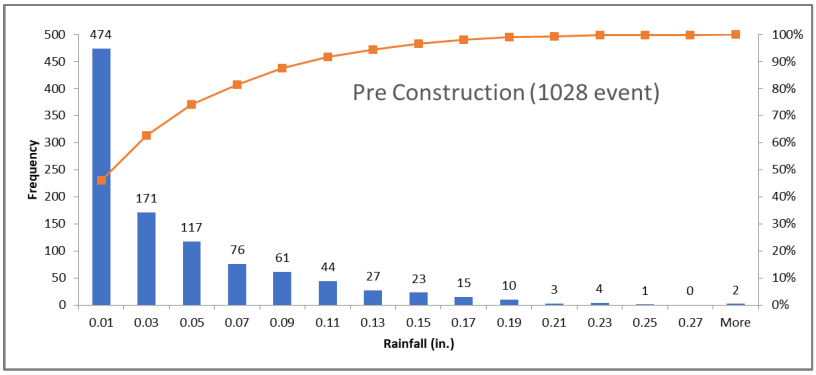

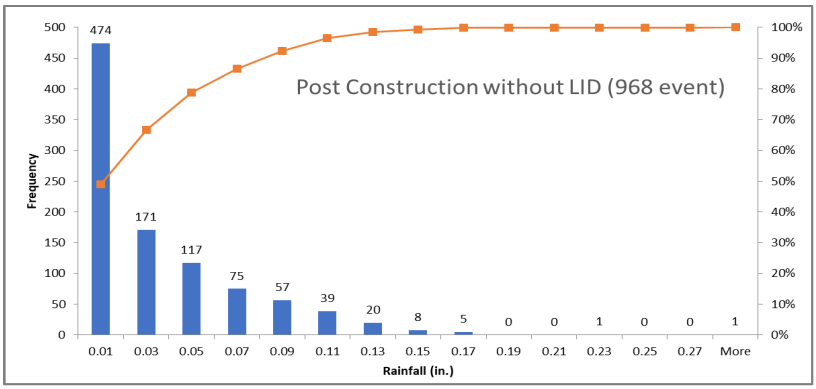

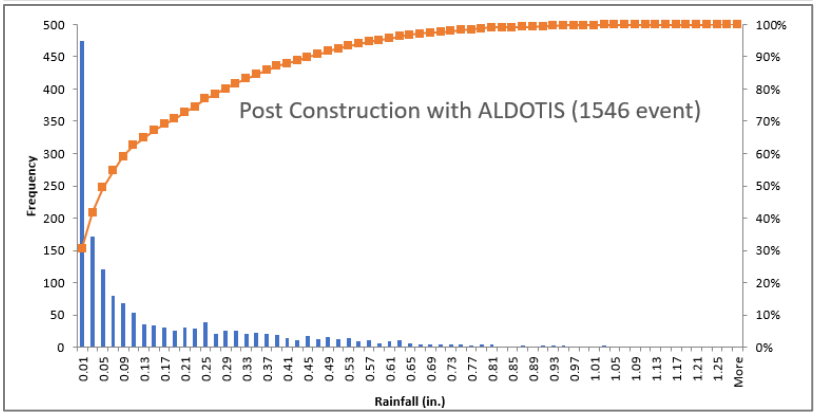

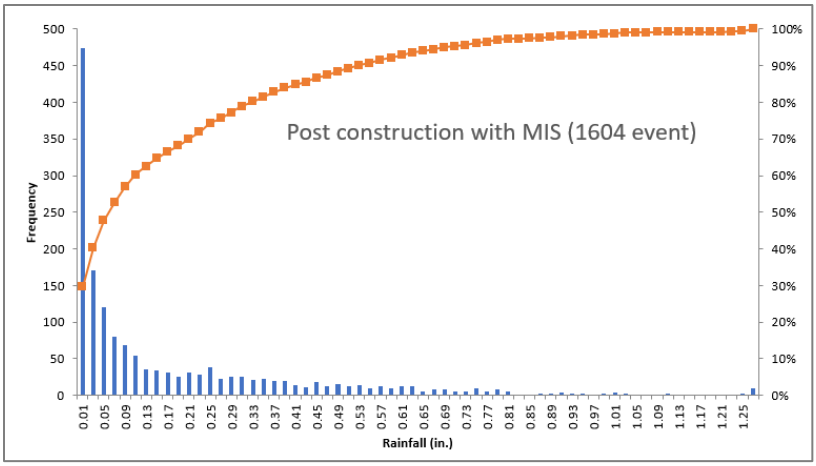

Figure 4.25 Rainfall Distributions (Histograms) for No-Runoff (R = 0) Events for Four Modeling Scenarios.

Table 4.22 provides a summary of rainfall and runoff characteristics for long-term simulations for four modeling scenarios. First, the number of events, total rainfall, and minimum and maximum rainfall for no-runoff (R = 0) events are determined. The post-construction scenario has 60 fewer events without a runoff, but two scenarios with infiltration swales have 518 or 576 more events compared to the pre-construction scenario. The pre-construction has 41.7 in. of rainfall without runoff over 15 years, and the post-construction with LID scenarios has 236.1 in. or 288.5 in. of rainfall that does not produce runoff. The maximum event rainfall that does not produce runoff increases from ~0.27 in. for no LID to 1.2 or 1.8 in. for having LID. The number of producing-runoff events (R>0) is significantly reduced with LID (from ~900 to ~300). Without LID, the minimum rainfall that produces runoff is 0.05 in., but with LID, it becomes 0.26 in. or 0.38 in. For the post-construction scenarios with LIDs, the overall runoff coefficient R_v for R>0 events is 0.40 or 0.39 (MIS) and reduces to 0.29 or 0.26 for all events because LIDs have many more events that do not produce runoff.

Table 4.22 Rainfall and Runoff Summary for Long-term Simulations for Four Scenarios.

Parameters to Summarize Runoff (R) Results	Pre-construction	Post-construction without LID	Post-construction with ALDOTIS[1]	Post-construction with MIS
No. events with R=0	1028	968	1546, 1510, 1468	1604
Total rainfall of R=0 events	41.7 in.	32.7 in.	**236.1, 202.6, 178.7 in.**	**288.5 in.**
Min rainfall for R=0 events	0.01 in.	0.01 in.	0.01 in.	0.01 in.
Max rainfall for R=0 events	**0.28 in.**	**0.27 in.**	**1.2 in.**	**1.8 in.**
No. events with R>0	**870**	**930**	**352, 399, 441**	**294**
Total runoff for R>0 events	255.36 in.	349.1 in.	249.7, 265.4, 282.8 in.	223.4 in.
Total rainfall of R>0 events	818.98 in.	828.0 in.	624.5, 658.5, 682.4 in.	572.2 in.
Overall R_v for R>0 events (all events)	0.31 (0.30)	0.42 (0.41)	0.40, 0.40, 0.41 (0.29, 0.31, 0.33)	0.39 (0.26)
Rainfall infiltrated/retained/ evaporated for R>0 events	0.65 in./event	0.51 in./event	1.06, 0.99, 0.91 in./event	1.19 in./event
Rainfall infiltrated/retained/ evaporated for all events	605.3 in.	511.6 in.	611.0, 595.6, 578.2 in.	637.3 in.
Min rainfall for R>0 events	0.05 in.	0.05 in.	**0.26, 0.24, 0.15 in.**	**0.38 in.**
Max rainfall for R>0 events	11.31 in.	11.31 in.	11.31 in.	11.31 in.
No. events with 0<R≤0.1 in.	569	410	55, 76, 92	43
Total rainfall of 0<R≤0.1 in.	239.3 in.	103.5 in.	49.2, 57.9, 62.2 in.	45.5 in.
No. events with R>0, Rainfall ≤ 0.1 in.	17	22	0	0
No. events with R>0.1 in.	301	520	297, 323, 349	251
No. events per year with R>0.1 in.	20.1	34.7	19.8, 21.5, 23.3	16.7

Note: [1] – Results for the soil-layer's saturated hydraulic conductivity of 0.93, 0.5, and 0.25 in./hr (1.86, 1.0, and 0.5 ft/d), respectively.

When the soil-layer's saturated hydraulic conductivity of 0.5, and 0.25 in./hr (1.0, and 0.5 ft/d) for ALDOTIS was used for long-term simulations, total rainfall producing no runoff decreases to 202.6 and 178.7 in. from 236.1 in. (Table 4.22) for 0.93 in./hr (1.86 ft/d) hydraulic conductivity, and the number of events producing runoff increases to 399 and 441 from 352, respectively. The minimum rainfall producing runoff decreases with the decrease of soil's hydraulic conductivity. Overall volumetric runoff coefficient R_v of ALDOTIS for all events increases from 0.29 to 0.33 (13.8% increase) when hydraulic conductivity decreases from 0.93 to 0.25 in./hr.

Figure 4.26 shows event runoff and runoff coefficient R_v versus runoff-producing (R>0) event rainfall for three post-construction scenarios, which has 930 (NoLID), 352 (ALDOTIS), and 294 (MIS) events (Table 4.22), respectively. The runoff coefficient R_v ranges from 0.01 to 0.96, with an average of 0.27 and a standard deviation of 0.19 for the post-construction without LID. Figure 4.26(b) shows four approximate trendlines when R_v is almost constant or increases with rainfall, and some events do not follow those patterns. There are many small rainfall events with runoff and small $R_v < 0.3$ for the post-construction without LID scenario. With LIDs (infiltration swales), runoff and runoff coefficients are decreased. For 352 events with R > 0, ALDOTIS had a maximum R_v decrease of 0.57 and an average R_v decrease of 0.11 with a standard deviation of 0.08. For 294 events with R > 0, MIS had a maximum R_v decrease of 0.59 and an average R_v decrease of 0.15 with a standard deviation of 0.10. Comparing MIS and ALDOTIS, the maximum R_v decrease was 0.40, and the average R_v decreased by 0.05 with a standard deviation of 0.05. This clearly shows that infiltration swales reduce surface runoff and runoff coefficients, and MIS performs better at reducing runoff than ALDOTIS does.

Table 4.23 summarize the runoff reduction and runoff information for two post-construction scenarios with infiltration swales from 15 years of the SWMM simulations. If ALDOTIS was installed for the post-construction site, it would have 928 events with a runoff reduction, and it reduced runoff of 99.4 in., MIS reduced runoff of 125.7 in. for 930 events over 15 years. The maximum runoff reduction is 0.68 in. and 0.87 in. for ALDOTIS and MIS, respectively, with 0.11 and 0.14 in. of event average reduction. Out of these runoff-reduction events, ALDOTIS and MIS made 350 and 294 events with runoff (R>0) to reduce total runoff of 58.1 in. and 70.5 in., respectively. Out of these 928 or 930 runoff-reduction events, ALDOTIS and MIS reduced 578 and 636 events to zero runoff, respectively. Out of all 1898 rainfall events, neither infiltration swales reduced the runoff for 968 events because these events did not produce the runoff under the post-construction without LID scenario (Table 4.22). These results indicate that MIS reduces more runoff than ALDOTIS does. Comparing Table 4.22 and Table 4.23, one will find two events (352 - 350) have no runoff reduction when R > 0 and SWMM outputs were in one-hour time intervals. When SWMM outputs were in 15-minute time intervals, those two events did have runoff reduction. MIS has runoff reduction for all events when R > 0 under post-construction without LID for both outputs from one-hour and 15-minute intervals.

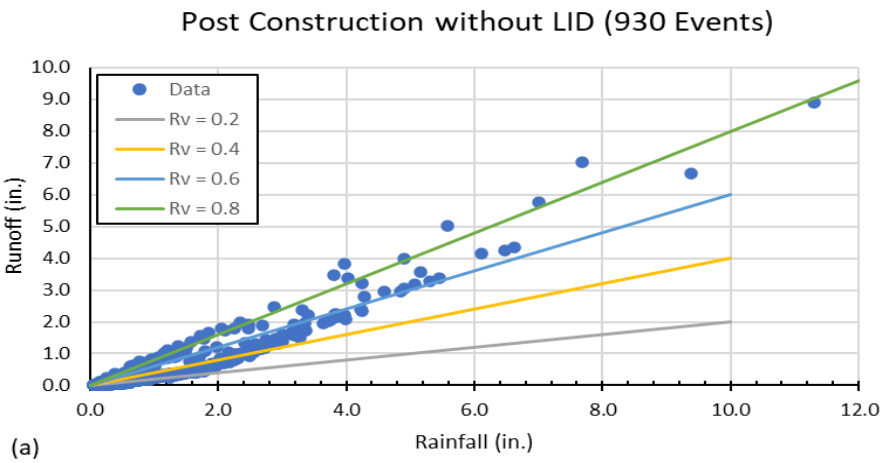

(a) Runoff

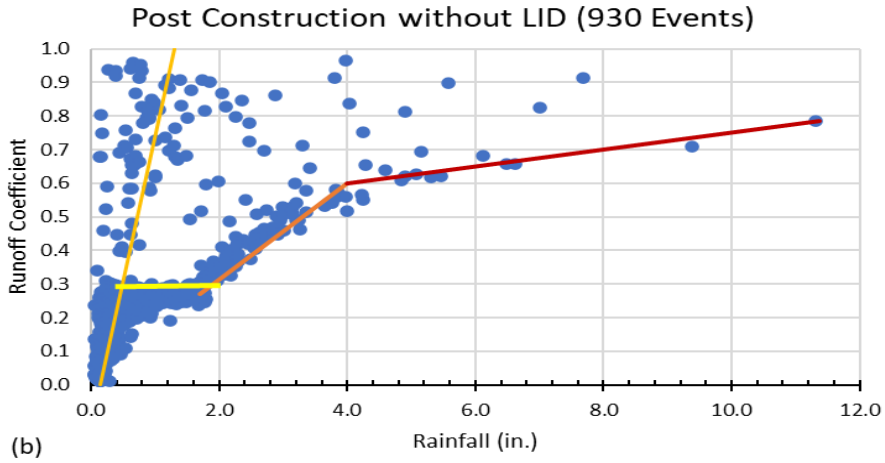

(b) Volumetric Runoff Coefficients R_v

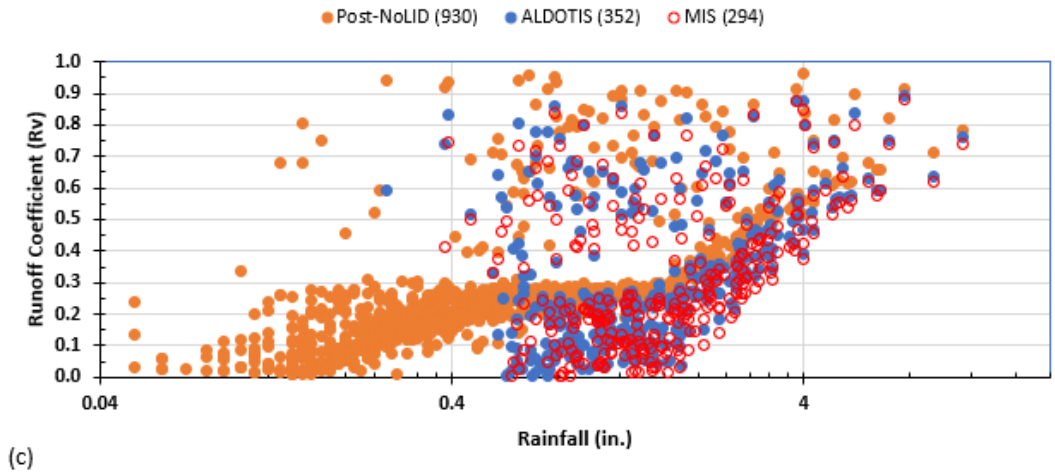

(c) Volumetric Runoff Coefficients R_v

Figure 4.26 (a) Runoff, (b) Volumetric Runoff Coefficients R_v for Post-Construction Without LID Scenario, and (c) Volumetric Runoff Coefficients R_v for three Post-Construction Scenarios versus Rainfall for Runoff Producing Events (R>0).

Table 4.23 Runoff Reduction or Runoff (in.) Results for Two Infiltration Swale Designs.

Parameters to Summarize Runoff (R) Results	Post-Construction with ALDOTIS	Post-Construction with MIS
No. events with runoff reduction	928 (578+350)	930 (636+294)
Event average ± standard deviation (total) of runoff reduction	0.11±0.093 (99.4)	0.14±0.124 (125.7)
Minimum runoff reduction	0.0014	0.002
Maximum runoff reduction	0.68	0.87
No. events with R>0 and runoff reduction	350	294
Total runoff with R>0 with reduction	247.9 in.	223.4
Average ± standard deviation of runoff with R>0 with reduction	0.71±1.025	0.76±1.063
Minimum runoff with R > 0 with reduction	0.002	0.002
Maximum runoff with R > 0 with reduction	8.61	8.38

Table 4.24 provides daily summary results from SWMM for four modeling scenarios so that we can compare them with ones in Table 4.4 derived from SWC presented in section 5.3.1. Using the same rainfall data, SWMM and SWC produce similar daily results except for evaporation when rainfall and runoff less than the threshold (e.g., 0.1 in. used) are excluded. In SWC, the user can only set one catchment with a few defaulted land use types and total percent impervious; however, the SWMM models five sub-catchments, and some results are normalized by sub-catchment area. Therefore, infiltration and evaporation losses for each sub-catchment were calculated first and added to get total infiltration and evaporation losses in the whole watershed, which were then divided by the watershed area. It takes much more effort to determine the results in Table 4.24 using SWMM outputs and Excel, but SWC internally processes those results in Table 4.4. The average annual evaporation from SWMM is, on average, 4.2 in. larger than one from SWC (Table 4.4). The average annual infiltrations for ALDOTIS and MIS from SWMM are 1.7 in. and 3.1 in., larger than those from SWC. SWC results show that ALDOTIS performs about the same as MIS, but SWMM can approve that MIS performs better than ALDOTIS.

Table 4.24 also provides results for the soil-layer's saturated hydraulic conductivity of 0.5, and 0.25 in./hr (1.0, and 0.5 ft/d) in addition to results using 0.93 in./hr (1.86 ft/d > 1.0 ft/d of the required minimum). Lower the soil-layer's saturated hydraulic conductivity, which is the maximum soil percolation rate, higher the surface runoff and smaller the infiltration by ALDOTIS. Therefore, it is recommended to make the soil layer have higher hydraulic conductivity for the implementation of the ALDOTIS.

Overall, both LID designs reduce runoff events effectively compared to post-development without LID, with the MIS providing the best overall performance in controlling stormwater runoff under Southern Alabama rainfall conditions.

Table 4.24 Daily Summary Results from SWMM for Four Modeling Scenarios for Southern Alabama.

Statistics [1]	Pre-Construction	Post-Construction w/o LID	Post-Construction with ALDOTIS [2]	Post-Construction with MIS
Average Annual Rainfall	57.4	57.4	57.4	57.4
Average Annual Runoff	17.02	23.27	16.65, 17.70, 18.93	14.89
Average Annual Evaporation)	5.93	5.51	5.94, 5.95, 5.95	5.92
Average Annual Infiltration	39.98	35.44	42.29， 42.29， 40.04	43.88
Days per Year with Rainfall	70.20	70.20	70.20, 70.40, 70.40	70.20
Days per Year with Runoff	21.67	37.73	22.00, 23.47, 25.53	18.47
Percent of Wet Days Retained	69%	46%	69%, 67%, 64%	74%
Smallest Rainfall w/ Runoff	0.11	0.11	0.12, 0.12, 0.12	0.12
Largest Rainfall w/o Runoff	0.87	0.87	1.69, 1.27, 1.27	1.69
Max Rainfall Retained	2.90	2.42	2.29, 2.46, 2.44	2.67

Note: 1 – Rainfall and runoff statistics are in in. and others in days, 2 - Results for the soil-layer's saturated hydraulic conductivity of 0.93, 0.5, and 0.25 in./hr (1.86, 1.0, and 0.5 ft/d), respectively.

4.3.6.3 Long-term Simulations of LIDs in Central and Northern Alabama

Long-term simulations of infiltration swales were also conducted in central and northern Alabama using climate data in Birmingham and Huntsville over 30 years (1/1/1990 to 1/1/2020). We hypothetically assumed the construction project with four scenarios in Southern Alabama occurs in Birmingham and Huntsville. Table 4.25 shows rainfall distributions of 3083 and 3255 events (6-hr inter-event dry period) for 30 years of rainfall data at Birmingham and Huntsville Airports, on average, about 103–109 events per year, fewer rainfall events than in Mobile. There are 36–37.5% of the rainfall events with rainfall ≤ 0.1 in., a total of 55.1–55.6 in. of rainfall (with an average depth of 0.05 in. per event). There are 68.6–68.9% and 84.8–85.7% of events with rainfall less than 0.5 in. and 1.0 in., respectively, in central and northern Alabama. Therefore, there are more events with rainfall between >0.1 in. and ≤0.5 in. compared to Mobile. For 2114 events with rainfall less than or equal to 0.5 in., it had a total of 246.9 in. of rainfall over 30 years (average 8.3 in. per year), which is 15.6% of total rainfall (1590.0 in. 0r 53.0 in. per year) at Birmingham.

Table 4.25 Event Rainfall Distributions at Birmingham and Huntsville.

Rainfall Ranges	Birmingham		Huntsville	
	No. Events	Percent Events	No. Events	Percent Events
(0, 0.1]	1,110	36.00%	1,220	37.48%
(0.1,0.5]	1,004	32.57%	1,024	31.46%
(0.5,1.0]	500	16.22%	547	16.80%
(1.0,1.5]	227	7.36%	226	6.94%
(1.5,2.0]	117	3.80%	106	3.26%
(2.0,2.5]	51	1.65%	57	1.75%
(2.5,3.0]	29	0.94%	20	0.61%
(3.0,3.5]	20	0.65%	16	0.49%
(3.5,4.0]	11	0.36%	16	0.49%
(4.0,4.5]	8	0.26%	8	0.25%
(4.5,5.0]	2	0.06%	7	0.22%
(5.0,5.5]	1	0.03%	1	0.03%
(5.5,6.0]			5	0.15%
(6.0,6.5]			1	0.03%
(6.5,7.0]	2	0.06%		
(8.0,8.5]	1	0.03%		
(12.0,12.5]			1	0.03%
Total	3,083	100.00%	3,255	100.00%

Note: Some 0.5 in. intervals were not shown when they did not have any rainfall events in both cities.

Table 4.26 summarizes a number or percent of runoff events for different runoff volume ranges for four modeling scenarios. The number of no-runoff rainfall events is listed first. The post-construction without LID had only 945 or 1,240 events (30.7–38.1% of all 3,083 or 3,255 rainfall events), but both post-construction with LID measures (ALDOTIS and MIS) had 2,352–2,758 events (76.3–84.7%) that did not produce any runoff. Infiltration swales performed much better in controlling runoff than the pre-construction scenario, which had 1,097 or 1,357 (35.6 or 41.7%) no-runoff-producing events. The pre-construction and the post-construction without LID scenarios still had a relatively large number of events (approximately from 260 to 14,00) that produced <0.1 or 0.1–0.2 in. runoff. The number of rainfall events that produce runoff of [0.0, 0.5] in. ranges from 2846 to 2939 for four scenarios, 92.3% to 95.3% of the total rainfall events over 30 years at Birmingham. The pre-construction scenario has 2,924 or 3,073 events, while the post-development without LID scenario has 78 or 61 fewer of these events. There are not many events (22–40, 0.71–1.23%) that produced 2 in. or more runoff for all scenarios.

Table 4.26 Number of Events for Different Runoff Ranges (0.1 or 0.5 in. Increment) for SWMM Long-term Rainfall Simulations of Four Scenarios at Birmingham and Huntsville.

Depth of Runoff volume	Pre-construction		Post-construction without LID		Post-construction with ALDOTIS		Post-construction with MIS	
	Birming.	Hunts.	Birming.	Hunts.	Birming.	Hunts.	Birming.	Hunts.
0.0	**1,097 35.6%**	**1,357 41.7%**	**945 30.7%**	**1,240 38.1%**	**2,352 76.3%**	**2,569 78.9%**	**2,561 83.1%**	**2,758 84.7%**
(0.0,0.1]	1,394 45.4%	1,325 40.7%	1,015 32.9%	879 27.0%	161 5.2%	166 5.1%	90 2.9%	84 2.6%
(0.1,0.2]	305	264	403	449	182	144	117	101
(0.2,0.3]	54	54	246	232	103	109	76	88
(0.3,0.4]	46	43	159	140	62	56	55	42
(0.4,0.5]	28	30	78	72	46	36	40	35
(0.5,0.6]	23	29	41	33	35	27	20	18
(0.6,0.7]	15	13	27	29	19	18	12	15
(0.7,0.8]	14	21	28	28	12	14	16	13
(0.8,0.9]	21	13	22	19	17	14	12	8
(0.9,1.0]	11	10	14	14	12	10	15	8
(1.0,1.5]	37	39	53	48	41	40	34	40
(1.5,2.0]	16	27	21	32	16	20	13	17
(2.0,2.5]	12	13	13	17	13	18	11	15
(2.5,3.0]	4	8	11	13	6	8	6	7
(3.0,3.5]	2	2	2	3	1	2	2	2
(3.5,4.0]	2	4	2	4	2	2	0	2
(4.0,8.9)	2	3	3	3	3	2	3	2

Table 4.27 provides a comprehensive summary of rainfall and runoff characteristics for four modeling scenarios for a total rainfall of 1,589.9 in. at Birmingham and 1,583.0 in. at Huntsville over 30 years. All results for Huntsville are given insider brackets from Table 4.27 to Table 4.29. The post-construction scenario has 152 or 117 fewer number of events without runoff, but two scenarios with infiltration swales have 1,212–1,256 or 1,401–1,464 more events compared to the pre-construction scenario. The pre-construction has 78.0 or 71.7 in. of rainfall without runoff over 30 years, and the post-construction with LID scenarios has 534.5–560.5 in. or 726.6–735.5 in. of rainfall that does not produce runoff. The maximum event rainfall that does not produce runoff increases from 0.2–0.27 in. for no LID to 1.3 or 1.8 in. for having LID because of surface ponding or internal storage. The number of producing-runoff events (R>0) is substantially reduced with LID (approximately from 2000 to 700 for ALDOTIS or approximately 500 for MIS). Without LID, the minimum rainfall that produces runoff is 0.01 in., but with LID, it becomes 0.25 in. or 0.12 in. For the post-construction scenarios with LIDs, the overall runoff coefficients for R>0 events are 0.30 or 0.32 (Huntsville) and reduced to 0.20 (ALDOTIS) or 0.16 (MIS) for all events because LIDs have many more events that do not produce runoff.

Table 4.27 Rainfall (in.) and Runoff (in.) Summary of Long-term Simulations for Four Scenarios at Birmingham and Huntsville (numbers inside brackets).

Parameters to Summarize Runoff (R) Results	Pre-construction	Post-construction without LID	Post-construction with ALDOTIS	Post-construction with MIS
No. events with R=0	1097 (1357)	945 (1240)	2,352 (2569)	2,561 (2758)
Total rainfall of R=0 events	78.0 (71.1)	57.7 (53.4)	534.5 (560.5)	726.6 (735.5)
Min rainfall for R=0 events	0.01 (0.01)	0.01 (0.01)	0.01 (0.01)	0.01 (0.01)
Max rainfall for R=0 events	0.25 (0.27)	0.25 (0.20)	1.29 (1.37)	1.80 (1.82)
No. events with R>0	1986 (1898)	2138 (2015)	731 (686)	522 (497)
Total runoff for R>0 events	322.57 (370.28)	525.70 (554.36)	312.43 (323.13)	256.36 (273.46)
Total rainfall of R>0 events	1511.95 (1511.83)	1532.27 (1529.54)	1055.4 (1022.35)	863.31 (847.44)
Overall R_v for R>0 events [all events]	0.21 [0.20] (0.24 [0.20])	0.34 [0.33] (0.36 [0.33])	0.30 [0.20] (0.32 [0.20])	0.30 [0.16] (0.32 [0.16])
Rainfall infiltrated/retained/ evaporated for R>0 events	0.60 (0.6) in./event	0.47 (0.48) in./event	1.06 (1.02) in./event	1.19 (1.15) in./event
Rainfall infiltrated/retained/ evaporated for all events	1267.4 (1212.7)	1064.2 (1028.5)	1277.5 (1259.8)	1333.6 (1309.4)
Min rainfall for R>0 events	0.01 (0.01)	0.01 (0.01)	0.25 (0.12)	0.25 (0.12)
Max rainfall for R>0 events	8.16 (12.03)	8.16 (12.03)	8.16 (12.03)	8.16 (12.03)
No. events with 0<R≤0.1 in.	1394 (1325)	1015 (879)	161 (166)	90 (84)
Total rainfall of 0<R≤0.1 in.	570.88 (584.69)	234.46 (220.53)	144.13 (146.45)	99.15 (88.05)
No. events with R>0, Rainfall ≤ 0.1 in.	166 (56)	237 (70)	0 (0)	0 (0)
No. events with R>0.1 in.	592 (573)	1045 (1124)	570 (520)	432 (413)
No. events per year with R>0.1 in.	39.5 (38.2)	69.7 (74.9)	38.0 (34.7)	28.8 (27.5)

Table 4.28 summarizes the runoff reduction and corresponding runoff information for two post-construction scenarios with infiltration swales in two cities. If infiltration swales were installed for the post-construction site at Birmingham or Huntsville, it would have 2,132 or approximately 2,010 events with a runoff reduction, and it reduced 215.4-231.4 in. of runoff for ALDOTIS or 271.0–281.0 in. of runoff for MIS over 30 years. Out of these runoff-reduction events, ALDOTIS and MIS made 725–680 and 516–495 events with runoff (R>0) to reduce total runoff of 307.1–319.7 in. and 251.5–271.3 in., respectively. Out of these 2,132 or approximately 2,010 runoff-reduction events, ALDOTIS and MIS reduced 1,407–1,329 and 1,616–1,518 events to zero runoff, respectively. Out of all 3,081 or 3,255 rainfall events at Birmingham or Huntsville, both infiltration swales did not reduce the runoff for 945 or 1,240 events because these events did not produce the runoff under the post-construction without LID scenario (Table 4.27). These results indicate that MIS reduces more runoff than ALDOTIS does in central and northern Alabama.

Comparing Table 4.27 and Table 4.28, one will find four events for ALDOTIS and two events for MIS at Huntsville have no runoff reduction when R > 0 and SWMM outputs were in a one-hour time interval. When SWMM outputs were in a 15-minute time interval, one event

for ALDOITIS and MIS still had no runoff reduction. However, six events for ALDOTIS and MIS at Birmingham have no runoff reduction when R > 0 and SWMM outputs were in a one-hour time interval. When SWMM outputs were in a 15-minute time interval, five events for ALDOTIS and MIS still had no runoff reduction.

Figure 4.27(a) shows rainfall hyetograph (from hourly rainfall data) and 15-minute runoff hydrographs on June 14, 2020, at Huntsville for post-construction scenarios. This rainfall event started at 5:00 am on June 14 and lasted 35 hours (for more than one day) with a total of 2.63 in. of rainfall (maximum intensity of 0.4 in./hr). For the post-construction without LID scenario, the runoff started at 5:15 am since the watershed had some impervious areas that produced runoff almost immediately. For the post-construction with ALDOTIS and MIS scenarios, the runoff started at 19:30 pm and 21:00 pm, respectively. Therefore, ALDOTIS and MIS had the runoff ponding for 14.5 or 15 hours before producing runoff. However, after LID produced the surface runoff, simulated discharges (cfs) were much larger than ones for the post-construction without LID scenario. These high discharges led to larger runoff volumes with ALDOTIS and MIS than the without-LID scenario. Figure 4.27(b) shows another example with no runoff reduction from LIDs on August 17, 2005, at Birmingham for post-construction scenarios. It was two events: the first lasted 2 hours for 0.3 in. of rainfall starting at 9:00 am, and the second lasted 7 hours for 0.9 in. of rainfall starting at 17:00 pm (with 6 hours of dry period from the first event). Both events produced surface runoff for the post-construction without LID scenario; however, for two with-LID scenarios, there was no runoff for the first event and high discharges and runoff volumes for the second event. These few events at Birmingham and Huntsville that did not have a runoff reduction for two LID scenarios may indicate potential issues of SWMM in its simplification of determining the overflow from LID facilities, which should be further studied in future research.

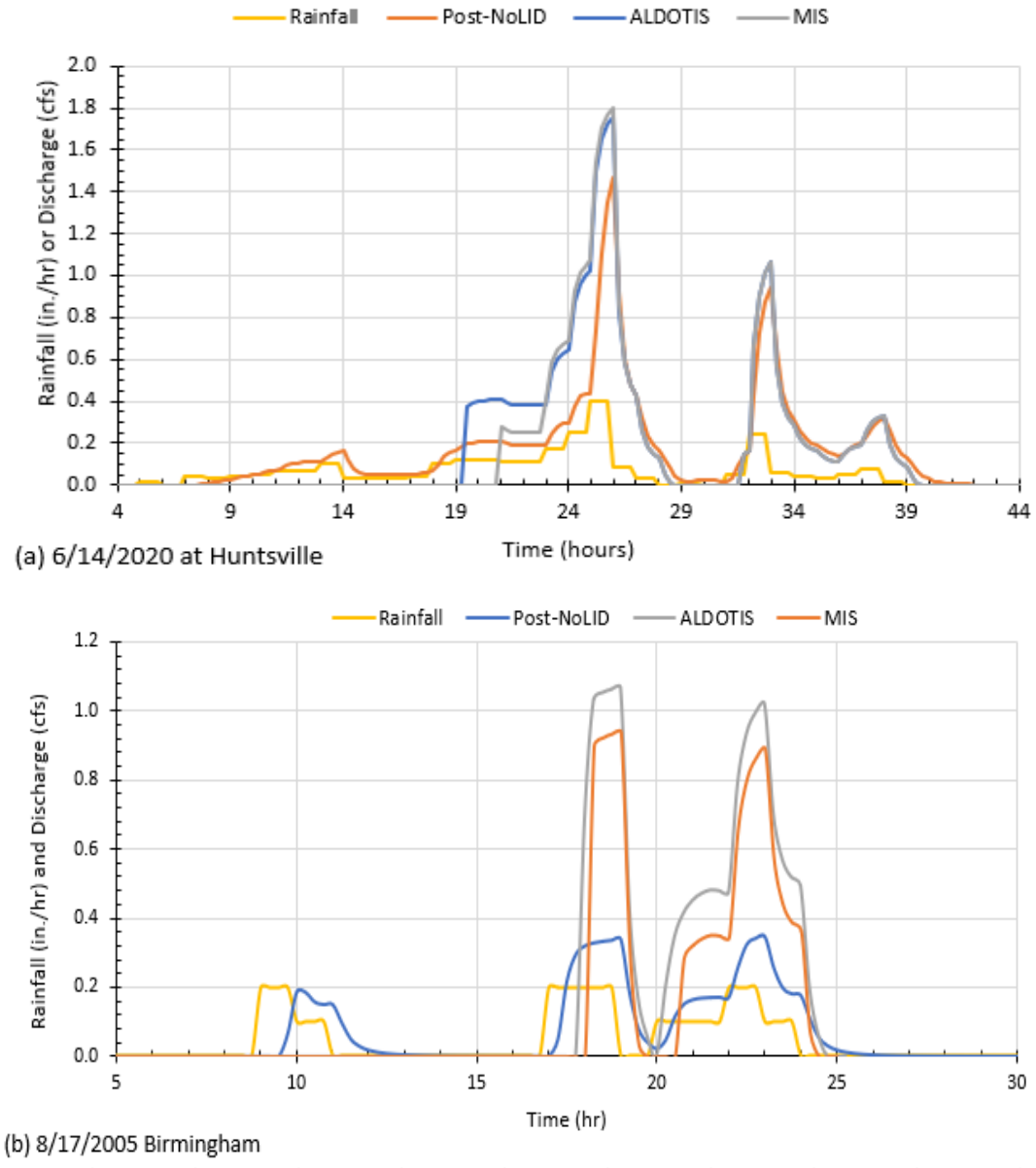

Figure 4.27 Rainfall Hyetograph and Runoff Hydrographs (a) on 6/14/2020 at Huntsville and (b) on 8/17/2005 at Birmingham for Post-Construction Scenarios.

Table 4.29 provides daily summary results from SWMM for four modeling scenarios in two cities so that we can compare them with results in Table 4.6 and Table 4.7 and derived from SWC presented in section 5.3.2. Using the same rainfall data, SWMM and SWC produce similar daily results, except evaporation when rainfall and runoff less than the threshold (e.g., 0.1 in. used) are excluded. The average annual evaporation from SWMM is larger than one from SWC.

Table 4.28 Runoff Reduction or Runoff (in.) Results for Two Infiltration Swale Designs at Birmingham and Huntsville (numbers inside brackets).

Parameters to Summarize Runoff (R) Results	Post-Construction with ALDOTIS	Post-Construction with MIS
No. events with runoff reduction	2132 [1407+725] (2014 [1329+685])	2132 [1616+516] (2014 [1518+496])
Average ± standard deviation (total) of runoff reduction	0.10±0.087 [215.4] (0.12±0.105 [231.8])	0.13±0.118 [271.0] (0.14±0.133 [281.4])
Minimum runoff reduction	0.002 (0.002)	0.002 (0.002)
Maximum runoff reduction	0.52 (1.72)	0.67 (1.82)
No. events with R>0 and runoff reduction	725 (685)	516 (496)
Total runoff with R>0 with reduction	307.1 (320.8)	251.5 (271.1)
Average ± standard deviation of runoff with R>0 with reduction	0.42±0.424 (0.47±0.706)	0.49±0.487 (0.55±0.768)
Minimum runoff with R > 0 with reduction	0.002 (0.002)	0.002 (0.002)
Maximum runoff with R > 0 with reduction	5.10 (9.34)	4.98 (9.23)

Table 4.29 Daily Summary Results from SWMM for Four Modeling Scenarios at Birmingham and Huntsville (numbers inside brackets).

Statistic	Pre-Construction	Post-Construction w/o LID	Post-Construction with ALDOTIS	Post-Construction with MIS
Average Annual Rainfall	53.0 (52.8)	53.0 (52.8)	53.0 (52.8)	53.0 (52.8)
Average Annual Runoff	10.75 (12.21)	17.52 (18.48)	10.41 (10.77)	8.55 (9.12)
Average Annual Evaporation	4.84 (5.29)	4.64 (4.64)	5.18 (5.50)	5.16 (5.47)
Average Annual Infiltration	42.65 (39.10)	37.43 (34.36)	44.50 (41.99)	46.02 (43.50)
Days per Year with Rainfall	71.10 (75.43)	71.10 (75.43)	71.10 (75.43)	71.10 (75.43)
Days per Year with Runoff	20.47 (20.90)	39.90 (40.53)	20.17 (19.40)	15.27 (15.47)
Percent of Wet Days Retained	71% (72%)	44% (46%)	72% (74%)	79% (79%)
Smallest Rainfall w/ Runoff	0.11 (0.11)	0.11 (0.11)	0.11 (0.11)	0.11 (0.11)
Largest Rainfall w/o Runoff	1.00 (0.91)	1.00 (0.91)	1.30 (1.47)	1.62 (2.89)
Max Rainfall Retained	2.96 (2.78)	2.51 (2.43)	2.82 (2.81)	2.94 (2.84)

4.4 EVALUATING THE INFILTRATION SWALES USING CIVILSTORM

CivilStorm is a powerful and comprehensive software application developed by Bentley Systems. It provides engineers and planners with the tools they need to effectively design, model, and optimize stormwater networks, ensuring infrastructure can handle a variety of storm scenarios and comply with environmental regulations. Despite platform functionality and interface differences, CivilStorm and SWMM can produce the same results under the same modeling conditions because CivilStorm allows users to select SWMM as the active numerical solver so that it integrates SWMM's core hydraulic and hydrologic computing engine into CivilStorm. The CivilStorm used for this study is linked to or compatible with SWMM release 5.1.013, and Bentley also claims that the current CivilStorm uses the most recent version of SWMM, i.e., SWMM 5.2. Bentley's numerical solver for CivilStorm is "GVF-Rational," i.e., gradually varied flow (GVF) for hydraulic and Rational Method for hydrological

simulations and calculations. The CivilStorm supports direct import and export of SWMM input files (*.inp), allowing the same SWMM model to run on both systems.

When the EPA SWMM is selected as the active numerical solver under CivilStorm, all SWMM hydrological methods can be used and implemented, including LID modeling. Therefore, the same model input data, e.g., subcatchment data in Table A.1 and LID modeling data in Table A.7, can be incorporated into CivilStorm despite different user interfaces. In this study, channel routing is not an important modeling task as only one drainage channel is included. Figure 4.28 shows subcatchment user interfaces for both CivilStorm and SWMM with basically the same input data; for example, Storage (Impervious depression) in CivilStorm is “Dstore-Imperv” in SWMM, Manning’s n (Impervious) in CivilStorm is “N-Imperv” in SWMM. Typically, CivilStorm fully spells out model parameter names, but SWMM uses abbreviated ones. In CivilStorm, the default unit for subcatchment slope is “ft/ft”, e.g., 0.005 ft/ft is 0.5% slope in SWMM. However, users can also change the slope unit in CivilStorm to “% slope” so that the imported data from the SWMM input data file can be used directly without any alterations. Not accounting for the catchment slope units will lead to different modeling results, for example, “0.5 ft/ft” is quite different from 0.5% slope. In SWMM, under “Infiltration Data,” users can select different infiltration methods and then input corresponding input data in another interface window, but CivilStorm allows entering all the infiltration input data under the same window (Figure 4.28).

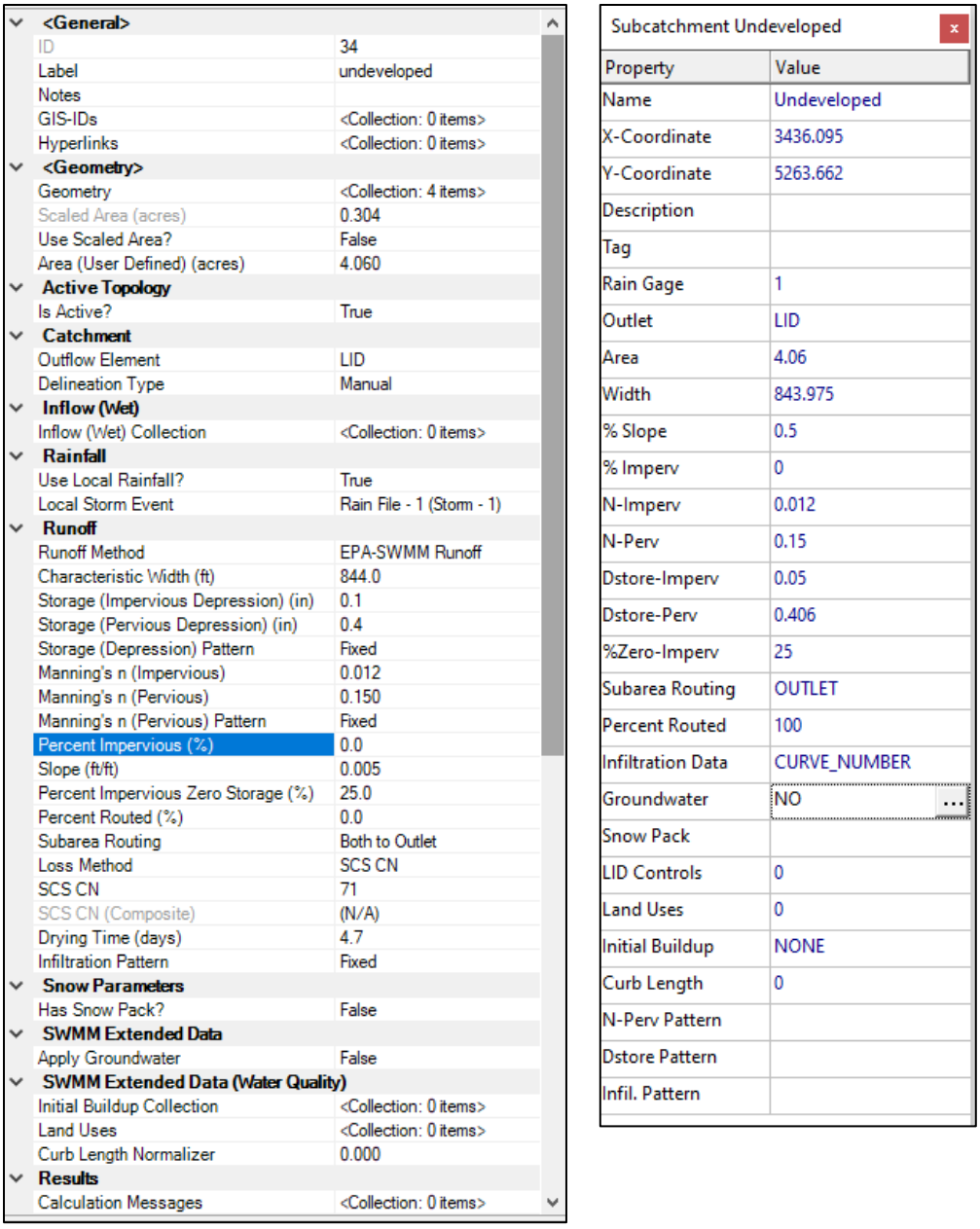

<General>	
ID	34
Label	undeveloped
Notes	
GIS-IDs	<Collection: 0 items>
Hyperlinks	<Collection: 0 items>
<Geometry>	
Geometry	<Collection: 4 items>
Scaled Area (acres)	0.304
Use Scaled Area?	False
Area (User Defined) (acres)	4.060
Active Topology	
Is Active?	True
Catchment	
Outflow Element	LID
Delineation Type	Manual
Inflow (Wet)	
Inflow (Wet) Collection	<Collection: 0 items>
Rainfall	
Use Local Rainfall?	True
Local Storm Event	Rain File - 1 (Storm - 1)
Runoff	
Runoff Method	EPA-SWMM Runoff
Characteristic Width (ft)	844.0
Storage (Impervious Depression) (in)	0.1
Storage (Pervious Depression) (in)	0.4
Storage (Depression) Pattern	Fixed
Manning's n (Impervious)	0.012
Manning's n (Pervious)	0.150
Manning's n (Pervious) Pattern	Fixed
Percent Impervious (%)	0.0
Slope (ft/ft)	0.005
Percent Impervious Zero Storage (%)	25.0
Percent Routed (%)	0.0
Subarea Routing	Both to Outlet
Loss Method	SCS CN
SCS CN	71
SCS CN (Composite)	(N/A)
Drying Time (days)	4.7
Infiltration Pattern	Fixed
Snow Parameters	
Has Snow Pack?	False
SWMM Extended Data	
Apply Groundwater	False
SWMM Extended Data (Water Quality)	
Initial Buildup Collection	<Collection: 0 items>
Land Uses	<Collection: 0 items>
Curb Length Normalizer	0.000
Results	
Calculation Messages	<Collection: 0 items>

Subcatchment Undeveloped

Property	Value
Name	Undeveloped
X-Coordinate	3436.095
Y-Coordinate	5263.662
Description	
Tag	
Rain Gage	1
Outlet	LID
Area	4.06
Width	843.975
% Slope	0.5
% Imperv	0
N-Imperv	0.012
N-Perv	0.15
Dstore-Imperv	0.05
Dstore-Perv	0.406
%Zero-Imperv	25
Subarea Routing	OUTLET
Percent Routed	100
Infiltration Data	CURVE_NUMBER
Groundwater	NO
Snow Pack	
LID Controls	0
Land Uses	0
Initial Buildup	NONE
Curb Length	0
N-Perv Pattern	
Dstore Pattern	
Infil. Pattern	

Figure 4.28 Subcatchment user interfaces for CivilStorm (left) and SWMM (right) for the "undeveloped" subarea for the Southern Alabama construction project.

The "scaled area" feature in the CivilStorm is a unique parameter in the process of entering data, unlike SWMM. In the CivilStorm, the scale area can be calculated automatically based on the physical geometry of the catchment as drawn or imported into the model. The software extracts the dimensions of polygons directly from map or GIS data. However, SWMM does not have this feature. Users must manually enter the total area of the subcatchments because SWMM cannot directly connect to GIS or geometric data for automatic area calculations. In CivilStorm, users can set the "Use scale area?" option to "True" or "False". If it is "False" (Figure 4.28), the user-defined area is used, e.g., Figure 4.28

shows “Scaled Area (acres)” is grey color, which means “not used”. Under “Area (User Defined) (acres)” a custom field allows users to input area manually, e.g., “4.06” in Figure 4.28. Then, the model uses the calculated polygon area if the option is “True” when CivilStorm integrates with Bently’s CAD software, i.e., MicroStation.

The use of units in SWMM and CivilStorm is another substantial difference. In SWMM, the user is restricted to choosing a single predefined system of units for the entire model, using the US Customary (imperial system) units such as feet, acres, cubic feet per second, or SI (metric system): units such as meters, hectares, cubic meters per second, etc. Once a unit system is selected, all inputs and outputs must conform to that system, and units cannot be mixed in SWMM (for example, some inputs use feet, and others use meters). However, a different system of units can be selected in the CivilStorm for each parameter, including length, area, flow, rainfall, and storage. These units can be changed in the model. CivilStorm provides flexibility on units of model parameters, but users must pay attention to units set by default, by another user, by the project team, etc.

The LID modeling practices differ substantially between the CivilStorm and SWMM regarding model setup. This difference is mainly for catchment from how LID facilities are integrated into the modeling process. SWMM provides direct integration of catchment (“LID Controls” in Figure 4.28), while CivilStorm requires adding a separate catchment to represent LID using “Low Impact Development” (not normal “Catchment”) under the Layout manual, even the LID facility is a part of the catchment. Figure 4.29 shows the CivilStorm watershed model for the same Southern Alabama construction project (Figure 4.18) that includes five subcatchments and a LID catchment (LI-1). For setting up LID facilities (e.g., BRC for infiltration swale) in CivilStorm, users must first set the basic information about LID using “Low Impact Development Controls” (Figure 4.30) under “Runoff” in the “Component” manual. Then, users should create a LID catchment and further set the area, number of units, and other attributes of LID in the LID catchment (Figure 4.31). Finally, the LID catchment is connected with other downstream catchments and/or outlets.

In comparison to setting LID in SWMM, first, users need to set the basic information of LID in the “LID Control Editor” (Figure 4.10), e.g., setup surface, soil, storage, and drain layers as shown in Figure 4.2, and then select a subcatchment and access “LID Controls” (Figure 4.28), where users connect the predefined LID type to the catchment by setting the LID surface area, number of units, and other attributes of LID as shown in Figure 4.11 or Figures A.15 and A.16. Therefore, CivilStorm’s “Low Impact Development Controls” in Figure 4.30 is the same as SWMM’s “LID Control Editor” in Figure 4.10 under “Hydrology”. SWMM uses four sub-windows (Figure 4.2) for users to specify LID basic information, but CivilStorm lumps all of them into one Window with four distinct sections (Surface, Soil, Storage, and Underdrain) for the data input (Figure 4.30).

After the basic information of the infiltration swale is inputted under “Low Impact Development Controls”, the next step is to connect a LID to a LID catchment. Figure 4.31 shows CivilStorm’s LID catchment (LI-1) with necessary input parameters for the Southern Alabama construction project for two scenarios: “False” (left) and “True” (right) of “Occupied Full Catchment?”. If a LID facility does not occupy the full catchment, the “False”

option is used, and “Percent Impervious Area Treated (%)” and “Percent Pervious Area Treated (%)” are two important parameters to allow CivilStorm to direct certain percent of the runoff from impervious or pervious area to the LID. If a LID facility occupies the full catchment, only “Top Width of Overland Flow Surface of Each Unit (ft)” and “Percent Initially Saturated (%)” should be specified as model input. The other three important inputs are to specify “Parent Catchment”, “Underdrain Flow Element”, and “Low Impact Development Control”. Figure 4.29 shows that the LID catchment LI-1 has the same area as the parent catchment LID (i.e., occupied full catchment), but LI-1 was moved parallelly northeast so that it can show clearly the connection between LI-1 catchment and LID catchment. It means all the runoff from the LID catchment will flow to the LI-1 catchment first, and LI-1’s surface runoff will flow to the parent catchment LID, then its outlet MH-1, and finally through channel CO-2 to outlet O-1. If LI-1 is smaller than the parent catchment LID, only the specified percent of the runoff from impervious and/or pervious areas flows to the LI-1 catchment, and the remaining percent of the upstream catchment runoff plus LI-1’s surface runoff flows to MH-1 directly. Underdrain outflow can flow to the outlet of the parent catchment or other junction.

It seems each LID catchment, e.g., LI-1, only allows to connect with one LID control facility; therefore, modelers must create multiple LID catchments (e.g., LI-2, LI-3, …, etc.) for connecting to several LID control facilities even if they have the same parent catchment. The only advantage could be the automatic computation of the LID areas from the LID catchment polygons when “Use Scaled Area” is set to “True.” However, SWMM does not need to create any LID catchments to connect a (parent) subcatchment to several LID facilities (Figure 4.11). In CivilStorm, if several LID facilities are connected to the same parent catchment, the sum of all the LID catchment areas should be smaller or equal to the area of the parent catchment. It is the same rule for the sum of the percent impervious or pervious areas treated to be smaller or equal to 100%.

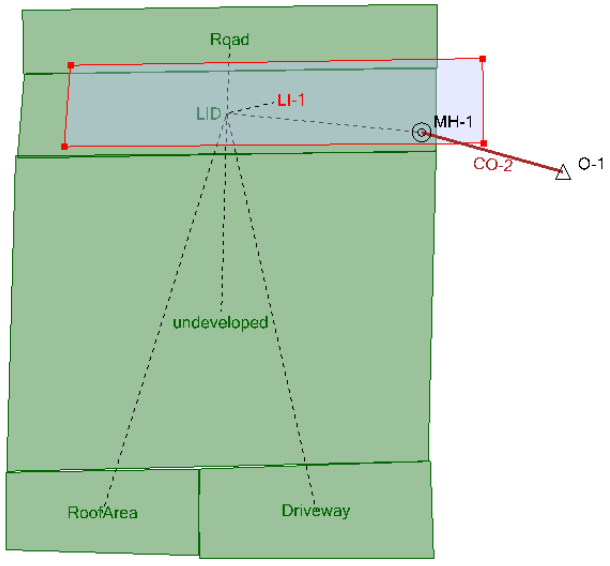

Figure 4.29 CivilStorm model with five subcatchments and a LID catchment (LI-1) for the Southern Alabama construction project.

CivilStorm also provides an opportunity for modelers to output detailed LID results into a separate file as SWMM does (Figure 4.11). In Figure 4.31 “Output Options” was selected as “Summary Results”, and the second option is “Detailed Results”. After “Detailed Results” is selected, the model must be rerun to get the detailed results for LID, but they are not directly saved in a specified file as SWMM does. To access them, right-click the LID catchment first, then click “Data Table” and choose by checking the available variables under Results as shown in Figure 4.32. There are 12 variables available to output the LID detailed results, and only nine variables are selected/checked for reporting the detailed results for infiltration swales in this study. After selecting LID variables and clicking the “OK” button, the detailed results as time series are shown in the “Graph: New Graph” window under the “Data” tab. When the “Graph” tab is selected, the detailed LID results are plotted in three panels (Figure 4.33, similar to SWMM results in Figure 4.13 and Figure 4.14): Infiltration rate (in./hr) including inflow, evaporation, and underdrain outflow, soil or pavement moisture (%), and depth (in.) for surface and storage layers. Both graph and time series data can be saved as separate files for further analysis using other software tools (e.g., Excel).

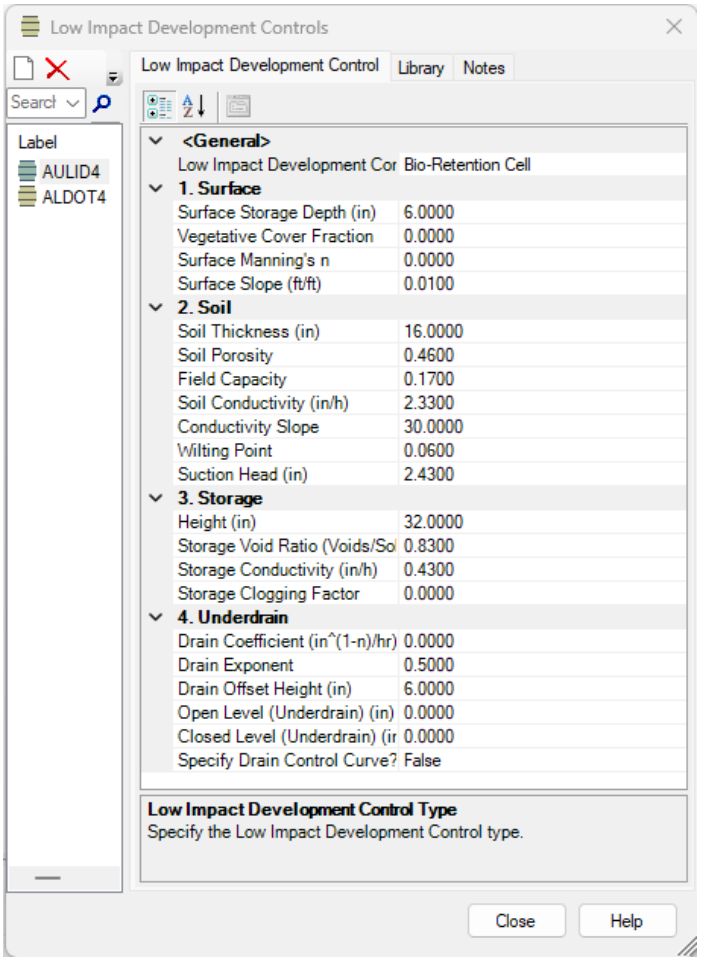

Figure 4.30 CivilStorm “Low Impact Development Controls” for the Southern Alabama construction project.

Despite some differences between CivilStorm and SWMM in the way of setting LID, they are basically the same in the function and type selection of LID, and both support the simulation and analysis of standard LID control measures. Both can simulate eight types of LID controls: Bio-Retention Cell, Rain Garden, Green Roof, Infiltration Trench, Permeable Pavement, Rain Barrel, Rooftop Disconnection, and Vegetative Swale.

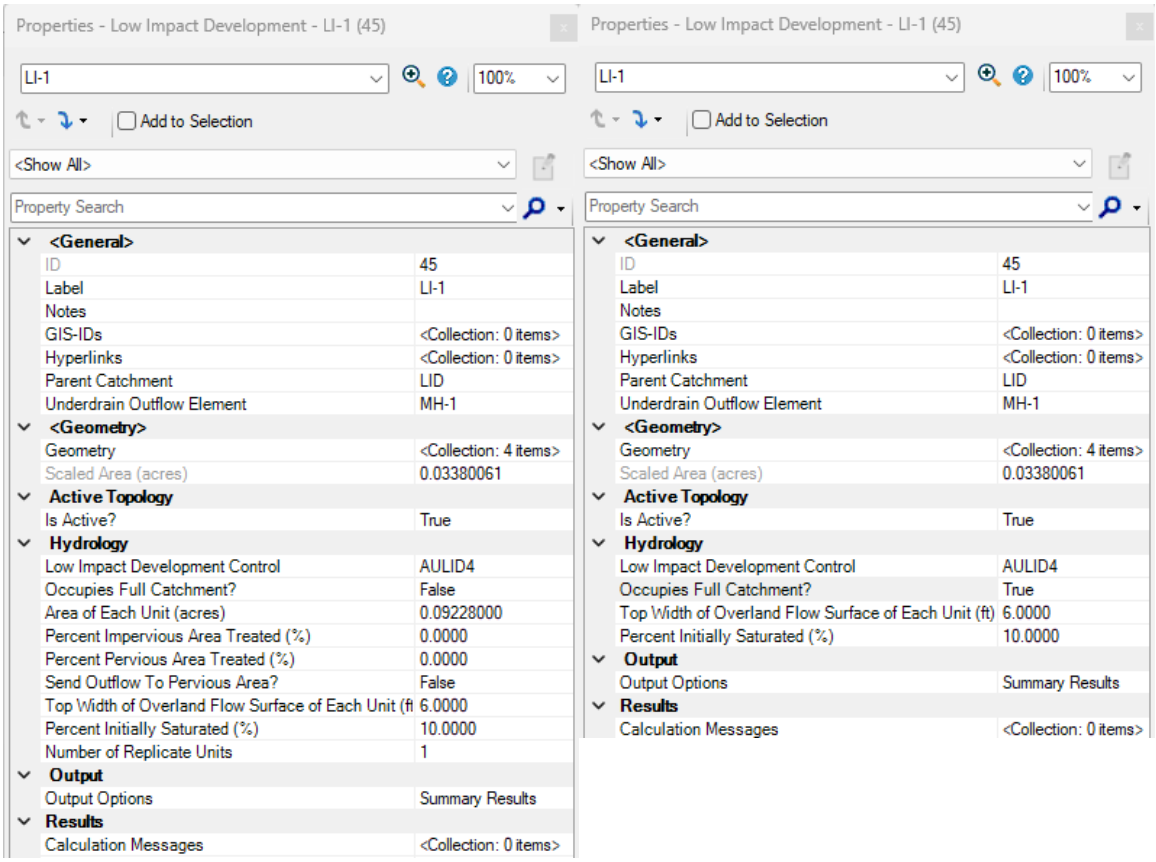

Figure 4.31 CivilStorm's LID catchment (LI-1) with necessary input parameters for the Southern Alabama construction project: "False" (left) and "True" (right) of "Occupied Full Catchment?"

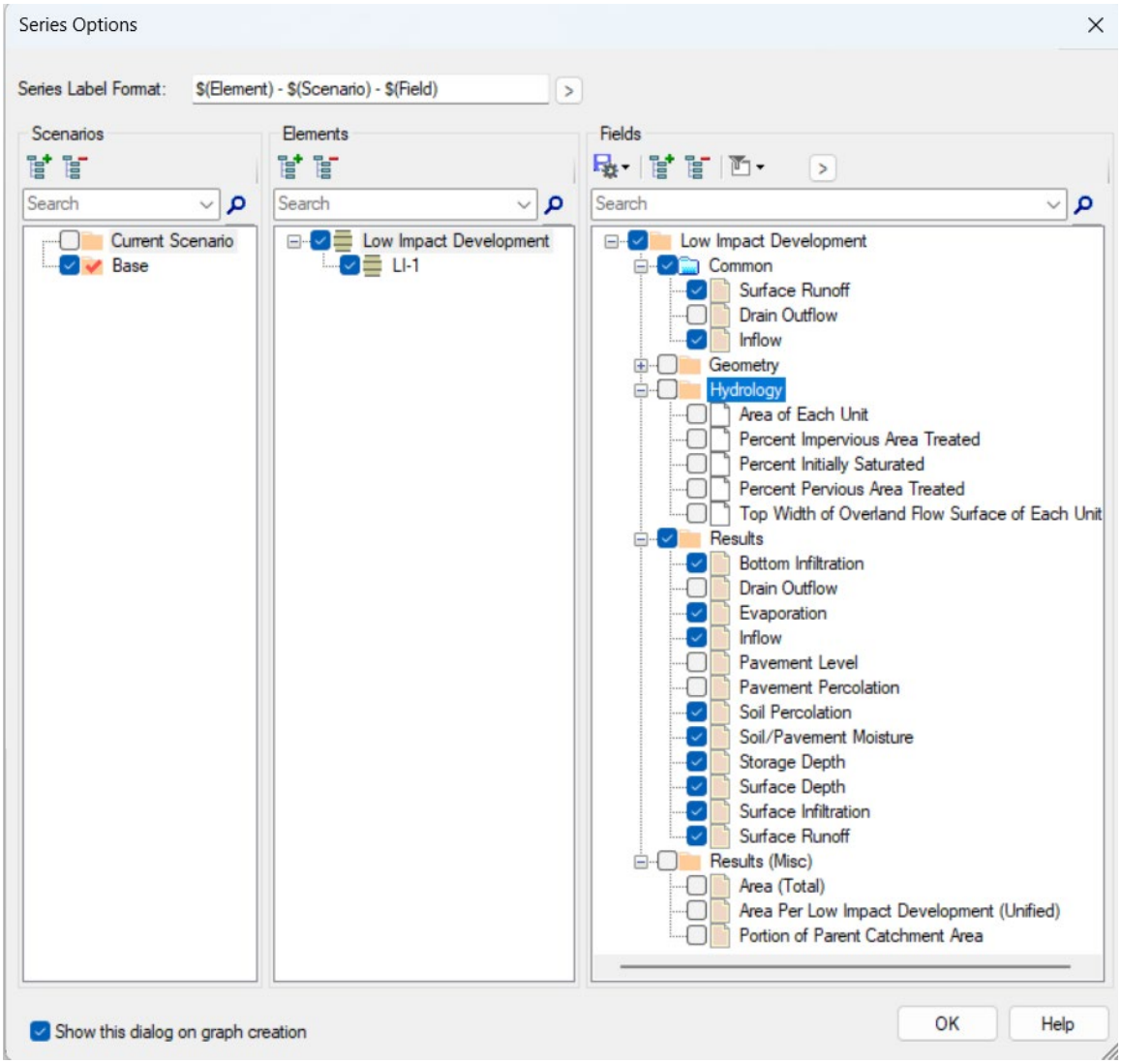

Figure 4.32 Series Option under Data Table from CivilStorm's LID catchment LI-1 to allow for the detailed output for a LID facility.

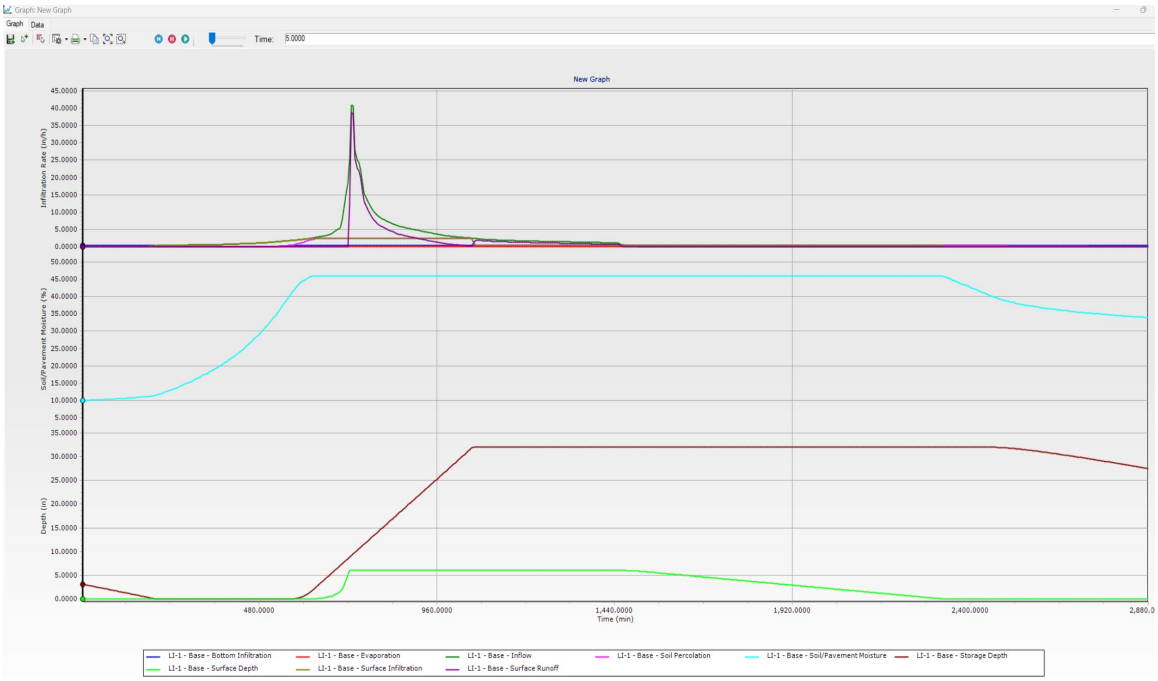

Figure 4.33 Example graphic results from the detailed output for a LID facility.

A CivilStorm model was created for the Southern Alabama construction project site (Figure 4.29) for the same four modeling scenarios with the same rainfall, e.g., 2.6 in. Type III rainfall with 15-min time interval for the model comparison and testing. When CivilStorm and SWMM use the same input parameters, rainfall data, and solver settings, they produce the same results, as shown in Figure 4.34. To better compare whether the results obtained by CivilStorm and SWMM are the same under the same conditions, three model runs were made and compared: (1) create the model in SWMM and run it in SWMM, (2) create the model in CivilStorm and run it in CivilStorm, and (3) create the model in SWMM and run it in the CivilStorm. In all four scenarios (Pre-construction, Post-construction without LID, with ALDOTIS and MIS), the surface runoff discharges simulated by SWMM, CivilStorm, and the SWMM model opened in CivilStorm overlap perfectly. This shows that all three configurations produce the same results using the same input data and solver Settings.

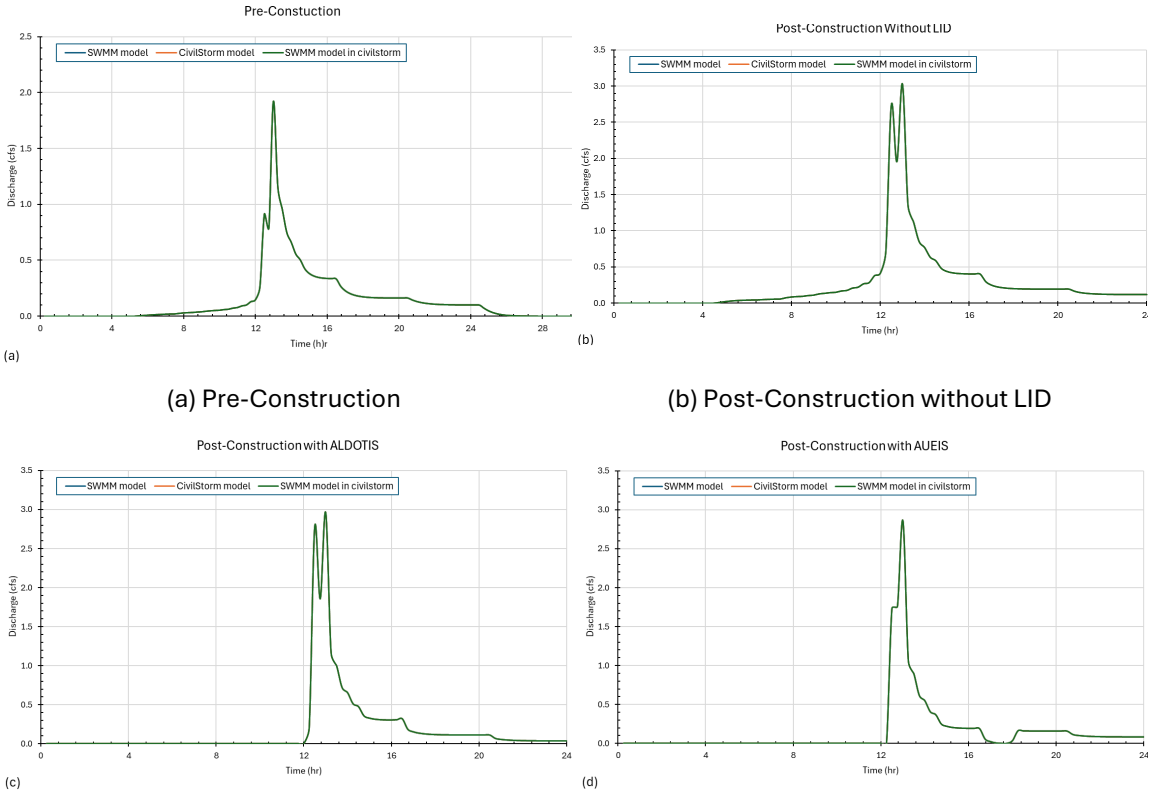

(a) Pre-Construction

(b) Post-Construction without LID

(c) Post-Construction with ALDOTIS

(d) Post-Construction with MIS.

Figure 4.34 Simulated Runoff Hydrographs from SWMM and CivilStorm for 15 min Time Step Type III 2.6 in. 24-hr Design Rainfall for Four Scenarios: (a) Pre-Construction, (b) Post-Construction without LID, (c) Post-Construction with ALDOTIS, and (d) Post-Construction with MIS.

CHAPTER 5. SUMMARY AND CONCLUSIONS

5.1 SUMMARY OF THE STUDY

In this study, a series of modified permeameters and infiltration rate testing columns were designed and constructed for small-scale tests encompassed using a 2.5 ft (0.76 m) long cylindrical 6 in. (15 cm) diameter PVC apparatus, which scaled down to fit the field-scale engineered media matrix designs. These cylindrical apparatuses were used to test multiple media designs simultaneously. They consisted of the modified permeability constant head tests (ASTM D2434), and constant-head and falling-head infiltration rate tests. These tests were used to measure the infiltration rates of the ALDOTIS design and different engineered media matrix designs. Figure 5.1 shows the small-scale engineered media matrix ALDOT design and the chosen MIS design.

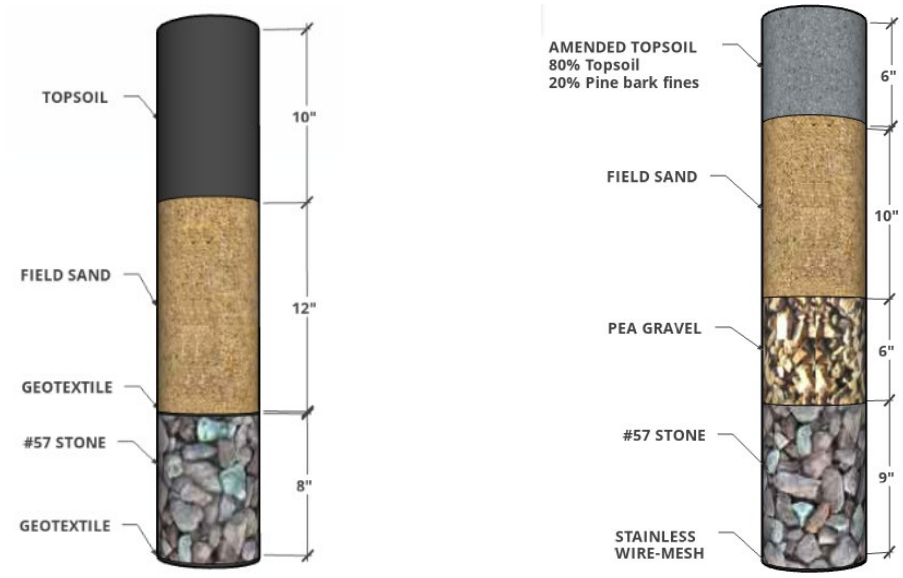

(a) ALDOTIS design (b) MIS design F3

Figure 5.1. Small-Scale Testing Designs

The selected MIS design (Figure 5.1) included 6 in. (15 cm) of an amended topsoil (80% topsoil and 20% pine bark fines by weight), 10 in. (25 cm) of fill sand, 6 in. (15 cm) of pea gravel, and 9 in. (23 cm) of #57 stone. Various MIS designs were tested using falling head and constant head infiltration rate apparatuses. An intermediate-scale infiltration chamber was designed and constructed to further test the ALDOT and modified (F3) infiltration swale designs.

Two field-scale infiltration swales based on the ALDOT and MIS or F3 designs (Figure 5.1) with two 6 in. ditch checks (Figures 3.18–3.20) were constructed at the AU-SRF, where the native soil is silty loam, a HSG B soil with field measured infiltration rates of 0.28 in./hr (0.7 cm/hr). These two swales were filled with water to the berm full height to determine the

drainage time and then to calculate average infiltration rates of these swales under the one-day and the three-day dry periods.

The modeling effort aims to develop an in-depth understanding of ALDOTISs in stormwater runoff control to mimic pre-construction hydrological performance. EPA SWC provides daily and annual simulation results for comparisons in runoff reductions of different scenarios, and SWMM results can be grouped by rainfall events with a 6-hour interevent dry period since dividing rainfall in the middle of the night (SWC method) could separate one rainfall event into two days and further results runoff greater than rainfall in some days. Various modeling tasks (design storms and long-term simulations) were performed for swales in different locations in Alabama (southern, central, and northern).

5.2 CONCLUSIONS

The following conclusions can be drawn from this study:

1. **From small-scale column tests, it was determined that the ALDOT topsoil was the major limiting factors affecting infiltration capacity.** Three 6 in. (15 cm) loose topsoil samples had measured falling-head infiltration rates from 0.27 ft/d to 1.39 ft/d with an average of 0.63 ft/d (Table 2.6, only one test's infiltration rate > 1.0 ft/d). Variations in infiltration rates of topsoil are due to soil consolidation (2 ft water head) and soil's heterogeneity. The modified permeability constant head test shows that topsoil permeability (Table 2.2) is higher than the minimum required infiltration rate specified in the LID Manual of Alabama (Dylewski et al. 2007), which is 1.0 ft/d (0.0083 in./min), however, the infiltration swale is seldom subjected to a 2-ft (0.6 m) constant head of water. The sandy topsoil used in this study has ~88% sand content and less than 2% silty content (Figure 2.1). ALDOT's topsoil (Section 650) for highway construction follows ASTM D 5268 and allows 2–20% by weight of organic material, 10–90% by weight of sand content (0.05–2 mm, from the Soil Science Society of America), and 10–90% by weight of silt (0.002–0.05 mm) and clay (< 0.002 mm) content, in portion of sample passing 10 Sieve (2 mm). Based on ASTM D 5268, ALDOT's topsoil could vary substantially in particle size distributions. In comparison to the topsoil used for this study (Figure 2.1, 88% sand), another topsoil can have quite different permeability, much lower than 1.16 ft/day (0.016 in./min, Table 2.2), with more fine silt and clay. This may not be important for various highway construction projects, but lower permeability is crucial to infiltration-based LIDs. Using topsoil with different permeabilities can result in variable performance of the infiltration swale to control the surface runoff and retain/store inflow.

2. Modified permeability constant head tests on five ALDOT swale designs (varying topsoil and sand heights) showed that three designs have permeability greater than 1.0 ft/d and two designs have permeability lower than 1.0 ft/d (0.24–0.48 ft/d) (Table 2.5). Table 5.1 summarizes the falling-head and constant head infiltration rate test results for ALDOTIS designs (e.g., removing geotextile, considering the consolidation, adding grass sod). Variations of infiltration rates are from three tested samples and three replicates for each

sample. Some tested infiltration rates were greater than 1.0 ft/d, but many are less than 1.0 ft/d, e.g., 0.16–0.24 ft/d (lowest rates in Table 5.1) which would result in more than 48 hours (2 days) of surface ponding. **Considering topsoil's heterogeneity and varying sand content, these small-scale tests indicate the current ALDOTIS design could perform satisfactorily (>1.0 ft/d infiltration rate) in some cases, but may not perform well in other situations.**

Table 5.1. Infiltration rate results for infiltration swale designs tested

Description	Design [1]	Measured infiltration rates (ft/d)	
		Falling head	Constant head
10" topsoil, 12" sand, 9" #57 stone	A_geo_geo	0.31±0.13 (0.16–0.54)	N/A
10" topsoil, 12" sand, 8" #57 stone	A-1G_geo_swm	0.62±0.27 (0.33–1.18)	0.46±0.059 (0.40–0.56)
10" topsoil, 12" sand, 9" #57 stone	A*_geo_geo_con	0.49±0.31 (0.23–1.28)	1.73±0.45 (1.16–2.31)
10" topsoil, 12" sand, 9.5" #57 stone	A*_geo_geo_con_grass	0.31±0.07 (0.24–0.43)	0.91±0.08 (0.79–1.04)

Note: [1] first "geo" - geotextile between sand/mixture and gravel layers and second "geo" – geotextile at the column bottom, "swm" – stainless wire mesh at the column bottom, "con" – consider topsoil's or mixture's sample consolidation under 2 ft (61 cm) of water head, "pea" – replace geotextile between sand/mixture and gravel layers with * (1, 4, and 6) inches of pea gravel, and "grass" – grass sod above the topsoil or the mixture (amended topsoil). [2]ALDOT calls for a minimum of 48 hr drawdown, which equates to 0.25 ft/d (7.6 cm/d) for a 6 in. (15 cm). tall check dam.*

3. **To enhance the infiltration capacity of the topsoil layer, the depth was reduced from 10 in. (25 cm) to 6 in. (15 cm) and amended with 20% pine bark fines by weight.** The amended topsoil had an average infiltration rate of 5.60 ft/day, i.e., 8.9 times higher than the infiltration rate obtained with topsoil alone, which was 0.63 ft/day (0.19 m/day). The modified swale Design B (Figure 2.7 and Table 2.9) with amended topsoil yielded an infiltration rate of 2.25 ft/d that was 7.25 times faster than the ALDOT swale's infiltration rate solely from pine bark fines amendment and decreasing the amount of topsoil.

4. **The geotextile layer decreased infiltration rates.** This was caused by fine soil particles from the sand layer migrating to the geotextile and clogging the material. To alleviate the reduction in infiltration rate capacity caused by the geotextile, a new 6 in. (15 cm) pea gravel layer was used as a substitute. **The addition of the pea gravel layer yielded an infiltration rate 2.66 times greater than ALDOT's design solely from using pea gravel rather than the geotextile.** Further analysis showed that minimal amounts of sand particles were penetrating through the pea gravel layer, and the pea gravel functioned effectively as a boundary layer separating the sand and the #57 stone. **In addition, removing the geotextile layer allows for installation of the infiltration swale without requiring laborers to enter the trench during construction – improving construction safety and reducing cost**. To properly install the geotextile layer, workers must climb down into the trench. Occupational Safety and Health Administration (OSHA) standards require a trench box be used when

vertical wall trenches of 5 ft (1.5 m) or greater unless the excavation is made entirely in stable rock. The depth of the infiltration swale, combined with the channel depth, triggers this requirement, adding substantial construction costs

5. **The #57 stone layer had the fastest infiltration rate because of its large air voids and high porosity**. The topsoil layer and the fill sand layer volumes were decreased to create more space, mostly for the pea gravel layer, but also for additional #57 stone. A MIS design is proposed from small-scale testing. The MIS design has 6 in. (15 cm) amended topsoil, 10 in. (25 cm) sand, 6 in. (15 cm) pea gravel (replacing the geotextile), and #57 stone layer (height depending on the swale depth, e.g., 26" stone of 4-ft swale) (Figure 5.1).

6. For the two field-scale infiltration swales, the average infiltration rate (evaluating the overall infiltration performance) for ALDOTIS was approximately 1.6 ft/d (0.49 m/d), whereas the MIS design displays an average infiltration rate of 5.2 ft/d (1.6 m/d). Therefore, the current ALDOTIS design using 10 in. (25.4 cm) topsoil with 88% sand content had infiltration rates higher than 1.0 ft/d, the Alabama LID minimum required infiltration rate. **The MIS design compared to the ALDOT swale had an improvement in infiltration rate of approximately 3.25 times.**

7. The topsoil used for this study contained a high (88%) sand content. ALDOT specifications allows for topsoil with lower sand contents that would affect infiltration performance. **When selecting materials for infiltration swale construction, sourcing sandy topsoil and testing topsoil for conductivity is recommended.**

8. Evaluating the infiltration performance for the one-day and the three-day dry periods, MIS (4.1–7.8 ft/d and 1.4–3.8 ft/d for three and one dry days, Figure 3.26) consistently outperformed ALDOTIS (1.7–2.4 ft/d and 1.3–1.5 ft/d for three and one dry days) in infiltration rates and drawdown times under different conditions. Increased rainfall frequency (shorter dry period) negatively impacted both swales, reducing infiltration rates and increasing drawdown times. **The MIS drawdown times were more sensitive to increased storm frequency compared to the ALDOTIS.** Despite longer drawdown times under frequent rainfall conditions, both swales fully drained within 24 hours for all tests.

9. **Data suggests the presence of an underdrain did not affect performance.** Evaluating the infiltration performance for the open and closed valves, the closed valve configuration exhibited slightly better performance (faster drawdown and higher infiltration rates) compared to the open valve in both swales. Seasonal variations potentially influenced performance. Open valve tests conducted in colder months (winter) showed slower infiltration compared to closed valve tests in warmer months (April-June). This could be due to temperature affecting water viscosity. More correlation is needed to confirm this relationship. Closed and open valve tests conducted in June showed similar performance, suggesting the underdrain may not have had a significant impact during the same season; however, underdrains could have a higher effect on performance in colder months.

10. **Evaluating the infiltration performance for seasonal variation, colder months showed slower infiltration and longer drawdown times for both infiltration swales (ALDOTIS and MIS). Warmer months, conversely, saw increased infiltration rates and faster drawdown times.**

11. **Evaluating the infiltration performance for wet and drier soils, both swales exhibited slower drawdown times and lower infiltration rates under wet soil initial conditions compared to drier conditions.** The MIS appeared less susceptible to the negative effects of soil moisture on infiltration compared to the ALDOT swale. This suggests the MIS' design or material composition may mitigate moisture influence.

12. **Evaluating the moisture content sensors, sensor data confirmed water infiltration, but absolute moisture content values were unreliable.** This is likely because water preferentially flowed through paths of least resistance, potentially missing some sensors. The time it took for water to reach sensors (time lag) was consistently lower for the MIS compared to the ALDOTIS at all depths except the deepest layer (unreliable data due to sensor malfunction in the ALDOTIS). The #57 stone layer sensor data (at the same depth in both swales) revealed a steeper initial rise in moisture content for the MIS, suggesting faster water movement. Despite having a smaller surface storage capacity, the MIS allowed water to reach the bottom #57 stone layer sensor significantly faster (1.7 hours) compared to the ALDOTIS. **This suggests the MIS design promotes faster infiltration.**

13. Large-scale testing also assessed maintenance needs associated with the infiltration swales. **Surveys of the swale surface showed no indication of settling over time.** With the modified swale providing higher hydraulic conductivity, the surface layer dries faster, reducing the chances of sod damage and compaction from mowing activities.

14. **Both SWC and SWMM can model the hydrological performance of several types of LID facilities.** The bio-retention cell is the most suitable LID type to represent the infiltration swales in drainage channels along the roadways that ALDOT implements for reducing the runoff in the construction project sites. ALDOT's infiltration swales have four layers (topsoil, sand, storage, and/or underdrain), but the bio-retention cells have three layers (soil, storage, and/or drain); therefore, the topsoil and sand layers are combined as an equivalent soil layer for SWC and SWMM modeling. The important parameters to model the infiltration swales are the surface berm height, soil layer's thickness and saturated hydraulic conductivity, storage layer thickness, and percentage of the catchment area with the runoff flowing into the swale. Two infiltration swale designs were modeled in this study: (1) ALDOTIS with 12 in. of topsoil, 12 in. of sand, and 24 in. of gravel layer (#57 stone) and (2) MIS design with 6 in. of mixture, 10 in. of sand, and 32 in. of gravel layer (pea gravel plus #57 stone).

15. EPA's SWC is designed for screening analysis to understand/model the runoff control performance of a single catchment with and without LID facilities. SWC has been used to model the four scenarios of a Southern Alabama construction project site: (1) pre-construction, (2) post-construction without LID, (3) post-construction with ALDOTIS, and (4) post-construction with MIS. Using limited input data summarized in Table 4.2 and Table 4.3, SWC runs for a long-term simulation (e.g., 15 years at Mobile, 30 years at Birmingham and Huntsville) to show the post-construction without LID increases the annual average runoff by 31.6% (from 16.62 in. to 21.89 in.) due to the increase of impervious area (10% to 27%) by the construction, the post-construction with LID reduces the runoff by 31.6% (from 21.89 in. to 14.97 in.) (Table 4.4). The post-construction with LID produces about 9.9% less of the annual runoff than the pre-construction scenario (from 16.62 in. to 14.64 in.). **The MIS**

performs slightly better in reducing the average annual runoff than ALDOTIS in the post-construction scenario. The same four scenarios were also modeled using SWC with Auburn, Birmingham, and Huntsville long-term rainfall data and had similar results as using Mobile rainfall data. SWC can consider the project site location and local soil property but use a few land use types (four pervious areas: forest, meadow, lawn, and desert) and lumped percent of impervious area to represent the complex construction project site as a single subcatchment.

16. Using the LID module for bio-retention cells, SWMM models were developed to mimic the water-filling events in two constructed infiltration swale designs at AU-SRF. **These SWMM models can reasonably predict the time series of surface water depth and the drawdown time for both designs when calibrated saturated hydraulic conductivities were used.** The measured drawdown time had large variations from one dry day (2.6 or 7.2 hours) to three dry days (8.5 or 12.5 hours) between events and from the first test in January (8.5 or 12.5 hours) to the last sets in October 2024 (0.3 to 1.2 hours). **The measured drawdown time for the ALDOTIS was always larger than for MIS.** For all field-scale tests presented in Chapter 4, the average measured drawdown time for the ALDOTIS ranged from 6.6 to 12.5 hours and from 1.0 to 8.5 hours for the MIS. Under the same test conditions, the average drawdown time for the MIS was 13% to 68% of ALDOTIS's drawdown time.

17. The Southern Alabama construction project site was further studied using SWMM under various design storms (95 percentile daily rainfall) by representing it using five subcatchments (Figure 4.18) with a set of LID parameters (Table 4.9). Under 2.6 in. Type III design storm, the post-construction without LID increases runoff by 52.7% (from 15,735 ft^3. to 24,035 ft^3), the post-construction with LID reduces the runoff by 35.2% or 44.4% (from 24,035 ft^3 to 15,590 or 13,365 ft^3) (Table 4.4). The post-construction scenario with LID produces about 0.9% to 15.1% less runoff than the pre-construction scenario (Table 4.9). The same four scenarios were also modeled using SWMM with other design rainfalls (2.0 to 2.8 in. Type II or III) and had similar results (Table 4.17). **The MIS performs much better in reducing surface runoff than ALDOTIS in the post-construction scenario under various design storms from south to north Alabama (Table 4.18).**

18. **SWMM can run long-term hydrological simulations to evaluate the runoff control performance of infiltration swales (ALDOTIS and MIS)**. A large percentage of rainfall events, e.g., 50% at Mobile, 36-37% in Birmingham and Huntsville, have a rainfall depth less than 0.1 in. (most produce no or very little runoff). At Mobile, 54.2% (1,028 events with 41.7 in. rainfall out of 1,898 events for 860.7 in. rainfall in 15 years), 51.0%, 81.5%, and 84.5% (1,604 events with 288.5 in. rainfall) of events under pre-construction, post-construction without LID, post-construction with ALDOTIS and with MIS, respectively, do not produce any surface runoff (Table 4.21). The maximum rainfall that does not produce runoff is 0.27 or 0.28 in. for pre- or post-construction without LID and increases to 1.2 in. for ALDOTIS or 1.8 in. for MIS (Table 4.22). Therefore, two infiltration swales capture additional 30.5–33.5% relatively smaller rainfall events in comparison to the post-construction without LID scenario and performs event better than the pre-construction scenario. The minimum rainfall that does not produce runoff is 0.05 in. for pre- or post-construction without LID and

increases to 0.26 in. for ALDOTIS or 0.38 in. for MIS (Table 4.22). **Therefore, these infiltration swales effectively eliminate or significantly reduce runoff for small rainfall events. Both infiltration swales at Mobile, Birmingham, and Huntsville can reduce runoff for almost all rainfall events by surface ponding and infiltration (Table 4.28).** For large rainfall events, two infiltration swales still result in the runoff reduction, which becomes smaller, and the runoff coefficient becomes larger (Figure 4.26). **The MIS design performed much better in reducing surface runoff than ALDOTIS in the post-construction scenario under long-term simulations (15 or 30 years) from south to north Alabama (Table 4.22 and Table 4.27).**

19. Through the long-term simulations at Mobile, Birmingham, and Huntsville, daily and annual rainfall-runoff results were generated (Table 4.24 and Table 4.29) and compared with the SWC results (Table 4.4, Table 4.7, and Table 4.8). **Both SWMM and SWC had similar results, except that the SWMM models produced larger evaporation losses than the SWC models.** The average annual evaporation from SWMM was, on average, 4.2 in. larger than one from SWC (Table 4.4) at Mobile. The average annual infiltrations for ALDOTIS and MIS at Mobile from SWMM are 1.7 in. and 3.1 in., larger than those from SWC. **SWC shows ALDOTIS performs about the same as MIS, but SWMM suggested that the MIS performs better than the ALDOTIS.**

20. **CivilStorm has an option to use the SWMM runoff solver so that it can produce the same hydrological results in studying the runoff control performance of infiltration swales for both design storm and long-term simulations** (Figure 4.34), even though CivilStorm requires some extra steps to set up the LID simulation model.

21. For the modeling study (conclusions 14–21), the soil's saturated hydraulic conductivity K_s was 0.93 in./hr (1.86 ft/d) for the ALDOTIS and 2.33 in./hr (4.66 ft/d) for the MIS, which are greater than 1.0 ft/d. When soil-layer's K_s of 1.0 ft/d (the required minimum LID infiltration rate) and 0.5 ft/d (half of the minimum) are used, the ALDOTIS reduces runoff infiltrated or stored from 39,622 ft^3 to 37,496 and 35,878 ft^3 (94–90% decrease) under 2.6 in. design storm in the Southern Alabama project site, respectively. If K_s becomes 1.0 ft/d for the ALDOTIS, the utilization percent for the full saturation in storage layer is 0%, and the maximum water level in storage layer is only 2.4 in. and 1.2 in. (stone layer is 12 or 24 in. for 4- or 5-ft swale). Decreasing the soil hydraulic conductivity leads to lower utilization rate of the storage layer (stone), which wastes the investment in making the swale deeper with additional stone or storage space. Long-term simulations also showed that the lower the soil-layer's saturated hydraulic conductivity, the higher the surface runoff and lower the infiltration by the ALDOTIS. **Therefore, it is recommended to have a topsoil layer with high hydraulic conductivity for the implementation of the ALDOTIS.**

5.3 Future Studies

This research aimed to provide greater understanding of the factors that affect the performance of infiltration swales. While significant findings were found through small-

scale, large-scale testing, and modeling experiments, opportunities still exist to further evaluate infiltration swales and improve their constructability and performance.

Topsoil was found to be the limiting layer in the performance of the infiltration swale. ALDOT's specifications currently allow for a wide range of topsoil makeups to be used in infiltration swales. Additional tests are recommended to better assess how topsoil composition affects overall performance of the infiltration swales.

Opportunities exist to further assess the composition of the engineered infiltration swale matrix. For example, understanding the performance of locally sourced materials, such as river chert, may allow for less expensive substitutions.

Retrofits could provide an opportunity to improve the performance of infiltration swales already deployed in the field. In-situ topsoil amendments, deep tillage, and other topsoil improvements can be assessed to determine if enhancements can be made. This can be especially important for infiltration swales that may not be meeting their infiltration expectations, or to provide maintenance if clogging becomes an issue over time.

While this study sought to evaluate maintenance needs, longer evaluation periods are recommended to fully understand how mowing and routine maintenance activities may affect performance of the infiltration swales. Furthermore, greater understanding of long-term infiltration performance is needed to understand when major maintenance or media replacement may be required.

REFERENCES

Abida, H., and Sabourin, J. F. (2006). "Grass Swale-Perforated Pipe Systems for Stormwater Management." *Journal of Irrigation and Drainage Engineering*, 132(1), 55-63.

Ackerman, D., and Stein, E. D. (2008). "Evaluating the effectiveness of best management practices using dynamic modeling." *Journal of Environmental Engineering*, 134(8), 628-639.

Ahmed, F., Gulliver, J. S., and Nieber, J. L. (2014). "Determining infiltration loss of a grassed swale." *World Environmental and Water Resources Congress 2014*, 8-14.

Ahmed, F., Gulliver, J. S., and Nieber, J. L. (2015). "Field infiltration measurements in grassed roadside drainage ditches: Spatial and temporal variability." *Journal of Hydrology*, 530, 604-611.

ALDOT (2014). "Guidelines For Operation. Subject: Post Development Stormwater Runoff Management for Small Frequent Rain Events." Alabama Department of Transportation (ALDOT), ed.Montgomery, AL.

ALDOT (2022). "Standard Specifications for Highway Construction." Alabama Department of Transportation (ALDOT), ed.Montgomery, AL.

Austin, P. J. (2024). "Constructing and evaluating large-scale infiltration swales for retaining and infiltrating roadway stormwater runoff." M.S., Auburn University, Auburn, AL 36849.

Bäckström, M. (2002). "Sediment transport in grassed swales during simulated runoff events." *Water science and technology : a journal of the International Association on Water Pollution Research*, 45 7, 41-49.

Barrett, M. (2005). "Performance comparison of structural stormwater best management practices." *Water environment research : a research publication of the Water Environment Federation*, 77, 78-86.

Bell, C. D., Wolfand, J. M., Panos, C. L., Bhaskar, A. S., Gilliom, R. L., Hogue, T. S., Hopkins, K. G., and Jefferson, A. J. (2020). "Stormwater control impacts on runoff volume and peak flow: A meta-analysis of watershed modelling studies." *Hydrological Processes*, 34(14), 3134-3152.

Bhaduri, B., Harbor, J., Engel, B., and Grove, M. (2000). "Assessing Watershed-Scale, Long-Term Hydrologic Impacts of Land-Use Change Using a GIS-NPS Model." *Environ. Manag.*, 26(6), 643-658.

Bjerg, P. L., Hinsby, K., Christensen, T. H., and Gravesen, P. (1992). "Spatial variability of hydraulic conductivity of an unconfined sandy aquifer determined by a mini slug test." *Journal of Hydrology*, 136(1), 107-122.

Carpenter, D. D., and Hallam, L. (2010). "Influence of planting soil mix characteristics on bioretention cell design and performance." *Journal of Hydrologic Engineering*, 15(6), 404-416.

Davis, A. P., Hunt, W. F., Traver, R. G., and Clar, M. (2009). "Bioretention Technology: Overview of Current Practice and Future Needs." *Journal of Environmental Engineering*, 135(3), 109-117.

Davis, A. P., Stagge, J. H., Jamil, E., and Kim, H. (2012). "Hydraulic performance of grass swales for managing highway runoff." *Water Res.*, 46(20), 6775-6786.

Davis, A. P., Stagge, J. H., Jamil, E., and Kim, H. (2012). "Hydraulic performance of grass swales for managing highway runoff." *Water Res.*, 46(20), 6775-6786.

Driscoll, E. D., Palhegyi, G. E., Strecker, E. W., and Shelley, P. E. (1989). "Analysis of storm event characteristics for selected rainfall gages throughout the United States." U.S. Environmental Protection Agency, Washington, D.C.

Dussaillant, A. R., Wu, C. H., and Potter, K. W. (2004). "Richards equation model of a rain garden." *Journal of Hydrologic Engineering*, 9(3), 219-225.
Dylewski, K. L., Brown, J. T. R., LeBleu, C. M., and Brantley, E. F. (2007). "Low Impact Development Handbook for the State of Alabama." Alabama Department of Environmental Management, Alabama Cooperative Extension System, and Auburn University, Montegomery, AL.
Ekka, S., and Hunt, W. (2020). *Swale Terminology for Urban Stormwater Treatment*.
Elhakim, A. (2016). "Estimation of soil permeability." *AEJ - Alexandria Engineering Journal*, 55.
Gohardoust, M. R., Sadeghi, M., Ziatabar Ahmadi, M., Jones, S. B., and Tuller, M. (2017). "Hydraulic conductivity of stratified unsaturated soils: Effects of random variability and layering." *Journal of Hydrology*, 546, 81-89.
Goyal, A., Morbidelli, R., Flammini, A., Corradini, C., and Govindaraju, R. S. (2019). "Estimation of Field-Scale Variability in Soil Saturated Hydraulic Conductivity From Rainfall-Runoff experiments." *Water Resources Research*, 55(9), 7902-7915.
He, Z., and Davis, A. P. (2011). "Process Modeling of Storm-Water Flow in a Bioretention Cell." *Journal of Irrigation and Drainage Engineering*, 137(3), 121-131.
Jiang, C., Li, J., Li, H., and Li, Y. (2019). "An improved approach to design bioretention system media." *Ecological Engineering*, 136, 125-133.
Khan, U. T., Valeo, C., Chu, A., and He, J. (2013). "A Data Driven Approach to Bioretention Cell Performance: Prediction and Design." *Water*, 5(1), 13-28.
Kirby, J. T., Durrans, S. R., Pitt, R., and Johnson, P. D. (2005). "Hydraulic resistance in grass swales designed for small flow conveyance." *Journal of Hydraulic Engineering*, 131(1), 65-68.
Kozlowski, T., and Ludynia, A. (2019). "Permeability Coefficient of Low Permeable Soils as a Single-Variable Function of Soil Parameter." *Water*, 11(12), 2500.
Lucas, W. C. (2004). "Green technology: The Delaware urban runoff management approach. A technical manual for designing nonstructural BMPs to minimize storm-water impacts from land development."Delaware Department of Natural Resources and Environmental Control Division of Soil and Water Conservation, Wilmington, Delaware.
Meter Group (2024). "Teros 10 Sensor - Simple Soil Water Content Sensor." <https://metergroup.com/products/teros-10/>.
MPCA (2021). "Minnesota Stormwater Manual: Alleviating compaction from construction activities."Minnesota Pollution Control Agency (MPCA), <https://stormwater.pca.state.mn.us/index.php/Alleviating_compaction_from_construction_activities>.
MPCA (2022). "Minnesota Stormwater Manual: BMPs For Stormwater Infiltration."Minnesota Pollution Control Agency (MPCA), <https://stormwater.pca.state.mn.us/index.php?title=File:BMPs_for_stormwater_infiltration_-_Minnesota_Stormwater_Manual.pdf>.
MPCA (2022). "Minnesota Stormwater Manual: Design criteria for infiltration."Minnesota Pollution Control Agency (MPCA), <https://stormwater.pca.state.mn.us/index.php?title=Design_criteria_for_infiltration>.
National Research Council (2009). *Urban Stormwater Management in the United States*, The National Academies Press, Washington, DC.
Paus, K. H., Muthanna, T. M., and Braskerud, B. C. (2015). "The hydrological performance of bioretention cells in regions with cold climates: seasonal variation and implications for design." *Hydrology Research*, 47(2), 291-304.

Ramirez Florez, D. A. (2024). "Evaluation of infiltration swale media using small- and intermediate-scale testing techniques." M.S., Auburn University, Auburn, AL 36839.

Rawls, W. J., Brakensiek, D. L., and Miller, N. (1983). "Green-Ampt infiltration parameters from soils data." *Journal of Hydraulic Engineering*, 109(1), 62-70.

Rossman, L. A. (2010). "Modeling low impact development alternatives with SWMM." *Journal of Water Management Modeling*.

Rossman, L. A., and Bernagros, J. T. (2019). "National Stormwater Calculator User's Guide (Version 2.0.0.1)." United States Environmental Protection Agency (USEPA), Cincinnati, OH.

Rossman, L. A., and Huber, W. C. (2016). "Storm Water Management Model Reference Manual, Volume I – Hydrology (Revised)." *EPA/600/R-15/162A*, National Risk Management Laboratory, Office of Research and Development, U.S. Environmental Protection Agency, Cincinnati, OH 45268.

Rossman, L. A., and Huber, W. C. (2016). "Storm Water Management Model Reference Manual, Volume III – Water Quality." *EPA/600/R016/093*, National Risk Management Laboratory, Office of Research and Development, U.S. Environmental Protection Agency, Cincinnati, OH 45268.

SEMCOG (2008). "Low impact development manual for Michigan."Southeast Michigan Council of Governments (SEMCOG), Detroit, Michigan.

Transportation For America (2013). "The Congestion Con." https://t4america.org/maps-tools/congestion-con/.

UNC (2024). "Post-Construction Stormwater Control Measures." *University of North Carolina (UNC)* https://ehs.unc.edu/topics/stormwater/program/post-construction-stormwater-control-measures/.

USDA (1986). "Urban hydrology for small watersheds." *Technical Release 55*, Natural Resources Conservation Service (NRCS), U.S. Department of Agriculture (USDA), Washington, D.C., USA.

USEPA (2009). "Technical Guidance on Implementing the Stormwater Runoff Requirements for Federal Projects under Section 438 of the Energy Independence and Security Act." *EPA 841-B-09-001*, United States Environmental Protection Agency (USEPA), Washington, DC 20460.

USEPA (2020). "Percent Impervious Area." *U.S. Environmental Protection Agency (USEPA), Enviroatlas* www.epa.gov/enviroatlas.

USEPA (2024). "Green Infrastructure." *US Environmental Protection Agency (USEPA)* https://www.epa.gov/green-infrastructure.

USEPA (2024). "Stormwater Discharges From Municipal Sources." *U.S. Environmental Protection Agency (USEPA)* https://www.epa.gov/npdes/stormwater-discharges-municipal-sources.

Winston, R. J., Dorsey, J. D., and Hunt, W. F. (2016). "Quantifying volume reduction and peak flow mitigation for three bioretention cells in clay soils in northeast Ohio." *Science of The Total Environment*, 553, 83-95.

Yang, Y., and Chui, T. F. M. (2018). "Optimizing surface and contributing areas of bioretention cells for stormwater runoff quality and quantity management." *Journal of Environmental Management*, 206, 1090-1103.

Zhang, X., Wendroth, O., Matocha, C., Zhu, J., and Reyes, J. (2020). "Assessing field-scale variability of soil hydraulic conductivity at and near saturation." *CATENA*, 187, 104335.

APPENDIX A: DEVELOPING A SWMM MODEL FOR INFILTRATION SWALES

To understand the performance of infiltration swales in controlling surface runoff using EPA SWMM, we first need to create a watershed or catchment model to represent the study area, then add infiltration swales as LID facilities. Appendix A provides some basic steps on how to develop a SWMM model for modeling infiltration swales. Some basic steps to set up and run a SWMM model can also be found in various SWMM tutorial documents and online videos, e.g., set certain project default options, map display options, and dimensions under View, and check the status bar at the bottom of the main window (e.g., auto-length off, offsets option as Depth).

Figure A.1 shows the user interface of EPA SWMM 5.2 for a post-construction scenario model for a Southern Alabama construction project site. At the top of the SWMM main window is a Menu bar with eight options (File, Edit, View, Project, Report, Tools, Window, and Help). Below the Menu bar is a Toolbar providing quick access to the most frequently used options. Below the Toolbar are three panels or windows: a "Project/Map" browser panel, a "Property/Action" panel of the selected project object/category, and a "Study Area Map" window. A vertical toolbar at the right side of the Study Area Map window provides quick access to add various basic SWMM components (e.g., rain gage, subcatchment, link, node, etc.) to the model/study area.

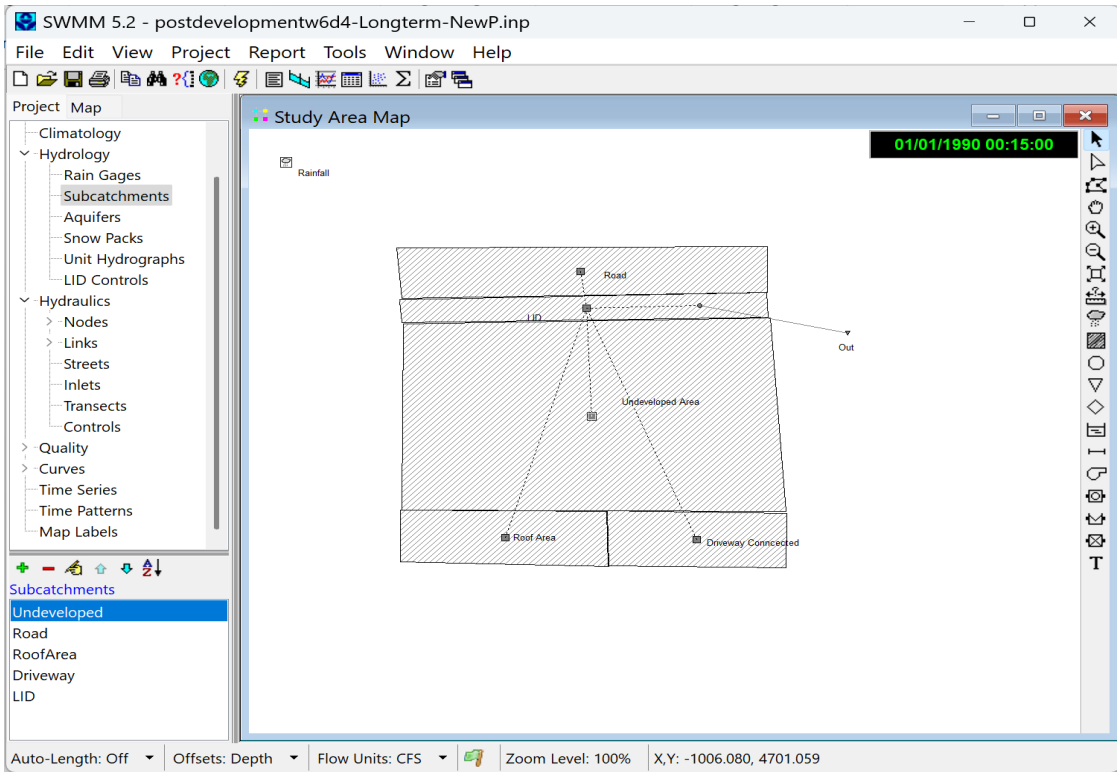

Figure A.1 SWMM 5.2 Project windows showing a post-construction scenario model for a Southern Alabama construction project site.

Under the “Project/Map” panel, one can access all objects to develop a SWMM to model infiltration swales. For example, using “Climatology” to set air temperature data for SWMM to determine/estimate evaporation loss; under “Hydrology”, using “Rain Gages” to set rainfall gages for SWMM hydrological model, using “Subcatchments” to add/edit subcatchments for a SWMM model (e.g., five subcatchments in Figure A.1), using “LID controls” to set basic parameters for two types of infiltration swales (ALDOTIS or MIS), using “Nodes” and “Links” to set junctions, outfall, and channels. using “Time Series” under “Curves” to set up rainfall time series data (design rainfall distributions). The following steps will provide more detailed information to complete various tasks to set up a SWMM model for the study.

A.1 Steps to Create Catchments in SWMM

Step 1: Open or Start a New SWMM Project

1. **Launch SWMM**: Open the SWMM software.
2. **Create a new Project:** If you continue work on an existing project, click on **File > Open** and navigate to your project file. Otherwise, create a new project by clicking **File > New**.

Step 2: Load Background Layers (Optional)

1. Go to **View > Backdrop > Load Backdrop**.
2. Browse to your .dxf, .shp, or raster file containing the map or catchment layout.
3. Load the backdrop to serve as a visual reference for drawing catchments.

Step 3: Define Catchment Elements

1. **Select the Subcatchment Tool**
    1) Navigate to the toolbar (right side of the Study Area Map, Figure A.1) and click on the **Subcatchment** tool  .
    2) The option 2 is to select “Subcatchments” under Hydrology in the Project browser panel, then click “  ” button in the Subcatchments property panel or select **Project** | **Add a New Subcatchment** from the main menu.
2. **Add a Subcatchment**:
    1) Click on the canvas (Study Area Map) where the first corner of the catchment is located.
    2) Drag your mouse to the next corner and click again.
    3) Repeat this process until the catchment outline is completed.
3. **Complete the Catchment**:
    1) After clicking the last corner, right-click and select **Complete Polygon** (or equivalent option).
    2) The subcatchment polygon will now be defined.

Step 4: Input Subcatchment Properties

1. Double-click on the newly created subcatchment to open the **Properties** window. The catchment properties are listed and explained in Table A.1.
2. Enter the following details:
    1) **Name/ID**: Assign a unique name or identifier.
    2) **Area**: Specify the catchment area in acres or hectares.
    3) **Width**: Enter the characteristic width for flow routing (overland flow length = Area/Width).

4) **Slope**: Input the catchment's average surface/terrain slope (%).
5) Continue to input all the available information in the Properties window as shown in Figure A.2. One may accept some default properties but should question whether these properties are appropriate for the study subcatchment or not.

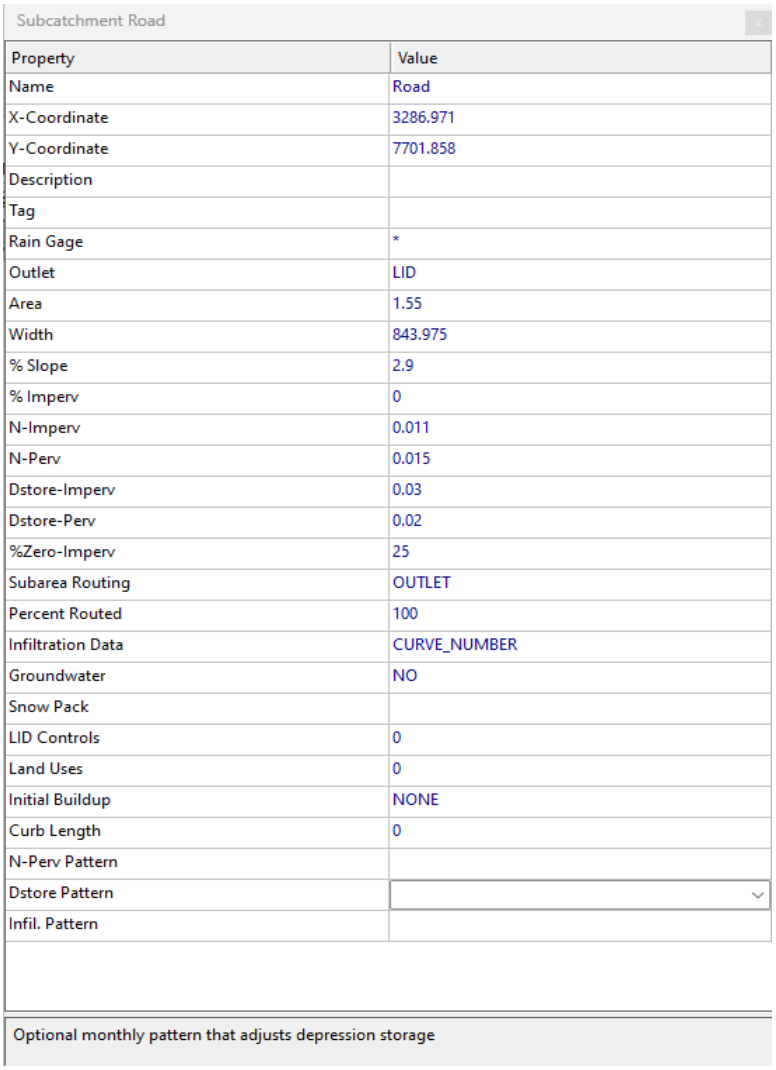

Figure A.2 Example of subcatchment properties in SWMM.

Table A.1 Parameters of Subcatchment in SWMM Hydrological Modeling.

Parameter	Description	Usage
Name	The unique identifier for the subcatchment in the model.	Each subcatchment should have a distinct name to differentiate between various watershed sections.
Rain Gage	Links the subcatchment to a rain gage that provides rainfall data for simulations.	The assigned rain gage ensures that the subcatchment uses the correct precipitation data during the simulation.

Outlet	Defines where runoff from the subcatchment goes (e.g., to a node, link, or another subcatchment).	This helps control how water moves through the stormwater network.
Area	The total area of the subcatchment (usually in acres or hectares)	This defines the surface area that contributes to runoff.
Width	The width of the subcatchment (characteristic width of the overland flow path).	This affects how quickly water flows off the subcatchment. Wider catchments generally have faster runoff.
Slope	The average slope (in percent) of the subcatchment area.	The slope affects the velocity of surface runoff, with steeper slopes typically leading to faster runoff and less infiltration.
% Impervious	Percentage of the subcatchment covered by impervious surfaces (e.g., roads, rooftops).	Impervious surfaces do not allow infiltration, so this percentage affects how much water directly contributes to surface runoff.
Impervious Surface Manning's n	Manning's roughness coefficient for the impervious portion of the subcatchment.	Manning's n values determine the roughness of the surface, affecting how quickly water moves across it. Impervious areas (like grass or soil) generally have lower roughness values than pervious areas.
Pervious Surface Manning's n	Manning's roughness coefficient for the previous portion of the subcatchment.	
Impervious Depression Storage	Depth of storage on impervious surfaces (in in. or mm).	Depression storage represents small surface depressions that trap water. Higher values mean more water is held temporarily before it runs off or infiltrates.
Pervious Depression Storage	Depth of storage on pervious surfaces (in in. or mm).	
Zero Percent Impervious	Percentage of the impervious area with no depression storage.	This parameter indicates the proportion of impervious surfaces that immediately contribute to runoff (e.g., sidewalks without depression).
Subarea Routing	Option: IMPERV, PERV, or OUTLET	Defines how water flows within the subcatchment. For instance: IMPERV: Runoff from pervious areas flows to impervious areas. PERV: Runoff from impervious areas flows to pervious areas. OUTLET: Both impervious and pervious areas directly drain to the outlet.
Percent Routed	The percentage of runoff routed between subareas.	Defines how much of the runoff from one part of the subcatchment is routed to another area before reaching the outlet.
Infiltration Parameters	**Horton Method**: Defines the rate at which water infiltrates into the soil over time (initial rate, final rate, and decay constant).	
	Green-Ampt Method: Uses soil suction head, hydraulic conductivity, and initial moisture deficit to calculate infiltration.	
	CN Method: Based on the NRCS CN, this method estimates runoff using the land cover, soil type, and rainfall data.	
	Usage: Infiltration models determine how much of the rainwater infiltrates into the soil and how much contributes to surface runoff.	
LID Controls	Specify if Low Impact Development (LID) practices, such as infiltration swales, permeable pavements, or green roofs, are applied to the subcatchment.	LID controls help manage stormwater runoff by encouraging infiltration, retention, and detention of rainwater, reducing the volume of water flowing directly to storm drains.
Groundwater Flow	Parameters that define the interaction between surface water and groundwater, such as aquifer properties, water table depth, and seepage characteristics.	Used if the model includes groundwater components that influence or are influenced by surface water.

A.3 Steps to Create Rainfall Data in SWMM

Creating rainfall data in SWMM involves defining the precipitation events that will be used for hydrological modeling. Below are the detailed steps:

Step 1: Create a Rain Gage

1. Open your SWMM project.
2. Navigate to the toolbar and click on the **Rain Gage** tool  , then select anywhere you want in the canvas or go to **Project>Hydrology> Rain Gage**, then select **Add** to create a new one.

Step 2: Create a Time Series Rainfall Event

1. **Go to the Time Series Tab**:

   Click on **Curves > Time Series** in the Project browser, then select **Add**  **Object** to create a new time series.
2. **Enter Rainfall Data**:
   1) Add Time Series Name, e.g., "2.6-Type III" for 2.6" Type III design rainfall, and Description (optional).
   2) Select "Use External data file named below" or "Enter time series data in the table below". Rainfall time series can be created in Excel or other tools, and then time-series data can be copied and pasted into the SWMM table or saved as a data (text) file as external data file.

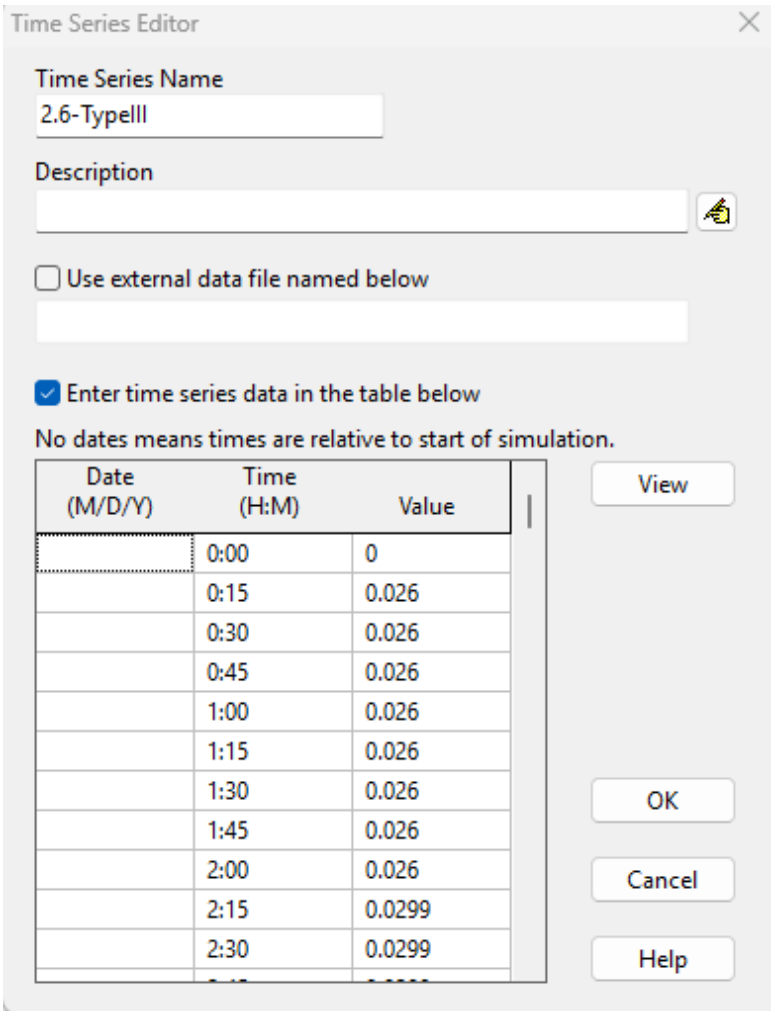

Figure A.3 Example of Rainfall Time Series Editor

3) Click **OK** to Save the Time Series

Step 3: Import/Link Time Series to Rain Gage

1. Double-click the icon of Rain Gage to open the properties of Rain Gage
2. **Import the File**:
    1) Edit the properties of Rain Gage to suit the time series, including key and required information: Name of rain gage, Rain Format, Time interval, Data Sources, Time Series Name, and Rain Units (Table A.2).
    2) Information on design rainfall is given in Figure A.4.

Table A.2 Rain information of a Rain Gage.

Property	Value	Description
Name	1	User-assigned name of rain gage.

Rain Format	INTENSITY/ VOULME/ CUMULATIVE	Rainfall data is provided as a rate (e.g., in./hr or mm/hr) / incremental depth (in. or mm) / cumulative depth (in. or mm).
Time Interval	0:05	Time resolution of rainfall data, SWMM provides nine options: 1, 5, 15, 20, and 30 minutes,1, 6, 12, and 24 hours.
Snow Catch Factor	1.0	Factor to adjust for snow catch efficiency (1.0 = no adjustment).
Data Source	TIMESERIES / FILE	Rainfall data is provided from a predefined time series in SWMM or an external data file.
TIME SERIES – Series Name	2.6-TypeIII-5min	The time series linked to the rain gage, likely a Type III storm at 5-min intervals.
DATA FILE – File Name, _ Station ID	e.g., Rain-72223513838.data, 72223513838	An external rainfall data file name, e.g., from NOAA rainfall data, and gage station ID
Rain Units	IN / MM	The unit of rainfall data. IN stands for in., and MM for millimeters.

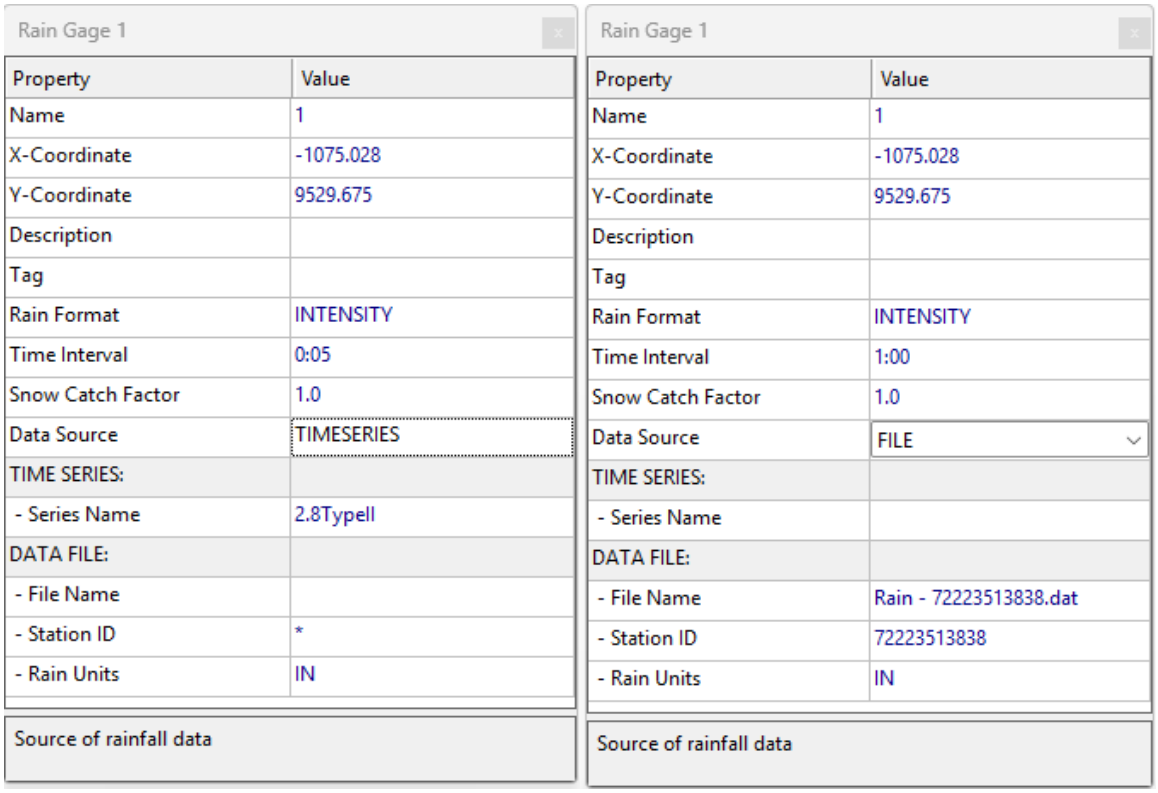

long-term rainfall from external data file (Left) design storm from SWMM time series (Right)

Figure A.4 Two examples of Rain Gage information: long-term rainfall from external data file (Left) or design storm from SWMM time series (Right).

Step 4: Assign the Rainfall to Subcatchments

1. Open the **Subcatchment Properties**.
2. Assign the Rain Gage Name (e.g., gage "1") to the **Rain Gage** field

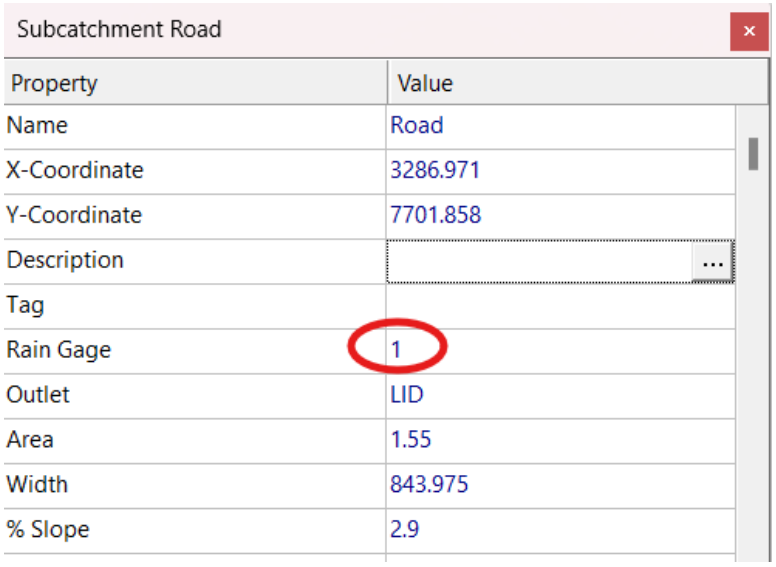

Figure A.5 Signing a rainfall gage "1" to a subcatchment "Road".

A.3 Steps to Create a Junction in SWMM

Step 1: Open the SWMM Project

Step 2: Select the Junction Tool

1. Locate the **Junction** tool in the toolbar or go to **Hydraulics > Node > Junction, then Add** under the Project.

Step 3: Add a Junction to the Network

1. **Place the Junction**:
   Click on the canvas where you want to place the junction. The junction will appear as a small circle or node.
2. **Name the Junction**:
   A default name (e.g., J1, J2) will be assigned automatically. Double-click the junction or right-click and select **Properties** to rename it.

Step 4: Define Junction Properties

1. Double-click the junction or right-click and select **Properties**.
2. Fill in the fields in the **Properties** window (Table A.3)

Table A.3 Junction properties explained.

Property	Value	Description
Name	1	Unique identifier for the junction.
Inflows	NO	No direct inflows have been assigned to this junction, or the molder provides inflow information.
Treatment	NO	No pollutant removal is applied at this junction, or no pollutants are simulated; otherwise, provide specific treatment information.
Invert Elevation	6.534	Elevation of the junction invert (in feet or meters, depending on model units).

Max. Depth	0	Maximum water depth (in ft or m), see Figure A.6.
Initial Depth	0	Initial water depth in the junction (in ft or m).
Surcharge Depth	0	Depth in excess of max depth before flooding. (in ft or m).
Ponded Area	0	Area available for ponding if flooding occurs (in ft^2 or m^2).

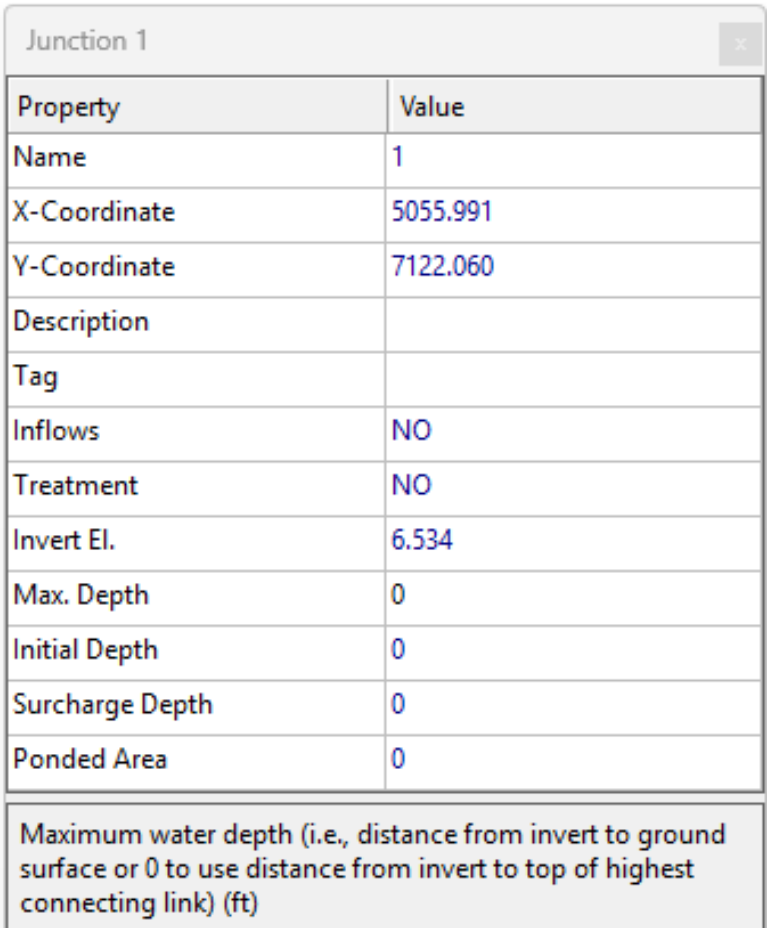

Figure A.6 Example of junction information.

Step 5: Connect the Junction to Subcatchments

1. Open the **LID Subcatchment Properties**.
2. Assign the Junction Name to the **Outlet** field (Figure A.7)

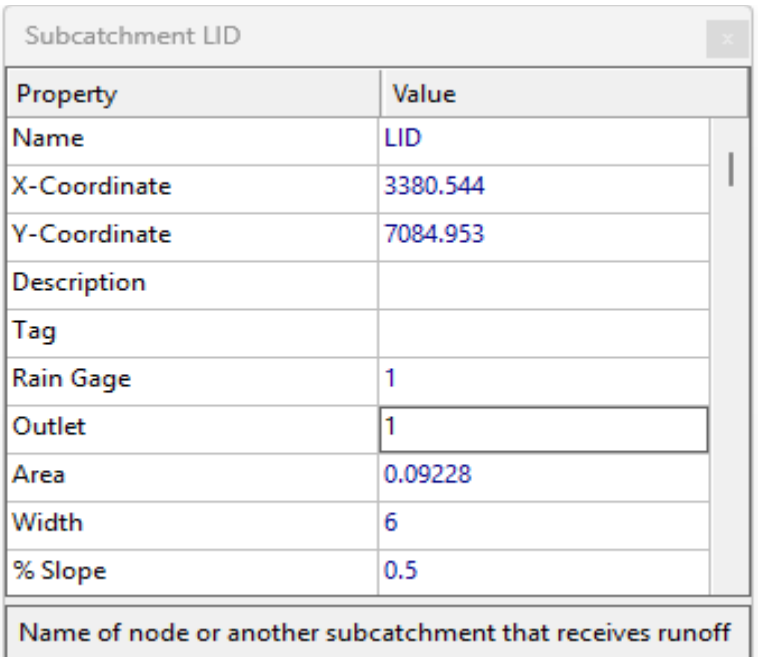

Figure A.7 Signing junction "1" as the outlet of a subcatchment "LID".

A.4 Steps to Create an Outfall in SWMM

Outfalls are terminal nodes of the drainage system used to define final downstream boundaries under the Dynamic-Wave flow routing. For other types of flow routing, they behave as a junction. Only a single link can be connected to an outfall node, and the option exists to have the outfall discharge onto a subcatchment's surface. The principal input parameters for outfalls include invert elevation, boundary condition type and stage description, and the presence of a flap gate to prevent backflow through the outfall.

Step 1: Open the SWMM Project

Step 2: Select the Outfall Tool

Locate the **Outfall** tool ▽ in the toolbar or navigate **Hydraulics> Node > Outfall** in the Project.

Step 3: Place the Outfall

1. **Click to Add the Outfall**:
   Click on the canvas at the location where the runoff exits the system. The outfall will appear as an outfall node.
2. **Name the Outfall**:
   A default name will be assigned. You can rename it by double-clicking the outfall or right-clicking and selecting **Properties**.

Step 4: Define Outfall Properties

1. Open the **Properties** window for the outfall by double-clicking on it.
2. Fill in the fields in the outfall **Properties** window. An outfall is a special node with all the basic node's property fields (Table A.3) plus a few additional fields shown in Table A.4. In this study, a simple free fall outfall is used (Figure A.8), which has a critical of the upstream conduit/channel at the outfall.

Table A.4 Additional fields of an outfall.

Property	Value	Description
Tide Gate	NO/YES	No/Yes whether a tide gate is present at the outfall.
Route To - Type	FREE / NORMAL / FIXED / TIDAL / TIMESERIES	The boundary conditions at an outfall can be described by any one of the following stage relationships: (1) the critical (free fall) or (2) normal flow depth in the connecting conduit, (3) a fixed stage elevation, (4) a tidal stage described in a table of tide height versus hour of the day, and (5) a user-defined time series of stage versus time.
Fixed Stage	0	Water elevation of a FIXED boundary condition (ft or m).
Curve Name	*	Name of tidal curve used for a TIDAL boundary condition (one can double-click to edit it)
Series Name	*	Name of time series used for a TIMESERIES boundary condition (one can double-click to edit it)

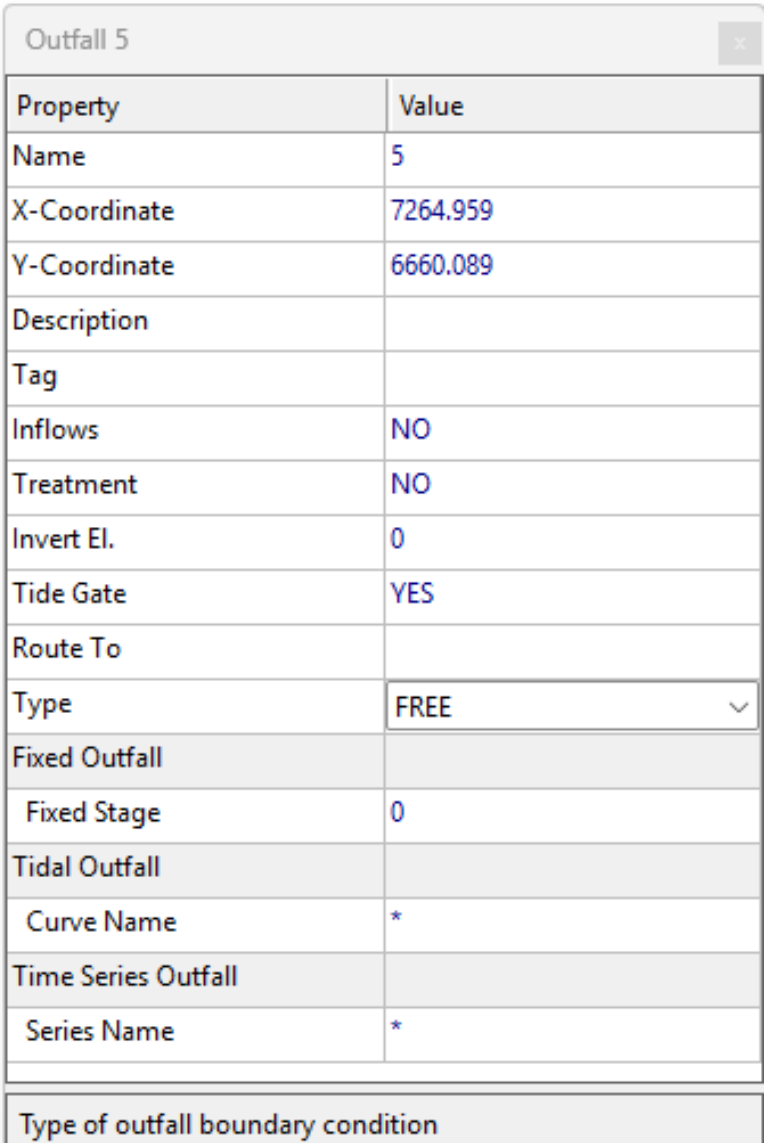

Figure A.8 Example of a free outfall.

A.5 Steps to Create a Conduit in SWMM

In SWMM, the conduit is used to present various pipes and channels under pressurized or open channel flow conditions. In this study, there is one trapezoidal channel (Figure A.9) that collects all runoff from all upstream subcatchments (Figure A.1). In ALODT practices, the drainage channel and infiltration swales are combined together, but the SWMM model separates them as two components: one LID control facility in LID subcatchment and a drainage channel. The LID control facility takes care of the runoff retention/infiltration/storage/evaporation, and the channel considers the flow routing.

Step 1: Open the SWMM Project

Step 2: Select the Conduit Tool

Locate the **Conduit** tool in the toolbar or go to **Hydraulics > Link > Conduit** in the Project.

Step 3: Add a Conduit

1. **Start the Conduit**:
   Click on the **upstream node** (e.g., a junction or outfall) where the conduit begins. (Click the junction we created before)
2. **End the Conduit**:
   Drag the cursor to the **downstream node** (e.g., another junction, outfall, or storage unit) and click to complete the conduit.
3. **Name the Conduit**:
   SWMM assigns a default name. You can rename it by double-clicking the conduit or right-clicking and selecting **Properties**.

Step 4: Define Conduit Properties

1. Double-click the conduit to open its **Properties** window.
2. Configure the following fields (**Table A.5**). Some specific values, e.g., inlet and outlet nodes are "1" and "5", are a specific project in this study. Various conduit shapes (Figure A.9) and corresponding parameters (Table A.6) can be selected and defined.

Table A.5 Conduit or Channel Properties.

Property	Value	Description
Name	"1"	Unique identifier for the conduit.
Inlet Node	"1"	The node where water enters the conduit.
Outlet Node	"5"	The node where water exits the conduit.
Shape	TRAPEZOIDAL	The cross-sectional shape of the conduit.
Max. Depth	"1"	Maximum allowable flow depth (ft or m).
Length	"384.36"	Length of the conduit (in ft or m).
Roughness	"0.03"	Manning's roughness coefficient, indicating surface roughness.

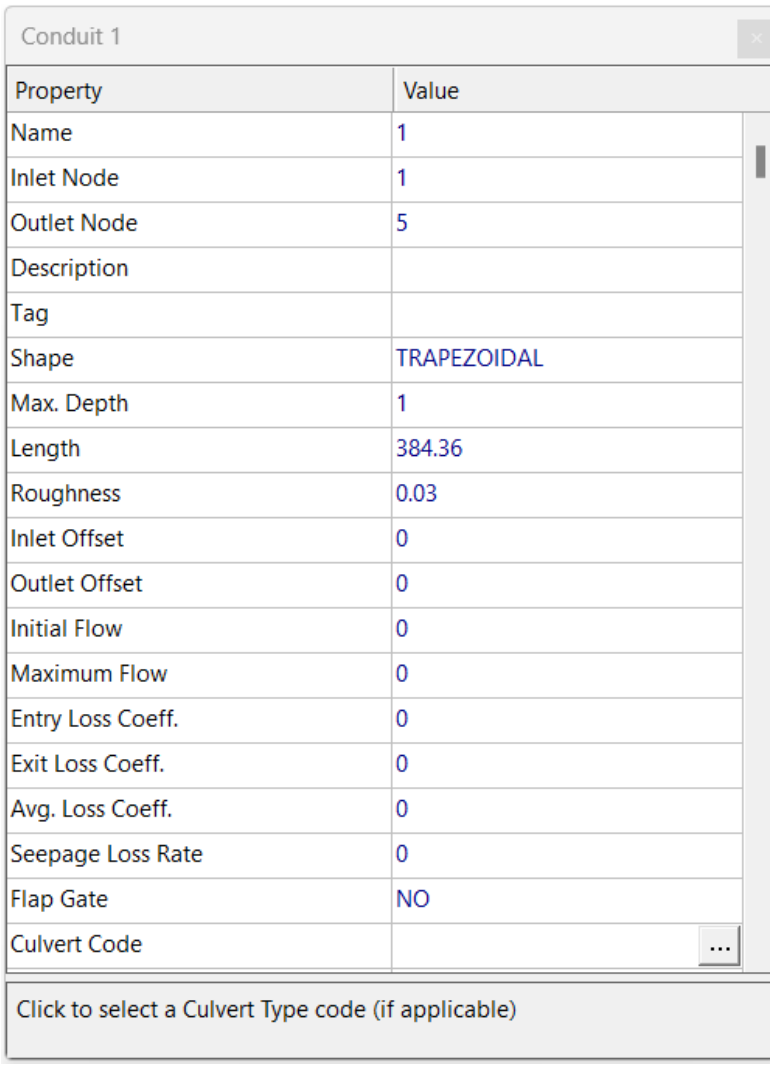

Figure A.9 Example of the conduit setup.

Table A.6 The details for the conduit in SWMM.

Property	Value	Description
Number of Barrels	1	Number of parallel conduits (barrels) modeled together.
Maximum Height	1	Height of the trapezoidal section (in ft or m).
Bottom Width	6	Width of the trapezoidal channel's bottom.
Left Slope	3	Horizontal-to-vertical slope ratio for the left side of the trapezoid.
Right Slope	3	Horizontal-to-vertical slope ratio for the right side of the trapezoid.

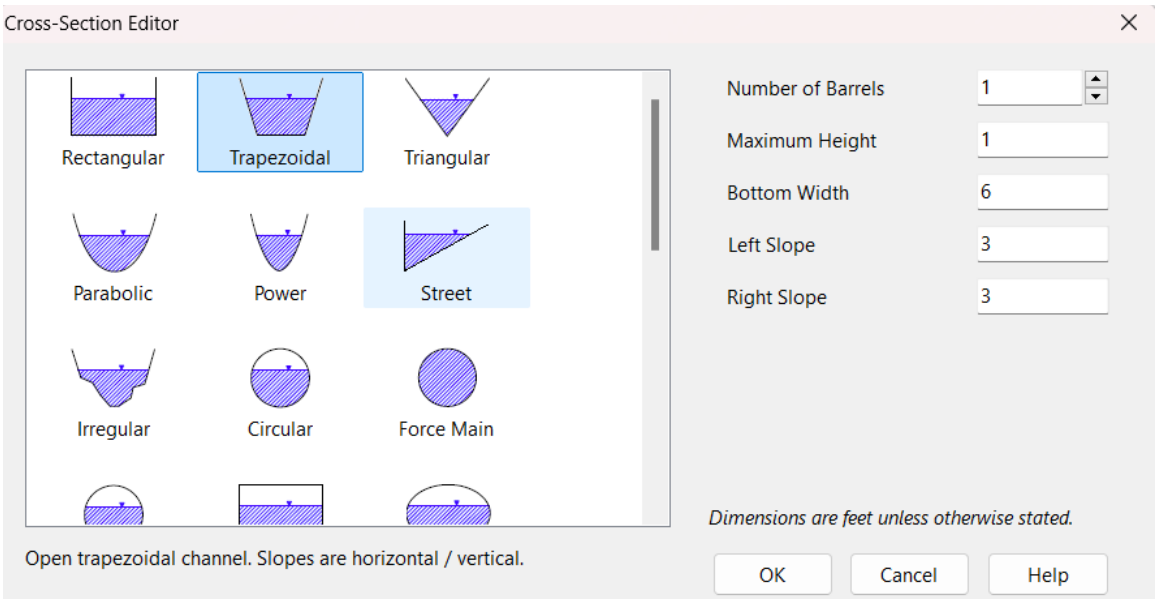

Figure A.10 Example of the conduit cross-section editor when the trapezoidal channel is selected.

A.6 Steps to Create a LID Control in SWMM

Creating the LID facilities in subcatchments is the most important step for this study. The first step is to access the LID controls and input/edit model parameters for four layers: surface, soil, storage, and drain (Figures A.11 to A.14). These LID related parameters have been discussed and explained in Table A.7.

Table A.7 Definition of SWMM's LID modeling parameters (Rossman and Huber 2016).

Layer	Parameter	Description
Surface	Berm Height (or Storage Depth), D_1	This depth is the depression storage or maximum freeboard or ponding depth for the surface layer. It corresponds to the height of a trapezoidal section for ditch check. It is measured in in. or millimeters.
	Vegetation Volume Fraction	The percentage of water storage volume occupied by vegetation is the space taken up by stems and leaves, not their surface area. Though usually negligible, this volume can reach 0.1 to 0.2 for dense vegetation inside LIDs.
	Surface Roughness	Manning's roughness coefficient (n) for overland flow over surface soil cover, pavement, roof surface, or a vegetative swale. Use 0 for other types of LIDs (n is not used for its calculation). It varies with the surface type and influences the runoff flow rate and the overall system performance.
	Surface Slope	A slope (in percentage) is suitable for roof surfaces, pavement, or vegetation swale, while a slope of 0 is used for other types of LIDs.
Soil	Thickness	The thickness of the soil layer varies, typically 18 to 36 in. (450 to 900 mm) for rain gardens, street planters, and other types of land-based bio-retention units, but only 3 to 6 in. (75 to 150 mm) for green roofs.
	Porosity	The pore space volume is the fraction of the total soil volume occupied by voids that surface runoff can fill.
	Field Capacity	The fraction of pore water remaining after complete drainage represents the soil's water volume that does not drain vertically.
	Wilting Point	In dry soils, the pore water volume is the fraction of bound water below which soil moisture cannot decrease.

	Conductivity	Hydraulic conductivity is the rate at which water flows through fully saturated soil, measured in in. or millimeters per hour.
	Conductivity Slope	This parameter plays a significant role in determining the infiltration/ percolation rate through the soil into the storage layer
	Suction Head	The average soil capillary suction of the wetting front, measured in in. or millimeters, is a key parameter used in the Green-Ampt infiltration model.
Storage	Thickness	The gravel layer's thickness or the rain barrel's height is typically 6 to 18 in. (150 to 450 mm) for gravel and 24 to 36 in. (600 to 900 mm) for rain barrels.
	Void Ratio	The void volume relative to the solid for gravel layers is usually between 0.5 and 0.75, called the void ratio. The porosity of the gravel layer is calculated as void ratio/(1 + void ratio).
	Seepage Rate	The infiltration rate of the underlying native soil, measured in in./hour or millimeters/hour, is usually the saturated hydraulic conductivity of Green-Ampt infiltration or the minimum penetration rate of Horton infiltration. If an impervious floor is present, 0 is used.
	Clogging Factor	The clogging factor is the total amount of treated runoff required to clog the layer divided by the void volume. Over time, clogging will reduce infiltration, primarily affecting access drains with permeable bottoms. Use 0 to ignore blocking.
Drain	Drain Coefficient and Drain Exponent	The drain coefficient C and exponent n determine the outflow rate from a drain based on the water height above the drain, using the equation $q = C\ h^n$, where q is the outflow and h is the water height. A typical n value is 0.5, making the drain behave like an orifice. If no drain is present, set C to 0.
	Drain Offset Height	This is the height of the drain line above the bottom of a storage layer or rain barrel (in. or mm).
	Open Level	The height in the drain's storage layer, measured in in. or mm, triggers the drain to open when water rises above it. A default value of 0 turns off this feature.
	Closed Level	The height (in in. or mm) in the drain's Storage Layer causes the drain to open automatically when the water level rises above it. The default is 0, which means that this feature is disabled.
	Control Curve	The height (in in. or mm) in the drain's Storage Layer causes the drain to close automatically when the water level falls below it. The default is 0.

Step 1: Open the SWMM Project

Step 2: Access the LID Controls Editor

1. Go to **Hydrology > LID Controls** in the Project to open the **LID Controls Editor** window.
2. Click **Add Object** to add a new LID control.

Step 3: Define the LID Control Type

1. In the **LID Controls Editor**, choose the type of LID control you want to create (Bio-Retention Cell, Rain Garden, Green Roof, Infiltration Trench, Permeable Pavement, Vegetative Swale, and Rain Barrel); we choose **Bio-Retention Cells** here to represent infiltration swales.
2. Assign a descriptive name for the LID control

Step 4: Configure LID Control Properties

1. **Surface Layer**:

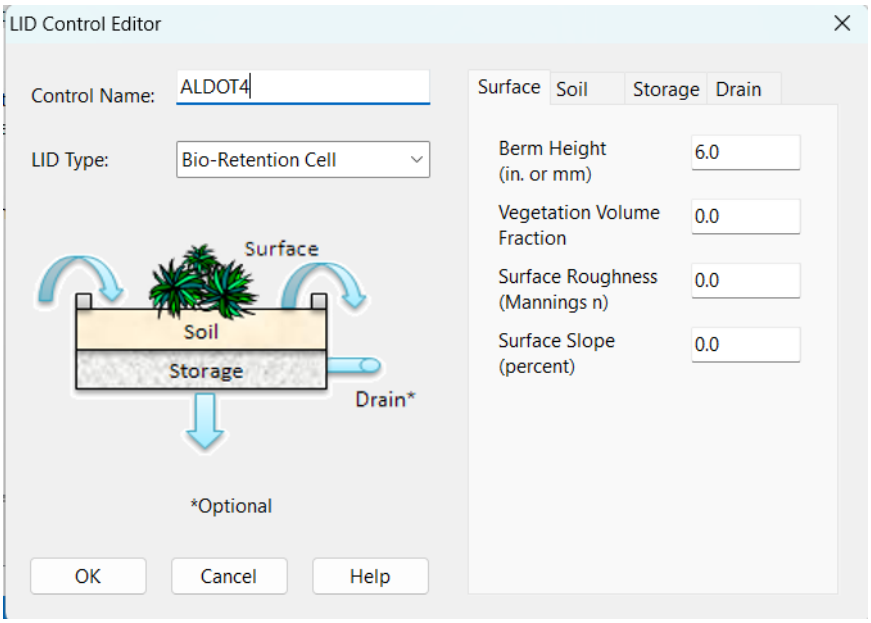

Figure A.11 Surface layer parameters for a LID facility.

Soil Layer:

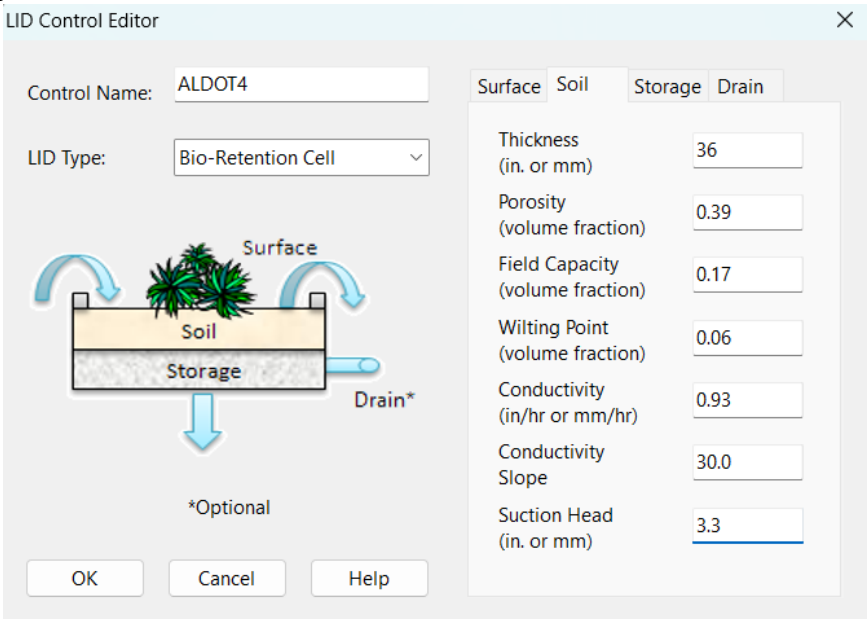

Figure A.12 Soil layer parameters for a LID facility.

2. **Storage Layer**:

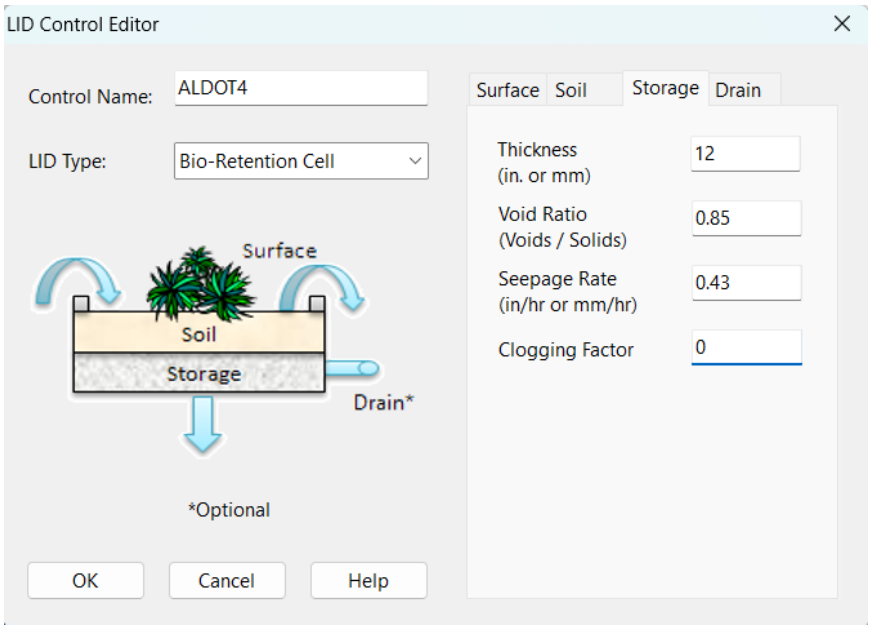

Figure A.13 Storage layer parameters for a LID facility.

3. **Drainage System**:

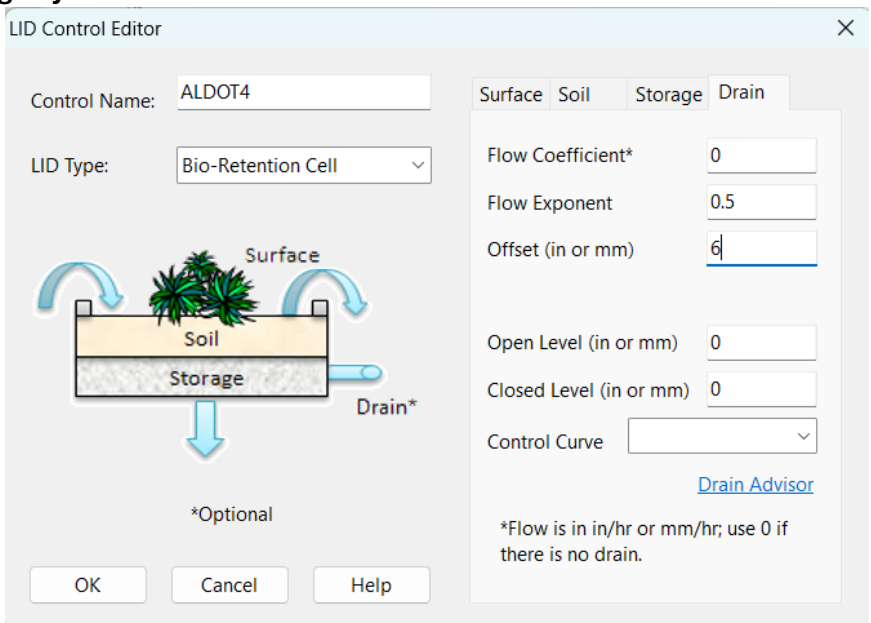

Figure A.14 Drain layer parameters for a LID facility.

Step 5: Assign the LID to a Subcatchment

1. Select the **Subcatchment** where the LID will be applied by double-clicking it.
2. Open the **LID Usage Editor**:

   Click the **LID Controls** button in the subcatchment properties window (Figure A.2 and **Figure 4.11**) to display "LID Controls for Subcatchment LID"

(Figure A.15) (subcatchment name “LID” changes with which subcatchment will add/have LID facilities).

3. Add the LID control:
    1) Click **Add** to associate the LID control with the subcatchment.

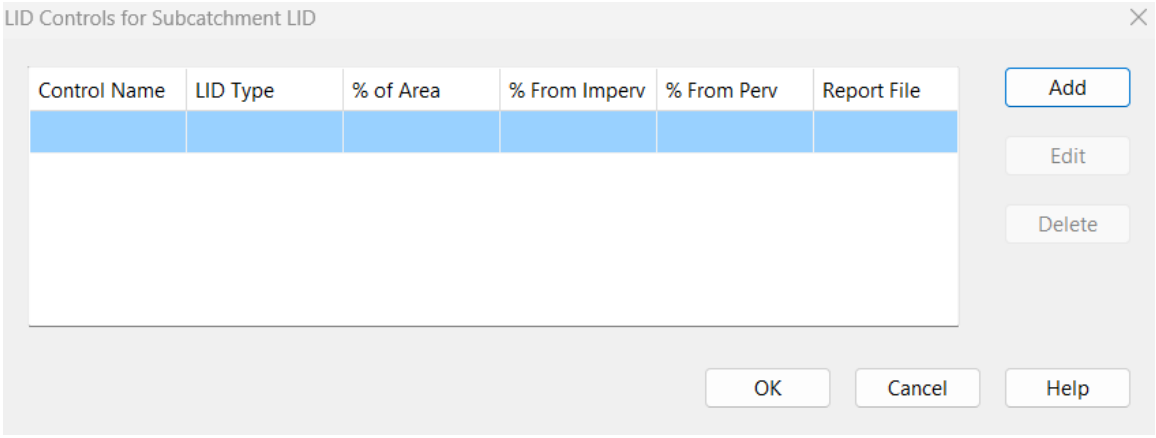

Figure A.15 Adding/editing/deleting LID controls for a subcatchment.

2) Specify the following parameters under “LID Usages Editor” (Figure A.16). Detailed explanations of these parameters and their significance are presented in Table A.8.

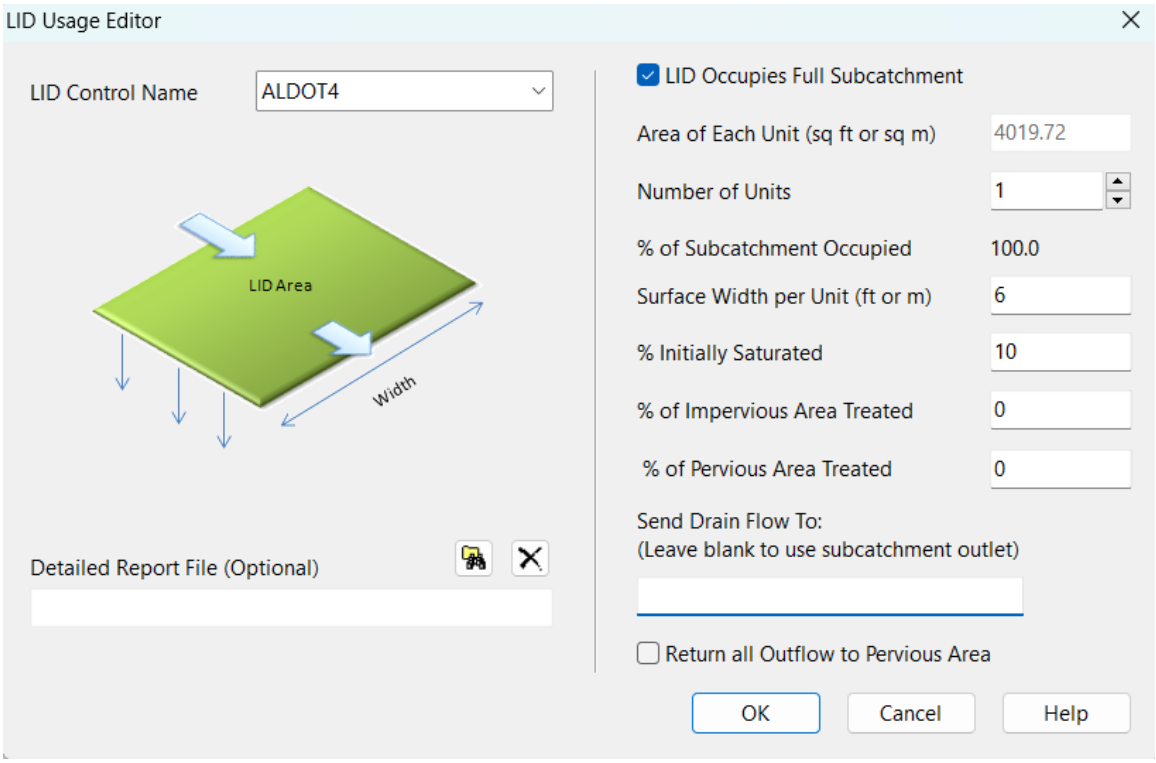

Figure A.16 Example setup of “LID Usage Editor” and parameter values.

4. Click OK to close the LID Usage Editor.

Table A.8 The Description of the LID Usage Editor Parameters

Name	Description
Control Name	Enter the name of the pre-defined LID control one wants to use in the subcatchment.
LID Occupies Full Subcatchment	Check this box if the LID control covers the entire subcatchment (it works independently and receives runoff from other subcatchments).
Area of Each Unit	The size of each LID unit (sq. ft or sq. m). If "LID Occupies Full Subcatchment" is selected, this field is disabled and automatically shows the total subcatchment area divided by the number of units. The label below updates to show how much of the area is used by the LID.
Number of Units	The number of identical LID units (e.g., rain barrels) in the subcatchment.
Surface Width Per Unit	The width of each unit's outflow edge (ft or m). For LIDs like roofs, trenches, or swales, this width is used to calculate how water flows off. For LIDs like rain gardens or rain barrels, set this to 0 as they don't use overland flow.
% Initially Saturated	For systems like rain gardens, green roofs, or bio-retention cells, this is how much water the soil contains at the start (0% is dry, 100% is fully saturated). For units with a storage layer, this shows the initial water depth in the storage.
% Impervious Area Treated	The percentage of impervious surfaces (like roofs or pavements) in the subcatchment whose runoff is managed by the LID. For example, if rain barrels collect runoff from roofs that make up 60% of the impervious area, this value is 60%. Use 0% for LIDs like green roofs that only handle direct rainfall. Ignore this if the LID covers the whole subcatchment.
% Pervious Area Treated	The percentage of pervious surfaces (like grass) in the subcatchment whose runoff is managed by the LID. Use 0% for LIDs like green roofs that only handle direct rainfall. Ignore this if the LID covers the whole subcatchment.
Send Drain Flow To	Specify where the drain flow from the LID should go (e.g., a Node or Subcatchment). Leave blank if the flow follows the subcatchment's outlet.
Return Outflow to Pervious Area	Check this box if you want the outflow from the LID to go back to the pervious area in the same subcatchment. If drain flow is sent elsewhere, only surface flow will return. This option is commonly used for Rain Barrels, Rooftop Disconnection, or Green Roofs.
Detailed Report File	Provide a file name to save detailed time-series results for the LID. Use the "browse" button to choose a file directory and enter a file name (e.g., MIS.txt) to save the detailed LID results or the "delete" button to remove it.

A.6 Steps to Set Simulation Options in SWMM

Step 1: Open the SWMM Project

Step 2: Access the Options Dialog

1. Go to **Project** to click the **Options** button on the toolbar.
2. The **Simulation Options** dialog box will appear, displaying various tabs for different types of settings.

Step 3: Configure General Simulation Options (Figure A.17)

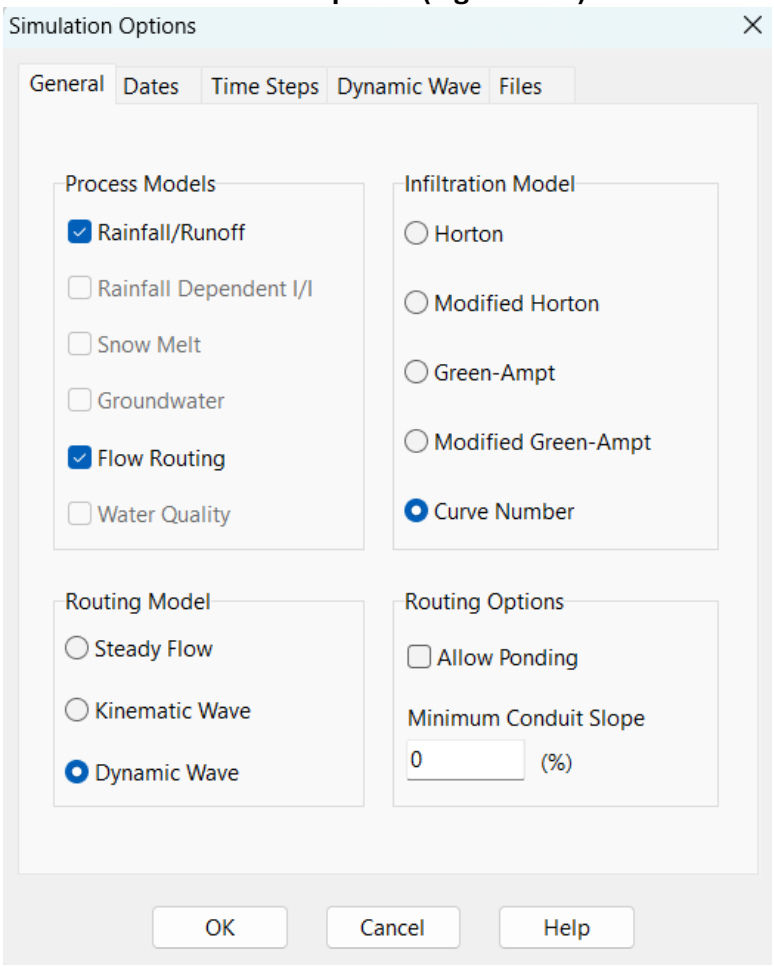

Figure A.17 Example setup of General Simulation Options.

Rainfall/Runoff and **Flow Routing** can simulate stormwater runoff and its transport through drainage systems.

Dynamic Wave routing model can accurately simulate the network's unsteady flow and backwater effect.

Curve Number infiltration model is a common model for rainfall-runoff estimation in urban and rural areas.

Step 4: Configure Date Settings

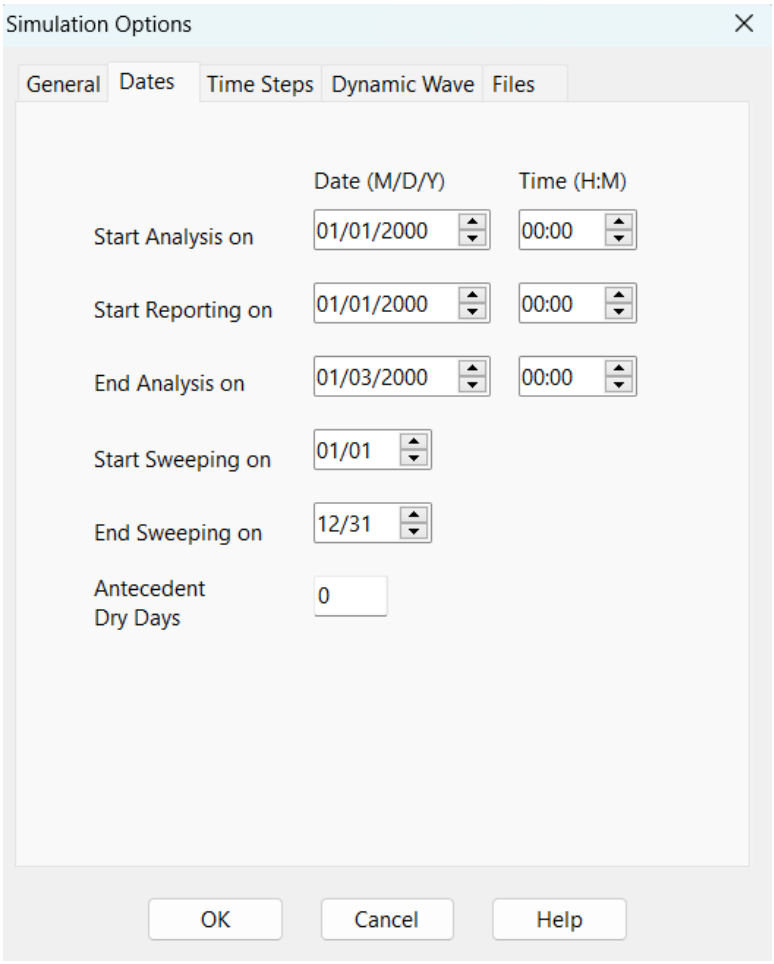

Figure A.18 Example setup of Dates for Simulation Options.

The simulation is set to run from **January 1, 2000**, at midnight (**00:00**) to **January 3, 2000**, at midnight (**00:00**) in Figure A.18.
Detailed results reporting starts at the beginning of the simulation (**01/01/2000, 00:00**).
Street sweeping (if modeled) is configured to occur year-round, from **January 1** to **December 31, but it is not used if runoff quality is not simulated**.
"Antecedent Dry Days" is set to **0**, meaning no pre-simulation dry period is considered for initializing soil or catchment conditions.

Step 5: Configure Time Steps Settings for Simulation (Figure A.19)

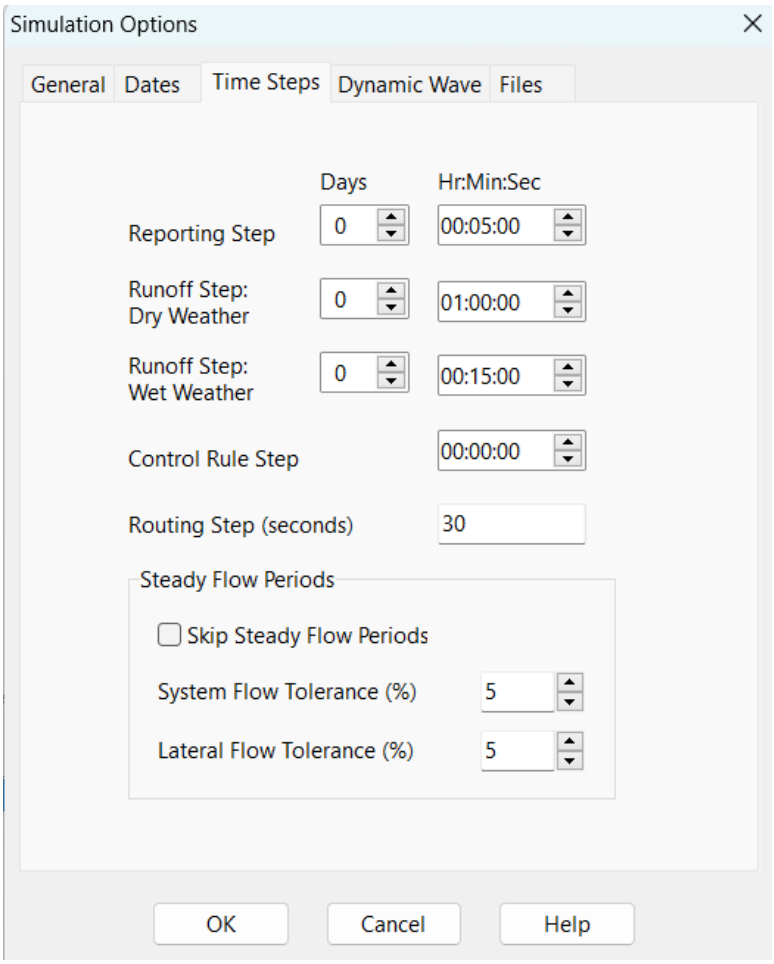

Figure A.19 Example setup of Time Steps for Simulation Options.

Reporting Step simulate results will be recorded every 5 minutes for analysis.
Runoff Step Dry Weather 1-hour intervals. **Runoff Step Wet Weather** 15-minute intervals.
Routing Step is set to 30 seconds, providing a detailed calculation for hydraulic routing.
Step 6: Configure Dynamic Wave Routing Settings (Figure A.20)

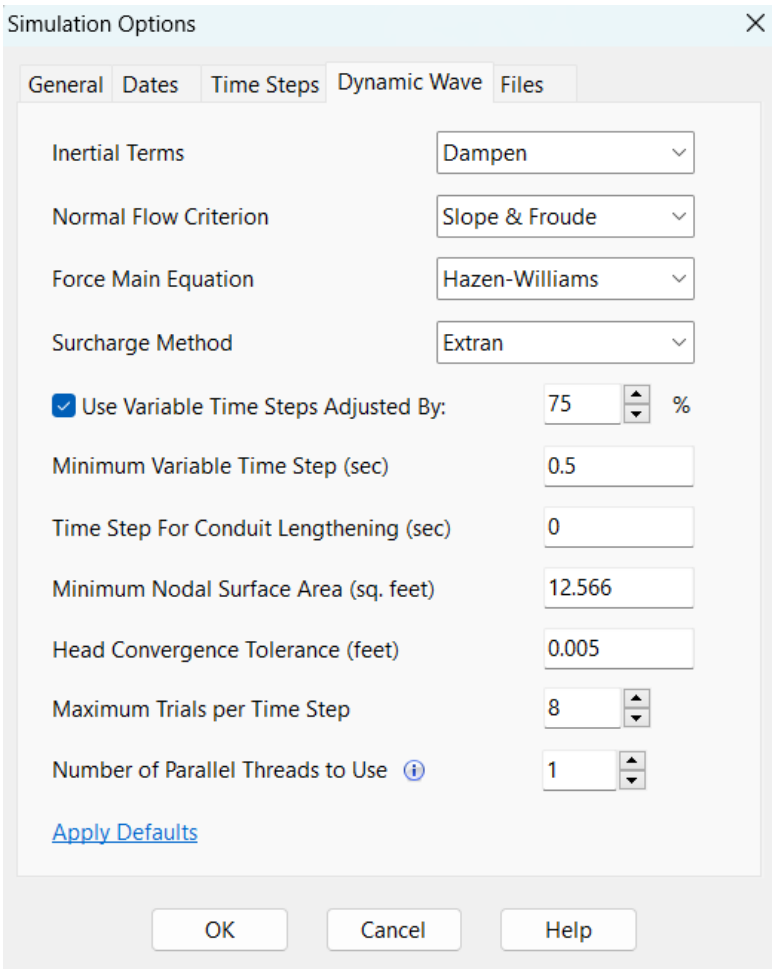

Figure A.20 Example setup of Dynamic Wave for Simulation Options.

A.7 Steps to Run the Model and Get Results in SWMM

Step 1: Run the Model

1. **Click Run**:
   Press the **Run** button (yellow arrow) on the toolbar.
2. **Monitor the Progress**:
   1) A progress bar will appear, showing the simulation status.
   2) Upon completion, a message will confirm whether the simulation ran successfully or encountered errors.

Step 5: View Results

SWMM provides multiple ways to review results:

1. **Scatter Plot (Figure A.21)**:
   1) Open the **Scatter Plot** 
   2) Select **Time Period** and **xy Variables** to create a **Scatter Plot** to view the scatter plot result

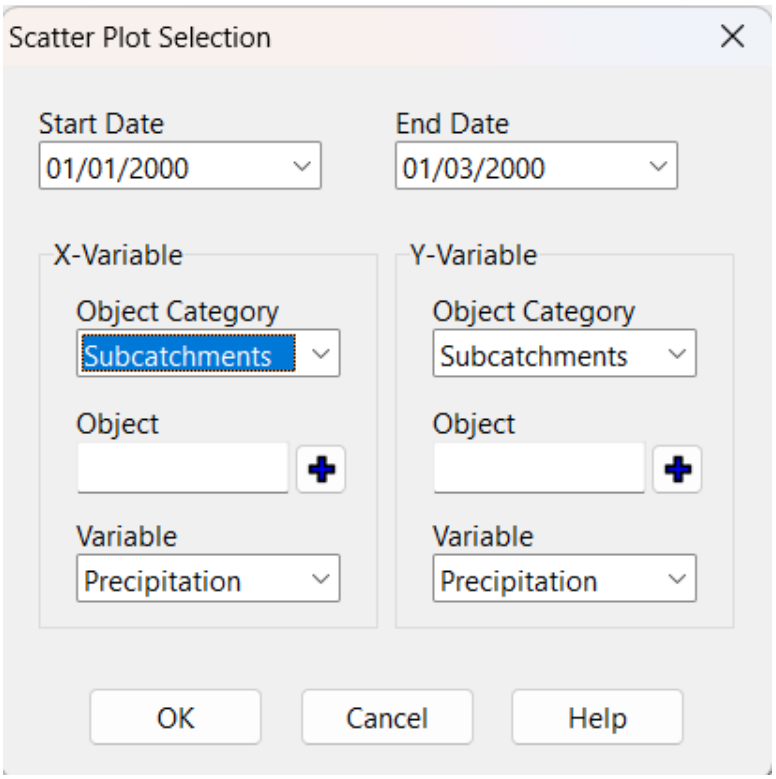

Figure A.21 Example setup of Scatter Plot Options.

2. **Time Series Table (Figure A.22)**:

    1) Open the **Time Series Table** 
    2) Select **Time Period** and **Data Series** to create a **Time Series Table** to view time series results.

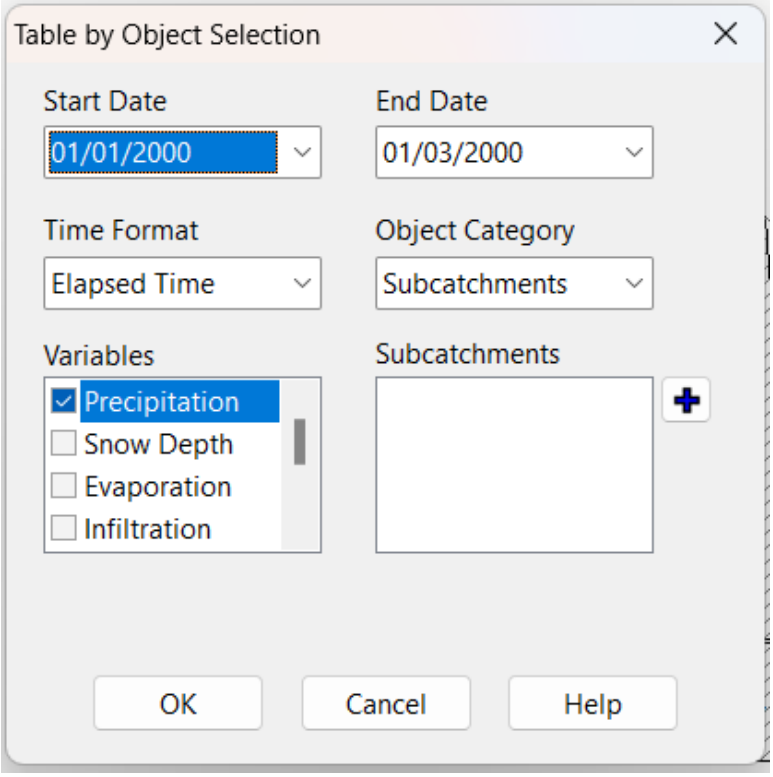

Figure A.22 Example setup of Time Series Table.

3. **Time Series Plot (Figure A.23)**:

    1) Open the **Time Series Plot** 
    2) Select **Time Period** and **Data Series** to create a **Time Series Result** to view time series results.

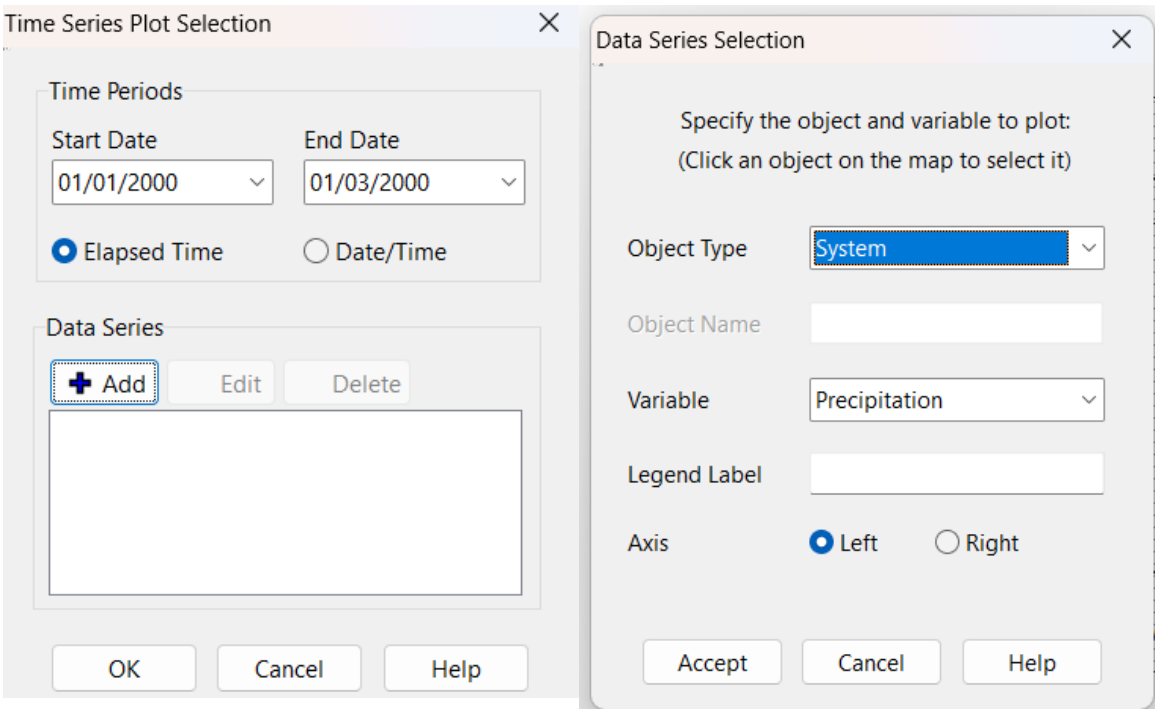

Figure A.23 Example setup windows of Time Series Plot.

4. **Profile Plots (Figure A.24)**:

    1) Open the **Profile Plots** 
    2) Select connected elements and create a **Profile Plot** to view longitudinal flow behavior.

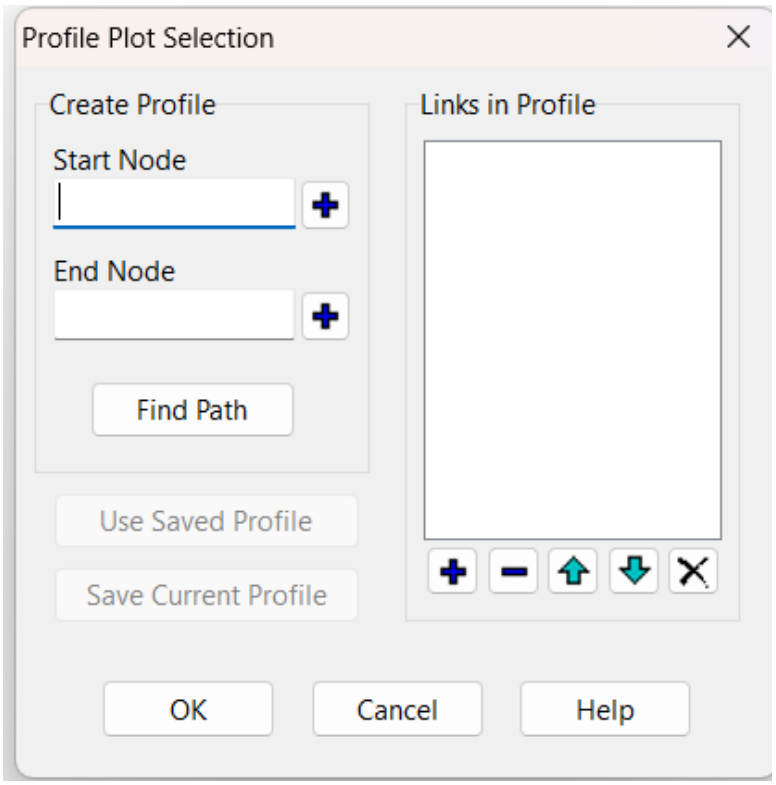

Figure A.24 Example setup of Profile Plots.

5. **Status Report**:

Open the **Status Report** , choose **Status Report** or **Summary Results**

In this study, the profile plot is not used. Since there is one open channel, dynamic wave routing may not make as much difference as kinematic wave routing.